UNIVERSITY OF OKLAHOMA

GRADUATE COLLEGE

EFFORTS TOWARDS THE SYNTHESIS OF FURAN CONTAINING BIOACTIVE COMPOUNDS

A DISSERTATION

SUBMITTED TO THE GRADUATE FACULTY

In partial fulfillment of the requirements for the

Degree of DOCTOR OF PHILOSOPHY

In Chemistry and Biochemistry

By

CHENXIN OU

Norman, Oklahoma

2023

EFFORTS TOWARDS THE SYNTHESIS OF FURAN CONTAINING BIOACTIVE COMPOUNDS

A DISSERTATION APPROVED FOR THE

DEPARTMENT OF CHEMISTRY AND BIOCHEMISTRY

BY THE COMMITTEE CONSISTING OF

Dr. Indrajeet Sharma, Chair

Dr. Yihan Shao

Dr. Susan Schroeder

Dr. Wei Qin

DEDICATION

I dedicate this dissertation to my parents for the unconditional love in my life.

ABSTRACT

Furan is a valuable subunit in pharmaceutical chemistry. However, there are still challenges in synthesizing furan-containing compounds. Two approaches have been attempted to address this issue. 1. Using enynal molecules as a carbene precursor for synthesizing functionalized furyl-pyrrolidines. A cascade approach was developed for synthesizing functionalized (2-furyl)-2-pyrrolidines, showcasing both convergence and remarkable stereoselectivity. This domino process proceeds through an N–H insertion into enynal-derived metal-carbenoid, followed by an intramolecular aldol reaction to provide pyrrolidines with high diastereoselectivity (>98:2). This chemistry utilizes Earth-abundant zinc chloride as a catalyst with loading as low as 1 mol%. This method operates under mild conditions and demonstrates high chemoselectivity by accommodating substrates bearing functionalities such as free alcohols, alkenes, and alkynes. 2 Towards the total synthesis of collybolide. Collybolide is a natural product that was first isolated from the fungus Collybia maculata. It has attracted attention due to its potential therapeutic applications, particularly in the treatment of pain and inflammation. Its complex structure, however, makes it a challenging target for total synthesis. Our route starts from simple glutamic acid. This route aimed to minimize the use of chiral reagents and catalysts to install all 6 stereocenters in Collybolide. So far, after 11 reactions, we have achieved the intermediate having 15 out of 22 carbon atoms and 4 out of 6 stereocenters in Collybolide without using any chiral reagents and catalysts other than glutamic acid. One of the significances of this route is that different from the traditional synthetic route, we installed furan moiety at a very early stage. Furan is known for its instability, however, in our route, it is stable throughout the synthetic pathway.

ACKNOWLEDGMENTS

First, I would like to thank my family. My parents, Jiangcun Chen and Wangguo Ou. You gave everything you could to create a wonderful environment for my childhood. You have supported all the decisions I made during my life. I am truly grateful for your sacrifice and giving.

Secondly, I would like to thank the University of Oklahoma and the Department of Chemistry and Biochemistry for allowing me to pursue my doctoral studies. Most importantly my mentor and Ph.D. advisor, Dr. Inderjeet Sharma. Thank you for accepting me into your group after Dr. Mao left this university. Also thank you for the training you gave and the knowledge and experience you shared with me. What I have learned will definitely help me in my future career.

I would like to thank the members of the Sharma Research Group –past and present for the help I received. Dr. Bidham Ghosh, Adam Alber, Prakash Kafle, Randy Welles, Surya Singh, Dr. Nicholas Massaro. You have been good friends with me. Such friendship has been a great experience during the years of my Ph. D. study.

I would also like to thank the members of my graduate committee, Dr. Yihan Shao, Dr. Susan Schroeder, Dr. Wei Qin. Additionally, I would like to thank my former committee members, Dr. Bayram Saparov and Dr. Scott Russell.

LIST OF FIGURES

LIST OF ABBREVIATIONS

A = alpha anomer

Å = Ångstrom

Ac = acetate group

al = aldehyde

Ar = aryl group

AcOH = acetic acid

A/A = acceptor/acceptor

B = beta anomer

Bn = benzyl group

Boc = tert-butyloxycarbonyl

BF_4 = tetrafluoroborate

BOX = bisoxazoline

Bu = butyl

Bz = benzoyl group

ºC = degrees Celsius (centigrade)

calc'd = calculated

d = doublet

D = dextrorotatory

DBU = 1,8-Diazabicyclo[5.4.0]undec-7-ene

DCE = 1,2 dichloroethane

DCM = dichloromethane

dd = doublet of doublets

DMAP = 4-dimethylaminopyridine

DMB = 2,4 dimethoxybenzyl

DMF = N,N-dimethylformamide

DMP = Dess-Martin periodinane

DMSO = dimethyl sulfoxide

DTBP= 2,6-Di-tert-butylpyridine

D/A = donor/acceptor

E = electrophile

ee = enantiomeric excess

EDCI = 1-Ethyl-3-(3-dimethylaminopropyl)carbodiimide

EDG = electron-donating group

en = alkene

esp = a,a,a’a,’-tetramethyl-1,3-benzenedipropionic acid

Et = ethyl

EtOAc = ethyl acetate

Equiv = equivalent

EWG = electron-withdrawing group

g = gram

h = hour

HMPA = hexamethylphosphoramide

HPLC = high-performance liquid chromatography

iPr = isopropyl

IR = infrared (spectroscopy)

J = coupling constant

KHMDS = potassium bis(trimethylsilyl)amide

LG = leaving group

m = multiplet or milli

M = metal or molar

Me = methyl

MeCN = acetonitrile

MHz = megahertz

MLn = metal catalyst with X ligands

MS = molecular sieves

m/z = mass to charge ratio

mol = mole(s)

$NaBH_4$ = sodium borohydride

*n*Bu = *n*-butyl

nd = not determined

NMR = Nuclear Magnetic Resonance

nr = no reaction

Nu = nucleophile

Nuc = nucleophile

o = ortho

one = ketone

p = para

p-ABSA = 4-acetamiobenzenesulfonyl azide

PF_6 = hexafluorophosphate

PG = protecting group

Ph = phenyl group

pH = hydrogen ion concentration in aqueous solution

q = quartet

R = alkyl group

Rf = retention factor

$Rh_2(OAc)_4$ = rhodium (II) acetate dimer

$Rh_2(oct)_4$ = rhodium (II) octanoate dimer

$Rh_2(HFB)_4$ = rhodium(II) Heptafluorobutyrate Dimer

RT = room temperature

s = singlet

sub = substrate

S_N1 = nucleophilic substitution unimolecular

S_N2 = nucleophilic substitution dimolecular

t = triplet

TBAF = tetra-n-butylammonium fluoride

tBu = tert-butyl

TBS = tert-butyldimethylsilyl

Tf = trifluoromethanesulfonyl (trifyl)

TFA = trifluoroacetic acid

THF = tetrahydrofuran

TLC = thin-layer chromatography

Ts = p-toluenesulfonyl (tosyl)

WHO = World Health Organization

X = anionic ligand or halide

yn = alkyne

TABLE OF CONTENTS

CHAPTER 1

The Introduction of Furan's Importance in the Pharmaceutical Field

1. Introduction

1.1. Furan

Furan is an aromatic cyclic ether possessing four carbon atoms and one oxygen atom. It is drawn with two carbon-carbon double bonds inside the ring while six π electrons from all four carbons and one oxygen generate aromaticity. The resonance energies of furan are 16 kcal/mol,[1] which is less than half of the resonance energies of benzene (36 kcal/mol).[1] Compared with other aromatic rings, furan is more reactive.[2] The lone pair of electrons on the oxygen atom can delocalize into the ring, making furan highly reactive towards electrophilic aromatic substitution. This means that furan tends to react at the 2-position (or alpha position relative to oxygen) in electrophilic aromatic substitutions due to the increased electron density in that position. Due to its electron-rich nature, furan is also susceptible to oxidation, particularly by potent oxidizing agents. Furan is sensitive to acid-catalyzed ring openings.[3] Furan can be protonated under acidic conditions, making it more susceptible to nucleophilic attack and potential ring-opening.[4] Furan can act as a diene in Diels-Alder reactions with dienophiles, resulting in the

formation of bicyclic compounds.[5] In this context, furan behaves as a highly reactive diene due to its s-cis conformation and the nature of the LUMO (Lowest Unoccupied Molecular Orbital), which has a significant contribution from the oxygen atom.

1.2. The versatile role of furans in facilitating molecular interactions

The presence of a furan moiety often conveys significant reactivity and a capacity to engage with various biological targets, such as enzymes and receptors. The means by which furan exerts its influence can be quite diverse.

Furans can experience π-π stacking interactions with target molecules. The phenomenon of π-π stacking is primarily an attractive, noncovalent interaction observed between two aromatic systems. A quintessential example would involve two aromatic rings approaching each other in such a way that their π electron clouds overlap. The furan ring, owing to its inherent aromaticity, can engage in such interactions quite effectively. This particular trait allows furan-containing compounds to interact preferentially with aromatic amino acid residues within proteins or with aromatic bases in nucleic acid structures like DNA. These interactions can profoundly influence the conformation, stability, and function of these macromolecules.

Hydrogen bonding is also a feature of furan interactions. Hydrogen bonds are fundamental in governing the structure and function of biological molecules. Typically, a hydrogen bond is formed between a partially positively charged hydrogen atom and a highly electronegative atom such as oxygen, nitrogen, or fluorine. While the furan ring itself does not serve as a hydrogen bond donor due to the absence of a proton linked to the oxygen atom, it can act as an efficient hydrogen bond acceptor. This capability arises

from the electronegative oxygen atom housed within the furan ring. Such interactions are integral in molecular recognition processes and in stabilizing multi-molecular complexes.

Furan can also lead to covalent bonding. Although furan boasts stabilization through aromaticity, it isn't entirely chemically inert. In specific scenarios, especially under enzyme catalysis, furan can engage in covalent interactions.[6] Certain enzymes might facilitate the breakdown of the aromatic ring or leverage the reactive nature of furan to form covalent bonds.[6-8] This potential makes furan an interesting molecule in drug design, where it can act as an irreversible enzyme inhibitor by forming a covalent linkage with the enzyme's active site, thus inactivating it.

1.3. Furan-containing pharmaceuticals

The bioactivity of furan-containing compounds has garnered significant interest in the field of pharmaceutical research. These compounds exhibit a wide array of biological properties that make them appealing candidates for drug development.

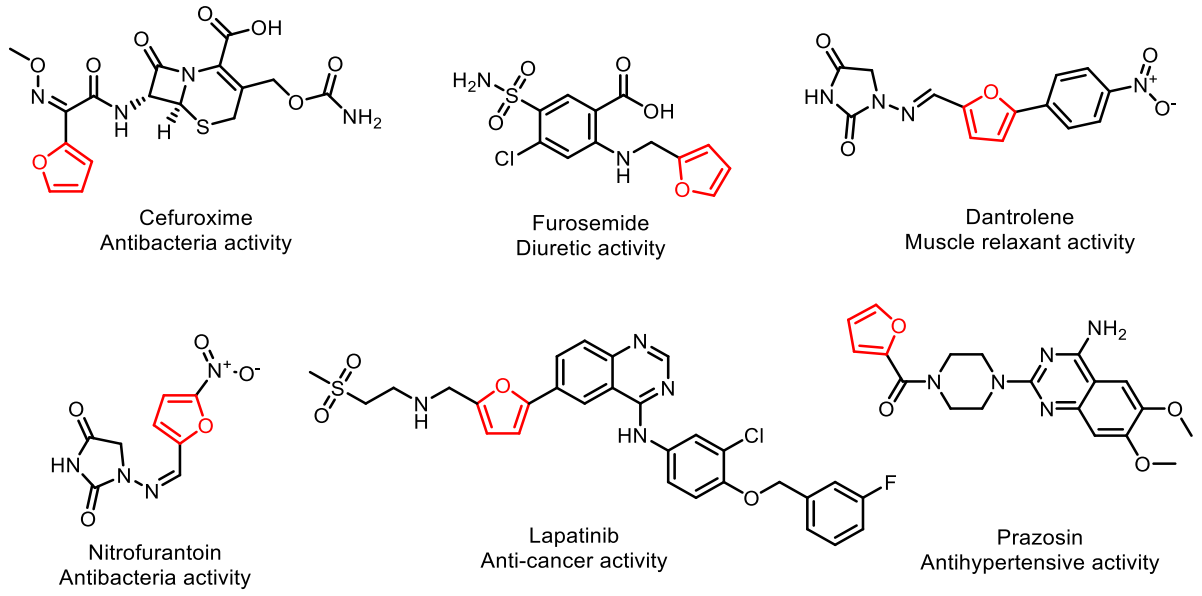

Figure 1.1. Examples of furan containing FDA-approved drugs.[7, 9-13]

1.3.1. Furan as an active pharmacophore

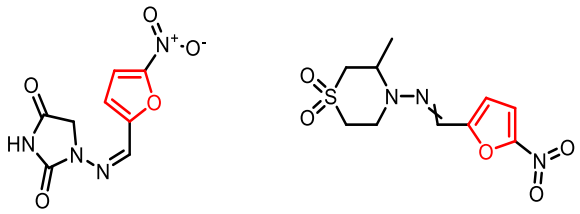

Figure 1.2. Nitrofurantoin (left) and Nifurtimox (right) as examples of furan serving as a pharmacophore for the drug molecules.

In the development of pharmaceutical chemistry, furan is discovered as one pharmacophore.[14-16] A pharmacophore is a vital concept in drug design and molecular pharmacology. It refers to an abstract description of molecular features that are necessary for molecular recognition of a ligand by a biological macromolecule. Essentially, a pharmacophore is the ensemble of steric and electronic features needed to ensure the

optimal supramolecular interactions with a specific biological target structure and to trigger or block its biological response.

Nitrofurantoin is an antibacterial medication prescribed for the treatment of urinary tract infections. It was first sold in 1953. Nitrofurantoin is on the World Health Organization's List of Essential Medicines.[17] It is available as a generic medication.[18] In 2020, it ranked as the 167th most frequently prescribed medication in the United States, with over 3 million prescriptions.[19] Nitrofurantoin is a typical nitrofuran antibiotic. It is readily reduced by bacterial flavoproteins (nitrofuran reductase) to multiple reactive intermediates. These intermediates damage ribosomal proteins, DNA, respiration, pyruvate metabolism, and other macromolecules within the cell. So far it is unknown which damage is primarily responsible for its bactericidal activity. However, the multi-target action of nitrofurantoin may be beneficial in the low development of bacterial resistance.[7] There are also other FDA-approved nitrofuran antibiotic available, such as Furazolidone, Nifuroxazide, and Nitrofurazone.[20-21]

Nifurtimox is an antiparasitic drug used for the treatment of Chagas disease. It is on the World Health Organization's List of Essential Medicines. While the mechanism of its action is not fully understood, it is believed that multiple reactive metabolites from Nifurtimox by the activation of nitroreductases are responsible for the parasite death.[22] This hypothesis is similar to the nitrofuran antibiotic mechanism of action.

1.3.2. Furan's role in enhancing drug binding affinity

Lapatinib is a small molecule tyrosine kinase inhibitor that targets both the epidermal growth factor receptor (EGFR) and human epidermal growth factor receptor 2

(HER2/neu).[12] It has been approved for the treatment of patients with advanced or metastatic breast cancer.[23] The furan ring is connected with the quinazoline core by a single bond. This allowed both conjugation and rotation, modulating the electronic interaction with the quinazoline core. The furan ring stabilizes the insertion of Lapatinib into a hydrophobic pocket that is specific to the inactive state of the ATP binding pocket of the EGFR family of receptor tyrosine kinases.[12]

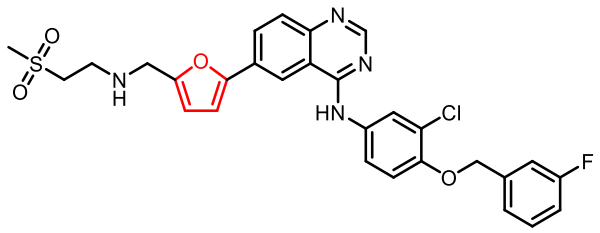

Figure 1.3. Furan-containing lapatinib as an example where furan increases the performance of the drug molecule.

1.3.3. Furan's role in enhancing drug permeability

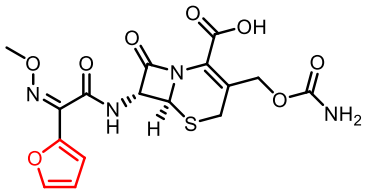

Figure 1.4. Furan-containing cefuroxime as an example where furan increases the permeability of the drug molecule.

Cefuroxime is an antibiotic against many bacteria including susceptible strains of Staphylococci and Streptococci, as well as a range of gram-negative organisms. It was patented in 1971 and received medical approval in 1977.[24] It is included in the World Health Organization's List of Essential Medicines.[17] In the United States, it ranked as the

325th most frequently prescribed medication in 2020, with over 800 thousand prescriptions.[25] Same as other f β-lactam antibiotics, the bactericidal effect of cefuroxime originates from inhibiting the crucial final transpeptidation step required for cross-linking, further disrupting the synthesis of peptidoglycan in the bacterial cell wall. As one of the second-generation cephalosporin antibiotics, the unique furan-linked oxyimino substructure in cefuroxime grants higher stability and permeability than others. It is less susceptible to beta-lactamase, thus having higher activity against Haemophilus influenzae, Neisseria gonorrhoeae, and Lyme disease.[26] In addition, unlike other second-generation cephalosporin antibiotics, cefuroxime can cross the blood–brain barrier.[26] One of the third-generation cephalosporin type antibiotics, Ceftiofur, also contains furan substructure.

1.3.4. Other examples of furan-containing pharmaceuticals

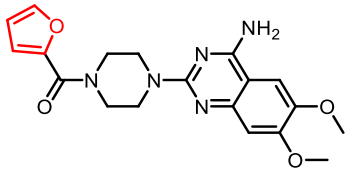

Figure 1.5. Furan-containing Prazosin as an example of antihypertensive drugs.

Prazosin is a medication that belongs to a class of drugs called alpha-1 blockers. It's primarily used to treat hypertension (high blood pressure) and symptoms associated with benign prostatic hyperplasia (BPH) in men.[27] Furthermore, it has found off-label use in managing nightmares related to post-traumatic stress disorder (PTSD).[28] While the furan ring is part of prazosin's chemical structure, its specific role in the medical action of the drug is not well-defined. The furan ring is likely involved in optimizing the drug's

pharmacokinetic properties, such as its absorption, distribution, metabolism, and excretion, rather than directly influencing its pharmacological effects.[29]

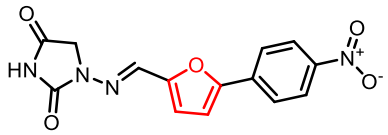

Figure 1.6. Furan-containing Dantrolene as an example for muscle relaxant.

Dantrolene is a commercial muscle relaxant. It inhibits Ca^{2+} ions release from sarcoplasmic reticulum stores by antagonizing ryanodine receptors, which lessens excitation-contraction coupling in muscle cells. It is also the primary clinical agent for malignant hyperthermia (MH) treatment. MH is a life-threatening disorder triggered by general anesthesia or drugs. While its mechanism was not fully understood, there was evidence that ryanodine receptor isoform 1 (RYR1) was associated with MH. RYR1 is the major calcium-releasing channel of the sarcoplasmic reticulum in the human body. The prolonged duration in the open state of RYR1 could be the cause of an enhanced efflux of calcium from the sarcoplasmic reticulum into the myoplasm. This altered effect of RYR1 is inhibited by dantrolene, restoring the normality of vital signs. However, the inhibition mechanism was not fully understood.[10]

1.4. Pharmaceutical liability of furan

Although furan plays an important role in medical chemistry, many furan-containing compounds are toxic. Their toxicity comes from oxidation of the furan ring in metabolism. After ingestion, furan is rapidly absorbed and distributed throughout the body. It's metabolized in the liver, primarily by the cytochrome P450 system.[6]

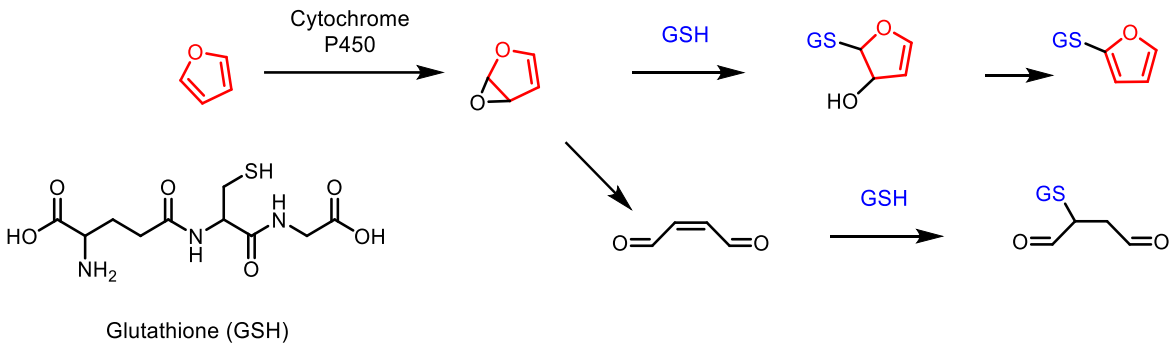

Figure 1.7. The representative mechanism for furan covalently binding to glutathione.[6]

Cytochrome P450, commonly abbreviated as CYP450 or simply P450, refers to a large and diverse superfamily of enzymes that play a critical role in the metabolism of a wide array of both endogenous and exogenous compounds. These enzymes are essential for the detoxification and clearance of various drugs and toxins from the body.

The cytochrome P450 oxidizes furans into reactive metabolites.[6] These metabolites aren't merely passive byproducts. They exhibit a pronounced affinity for DNA, leading to potential bindings. Such interactions can distort the DNA structure, paving the way for mutations that could disrupt normal cellular functions or even initiate carcinogenic processes.

The repercussions of furan oxidation extend beyond DNA interactions. One notable consequence is the depletion of Glutathione (GSH), an essential antioxidant in cells. When furan's oxidation diminishes GSH levels, cells, especially hepatocytes, become vulnerable—even micromolar concentrations can compromise their viability. Additionally, furan's impact on cellular energetics is profound. It not only depletes ATP, the primary energy molecule in cells, in isolated hepatocytes but also disrupts the

oxidative phosphorylation process, a vital energy-producing pathway. This disruption occurs both in test-tube experiments (*in vitro*) and in living organisms (*in vivo*), underscoring the broad and potentially harmful impact of furan on cellular bioenergetics. [6, 30]

1.5. Examples of non-toxic furan pharmaceuticals

1.5.1. A non-oxidative metabolism pathway leads to no toxicity

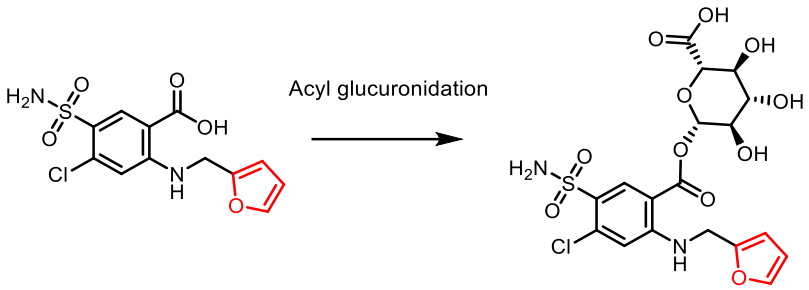

Figure 1.8. Major metabolization pathway of Furosemide leads to no toxicity

As mentioned previously, the utilization of furan in the pharmaceutical industry is well-established, with several FDA-approved drugs containing this moiety. The relatively non-toxic nature of these drugs is noteworthy, especially when contrasted with the inherent toxicity often associated with furan compounds.[9] A major metabolism pathway being non-oxidative decreases the toxicity of the compound. Furosemide serves as a prime example of a furan-containing pharmaceutical with a safety profile that has stood the test of time. As a potent loop diuretic, it is prescribed for conditions such as edema resulting from heart failure, liver scarring, or kidney disorders. Furosemide binds to the Na-K-2Cl cotransporter (NKCC) in the thick ascending limb of the loop of Henle, blocking tubular reabsorption of sodium and chloride.[31] Such inhibition increases the excretion of water along with sodium, chloride, and other ions.[9] It is on the World Health Organization's List of Essential Medicines.[17] In the United States, it is available as a generic

medication.[32] In 2020, it was the nineteenth most commonly prescribed medication in the United States, with more than 26 million prescriptions.[19] While the specific reason is still unknown, the major route of furosemide metabolism is glucuronidation rather than oxidation in humans.[33]

1.5.2. A major metabolism pathway without the involvement of GSH leading to reduced toxicity

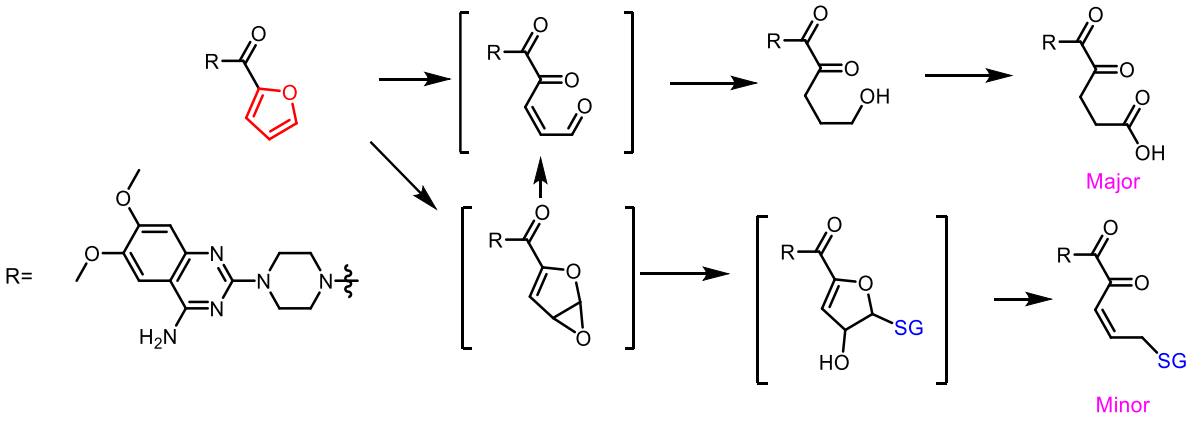

Figure 1.9. Metabolism of prazosin. No toxicity by forming GSH inactive intermediates as the major pathway.[34]

While oxidation of furan may lead to depletion of GSH and further health issues, it is not always the case. Formation of GSH inactive intermediate after oxidation of furan ring also reduces the toxicity. Prazosin is a medication used to treat high blood pressure, symptoms of an enlarged prostate, and nightmares related to post-traumatic stress disorder (PTSD).[27-28] In 2020, it was the 190th most commonly prescribed medication in the United States, with more than 2 million prescriptions.[19] After the oxidation of the furan ring, diketone aldehyde was immediately formed as the major intermediate, and this

intermediate does not couple with GSH. GS-coupled diketone was detected as a minor product.[34]

1.5.3. Furan-containing compounds inhibition of P450 leads to reduced toxicity

The furan ring-oxidized metabolite inhibits P450, allowing other molecules not to be oxidized. The overall toxicity of the compound is thus affected. For example, L-754,394 is a potent inhibitor of the HIV-1 encoded protease, so it is identified as an experimental anti-HIV agent. Then it is later identified as a P450 inhibitor.[35] However, inhibition of P450 may lead to drug-drug interactions, altered drug response, and delayed clearance of drugs, so it needs to be seriously considered especially when multiple drugs are used concurrently.

1.5.4. A reliable structure to avoid furan-containing compound being oxidized by P450 is underdeveloped

The bioactivity of furan-containing compounds has been acknowledged and explored in various medical chemistry domains. These compounds demonstrate an ability to engage with biological systems, modulating enzyme functions, receptor interactions, and various other cellular pathways. Such interactions have paved the way for potential drug candidates that could address a spectrum of medical conditions. However, with the promise of bioactivity comes the specter of toxicity. Furan's metabolic fate has been linked to the generation of reactive intermediates that could be detrimental to cellular health. These intermediates, formed particularly due to the oxidation of the furan ring, can interact with vital cellular components, including DNA, posing potential risks of mutagenicity and other related hazards. Given this double-edged nature of furan, a pressing question

emerges: How can we harness the therapeutic potential of furan while mitigating its associated risks? The answer, unfortunately, remains elusive. Although significant strides have been made in understanding the biological interactions of furan, a definitive strategy to optimize its bioactivity while curtailing its toxicity is yet to be established. It becomes evident that a deeper dive into the molecular intricacies of furan is paramount. Comprehensive studies, employing cutting-edge techniques in molecular biology, pharmacology, and toxicology, are needed to decipher the underpinnings of furan's behavior in biological systems. By doing so, the scientific community might find a roadmap to design furan-based compounds that deliver therapeutic benefits without compromising safety.

1.6. Furan-containing natural products

1.6.1. Furan as an important bioactive substructure

Due to various interaction possibilities provided by the furan ring, many furan-containing natural products have been identified as possessing therapeutic potential, demonstrating a variety of pharmacological properties that can be harnessed for medical applications. Such potentials include but are not limited to antimicrobial, anticancer, anti-inflammatory, and antiviral properties.

Furan derivatives have exhibited remarkable antimicrobial activities, effectively inhibiting the growth and proliferation of various bacterial and fungal pathogens.[36] This antimicrobial potential is particularly relevant in the current global scenario, where antibiotic resistance has emerged as a major public health concern. The unique structures of furan-containing compounds allow them to interact with bacterial and fungal cellular components, disrupting essential biological processes and ultimately leading to the death

of the pathogens. Several studies have reported the efficacy of furan derivatives against drug-resistant strains of bacteria, highlighting their potential as alternative therapeutic agents in the fight against antibiotic resistance.[37] 2,5-Bis(hydroxymethyl)furan is discovered in many bio-sources including the fungus *Phellinus linteus*.,[38] the ascomycete *Xylaria longipes*;[39] the phytopathogen fungus *Colletotrichum acutatum*,[40] and the marine-derived fungi *Paecilomyces sp*.[41] It shows antimicrobial activity against *methicillin-resistant Staphylococcus aureus* (MRSA).[42]

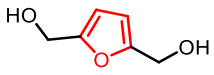

Figure 1.10. Furan-containing 2,5-Bis(hydroxymethyl)furan as an example for natural products with antimicrobial activity.

Furan-containing compounds have also demonstrated potent anticancer activities, making them attractive candidates for the development of novel anticancer agents. These compounds are known to interfere with various cellular processes that are crucial for cancer cell survival and proliferation, such as DNA replication, cell cycle progression, and apoptosis. Furthermore, furan derivatives have shown the ability to modulate the expression of specific genes involved in cancer development, thereby inhibiting the growth and spread of cancer cells. The anticancer potential of furan-containing natural products has been validated in numerous in vitro and in vivo studies, providing a strong foundation for their further development as anticancer agents.[43-44] 5.-(Hydroxymethyl)furan-2-carboxylic acid was extracted from the fungi *Aspergillus spp. Gibbererlla fujikuroi, Helminthosporium maydis and Pyricularia grisea.*[45] Other than

antimicrobial activities against *Bacillus subtilis* and *Staphylococcus aureus*,[46] it also shows antitumor activity.[45]

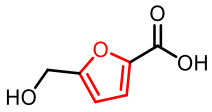

Figure 1.11. Furan-containing 5-(Hydroxymethyl)furan-2-carboxylic acid as an example for natural products with anticancer activity.

The anti-inflammatory properties of furan derivatives are another area of therapeutic interest. Inflammation is a complex biological response that plays a crucial role in various pathological conditions, including autoimmune diseases, allergies, and chronic inflammatory disorders. Furan-containing compounds have been shown to modulate the activity of various inflammatory mediators, such as cytokines and prostaglandins, thereby attenuating the inflammatory response. These anti-inflammatory effects make furan derivatives promising candidates for the development of novel anti-inflammatory agents that can be used in the treatment of various inflammatory disorders. Serfurosterone A is phytoecdysteroids isolated from the methanolic extract of the roots *of Serratula wolffii* (Asteraceae).[47] It is related to insect hormones. While these hormones primarily function in the insect realm, they have also garnered scientific interest because of their diverse biological effects on other organisms. Serfurosterone A shows anti-neuroinflammatory activity with inhibited 26.0% NO production.[48]

Furthermore, furan-containing natural products have exhibited antiviral activities against a range of viral pathogens. These compounds can interfere with various stages of the viral life cycle, including viral entry, replication, and assembly, thereby inhibiting the

infection, and spread of the virus. The antiviral potential of furan derivatives is of particular significance given the ongoing global efforts to combat viral infections, including emerging and re-emerging viral diseases. Mumefural was isolated from the fruit juice concentrate of *Prunus mume* (*Rosaceae*). Its activity against the pandemic influenza A(H1N1) virus was observed by Sriwilaijaroen *et al.*[49]

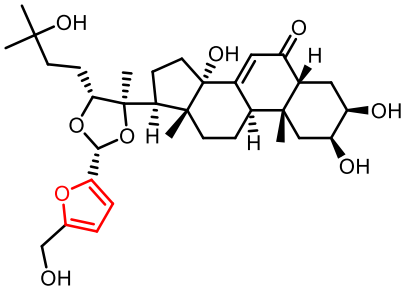

Figure 1.12. Furan-containing Serfurosterone A as an example for natural products with anti-inflammatory properties.

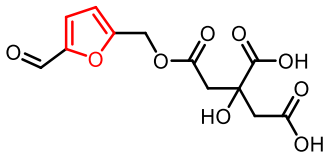

Figure 1.13. Furan containing Mumefural as an example for natural products with anti-viral properties.

Several furan derivatives have been studied for their potential analgesic (pain-relieving) effects. One of the mechanisms proposed for their analgesic activities is interactions with Opioid Receptors.[50-51] Salvinorin A (Sal A) is a diterpene lactone, devoid of any nitrogen atoms. Extracted primarily from the leaves of *Salvia divinorum*, a plant native to the isolated cloud forests of Mexico. The global scientific community's interest

in Sal A originates from its being different from other opioids. It is the first known opioid without nitrogen atoms, which revealed a new potential in pharmaceutical chemistry.

1.6.2. Furanoterpenoids as an important bioactive scaffold

Furanoterpenoids are a subclass of terpenoids that contain a furan ring within their molecular structure. Terpenoids are a large and diverse class of naturally occurring organic compounds derived from the five-carbon isoprene unit. Furan, on the other hand, is a heterocyclic compound consisting of a five-membered ring with four carbon atoms and one oxygen atom. The fusion of these two entities results in furanoterpenoids.

These compounds are particularly interesting because they combine the vast structural diversity of terpenoids with the unique reactivity of the furan ring. Found in various plants, marine organisms, and some fungi, furanoterpenoids have been the subject of extensive research due to their complex structures and promising biological activities.[52-55] Many furanoterpenoids exhibit a range of pharmacological effects, including anti-inflammatory, antibacterial, antifungal, and antitumor activities.[52]

The biosynthesis of furanoterpenoids typically begins with the formation of basic terpenoid skeletons through the isoprenoid pathway. Specific enzymes then introduce and modify the furan ring, leading to the plethora of furanoterpenoid structures found in nature. Given their potential therapeutic benefits, the chemical synthesis, biosynthesis, and biological evaluation of furanoterpenoids remain areas of active research in the field of natural product chemistry.

Salvinorin A (Sal A) is a non-nitrogenous diterpene extracted from the Mexican mint *Salvia divinorum*. Sal A has been reported to be a hallucinogen,[56] but its mechanism

of action was unclear for years until Roth et al. reported Sal A to be a selective κ opioid agonist.[50] Opioids are substances that bind to opioid receptors. Medically, some of them, such as morphine, oxycodone, buprenorphine, etc., are legally prescribed for pain relief. Opioids are classified as Mu (μ), delta (δ), and kappa (κ) opioids, corresponding to μ, δ, and κ opioid receptors, which are the three major opioid receptors in the brain.[57] Each type of opioid only activates the corresponding receptor. Activation of μ-opioid receptor by an agonist like morphine causes analgesia, sedation, and slightly reduced blood pressure with side effects including itching, nausea, euphoria, decreased respiration, and miosis. δ agonists cause stronger analgesic effects and fewer side effects than mu-opioid agonists. However, δ agonists are poor analgesics in acute pain, and they provide heavy potentiation to any mu agonism. κ agonists are strong analgesics like μ agonists but with fewer side effects on respiration and digestion systems. However, the side effects, including dysphoria and hallucinations, limit its usage clinically.[58] The discovery of Sal A being a κ agonist is striking because it was the first opioid agonist without nitrogen atoms in the molecule. Until this discovery, a positively charged nitrogen atom was considered essential to have a high affinity to opioid receptors.[59] This finding suggested the mechanism of action of Sal A was different from all known opioids at that time. Sal A was also the first natural product identified to be a selective κ opioid agonist. Research suggests that dysphoric effects of the kappa-opioid receptor (κOR) agonists result from the activation of p38 MAPK pathway. This pathway is separate from the G protein pathway, which causes a sedation effect. G protein-biased kappa agonists were hypothesized to have antipruritic effects with fewer side effects.

Riley et. al. synthesized fifty Sal A derivatives which have substitutions on the furan motif.[60] Most substitutions except one example decreased its activity and sterically less demanding substitutions are preferred. Suggesting its binding in a congested portion of the binding pocket.[60]

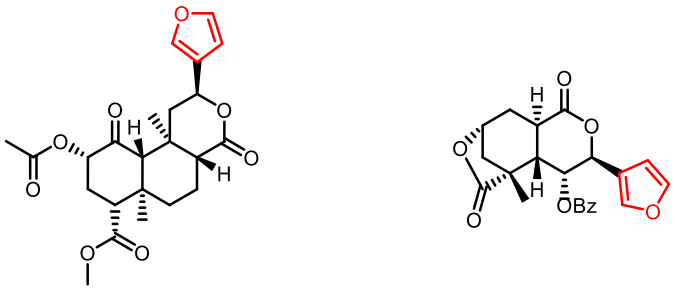

Figure 1.14. Sal A (left) and Collybolide(right) both belong to furanoterpenoids showing selectivity against κOR

Collybolide is a natural product isolated from the fungus *Collybia maculate*. The structure of collybolide contains a similar furyl-δ-lactone motif. Like Sal A, collybolide is identified as a selective κOR agonist.[51] It is a potential therapeutic drug targeting κOR, which may develop analgesic medicines without dysphoric effects.[51]

1.7. Synthesis of furan and its derivatives

The medical potential of furan-containing compounds has greatly influenced the landscape of synthetic chemistry. As the demand for furan derivatives in medicinal applications grows, so does the impetus for synthetic chemists to develop innovative, efficient, and green methodologies for their production. There are multiple developed methods to produce furan rings, including two name reactions: Paal-Knorr Synthesis and Feist-Benary Synthesis.[61-62] Recently, more efforts towards the development of metal-catalyzed furan cyclization reactions for furan synthesis.[63] However, some limitations still

exist, including compatibility with sensitive functional groups and a low variety of substituents. Therefore, further development of furan synthesis is required.[64]

1.7.1. Biosynthesis of furan

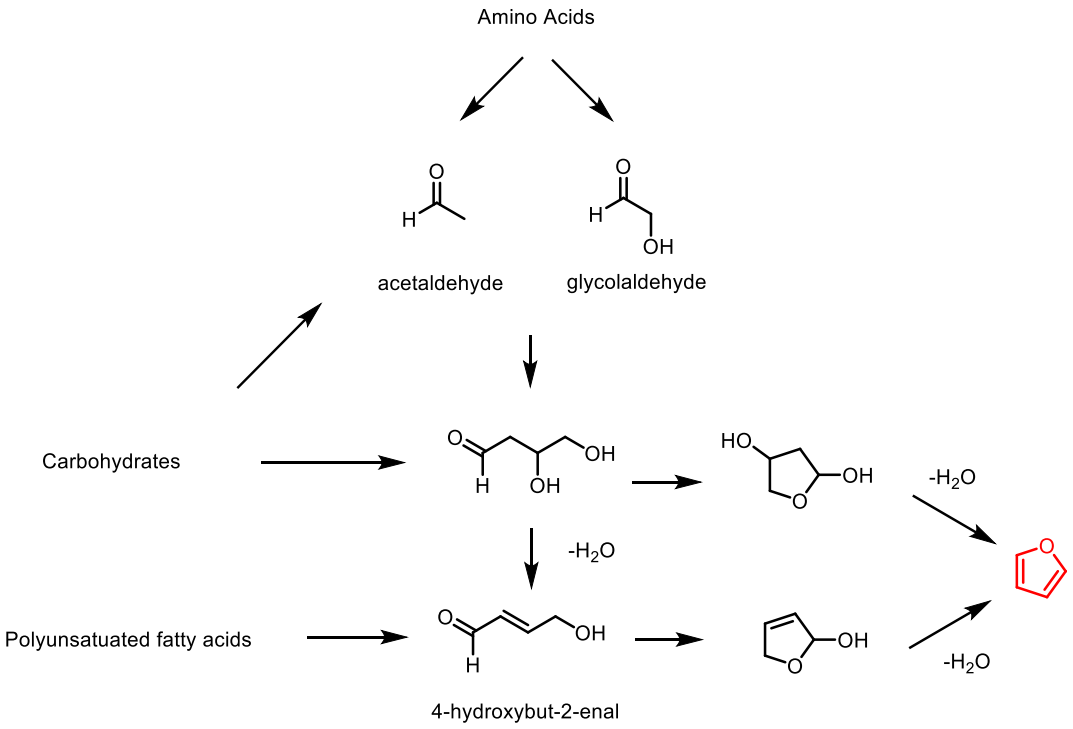

Figure 1.15. Proposed pathways of formation of furan from amino acids, carbohydrates, and poly-unsaturated fatty acids as three main groups of sources[65]

The formation of furan can be derived from various biological sources, primarily falling within three main categories: amino acids, carbohydrates, and polyunsaturated fatty acids.[65] Amino acids, which are the building blocks of proteins, can undergo a series of thermal or chemical reactions, leading to the breakdown and rearrangement of their carbon skeletons to form furan structures. Similarly, carbohydrates, which are organic molecules comprising carbon, hydrogen, and oxygen, can be subjected to dehydration and other chemical transformations to yield furans. The process typically involves the

dehydration of sugars, where furan forms as a result of the cyclic structure of some sugars and the release of water. On the other hand, polyunsaturated fatty acids, characterized by multiple double bonds in their carbon chain, can form furans through oxidative processes. The presence of multiple double bonds makes these fatty acids susceptible to oxidation, leading to complex reactions that can produce furan rings as intermediates or end products. The ability to generate furan from these diverse biological sources underscores its widespread occurrence and importance in various industrial and synthetic applications.[65]

1.7.2. Paal-Knorr synthesis

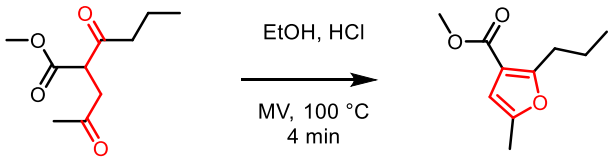

Figure 1.16. Microwave-assisted Paal-Knorr Synthesis of furan[66]

Paal-Knorr Synthesis is a traditional reaction to convert 1,4-diones into furans. The reaction condition was determined by Carl Paal and Ludwig Knorr.[67-68] The one carbonyl group in the molecule is protonated and then attacked by the other carbonyl group, forming the five-member ring. The furan ring is then formed via the elimination of the water molecule.[61] The hash condition of prolonged heating time together with strong Lewis acid (phosphorus (V) oxide, zinc chloride, etc) or Bronsted acid (sulfuric acid) was considered one of the major disadvantages of this reaction. Microwave has been applied to this reaction to improve the reaction.[66]

1.7.3. Feist-Benary synthesis

Feist-Benary Synthesis is another name reaction to produce substituted furans from α-halogen ketones and β-dicarbonyl compounds.[69] The first step of this reaction is condensation reaction as the diketone central carbon in β-dicarbonyl compounds attacks the carbonyl in β-dicarbonyl compounds. The five-member ring is formed by enol kicking out the halogen atom. This reaction provides a wide range of substituted furans due to the easy access to different α-halogen ketones and β-dicarbonyl compounds as starting materials. However, some α-halogen ketones give alkylation of diketone product instead.[70]

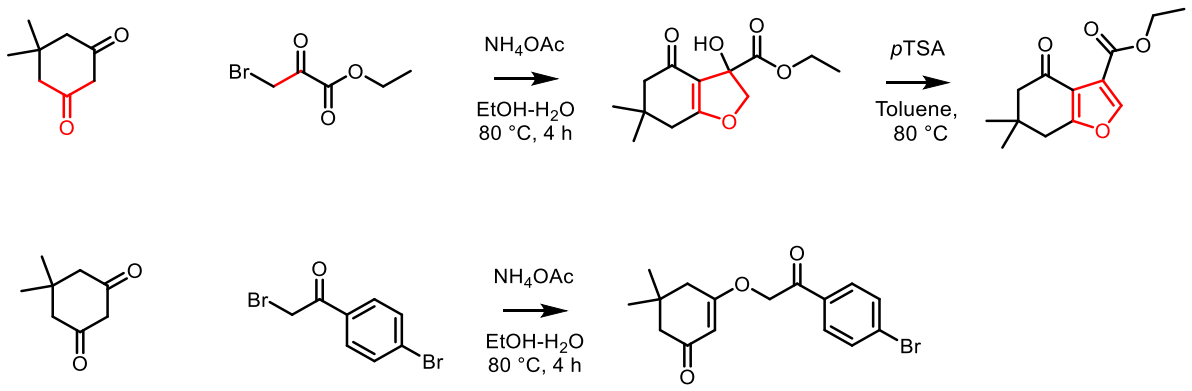

Figure 1.17. An example of Feist-Benary Synthesis and illustration of side reaction. [70]

1.7.4. Synthesis of multi-substituted furans *via* cyclization reactions

Most routes of multi-substituted furan synthesis involved cyclization reactions. Metal-catalyzed cycloisomerization reactions of unsaturated acyclic precursors usually only require mild conditions. This advantage makes them a favored approach in furan synthesis. Different metals like g Rh(I), Ag(I), Au(III), and Pd(0/II) can catalyze the cyclization of allenyl ketone[71], alcohol[72], and epoxide[73] into furans. However, alkynes are preferred due to their easier access over corresponding allenes. The research focus in

this area now is to expand the scope of suitable starting materials for these transformations and minimize the restrictions in functional substitution.[64]

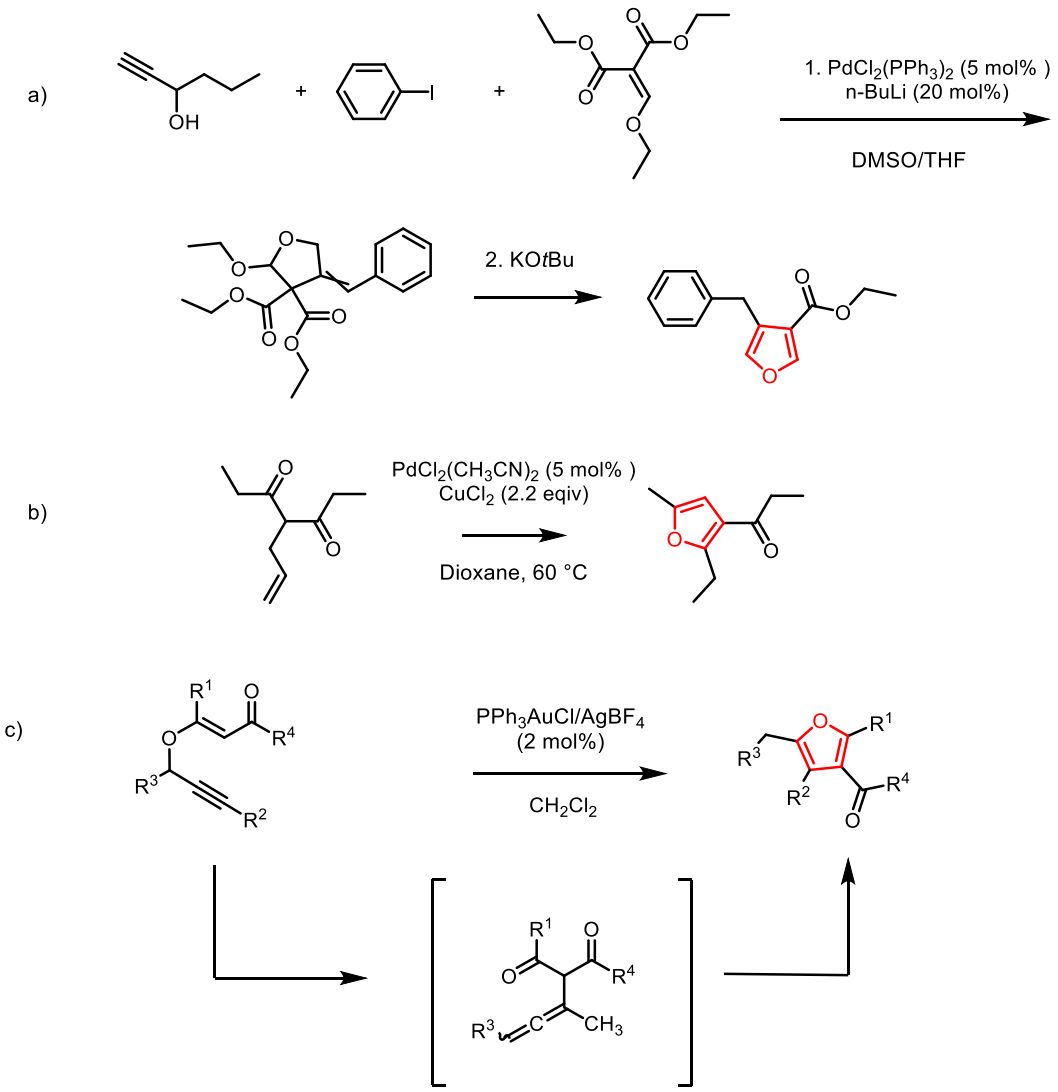

Figure 1.18. Different cyclization reactions were developed for furan synthesis.[74-76]

Many metal-catalyzed furan syntheses have been reported. A one-pot three-component system for C3-C4 disubstitution furans was developed by Garcon et al.[74] By using a Palladium catalyst, a two-step furan synthesis was accomplished from 3 simple and easily available starting materials. Widenhoefer et al. aimed to use alkenes instead

of alkynes and allenes to expand the scope of starting materials in this field.[75] They used $CuCl_2$ as an oxidant to compensate for the usage of alkenes instead of alkynes. Fair to good yield was achieved with limited substrate scope. A tetrasubstituted furans synthesis by a cascade reaction of a propargyl-Claisen rearrangement and hetero-cyclization was published by Kirsch et al. [76] They creatively used propargyl vinyl ethers as a precursor to generate -allenyl diketone intermediate in situ via [3,3]-sigmatropic rearrangement. A variety of substituted propargyl esters can be easily produced from corresponding propargyl alcohols. The electron-withdrawing group at the C-3 position was also not limited by esters but also ketones and amides. This makes this reaction possible for a wide range of multi-substituted furans. In addition, this reaction tolerates air and moisture. No e special precautions are needed to remove air and water from the reaction.

1.7.5. Formation of furan as a driving force to form carbene

During the literature search, enyn-als/-ones attracted my attention. enyn-als/-ones are organic compounds characterized by the presence of a triple bond (yne) and a double bond (ene) conjugated with either an aldehyde (-al) or a ketone (-one) functional group. In 1976, Ohloff and co-workers published their work where the zinc catalyst coordinates with a non-conjugated alkene-alkyne-ester to preform cyclopropanation via a zinc carbenoid. [77] Due to the low yield, such a zinc carbenoid approach was not utilized in organic synthesis. Inspired by this approach, a zinc(II) furylcarbeniod system was published by Vicente *et al*. in 2012.[78] In this work, a conjugated alkene-alkyne-ketone was formed in situ, leading to the formation of poly-substituted furan. The formation of a zinc(II) furylcarbeniod is proposed as the reactive intermediate. The computational study also

agreed with the formation of the zinc(II) furylcarbeniod. In this reaction, the formation of the furan ring is a driving force for cyclization and carbenoid formation.

1.7.6. Carbenes and carbenoids

Carbenes in organic chemistry refer to a neutral, divalent carbon species containing six electrons. Carbenes are classified as Fischer carbenes and Schrock carbenes, based on diffenrent electron configurations.[79] Fischer carbenes have an sp^2 hybridized carbon center with paired electrons filled in one of the sp^2 orbitals while the P orbital is empty. Fischer carbenes are also known as singlet carbenes because the antiparallel electron pair in the sp2 orbital results in *a singlet* state and a net spin of zero. Schrock carbenes are either sp2 or sp hybridized. The spins of the two unpaired electrons are parallel and have the same direction, occupying two different orbitals. This *triplet* state makes a net spin of one and paramagneticity. Therefore, Schrock carbenes are also called triplet carbenes. Fischer carbenes are generally more stable than Schrock carbenes, allowing better control of reactivity in organic synthesis.

Like carbenes, carbenoids can exist as Fischer-type or Schrock-type. The Fischer-type carbeniods are usually formed with metal centers at a low oxidation state, while Schrock-type carotenoids are usually formed with metal centers at a high oxidation state. Such a difference creates different reactivity in two carbeniods. Carbenes and carbeniods received close attention in organic synthesis due to their ambiphilic nature. Having a free p orbital and a free sp2 lone pairs, carbenes, and carbeniods have both electrophilic and nucleophilic reactivity. While ambiphilic synthons serve as valuable resources for accessing a variety of valuable scaffolds in organic synthesis, their full development is

still underway. Fischer carbenes exhibiting partial positive charge on carbon are initially electrophilic, which were utilized in this dissertation.

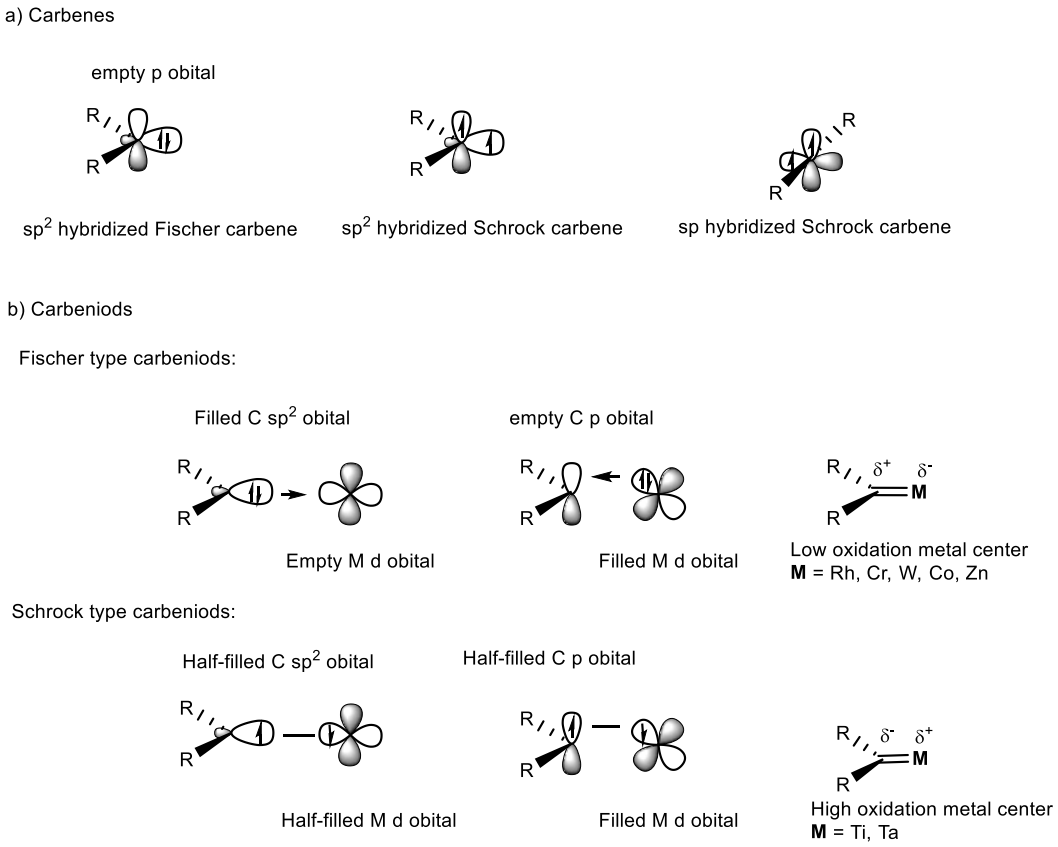

Figure. 1.19. Illustration of Fischer carbenes and Schrock carbenes and their corresponding carbeniods.

1.7.7. Diazo compounds as the most used carbene precurosors

Diazos is one of the most effective sources of carbenes and carbeniods. Two linked nitrogen atoms (azo, −N=N−) at the terminal position are called a diazo group. A charge-neutral organic compound with a carbon atom binding to a diazo group is called a diazo compound, or in short, a diazo. Diazos can generate carbenes or carbeniods under

thermal conditions, ultraviolet, or metal catalysts.[80] Over the past decades, diazo chemistry has been deeply studied. Diazo carbenes were widely used for many reactions in organic syntheses, such as cyclopropanation[81], X-H activation[82], and Wolff rearrangement[83]. The stability of diazo increases with the negative charge resonance being stabilized by the neighboring electron-withdrawing group.[84] Based on neighboring groups being electron withdrawing or donating, diazos can be classified as donor/donor (D/D), donor (D), donor/acceptor (D/A), acceptor (A), and acceptor/acceptor (A/A).[84] The stabiliy of diazos increases from D/D to A/A since the negative charge can delocolize to the neigbering groups. In general, A/A diazos are too stable that requries harsh reaction conditions, while D/D and D diazos are too sensitive to be utilized in the synthesis. D/A daizos showed hight utility because they produces more stable carbene intermediates than the traditional diazos, which allows high selectivity in asymmetric C-H activation, cyclopraoanation and other reactions.[85]

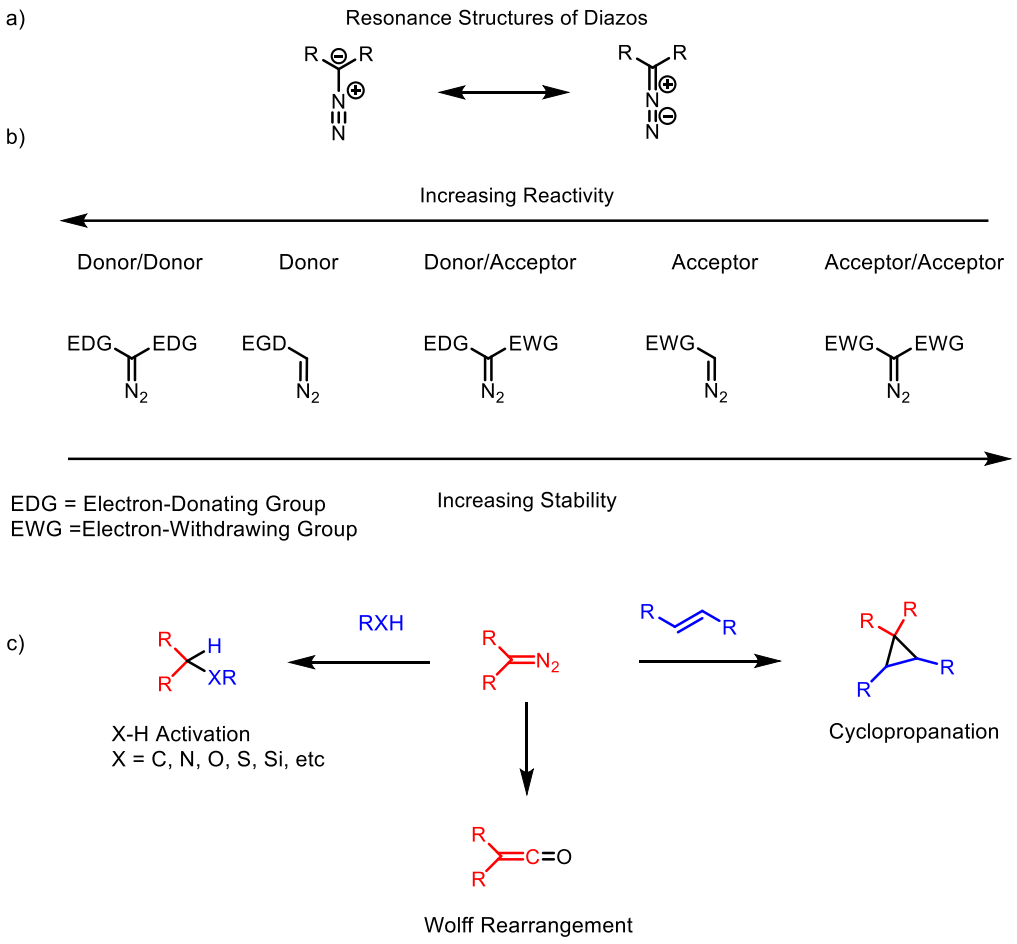

Figure. 1.20. Illustration of a) diazo resonance structure. b) Donnor/Acceptor clacification of diazos. c) Common diazo reactions.

During the last decades, diazo chemistry has been rapidly developed as a part of carbene chemistry.[79, 86] However, diazos are potential exposives, which limits their use.[87] On the other hand, enyn-als/-ones generate similar carbenionds as diazos.[87] They are benchtop stable and they do not generate N_2 gas during the reaction. These factors make enyn-als/-ones good substituents for diazos. After the discovery of enyn-als/-ones, much work has been done to utilize enyn-als/-ones as carbenoid precursors instead of diazos. As a result, Rhodium catalysts, which are most commonly used in diazo chemistry, are heavily used in enyn-als/-ones chemistry.[84-85] In addition, while enyn-als/-ones produce

similar carbeniods as diazos, no enyn-als/-ones cascade reaction was reported while many cascade reactions were reported with diazos.[88-92]

Metal carbenoid intermediates, notable for their ability to engage in a diverse array of unconventional reactions, pave the way for innovative synthetic strategies. These intermediates are efficiently generated through metal-catalyzed nitrogen extrusion from diazo compounds. Their reactivity intimately ties with the carbenoid structure, leading to their categorization into three principal groups: acceptor, acceptor/acceptor, and donor/acceptor (See **Figure 1.20**). Acceptor groups commonly include keto, nitro, cyano, phosphonyl, and sulfonyl, whereas vinyl, aryl, and heteroaryl typically serve as donor groups. Exhibiting predominantly electrophilic characteristics, the carbenes become more reactive and less selective with the presence of acceptor groups, while the opposite tends to be true with donor groups.[84] In the realm of total synthesis, carbenoids without a donor group are principally employed in intramolecular reactions. A burgeoning field in total synthesis involves the utilization of donor/acceptor-carbenoids due to their significantly enhanced selectivity compared to their conventional counterparts.[84]

1.7.8. The comparison between enyn-als/-ones vs diazos

While both enyn-als/-ones and diazos generate similar carbenoids, enyn-als/-ones do not generate nitrogen gas during the reaction or decomposition. In addition, enyn-als/-ones are benchtop stable without catalysis. Therefore, enyn-als/-ones are considered safer replacements for diazos.[87] Enyn-als/-ones also provide synthetic versatility. As mentioned earlier, D/D and D carbenoids are difficult to make through the diazo approach. However, they can be easily achieved by enyn-als/-ones, since one end of the carbenoids is newly formed furan and the other end is the terminal group of alkyne functionality which

can attach to both donor and acceptor groups. Enyn-als/-ones are proposed to generate similar carbene as diazos, and many reactions have been developed, such as X-H activation[93-96], and cyclopropanation[78]. However, cascade reactions are very rare with enyn-als/-ones. The only example of cascade reaction with enyn-als/-ones is developed by Hu *et al*.[97] Therefore, there is a huge potential of enyn-als/-ones to be developed. I hypothesized that there is a huge potential in enyn-als/-ones chemistry for cascade reaction capability. In addition, earth-abundant metal are hypothesized to replace rhodium as catalysts.

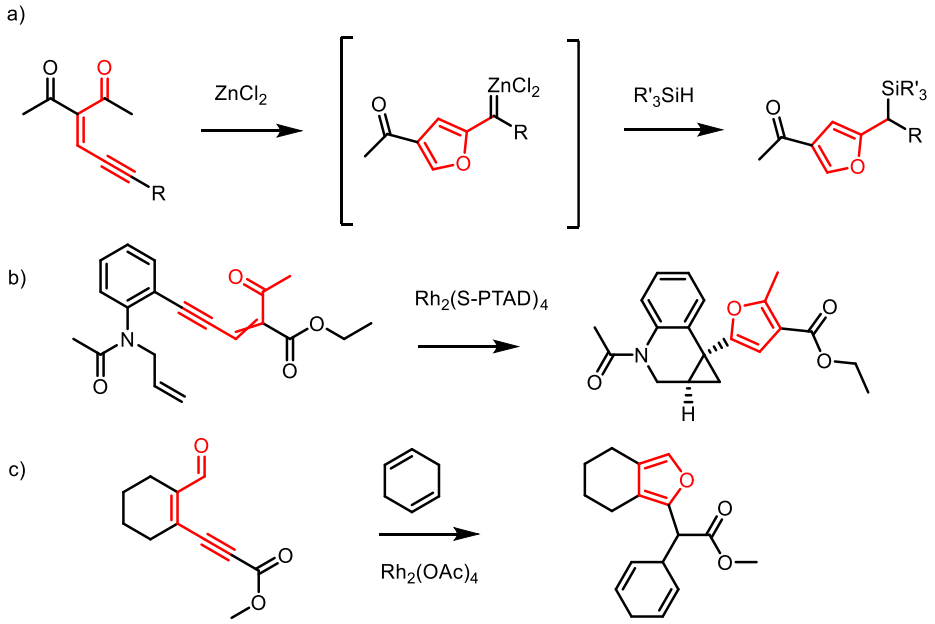

Figure 1.21. Enyn-als/-ones reactions a)Si-H activation,[78] b) Cyclopropanation,[81]c) C-H activation[93]

1.8. Synthesis furan-containing natural products

1.8.1. Total synthesis of ricciocarpin A

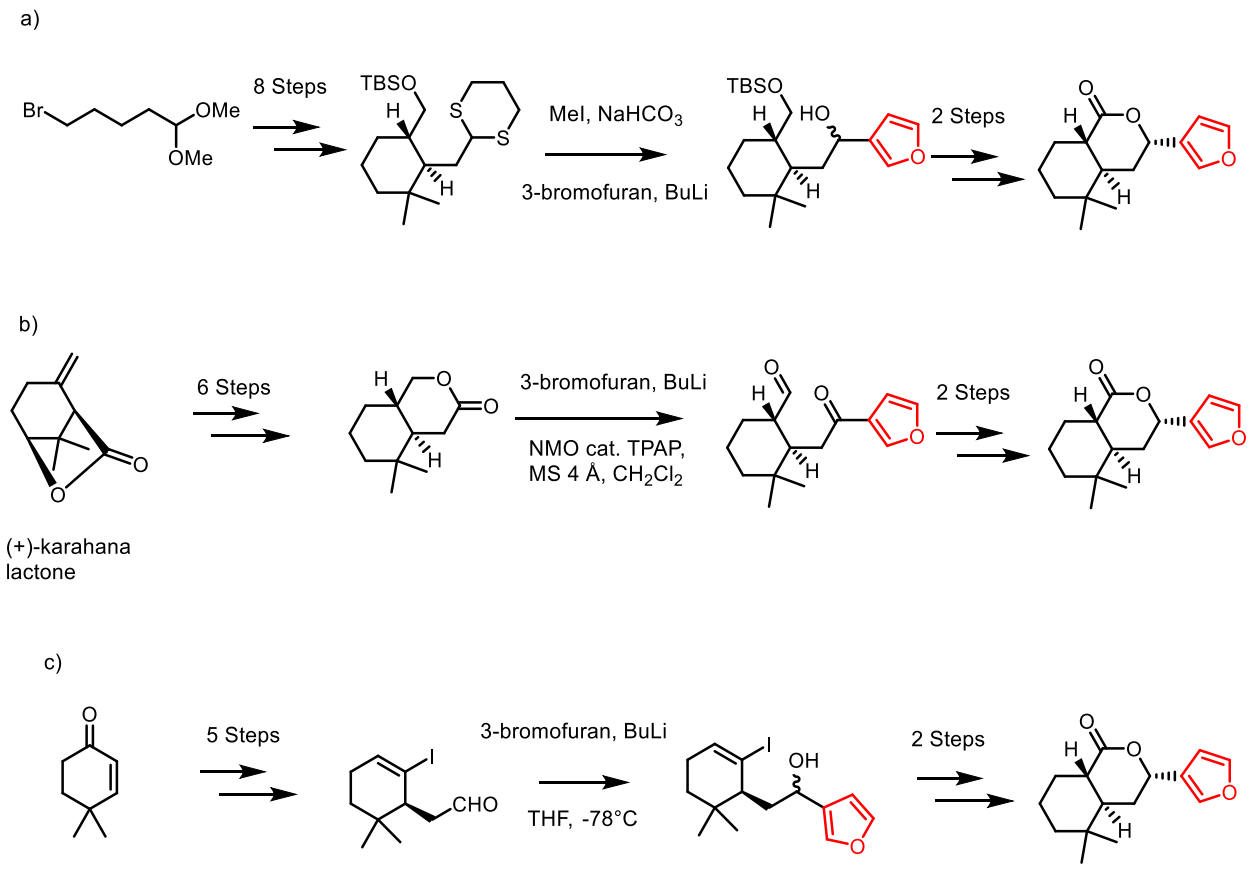

Figure 1.22. Total synthesis of Ricciocarpin A. Different synthetic routes developed by: a)Ihara e*t al*. [98] b) Palombo *et al*. [99] c) Jan *et al.* [100]

Ricciocarpin A was first isolated from the liverwort *Ricciocarpos natans*.[98] It has a high molluscicidal effect against the water snail *Biomphalaria glabrata*, one of the vectors of schistosomiasis *(bilharziasis).* Similar to antibiotics, molluscicides also face the problems of the development of resistance, toxicity to non-target organisms, and increasing cost of their synthesis.

Ricciocarpin A's interesting structure of a δ-lactone functionality connected with a 3-furyl group and bioactive usage attracted a lot of synthetic attention. The molluscicidal

study by Tiefensee *et al.*[101] suggests that the furan ring in the molecule plays an important role in its molluscicidal effect. Replacing the furan ring with a cardiac y-lactone visibly reduced IC50 from 11 ppm to 43 ppm. Its lactone scaffold may also be associated with its molluscicidal effect.[101] Different routes of its total synthesis have been developed.[98-100] While starting from different starting materials, a common trend can be found in those routes: the furan motif is fused into the molecule at a late stage. In addition, most of these routes relied on a nucleophilic attack of lithiated furan to aldehyde or ester. This requires basic sensitive groups to be protected so that the aldehyde or ester is the only reactive functional group with lithiated furan, thus putting a limit to the synthetic routes.

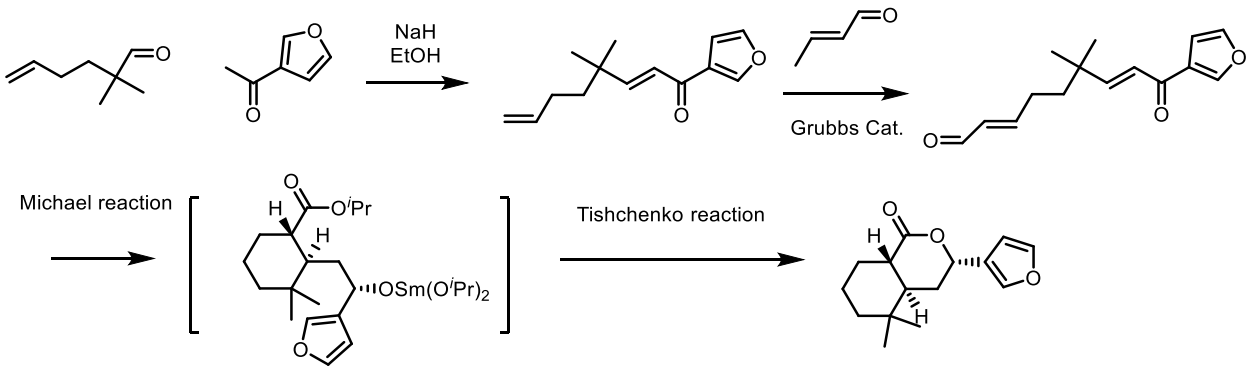

Figure 1.23. Total synthesis of Ricciocarpin A by Anna Michrowska and Benjamin List.[102]

Notably, Nobel prize winner Benjamin List also developed a synthetic route for Ricciocarpin A.[102] In this route, unlike other developed routes, this route installed furan at the beginning. The key reaction is a three-step cascade reaction. They managed to perform a sequence of reduction, Micheal addition and Tishchenko reaction in one-pot.[102] While it is generally believed that furan is a liability in natural product synthesis, this route

is a good example that installing furan into the molecule at an early stage allows more possibilities in total synthesis.

1.8.2. Metallation of furan

While different methods, including metal-catalyzed cyclization, have been developed for furan synthesis. In the synthetic field, the most common way to incorporate furan into the target molecule is the metallation of Furan.

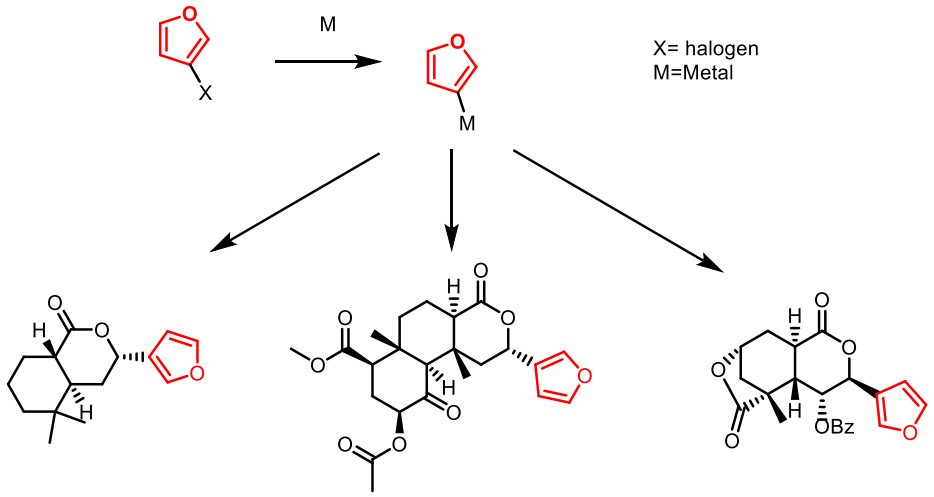

Figure 1.24. Metallation of Furan leads to the total synthesis of furan-containing natural products.

Furan undergoes a metal-induced activation process, where a metal atom, often from a strong base or a metal reagent, forms a bond with one of the carbons of the furan ring. This metallated furan intermediate can then act as a nucleophile or a building block, allowing chemists to introduce various substituents or even stitch the furan ring onto larger molecular frameworks.

Furan metallation stands out as a pivotal technique in the domain of organic synthesis, primarily due to its sheer versatility. This method grants chemists a passport to

a plethora of synthetic possibilities. When furan undergoes metallation, it can be further functionalized with a broad spectrum of electrophiles. This opens up avenues for creating an extensive array of derivatized furan compounds, catering to various applications and research purposes. Another significant advantage of this technique is its capacity for reactivity control. The choice of metals or specific conditions can determine the site of metallation on the furan ring. This element of control is crucial as it paves the way for regioselective functionalization, allowing chemists to precisely direct the subsequent reactions to a desired position on the furan molecule. Moreover, furan metallation has established itself as a strategic linchpin in synthetic routes.[103] The introduction of functional groups post-metallation can serve as key intermediates, setting the stage for subsequent transformative steps that might be challenging to achieve otherwise. Additionally, the efficiency of the method often shines through in many cases where the metallation of furan, followed by its reactions, can yield products in commendably high quantities. This efficiency not only streamlines the synthetic process but also makes it more economically viable in the long run.

While furan metallation boasts various benefits, it is not without its set of challenges and disadvantages. One of the primary concerns with this technique is its potential for undesired side reactions.[104] Given furan's sensitivity, especially when metalated, there's an inherent risk of over-reaction or unwanted transformations that can complicate the synthesis and decrease the yield of the desired product. The presence of metal residues post-metallation can also pose issues, especially if the final compound is intended for pharmaceutical or biologically active applications where purity is paramount. Regioselectivity, although a strength in some contexts, can also emerge as a double-

edged sword. Achieving consistent regioselectivity demands meticulous optimization of reaction conditions. This often requires an exhaustive investigation of different metals, ligands, and conditions, making the process time-consuming and resource-intensive. Furthermore, the requirement for specific, sometimes rare, or expensive metals and reagents can elevate the overall cost of synthesis. In large-scale industrial applications, these costs can become a significant concern. Lastly, metallation, especially when employing certain metals, might necessitate strict anhydrous and inert conditions to prevent degradation or unwanted reactions, adding another layer of complexity to the procedure.

Synthesis of furan-containing natural products has been achieved by different groups. However, keeping a furan moiety throughout the synthesis is still challenging. Several factors contribute to these challenges. For one, the furan ring is sensitive to a variety of conditions, including acids and certain oxidizing agents.[3, 105] This sensitivity can lead to unwanted side reactions during synthesis, especially when working with multifunctional molecules.[104] Additionally, the strategies for furan ring installation often require high precision, given that the furan moiety needs to be positioned accurately within the desired molecular architecture. The medical potential of furan-containing compounds has greatly influenced the landscape of synthetic chemistry.[103-104] As the demand for furan derivatives in medicinal applications grows, so does the impetus for synthetic chemists to develop innovative, efficient, and green methodologies for their production. The interplay between medicinal needs and synthetic capabilities drives the need for novel methodologies to emerge.

1.9. Specific aims

This thesis tried to address the issue that synthesizing furan containing bioactive compounds is still challenging. Developing novel methodologies for producing furan derivatives is required. Since both broad-spectrum synthesis and targeted synthesis can contribute to solving this issue, two specific aims were proposed. The first aim is to harvest the possibilities of the potential of enyn-als/-ones, utilizing them as a novel carbene precursor to perform cascade reactions as a broad-spectrum synthesis of furan-containing bioactive compounds. Detailed in **Chapter 2**, this aim leads to the development of a new methodology to synthesis of furyl-pyrrolidines with high diastereoselectivity under earth abundant zinc catalysis. The second aim is to develop targeted synthesis of furan derivatives and exploring the possibilities to develop a methodology to incorporate furan in the early stage of collybolide synthesis. In **Chapter 3**, intermediates were synthesized toward the total synthesis of furan-containing natural product collybolide and its analogues. Following my synthesis route, the bicyclic core of the molecule has been successfully achieved. The final intermediate achieved 15 out of 22 carbon atoms and 4 out of 6 stereo centers from collybolide.

1.10. REFERENCES FOR CHAPTER 1

1. Smith, M. B., *March's advanced organic chemistry: reactions, mechanisms, and structure*. John Wiley & Sons: 2020.

2. Boto, A.; Alvarez, L., Furan and its derivatives. *Heterocycl. Nat. Prod. Synth.* **2011**, 97-152.

3. Dean, F. M., Recent advances in furan chemistry. Part I. *Adv. Heterocycl. Chem.* **1982,** *30*, 167-238.

4. Liang, X.; Haynes, B. S.; Montoya, A., Acid-Catalyzed ring opening of furan in aqueous solution. *Energy Fuels* **2017,** *32* (4), 4139-4148.

5. Kappe, C. O.; Murphree, S. S.; Padwa, A., Synthetic applications of furan Diels-Alder chemistry. *Tetrahedron* **1997,** *53* (42), 14179-14233.

6. Peterson, L. A., Reactive metabolites in the biotransformation of molecules containing a furan ring. *Chem. Res. Toxicol.* **2013,** *26* (1), 6-25.

7. McOsker, C. C.; Fitzpatrick, P. M., Nitrofurantoin: mechanism of action and implications for resistance development in common uropathogens. *J. Antimicrob. Chemother.* **1994,** *33* (suppl_A), 23-30.

8. Burka, L. T.; Washburn, K. D.; Irwin, R. D., Disposition of [14C] furan in the male F344 rat. *J. Toxicol. Environ. Health A* **1991,** *34* (2), 245-257.

9. Ponto, L.; Schoenwald, R. D., Furosemide (frusemide). A pharmacokinetic/pharmacodynamic review (Part I). *Clin. Pharmacokinet.* **1990,** *18* (5), 381-408.

10. Krause, T.; Gerbershagen, M.; Fiege, M.; Weisshorn, R.; Wappler, F., Dantrolene–a review of its pharmacology, therapeutic use and new developments. *Anaesthesia* **2004,** *59* (4), 364-373.

11. McLeod, D. C.; Tartaglione, T. A.; Polk, R. E., Review of the New Second-Generation Cephalosporins: Cefonicid, Ceforanide, and Cefuroxime. *Drug Intell. Clin. Pharm.* **1985,** *19* (3), 188-198.

12. Wilson, J. N.; Liu, W.; Brown, A. S.; Landgraf, R., Binding-induced, turn-on fluorescence of the EGFR/ERBB kinase inhibitor, lapatinib. *Org. Biomol. Chem.* **2015,** *13* (17), 5006-5011.

13. Taylor, J.; Twomey, T.; Schach von Wittenau, M., The metabolic fate of prazosin. *Xenobiotica* **1977,** *7* (6), 357-364.

14. Munro, T. A.; Rizzacasa, M. A.; Roth, B. L.; Toth, B. A.; Yan, F., Studies toward the pharmacophore of salvinorin A, a potent κ opioid receptor agonist. *J. Med. Chem.* **2005,** *48* (2), 345-348.

15. Zuma, N. H.; Aucamp, J.; van Rensburg, H. D. J.; David, D. D., Synthesis and in vitro antileishmanial activity of alkylene-linked nitrofurantoin-triazole hybrids. *Eur. J. Med. Chem.* **2023,** *246*, 115012.

16. Sadlowski, C.; Park, B.; Borges, C. A.; Das, S.; Kerr, D. L.; He, M.; Han, H.; Riley, L.; Murthy, N., Nitro sulfonyl fluorides are a new pharmacophore for the development of antibiotics. *Mol. Syst. Des. Eng.* **2018,** *3* (4), 599-603.

17. World Health, O. *World Health Organization model list of essential medicines: 21st list 2019*; World Health Organization: Geneva, 2019, 2019.

18. Al-Jazairi, A. S.; Al-Ghamdi, M. A.; Al-Suhaibani, L. K.; Abu-Riash, T.; Assfoor, A. b.; Alsergani, H.; Alburaiki, J., The clinical and Practice Dilemma of Frequent Switching Among Generic Medications: Magnitude and Patient Safety Prospective. *Hosp. Pharm.* **2023**, 00185787231151858.

19. Kane, S. The Top 300 of 2020. https://clincalc.com/DrugStats/Top300Drugs.aspx. (accessed December 1).

20. Grayson, M. L.; Whitby, M., 88 Nitrofurans: Nitrofurazone, Furazolidone and Nitrofurantoin. *The Use of Antibiotics* **2010,** *1195*.

21. Kannigadu, C.; Aucamp, J.; N'Da, D. D., Synthesis and in vitro antileishmanial efficacy of benzyl analogues of nifuroxazide. *Drug Dev. Res.* **2021,** *82* (2), 287-295.

22. Wilkinson, S. R.; Taylor, M. C.; Horn, D.; Kelly, J. M.; Cheeseman, I., A mechanism for cross-resistance to nifurtimox and benznidazole in trypanosomes. *Proc. Natl. Acad. Sci.* **2008,** *105* (13), 5022-5027.

23. Gene-Expression Signatures may Influence Future Treatment Options for Breast Cancer. *Womens Health* **2010,** *6* (2), 171-173.

24. Fischer, J.; Ganellin, C. R., Analogue-based drug discovery. *Chemistry International--Newsmagazine for IUPAC* **2010,** *32* (4), 12-15.

25. Kane, S. Cefuroxime. https://clincalc.com/DrugStats/Drugs/Cefuroxime. (accessed December 1).

26. Root, R. K.; Waldvogel, F.; Corey, L.; Stamm, W. E., *Clinical infectious diseases: a practical approach*. Oxford University Press, USA: 1999.

27. Graham, R. M.; Pettinger, W. A., Prazosin. *N. Engl. J. Med.* **1979,** *300* (5), 232-236.

28. Kung, S.; Espinel, Z.; Lapid, M. I. In *Treatment of nightmares with prazosin: a systematic review*, Mayo Clin. Proc., Elsevier: 2012; pp 890-900.

29. Bolognesi, M. L.; Budriesi, R.; Chiarini, A.; Poggesi, E.; Leonardi, A.; Melchiorre, C., Design, synthesis, and biological activity of prazosin-related antagonists. Role of the piperazine and furan units of prazosin on the selectivity for α1-adrenoreceptor subtypes. *J. Med. Chem.* **1998,** *41* (24), 4844-4853.

30. Bakhiya, N.; Appel, K. E., Toxicity and carcinogenicity of furan in human diet. *Arch. Toxicol.* **2010,** *84*, 563-578.

31. Dowd, F. J.; Johnson, B.; Mariotti, A., *Pharmacology and therapeutics for dentistry-E-book*. Elsevier Health Sciences: 2016.

32. Medina-Lopez, J. R.; Dominguez-Reyes, A.; Hurtado, M., Comparison of Generic Furosemide Products by In Vitro Release Studies using USP Apparatus 2 and 4. *Dissolution Technol.* **2021,** *28* (1), 14-23.

33. Nakahama, H.; Miwa, Y.; Yamaji, A.; Orita, Y.; Fukuhara, Y.; Yanase, M.; Kamada, T.; Sonoda, T.; Ishibasi, M.; Ichikawa, Y., The urinary excretion of frusemide and its metabolites by kidney transplant patients. *Eur. J. Clin. Pharmacol.* **1987,** *32*, 313-315.

34. Erve, J. C. L.; Vashishtha, S. C.; Ojewoye, O.; Adedoyin, A.; Espina, R.; DeMaio, W.; Talaat, R. E., Metabolism of prazosin in rat and characterization of metabolites in plasma, urine, faeces, brain and bile using liquid chromatography/mass spectrometry (LC/MS). *Xenobiotica* **2008,** *38* (5), 540-558.

35. Sahali-Sahly, Y.; Balani, S. K.; Lin, J. H.; Baillie, T. A., In vitro studies on the metabolic activation of the furanopyridine L-754,394, a highly potent and selective

mechanism-based inhibitor of cytochrome P450 3A4. *Chem. Res. Toxicol.* **1996,** *9* (6), 1007-1012.

36. Saeid, H.; Al-sayed, H.; Bader, M., A Review on Biological and Medicinal Significance of Furan. *Alq J Med App Sci.* **2023,** *6* (1), 44-58.

37. Alizadeh, M.; Jalal, M.; Hamed, K.; Saber, A.; Kheirouri, S.; Pourteymour Fard Tabrizi, F.; Kamari, N., Recent updates on anti-inflammatory and antimicrobial effects of furan natural derivatives. *J. Inflammation Res.* **2020**, 451-463.

38. Song, K.; Cho, S.; Ko, K.; Han, M.; Yoo, I. D., Secondary metabolites from the mycelial culture broth of Phellinus linteus. *Appl. Biol. Chem.* **1994,** *37* (2), 100-104.

39. Schneider, G.; Anke, H.; Sterner, O., Xylaramide, a new antifungal compound, and other secondary metabolites from Xylaria longipes. *Zeitschrift Für Naturforschung C* **1996,** *51* (11-12), 802-806.

40. Mancilla, G.; Jimenez-Teja, D.; Femenia-Rios, M.; Macias-Sanchez, A. J.; Collado, I. G.; Hernandez-Galan, R., Novel macrolide from wild strains of the phytopathogen fungus Colletotrichum acutatum. *Nat. Prod. Commun.* **2009,** *4* (3), 1934578X0900400316.

41. Mosadeghzad, Z.; Zuriati, Z.; Asmat, A.; Gires, U.; Wickneswari, R.; Pittayakhajonwut, P.; Farahani, G., Chemical components and bioactivity of the marine-derived fungus Paecilomyces sp. collected from Tinggi Island, Malaysia. *Chem. Nat. Compd.* **2013,** *49*, 621-625.

42. Romashov, L. V.; Kucherov, F. A.; Kozlov, K. S.; Ananikov, V. P., Bio-Derived Furanic Compounds with Natural Metabolism: New Sustainable Possibilities for Selective Organic Synthesis. *Int. J. Mol. Sci.* **2023,** *24* (4), 3997.

43. Lu, D.; Zhou, Y.; Li, Q.; Luo, J.; Jiang, Q.; He, B.; Tang, Q., Synthesis, in vitro antitumor activity and molecular mechanism of novel furan derivatives and their precursors. *Anticancer Agents Med. Chem.* **2020,** *20* (12), 1475-1486.

44. Altowyan, M. S.; Soliman, S. M.; Haukka, M.; Al-Shaalan, N. H.; Alkharboush, A. A.; Barakat, A., Synthesis, characterization, and cytotoxicity of new spirooxindoles engrafted furan structural motif as a potential anticancer agent. *ACS omega* **2022,** *7* (40), 35743-35754.

45. Munekata, M.; Tamura, G., Antitumor activity of 5-hydroxymethyl-2-furoic acid. *Agric. Biol. Chem.* **1981,** *45* (9), 2149-2150.

46. Jadulco, R.; Proksch, P.; Wray, V.; Sudarsono; Berg, A.; Gräfe, U., New Macrolides and Furan Carboxylic Acid Derivative from the Sponge-Derived Fungus Cladosporium herbarum. *J. Nat. Prod.* **2001,** *64* (4), 527-530.

47. Liktor-Busa, E.; Simon, A.; Toth, G.; Bathori, M., The first two ecdysteroids containing a furan ring from Serratula wolffii. *Tetrahedron Lett.* **2008,** *49* (11), 1738-1740.

48. Li, J.; Zeng, K.-W.; Shi, S.-P.; Jiang, Y.; Tu, P.-F., Anti-neuroinflammatory constituents from Polygala tricornis Gagnep. *Fitoterapia* **2012,** *83* (5), 896-900.

49. Sriwilaijaroen, N.; Kadowaki, A.; Onishi, Y.; Gato, N.; Ujike, M.; Odagiri, T.; Tashiro, M.; Suzuki, Y., Mumefural and related HMF derivatives from Japanese apricot fruit juice concentrate show multiple inhibitory effects on pandemic influenza A (H1N1) virus. *Food Chem.* **2011,** *127* (1), 1-9.

50. Roth, B. L.; Baner, K.; Westkaemper, R.; Siebert, D.; Rice, K. C.; Steinberg, S.; Ernsberger, P.; Rothman, R. B., Salvinorin A: A potent naturally occurring nonnitrogenous κ opioid selective agonist. *Proc. Natl. Acad. Sci.* **2002,** *99* (18), 11934-11939.

51. Gupta, A.; Gomes, I.; Bobeck, E. N.; Fakira, A. K.; Massaro, N. P.; Sharma, I.; Cavé, A.; Hamm, H. E.; Parello, J.; Devi, L. A., Collybolide is a novel biased agonist of κ-opioid receptors with potent antipruritic activity. *Proc. Natl. Acad. Sci.* **2016,** *113* (21), 6041-6046.

52. Li, H.; Peng, Y.; Zheng, J., Metabolic activation and toxicities of furanoterpenoids. In *Advances in Molecular Toxicology*, Elsevier: 2016; Vol. 10, pp 55-97.

53. Abdjul, D. B.; Yamazaki, H.; Kanno, S.-i.; Wewengkang, D. S.; Rotinsulu, H.; Sumilat, D. A.; Ukai, K.; Kapojos, M. M.; Namikoshi, M., Furanoterpenes, new types of protein tyrosine phosphatase 1B inhibitors, from two Indonesian marine sponges, Ircinia and Spongia spp. *Bioorg. Med. Chem. Lett.* **2017,** *27* (5), 1159-1161.

54. Hyodo, H.; Uritani, I.; Akai, S., Production of Furano-terpenoids and other Compounds in Sweet Potato Root Tissue in Response to Infection by various Isolates of Ceratocystis fimbriata. *J. Phytopathol.* **1969,** *65* (4), 332-340.

55. Chakraborty, K.; Thilakan, B.; Raola, V. K., Antimicrobial polyketide furanoterpenoids from seaweed-associated heterotrophic bacterium Bacillus subtilis MTCC 10403. *Phytochemistry* **2017,** *142*, 112-125.

56. Valdés, L. J., Salvia divinorum and the unique diterpene hallucinogen, Salvinorin (divinorin) A. *J. Psychoactive Drugs* **1994,** *26* (3), 277-283.

57. Stein, C., Opioid receptors. *Annu. Rev. Med.* **2016,** *67*, 433-451.

58. Pradhan, A. A.; Smith, M. L.; Kieffer, B. L.; Evans, C. J., Ligand-directed signalling within the opioid receptor family. *Br. J. Pharmacol.* **2012,** *167* (5), 960-969.

59. Prisinzano, T. E., Neoclerodanes as Atypical Opioid Receptor Ligands. *J. Med. Chem.* **2013,** *56* (9), 3435-3443.

60. Riley, A. P.; Groer, C. E.; Young, D.; Ewald, A. W.; Kivell, B. M.; Prisinzano, T. E., Synthesis and κ-Opioid Receptor Activity of Furan-Substituted Salvinorin A Analogues. *J. Med. Chem.* **2014,** *57* (24), 10464-10475.

61. Amarnath, V.; Amarnath, K., Intermediates in the Paal-Knorr Synthesis of Furans. *J. Org. Chem.* **1995,** *60* (2), 301-307.

62. Bansal, R. K., *Heterocyclic chemistry*. New Age International: 2020.

63. Moran, W. J.; Rodríguez, A., Metal-catalyzed furan synthesis. A review. *Org. Prep. Proced. Int.* **2012,** *44* (2), 103-130.

64. Kirsch, S. F., Syntheses of polysubstituted furans: recent developments. *Org. Biomol. Chem.* **2006,** *4* (11), 2076-2080.

65. Vranová, J.; Ciesarová, Z., Furan in Food - a Review. *Czech J. Food Sci.* **2009,** *27* (1), 1-10.

66. Minetto, G.; Raveglia, L. F.; Sega, A.; Taddei, M., Microwave-Assisted Paal–Knorr Reaction – Three-Step Regiocontrolled Synthesis of Polysubstituted Furans, Pyrroles and Thiophenes. *Eur. J. Org. Chem.* **2005,** *2005* (24), 5277-5288.

67. Paal, C., Ueber die Derivate des Acetophenonacetessigesters und des Acetonylacetessigesters. *Berichte der deutschen chemischen Gesellschaft* **1884,** *17* (2), 2756-2767.

68. Knorr, L., Synthese von Furfuranderivaten aus dem Diacetbernsteinsäureester. *Berichte der deutschen chemischen Gesellschaft* **1884,** *17* (2), 2863-2870.

69. Feist, F., Studien in der Furan-und Pyrrol-Gruppe. *Berichte der deutschen chemischen Gesellschaft* **1902,** *35* (2), 1537-1544.

70. Ghazvini, M.; Shahvelayati, A. S.; Sabri, A.; Nasrabadi, F. Z., Synthesis of furan and dihydrofuran derivatives via Feist–Benary reaction in the presence of ammonium acetate in aqueous ethanol. *Chemistry of Heterocyclic Compounds* **2016,** *52*, 161-164.

71. Sniady, A.; Wheeler, K. A.; Dembinski, R., 5-Endo-D ig Electrophilic Cyclization of 1, 4-Disubstituted But-3-yn-1-ones: Regiocontrolled Synthesis of 2, 5-Disubstituted 3-Bromo-and 3-Iodofurans. *Org. Lett.* **2005,** *7* (9), 1769-1772.

72. Gabriele, B.; Salerno, G.; Lauria, E., A general and facile synthesis of substituted furans by palladium-catalyzed cycloisomerization of (Z)-2-en-4-yn-1-ols. *J. Org. Chem.* **1999,** *64* (21), 7687-7692.

73. Hashmi, A. S. K.; Sinha, P., Gold catalysis: mild conditions for the transformation of alkynyl epoxides to furans. *Advanced Synthesis & Catalysis* **2004,** *346* (4), 432-438.

74. Garçon, S.; Vassiliou, S.; Cavicchioli, M.; Hartmann, B.; Monteiro, N.; Balme, G., An effective one-pot synthesis of 3-benzylfurans and their potential utility as versatile precursors of 3, 4-dibenzyltetrahydrofuran lignans. Formal synthesis of (±)-burseran. *J. Org. Chem.* **2001,** *66* (11), 4069-4073.

75. Han, X.; Widenhoefer, R. A., Palladium-catalyzed oxidative alkoxylation of α-alkenyl β-diketones to form functionalized furans. *J. Org. Chem.* **2004,** *69* (5), 1738-1740.

76. Suhre, M. H.; Reif, M.; Kirsch, S. F., Gold (I)-catalyzed synthesis of highly substituted furans. *Org. Lett.* **2005,** *7* (18), 3925-3927.

77. Strickler, H.; Davis, J. B.; Ohloff, G., Zur cyclisierung von dehydrolinalylacetat in gegenwart von zinkchlorid. *Helvetica Chimica Acta* **1976,** *59* (4), 1328-1332.

78. Vicente, R.; González, J.; Riesgo, L.; González, J.; López, L. A., Catalytic Generation of Zinc Carbenes from Alkynes: Zinc-Catalyzed Cyclopropanation and Si H Bond Insertion Reactions. *Angew. Chem.* **2012,** *124* (32), 8187-8191.

79. Kirmse, W., *Carbene chemistry*. Elsevier: 2013; Vol. 1.

80. Regitz, M., *Diazo compounds: properties and synthesis*. Elsevier: 2012.

81. Zhu, D.; Chen, L.; Zhang, H.; Ma, Z.; Jiang, H.; Zhu, S., Highly Chemo- and Stereoselective Catalyst-Controlled Allylic C−H Insertion and Cyclopropanation Using Donor/Donor Carbenes. *Angew. Chem. Int. Ed.* **2018,** *57* (38), 12405-12409.

82. Xiang, Y.; Wang, C.; Ding, Q.; Peng, Y., Diazo Compounds: Versatile Synthons for the Synthesis of Nitrogen Heterocycles via Transition Metal-Catalyzed Cascade C–H Activation/Carbene Insertion/Annulation Reactions. *Advanced Synthesis & Catalysis* **2019,** *361* (5), 919-944.

83. Meier, H.; Zeller, K. P., The Wolff rearrangement of α-diazo carbonyl compounds. *Angew. Chem. Int. Ed.* **1975,** *14* (1), 32-43.

84. Davies, H. M.; Denton, J. R., Application of donor/acceptor-carbenoids to the synthesis of natural products. *Chem. Soc. Rev.* **2009,** *38* (11), 3061-3071.

85. Davies, H. M.; Walji, A. M., Rhodium (II)-stabilized carbenoids containing both donor and acceptor substituents. *Modern Rhodium-Catalyzed Organic Reactions* **2005**, 301-340.

86. Arduengo, A. J.; Bertrand, G., Carbenes introduction. ACS Publications: 2009; Vol. 109, pp 3209-3210.

87. Ma, J.; Zhang, L.; Zhu, S., Enynal/enynone: a safe and practical carbenoid precursor. *Curr. Org. Chem.* **2016,** *20* (1), 102-118.

88. Nicolle, S. M.; Lewis, W.; Hayes, C. J.; Moody, C. J., Stereoselective Synthesis of Functionalized Pyrrolidines by the Diverted N− H Insertion Reaction of Metallocarbenes with β-Aminoketone Derivatives. *Angew. Chem. Int. Ed.* **2016,** *55* (11), 3749-3753.

89. Jing, C. C.; Xing, D.; Gao, L. X.; Li, J.; Hu, W. H., Divergent Synthesis of Multisubstituted Tetrahydrofurans and Pyrrolidines via Intramolecular Aldol-type Trapping of Onium Ylide Intermediates. *Chem-Eur J* **2015,** *21* (52), 19202-19207.

90. Liu, K.; Zhu, C.; Min, J.; Peng, S.; Xu, G.; Sun, J., Stereodivergent Synthesis of N-Heterocycles by Catalyst-Controlled, Activity-Directed Tandem Annulation of Diazo Compounds with Amino Alkynes. *Angew. Chem. Int. Ed.* **2015,** *54* (44), 12962-12967.

91. Chinthapally, K.; Massaro, N. P.; Ton, S.; Gardner, E. D.; Sharma, I., Trapping rhodium vinylcarbenoids with aminochalcones for the synthesis of medium-sized azacycles. *Tetrahedron Lett.* **2019,** *60* (46), 151253.

92. Hunter, A. C.; Almutwalli, B.; Bain, A. I.; Sharma, I., Trapping rhodium carbenoids with aminoalkynes for the synthesis of diverse N-heterocycles. *Tetrahedron* **2018,** *74* (38), 5451-5457.

93. Miki, K.; Kato, Y.; Uemura, S.; Ohe, K., Catalytic Nucleophilic Addition Reaction to (2-Furyl) carbene Intermediates Generated from Carbonyl–Ene–Ynes. *Bull. Chem. Soc. Jpn.* **2008,** *81* (9), 1158-1165.

94. González, J.; González, J.; Pérez-Calleja, C.; López, L. A.; Vicente, R., Zinc-Catalyzed Synthesis of Functionalized Furans and Triarylmethanes from Enynones and Alcohols or Azoles: Dual X H Bond Activation by Zinc. *Angew. Chem. Int. Ed.* **2013,** *52* (22), 5853-5857.

95. Wu, W.; Chen, Y.; Li, M.; Hu, W.; Lin, X., Access to Polysubstituted (Furyl) methylthioethers via a Base-Promoted SH Insertion Reaction of Conjugated Enynones. *J. Org. Chem.* **2019,** *84* (22), 14529-14539.

96. Tseberlidis, G.; Caselli, A.; Vicente, R., Carbene XH bond insertions catalyzed by copper (I) macrocyclic pyridine-containing ligand (PcL) complexes. *J. Organomet. Chem.* **2017,** *835*, 1-5.

97. Hong, K.; Shu, J.; Dong, S.; Zhang, Z.; He, Y.; Liu, M.; Huang, J.; Hu, W.; Xu, X., Asymmetric Three-Component Reaction of Enynal with Alcohol and Imine as An Expeditious Track to Afford Chiral α-Furyl-β-amino Carboxylate Derivatives. *ACS Catal.* **2022,** *12* (22), 14185-14193.

98. Ihara, M.; Suzuki, S.; Taniguchi, N.; Fukumoto, K., Deconjugation of α, β-unsaturated esters and an intramolecular Michael reaction of bis-α, β-unsaturated esters with trialkylsilyl trifluoromethanesulfonate in the presence of tertiary amine: synthesis of (±)-ricciocarpin A. *J. Chem. Soc., Perkin Trans. 1* **1993,** (19), 2251-2258.

99. Palombo, E.; Audran, G.; Monti, H., Enantioselective synthesis of (+)-ricciocarpin A using an auxiliary hydroxyl group and a diastereofacial selectivity based methodology. *Synlett* **2005,** *2005* (13), 2104-2106.

100. Jan, N.-W.; Liu, H.-J., An enantioselective total synthesis of (+)-ricciocarpin A. *Org. Lett.* **2006,** *8* (1), 151-153.

101. Wurzel, G.; Becker, H.; Eicher, T.; Tiefensee, K., Molluscicidal properties of constituents from the liverwort Ricciocarpos natans and of synthetic lunularic acid derivatives. *Planta Med.* **1990,** *56* (05), 444-445.

102. Michrowska, A.; List, B., Concise synthesis of ricciocarpin A and discovery of a more potent analogue. *Nat. Chem.* **2009,** *1* (3), 225-228.

103. Majumdar, K. C.; Chattopadhyay, S. K., *Heterocycles in natural product synthesis*. John Wiley & Sons: 2011.

104. Raczko, J.; Jurczak, J., Furan in the synthesis of natural products. *Stud. Nat. Prod. Chem.* **1995,** *16*, 639-685.

105. Makarov, A. S.; Uchuskin, M. G.; Trushkov, I. V., Furan oxidation reactions in the total synthesis of natural products. *Synthesis* **2018,** *50* (16), 3059-3086.

CHAPTER 2

The Synthesis of 2-Furyl-pyrrolidines as a Furan-Containing Libraries

2.1. Introduction

Our research group has been working on diazo carbenoids for years. Enyn-als/-ones provide a new approach to carbenoids with the advantage of no gas generation compared with diazos. In addition, enyn-als/-ones generate furan moiety in the product molecule. This brought the idea of using enyn-als/-ones as novel carbenoid precursors for synthesizing furan-containing compounds.

2.2. Enyn-als/-ones

Enyn-als/-ones are newly developed. In 1995, Nakatani *et al.* reported the formation of furyl alcohol from enynone under photoirradiation at 366 nm in water.[1] Later, they tested different alcohols and confirmed the generation of carbene as the intermediate.[2] In 2002, the furyl metal carbenes were isolated by Uemura *et al.* using enynone starting materials.[3] To generate the metal carbenes, three equivalent of metals were used. Later, cyclopropanation of such carbene was achieved with 5 mol% chromium catalysts by the same group in 2004.[4] In the same study, rhodium acetate was discovered

as a better catalyst than chromium for this reaction. In 2008, C-H,N-H, S-H, O-H and Si-H insertion were achieved by the same group under rhodium catalysis.[5]

In 2012, Vicente et *al.* published the generation of a zinc carbene using enynal approch.[6] The computational study suggests that zinc carbene is more stable than zinc carbeniod in this case. Compared with pervious literature known zinc carebenes or carbenoids, their method was the first catalitic zinc method. They applied this zinc carbene to Si-H insertion and cycloadddtion. Later, they also applied this zinc carbene to N-H and O-H insertion.[7]

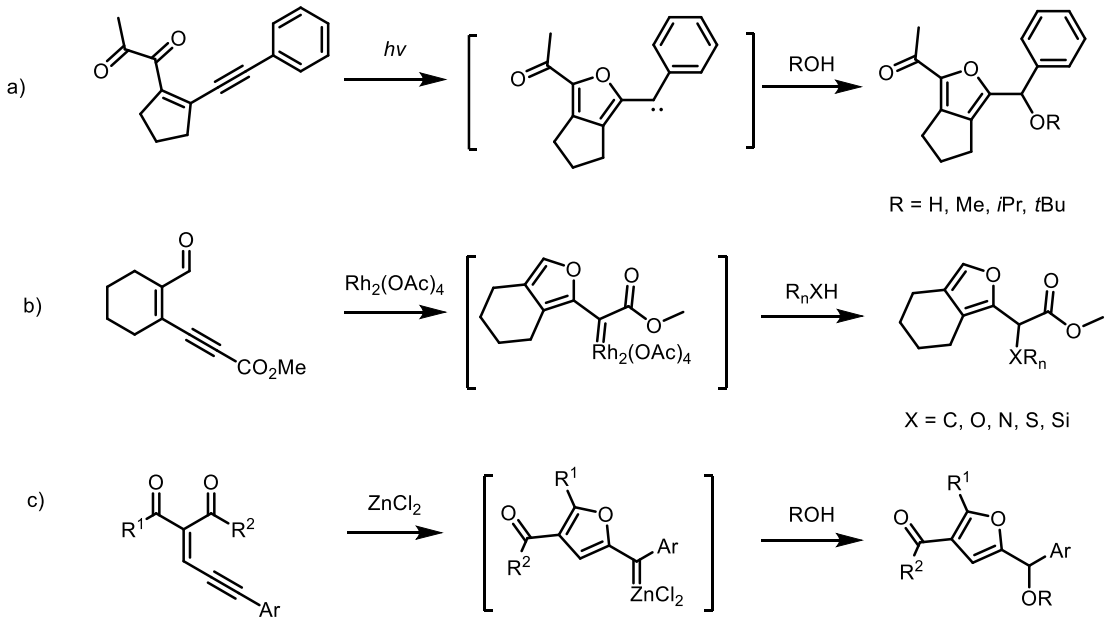

Figure 2.1. Enyn-als/-ones generates carbenes or metal carbenes under different conditions[1, 5, 7]

There is mechanistic similarity between the formation of carbeniodes from diazos and enynones. As mentioned in previous chapters, the driving force of enyn-als/-ones generating carbene is the formation of furan rings. The mechanism is illustrated in the

scheme. The lone pair electrons on oxygen attack the alkyne, pushing alkyne electrons to form a carbon-zinc bond. The d electrons on zinc back push the electron to quench the positive charge on oxygen, forming the furan moiety and carbeniod simultaneously. In the case of diazos, the electron on carbon will first bond to metal catalysts, then the d electrons on rhodium back push the electron to kick out nitrogen gas, forming carbeniods.

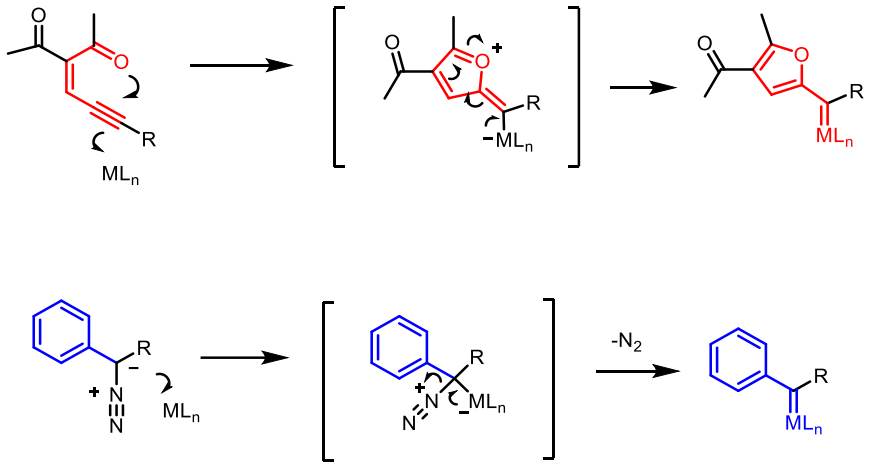

Figure 2.2. Similar carbenes formed from enynone precursor and diazo precursor where both carbenes have an adjacent aromatic ring

The structure of enynal derived carbenes and diazo derived carbenes are highly similar to each other (**Figure 2.2.**). On the other hand, without a diazo substructure, the enynals/enynones are bench-top stable without catalysts. The formation of furan substructure instead of nitrogen gas also provides much less risk in storing the carbeniod precursors. Therefore, enynals and enyones are considered as a safer replacement of diazos. However, during the literature search before the initiation of the project, it was noticed that no cascade reaction was developed with enyn-als/-ones, while many examples of cascade with diazos.[8-12]

2.3. Cascade reaction

Cascade reactions, also known as domino or tandem reactions, represent a fascinating and efficient approach in the realm of organic synthesis.[13] These processes involve multiple bond-forming transformations that occur sequentially in a single reaction flask without the need for isolating intermediate compounds. This characteristic offers a myriad of advantages, such as enhanced atom economy, reduced waste, shorter reaction times, and often, increased yields. By streamlining multiple steps into one pot, cascade reactions can be both economically and environmentally beneficial, reducing the consumption of reagents, solvents, and energy. The inherent beauty of cascade reactions lies in their ability to rapidly build molecular complexity from simple starting materials, making them invaluable tools for constructing intricate molecules, including natural products and drug candidates. Over the years, the strategic design and execution of cascade reactions have emerged as a pinnacle of creativity and efficiency in modern synthetic chemistry.

2.3.1. Diazo carbene O-H insertion/aldol reaction cascade

Diazo carbenes have been used to develop cascade reactions for functionalized tetrahydrofuran synthesis. Functionalized tetrahydrofurans (THFs) hold significant importance in organic chemistry, particularly in the synthesis of natural products and pharmaceuticals. Their unique structural and chemical properties make them versatile intermediates in various synthetic pathways. Functionalized tetrahydrofurans are integral to various fields of chemistry, from natural product synthesis to drug development and materials science. Their structural diversity and the ability to undergo a wide range of chemical transformations make them invaluable tools in the chemist's repertoire. The

ongoing research and development in the functionalization of THFs continue to open new possibilities in science and technology.

In 2009, Hu *et al*. reported a one-pot cascade method to synthesize fully substituted tetrahydrofurans, utilizing aryldiazoacetates and allyl alcohols.[14] In this process, the Rh-catalyzed decomposition of diazoacetates combined with secondary alcohols leads to an O-H insertion product, characterized by outstanding diastereoselectivity. This is followed by an intramolecular Michael-type addition, culminating in the formation of the targeted tetrahydrofurans with exceptional stereoselective control.

Suga *et al.* reported three-component reactions involving aromatic aldehydes, α-alkyl-α-diazo esters, and 2-alkenoic acid derivatives in 2013.[15] These reaction are conducted in the presence of metal salts such as $Ni(BF_4)_2 \cdot 6H_2O$ and $Co(BF_4)_2 \cdot 6H_2O$. These metal salts not only selectively facilitate the cycloadditions with olefinic dipolarophiles but also significantly enhance the diastereoselectivities of the reactions. Additionally, when using (S)-3-(2-alkenoyl)-4-isopropyl-2-oxazolidinones as dipolarophiles in the synthesis of chiral tetrahydrofuran derivatives, these salts induce an unexpected form of diastereoselective asymmetric induction. This outcome is particularly notable as it deviates from typical expectations of Lewis acid-catalyzed cycloadditions involving bidentate-type dipolarophiles.

Moody et al. also published cascade reactions for the synthesis of highly substituted tetrahydrofurans in 2015.[16] These reactions of diazocarbonyl compounds with β-hydroxyketones, catalyzed by either copper or rhodium, result in the formation of highly substituted tetrahydrofurans exhibiting excellent diastereoselectivity. This efficient single-

step process initially proceeds as a carbene O-H insertion reaction, followed by an intramolecular aldol reaction under mild conditions, demonstrating a unique pathway of synthesis.

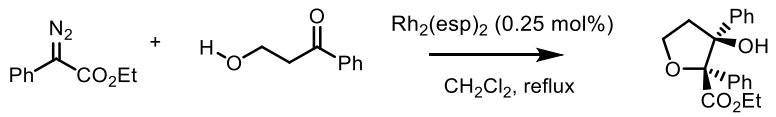

Figure 2.3. Diazo carbene O-H insertion/aldol reaction cascade developed by Moody *et al*.[16]

2.3.2. Diazo carbene N-H insertion/aldol reaction cascade

Diazo carbenes have been used to develop cascade reactions for pyrrolidine synthesis. Pyrrolidine has the structure of a five-member heterocyclic ring containing four carbon atoms and one nitrogen atom. Pyrrolidine is a common substructure in many alkaloids and other bioactive natural products.[8] Examples include the following: Broussonetinine A is a natural alkaloid that is found in the plant *Broussonetia kazinoki*.[17] It is a strong inhibitor of α- and β-glucosidase, β-galactosidase and α- and β-mannosidase.[17] Another example, lepadiformine, was isolated from the ascidian *Clavelina lepadiformis*.[18] It has been found to exhibit cytotoxic and antiproliferative effects against various cancer cell lines.[18]

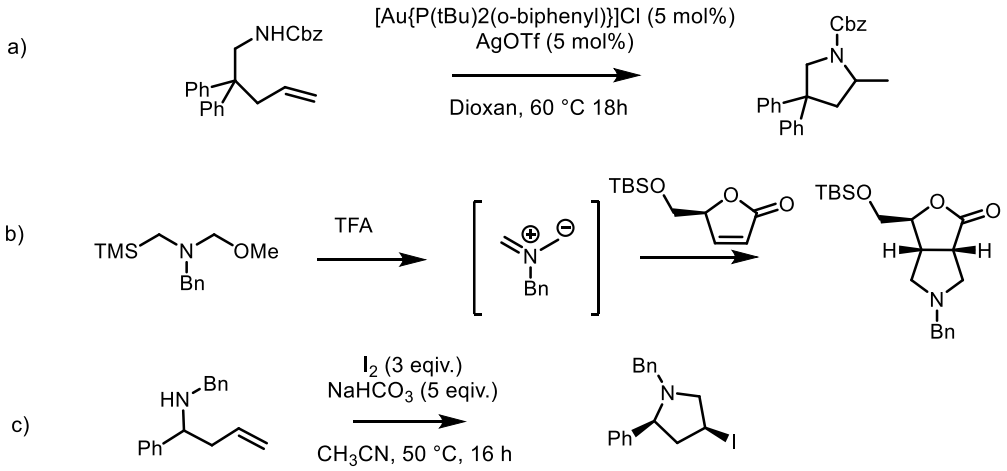

Figure 2.4. Different non-diazo approaches to pyrrolidine synthesis.[19-21]

Due to its abundance in pharmaceuticals, agrochemicals, and other organic compounds, great efforts have been devoted to developing different methodologies for multi-substituted and asymmetric pyrrolidines. Many routes have been developed for synthesizing pyrrolidines and proline derivatives. Hydroamination[19], azomethine ylide cycloaddition[20], iodocyclisation[21], etc., can lead to pyrrolidine synthesis. Recently, diazo approaches to pyrrolidines have been investigated by different researchers **(Figure 2.3.).**

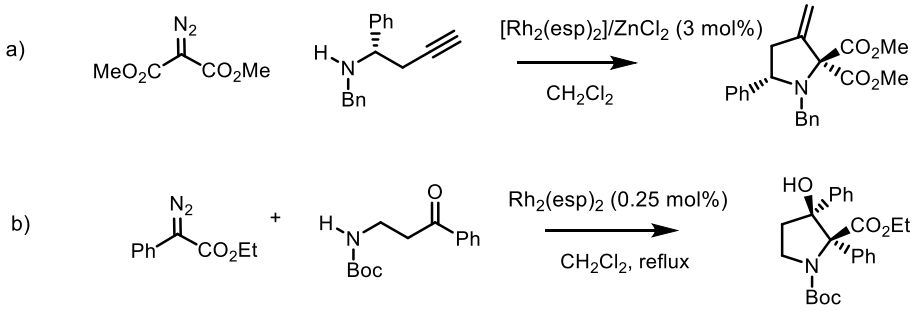

Figure 2.5. Different diazo approaches to pyrrolidine synthesis.[8]

Hu *et al*. have innovated a three-component reaction involving diazo compounds, anilines, and 4-oxo-enoates in 2013,[22] achieving variability in the reaction pathway by

manipulating the order of substrate addition. This method can follow one of two routes: either an aza-Michael addition followed by ylide formation and intramolecular aldol addition to produce pyrrolidines, or an initial ylide formation leading to a Michael addition, resulting in the formation of linear α-amino ester derivatives. Aza-Michael addition pathway yielded diverse, polyfunctional pyrrolidines with high diastereoselectivity and good overall yields.

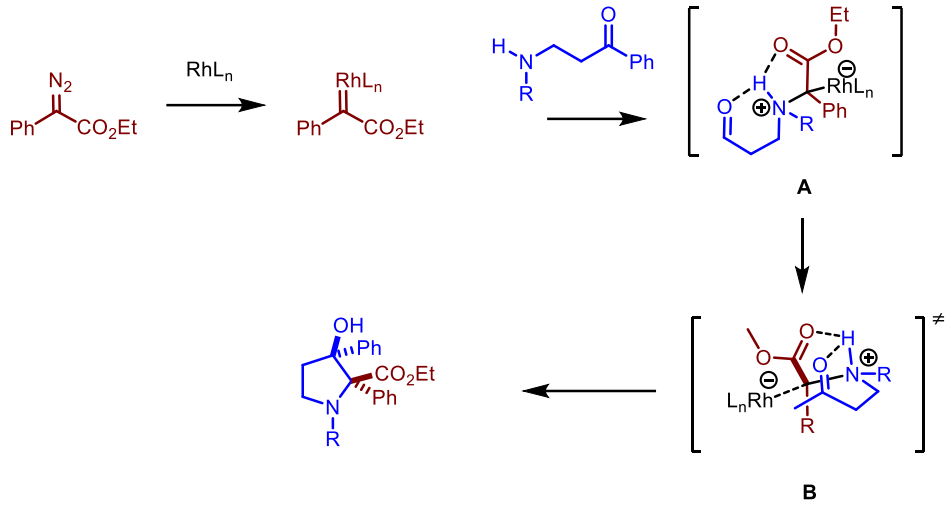

Figure 2.6. Proposed mechanism of diazo approach to pyrrolidine developed by Moody *et al.*[8]

A new approach for synthesizing five-membered N-heterocycles has been established by Sun et al. in 2015,[23] which captures intermediates generated in situ. This method includes a copper-catalyzed process, where annulation is achieved through the formation of allenoates followed by an intramolecular hydroamination. Additionally, a rhodium-catalyzed pathway is utilized, characterized by the insertion of a carbenoid into the N-H bond, leading to a subsequent Conia-ene cyclization.

The Moody group reported a system that consists of N-H insertion to donor/acceptor (D/A) diazos, followed by an aldol reaction.[8] Their proposed mechanism is shown in **Figure 2.6**. They used phenyl-ester diazos which are D/A diazos as carbene precursors. Then the lone pair of the nitrogen atom is inserted into the empty orbitals of carbene, forming the insertion product **A**. Then a five-member-ring intermediate **B** leads to the aldol reaction which generates the final products. They claimed that the hydrogen bond between N-hydrogen and two oxygens is the source of diastereoselectivity. This route provides a new possibility to synthesize functionalized pyrrolidines with high atomic economy.

2.3.3. Selection of the enynal for the novel cascade reaction

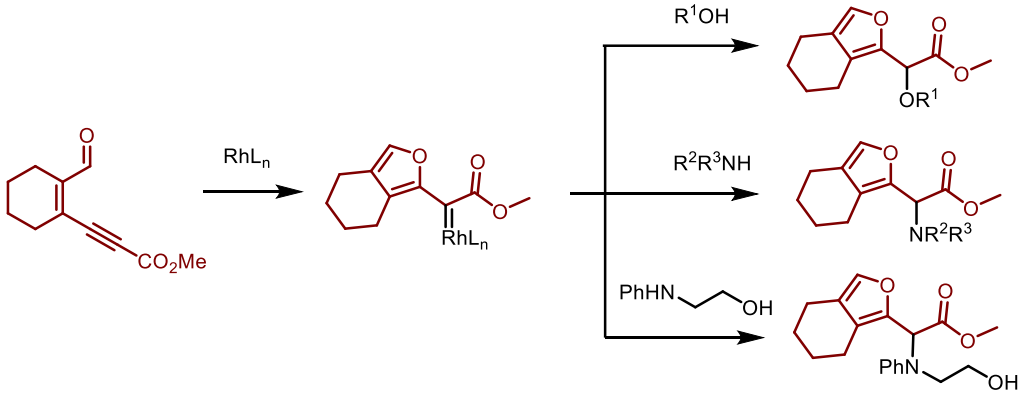

Figure 2.7. The N-H insertion of fury carbene developed by the Ohe group.[5]

In 2008, the Ohe group published X-H activation of enynal initiated furyl careben.[5] In this research, a cyclic enynal was used to perform O-H and N-H insertion after the formation of furyl carbene. They also find the selectivity of such carbene favors nitrogen over oxygen. When both nitrogen and oxygen were both available, only nitrogen was instered.[5] This furyl carbene is a typical D/A carbene where furan group is the doner and

ester group is the acceptor. Since the O-H and N-H insertion were known, this enynal was selected to be a template for the hypothetic enynal cascade reaction.

2.4. Hypothesis

So far, the enynal approach has been utilized for X-H functionalization and cyclopropanation. However, unlike diazos having many examples of cascade reactions[8, 24], cascade reactions using enynals/enynones are still underdeveloped. The first cascade reaction with enynal is developed by the Hu group.[25] Therefore, I hypothesized that the following reaction as an enynal cascade(**Figure 2.8.**). In addition, different metals were reported to catalyze enynal reactions, such as zinc, copper, and iron. I hypothesized that rhodium could be replaced in this reaction. These metals will be tested for the generation of target molecules.

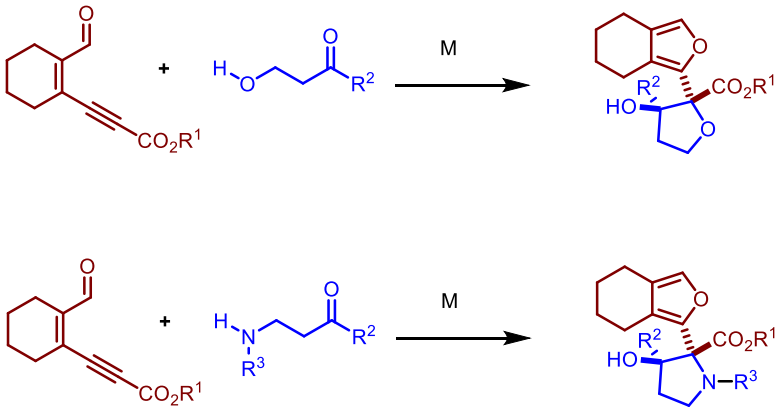

Figure 2.8. Hypothetic enynal cascade reaction to generate functionalized tetrahydrofurans and pyrrolidines

2.5. Synthesis of enynal 1a

To test our hypothesis, we designed the reaction between enynal **1a** and aminoketone **2a**. The synthesis of **1a** followed a reported route[26] (**Figure 2.9.**). Initially,

Cyclohexanone **4** was treated with tribromophosphine and DMF for a Vilsmeier–Haack type reaction. A bromo-aldehyde **5** was generated with a 51% yield. The reaction mechanism involves the formation of the Iminium ion **4**. After the enol form of cyclohexanone was added to the Iminium ion, the enol was reacted with tribromo phosphene to make alcohol into a leaving group ($OPBr_2$). This leaving group is eventually replaced by bromine to yield bromo-aldehyde **5.** The reaction mechanism is shown in **Figure 2.10**.

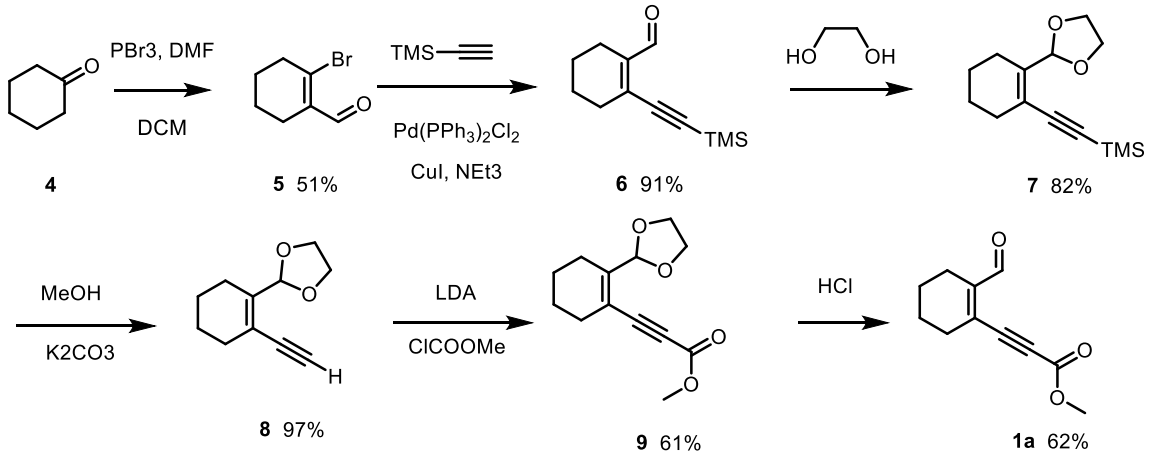

Figure 2.9. Synthesis of enynal **1a** following the reported procedure[26]

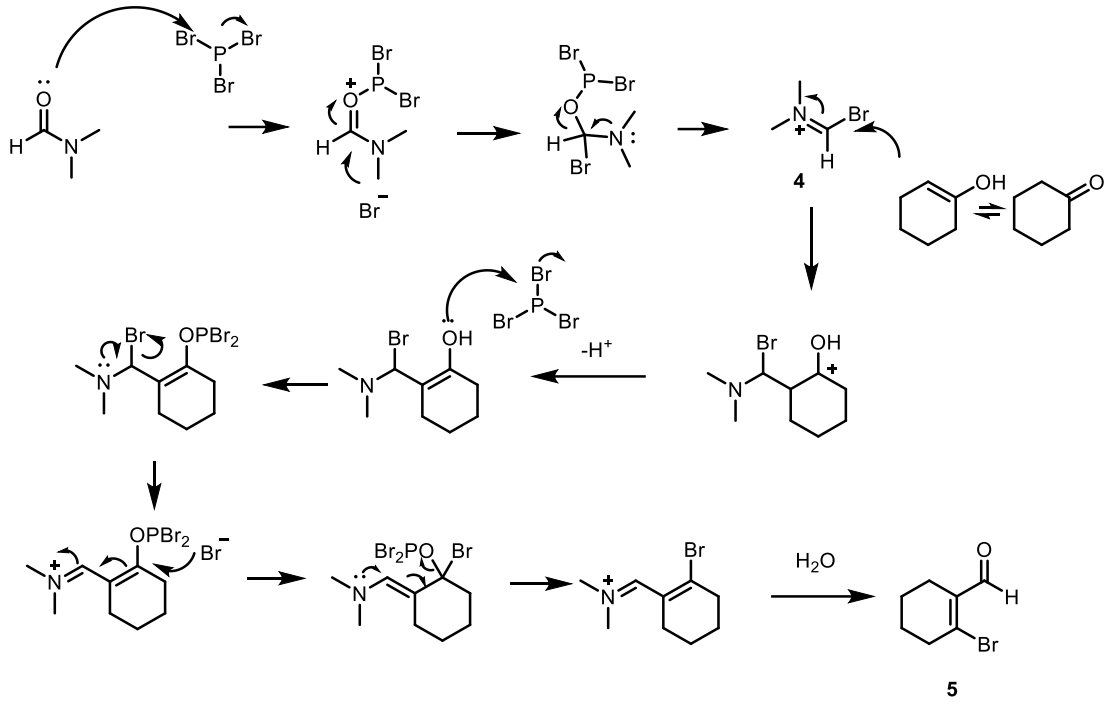

Figure 2.10. Proposed mechanism for the generation of **5** from cyclohexanone.

Later, the bromoaldehyde **5** underwent a Sonogashira coupling to couple with the TMS alkyne. The TMS group increased the boiling point of alkyne to keep it in the liquid form at 60 °C. The Sonogashira coupling is a highly regarded and widely used organic reaction in synthetic chemistry,[27-28] offering an efficient route to form carbon-carbon bonds between terminal alkynes and aryl or vinyl halides. Pioneered by Kenkichi Sonogashira, Yoshihiko Tohda, and Nobue Hagihara in the late 1970s,[29] this cross-coupling reaction utilizes a palladium catalyst in combination with a copper co-catalyst and an amine base to facilitate the bond formation[29] (**Figure 2.11.**). Due to its versatility and reliability, the Sonogashira coupling has been instrumental in the synthesis of complex molecules, natural products, pharmaceuticals, and materials, especially in the realm of conjugated polymers and organic electronic devices. The reaction's ability to form carbon-carbon

bonds under relatively mild conditions and with a broad substrate scope has positioned it as an invaluable tool in modern organic synthesis.

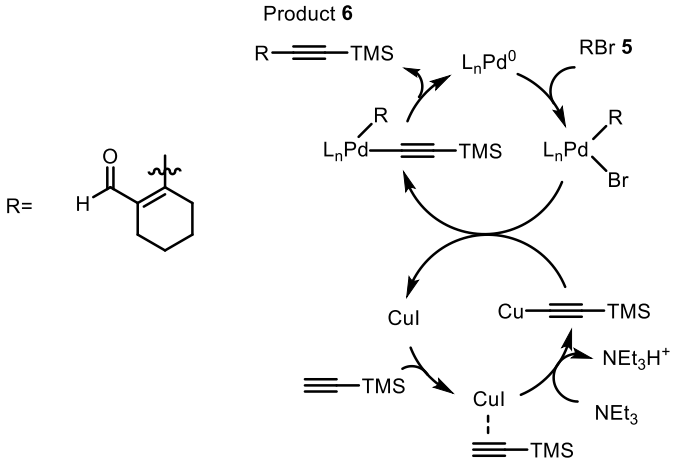

Figure 2.11. Proposed mechanism for the generation of **6** via Sonogashira coupling

Then the aldehyde was protected with ethane glycol to form acetal **7**, followed by deprotection of alkyne to give **9**. Then, the ester group was installed with n-butyl lithium. Finally, the aldehyde was deprotected to get **1a**.

2.6. Attempt of O-H insertion using enynal as a carbene precusor

After obtaining enynal **1**, O-H insertion was immediately tested with two keto-alcohols. However, aldol product was not detected under rhodium catalysis for alcohol starting materials. The reactions yielded degradation of enynal **1a**, but no insertion or aldol product was observed. These results suggest the formation of rhodium carbene, but no further O-H insertion. The reactivity difference between diazo and enynal was observed. Such reactivity difference was thought to originate from electron rich nature of the furan ring. Metal carbenes are generally electrophilic, and the donor group makes the metal carbene more selective but less reactive.[30] As mentioned in **Chapter 1**, furan is

much more electron rich than benzene. Therefore, the lower reactivity of furyl carbene compared with phenyl carbene was to blamed for the result of no insertion reactions.

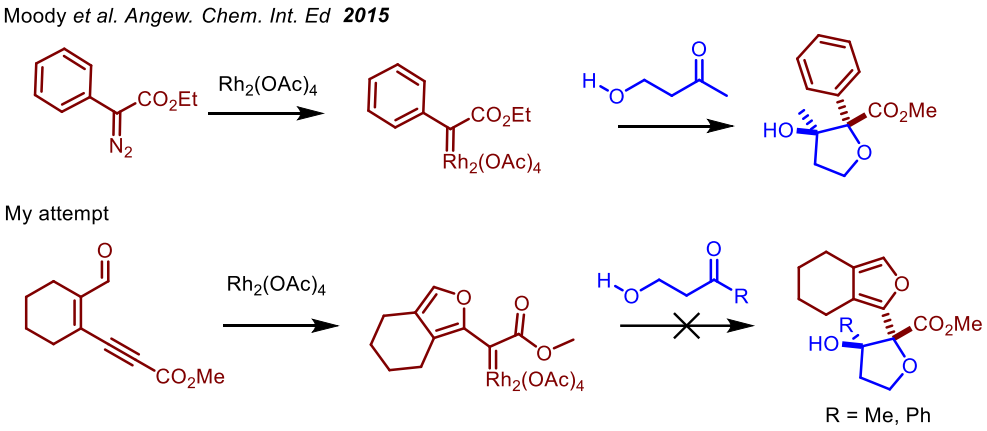

Figure 2.12. Enynal **1a** with keto-alcohol did not yield the expected product, compared with the Moody paper[16]

2.7. Synthesis of keto-aniline 2a

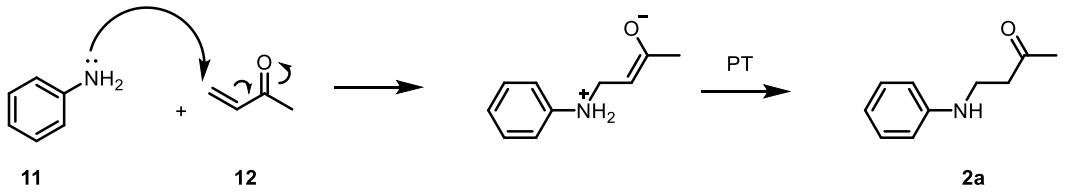

Figure 2.13. Formation of beta-aminoketone **2a**

The unsuccessful attempts of O-H insertion suggested a better nucleophile is required. It turned the research towards N-H insertion cascades, since nitrogen is a better nucleophile than oxygen.[31] The keto-aniline **2a** was synthesized following the reported one-step synthesis (**Figure 2.13.**).[32] 11 and 12 were stirred for overnight without solvents and catalysts. Product **2a** was isolated by flash column chromatography. This reaction was a typical aza-Michael addition reaction. 2**a** was obtained with a 75% yield.

2.8. Screening of reaction conditions

With both **1a** and **2a** in hands, $Rh_2(OAc)_4$ was initially tested at RT in DCM. The reaction was monitored with TLC. Under the Ninhydrin stain, two new compounds formed. These two spots were later identified as insertion and aldol products respectively. After consumption of the starting material on TLC, 1,3,5-trimethoxybenzen was added to the reaction mixture as an internal standard. To our delight, the aldol product was obtained with a 43% yield from the crude NMR. Insertion product was also detected from the reaction mixture (23% yield, Entry 1, P133). Then the reaction was repeated under reflux condition, heating resulted in more aldol product (59%) and less insertion product (18% yield, Entry 2, P133).

After the initial success of making the aldol product, optimization of the reaction was performed (**Table 1.**). We started by testing different metal catalysts reported to generate carbenoids with enynals, Rh(II), Cu(I), Zn, and Fe(II). It turned out that Znic Chloride produced the highest aldol product than other catalysts tested (Entry 8, P136). The zinc chloride reaction in DCM was also repeated at RT. This pair of results was consistent with the $Rh_2(OAc)_4$ reaction, which showed higher temperatures favored the formation of aldol product. However, heating the reaction mixture overnight led to the degradation of the product, so a higher temperature was not applied to avoid thermal degradation.

Table 1. Optimization table for the N-H insertion / aldol cascade reaction

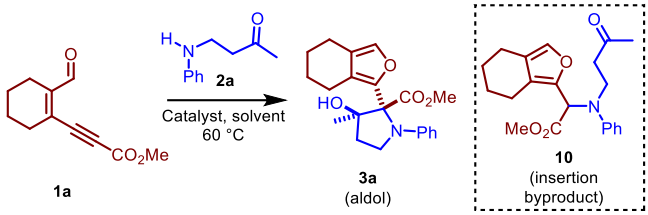

Entry[a]	Catalyst (mol%)	Solvent	Time	Yield (3**a**)[b]	Yield (**10**)[b]
1[c]	$Rh_2(OAc)_4$ (10)	CH_2Cl_2	16 h	43	23
2	$Rh_2(OAc)_4$ (10)	CH_2Cl_2	8 h	59	18
3	$Rh_2(esp)_2$ (10)	CH_2Cl_2	8 h	45	13
4	$Rh_2(TFA)_4$ (10)	CH_2Cl_2	8 h	54	9
5	$Rh_2(TPA)_4$ (10)	CH_2Cl_2	8 h	0	0
6	$Rh_2(HFB)_4$ (10)	CH_2Cl_2	8 h	19	16
7[c]	$ZnCl_2$ (20)	CH_2Cl_2	16 h	40	33
8	$ZnCl_2$ (20)	CH_2Cl_2	8 h	65	11
9	$[CuOTf]_2$•tol (20)	CH_2Cl_2	8 h	49	7
10	$Fe(BF_4)_2$ (20)	CH_2Cl_2	8 h	31	6
11	$ZnCl_2$ (20)	DCE	6 h	69	10
12	**$ZnCl_2$ (20)**	**PhCl**	**6 h**	**75**	**11**
13	$ZnCl_2$ (20)	Toluene	6 h	70	16
14	$ZnCl_2$ (20)	$PhCF_3$	6 h	75	17
15	$ZnBr_2$ (20)	PhCl	6 h	72	0
16	ZnI_2 (20)	PhCl	6 h	75	0
17	$Zn(OTf)_2$ (20)	PhCl	6 h	71	0
18	-	PhCl	3 d	26	0
19	*hν*	PhCl	8 h	0	0
20	$ZnCl_2$-TmBox(20)	PhCl	6 h	0	0

[a] Reaction conditions: **1a** (85 μmol), **2a** (50 μmol), catalyst, solvent (1.5 mL), temperature (60 ºC). [b] Yield was determined by ^{1}H NMR using 1,3,5-trimethoxy benzene as an internal standard. [c] Room temperature. (NMRs in P133-142)

Different solvents were tested with zinc chloride at 60 °C. Chlorobenzene gave the highest **3a** yield (75%, Entry 12, P138). Different zinc salts comparison gave similar results in terms of **3a** yield: all around 70-75% yield, while most of the zinc salts did not give only **3a** without formation of **10** (Entry 15-17, P139-140). TmBox ligand was used as a model to test the potential of inducing steroerosectivity to the reaction. TmBox ligand is one of the Box ligand family. Many chiral versions of Box ligands were developed for asymmetric catalysis. Unfortunately, after 6 h, no product was detected from crude NMR with addition of TmBox ligand (Entry 20, P142). Light irradiation at 365 nm was also tested, however, a complex mixture with heavy degradation was detected (Entry 19, P142). Finally, no catalyst experiment was carried out, after three days, the formation of **3a** was 26%, suggesting catalysts are needed in this reaction (Entry 18, P141). The result of no zinc catalyst gave a higher yield than zinc TmBox might result from zinc Tmbox decomposing the product without any catalytic effect. Considering zinc chloride is a strong Lewis acid, we hypothesize that zinc chloride did not only facilitate the formation of carbene, but also catalyze the aldol reaction. To sum up, the optimized reaction condition was in chlorobenzene at 60 °C with zinc chloride as the catalyst.

2.9. Substrate scope test

Once we had set the optimal reaction parameters, we proceeded to investigate the reaction breadth between enynal 1a and an assortment of phenyl-substituted aminoketones **2** (as illustrated in **Figure 2.14.**). We successfully produced a series of related products 3, achieving yields that spanned from moderate to impressive. Notably, halogen substitutions at the para-position on the phenyl group led to high yields of the aldol products (**3b**, **3c**). When halogens were introduced at both ortho and para sites, the

reactivity remained consistent, producing the relevant aldol derivatives in commendable yields (3d). Electron-withdrawing groups on the phenyl ring facilitated the reaction, steering it towards the desired aldol products. Specifically, the -nitro group at the para-position proved highly effective, resulting in an exemplary aldol yield (**3e**).

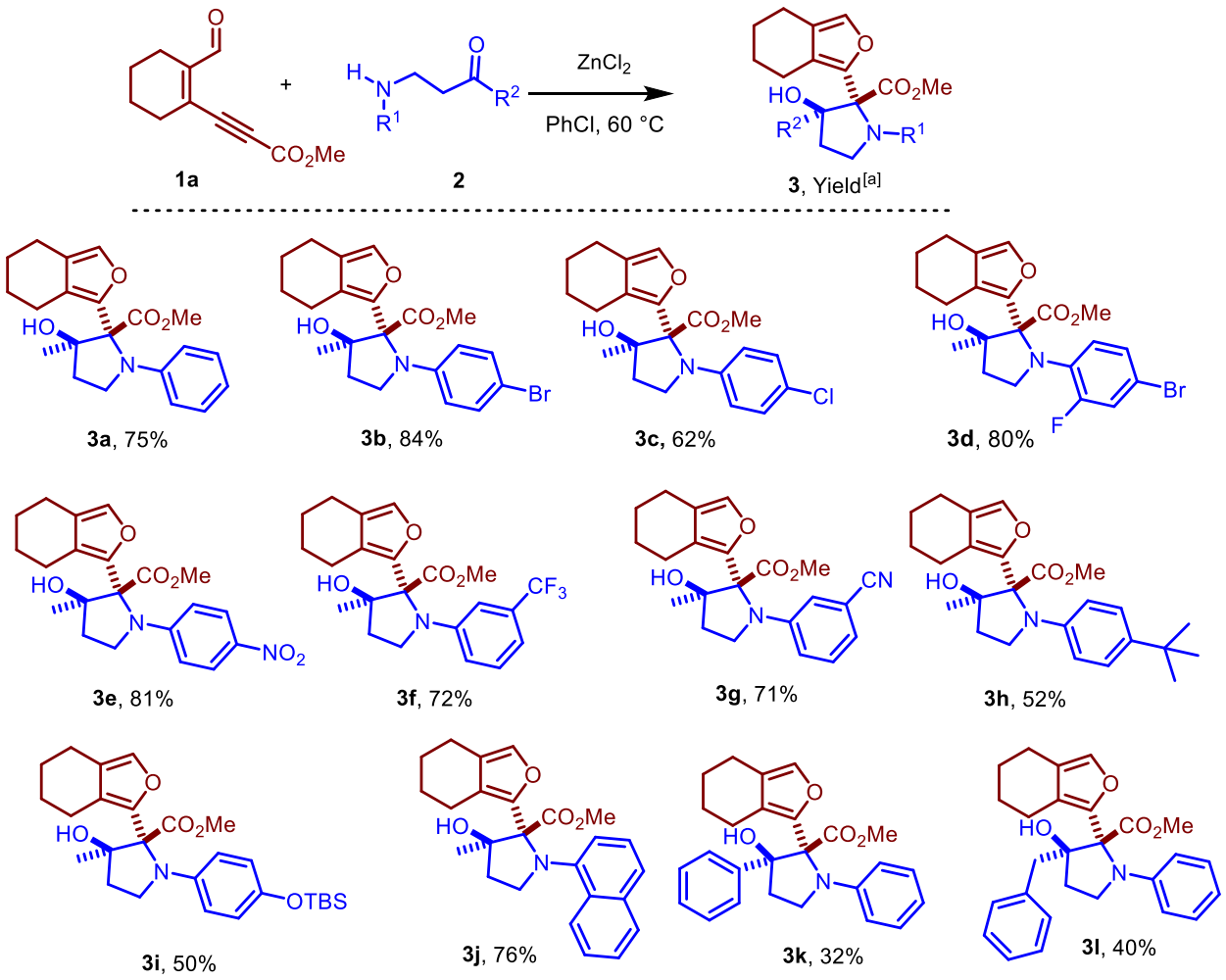

Figure 2.14. Different aldol products **3** were successfully made after verifying the substitution on the phenyl ring and replacement of the methyl group.

The cascade reaction also accommodated meta-substituted -trifluoromethyl and -cyano aminoketones, although the yields were somewhat decreased (**3f**, **3g**). Aminoketones with electron-releasing groups also displayed good reactivity, even though

their yields were marginally lower (**3h**, **3i**). Similarly, substituting the N-phenyl for a naphthyl variant maintained the reaction's efficacy, yielding an aldol product in a satisfactory manner (**3j**).

Following our initial findings, we focused on examining how electronic and steric properties influenced the ketone function in β-aminoketones by replacing the methyl group with phenyl and benzyl units. This alteration led to reduced yields in the corresponding aldol derivatives (**3k**, **3l**), and we also noted the presence of insertion and some unidentified byproducts.

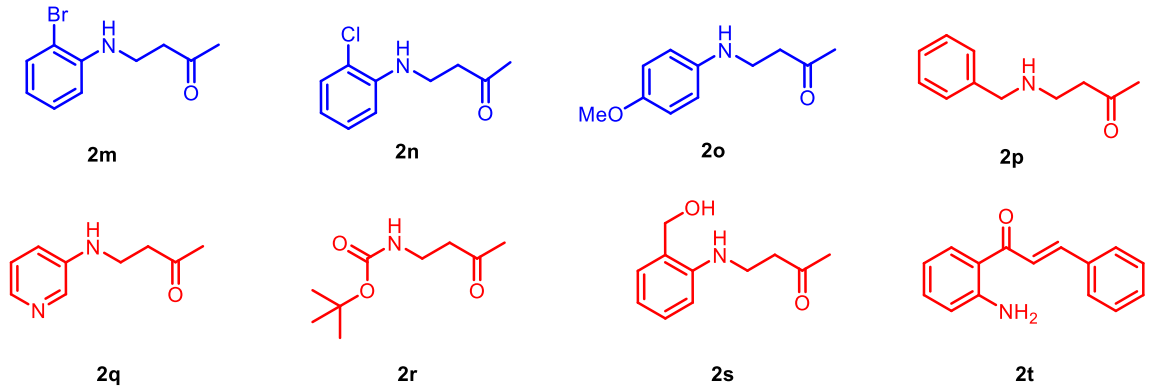

Figure 2.15. Animoketones that did not give clean reactions. Blue: products were mixed with impurities. Red: no production of the product.

Other than these aminoketones which gave clean reactions, there are other aminoketones that gave complicated mixtures after reactions (**Figure 2.15.**). Surprisingly, both **2m** and **2n** gave only around 40% yield. These two products were unable to be purified by flash column chromatography. **2o** gave a 26% yield, and the product was unable to be purified by flash column chromatography. **2s** and **2t** yielded degreadation of enynal, while **2p, 2q** and **2r** completely deactivated zinc chloride, leading to no reaction.

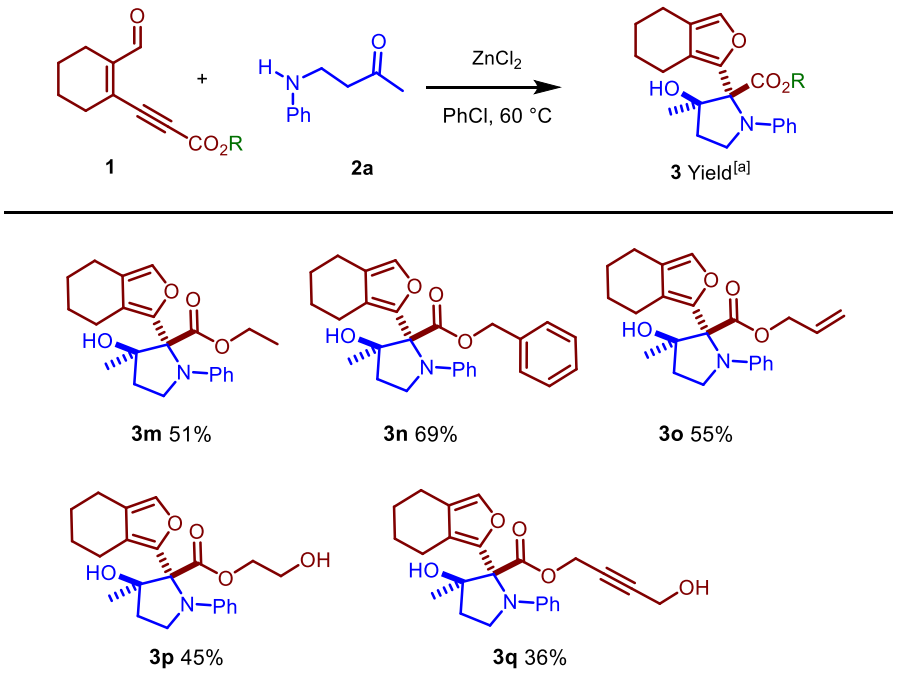

Figure 2.16. Different aldol products **3** were successfully made after verifying the substitution on the ester group.

After a successful examination of the substrate range for aminoketones, we shifted our attention to the N–H insertion/aldol reaction with various ester-substituted enynals (as shown in **Figure2.16.**). We found that replacing the methyl ester with bulkier groups resulted in lower product yields (**3m**, **3n**). However, it was uplifting to see that esters with alkene and alkyne groups were compatible, yielding the desired products in noteworthy amounts (**3o**, **3q**). Remarkably, the N–H insertion proceeded seamlessly even when free alcohols were present, leading to the desired aldol products in satisfactory yields (**3p**, **3q**). The distinct chemoselectivity of the insertion/aldol reaction in the presence of alkene, alkyne, and free alcohol groups underscores the robustness of our refined cascade methodology.

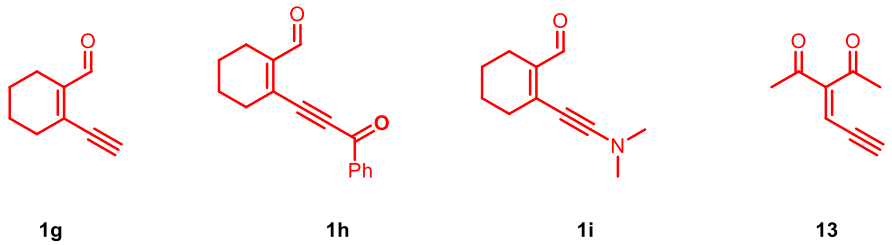

Figure 2.17. Enynals that did not give clean reactions.

Some other enyn-als/-ones were tested, but yielded no corresponding aldol product (**Figure 2.12.**).I used **1g** as a representation of D-carbenoid, but only degradation of **1g** was observed. I then tested **1h** and **1i** as different D/A carbenoids. However, 1h yielded Micheal addition while **1i** yielded only insertion product. **13** was tested as a different enynone. Unfortunately, degradation was again observed as **1g**.

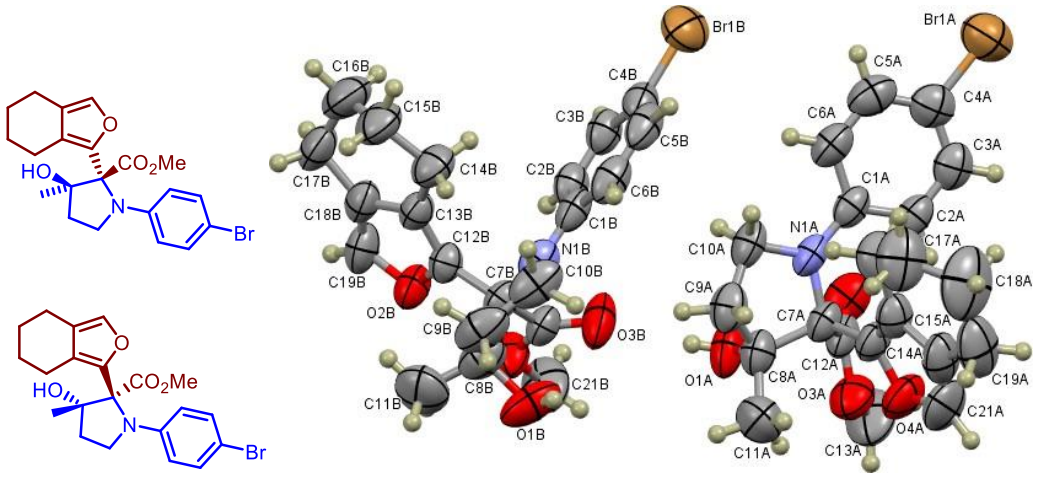

Figure 2.18. Crystal structure of **3b** suggests only formation of a pair of enantiomers.

All the compounds isolated show high diastereoselectivity based on NMR analysis. After crystallography, this diastereoselectivity is confirmed (**Figure 2.18.**). Only 2 isomers which the hydroxyl group and ester group are cis to each other are generated. This result is consistent with the corresponding diazo cascade system published by Moody *et al*.[8]

Lastly, a 1 mmol scale experiment between **1a** and **2b** was conducted with 1 mol% zinc chloride loading. The reaction yielded 75% aldol product **3b**, which showed the high turnover number of this simple zinc catalyst.

2.10. Potential binding between zinc and the aminoketone

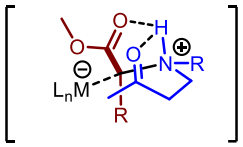

C

ML_n= $Rh_2(OAc)_4$ or $ZnCl_2$

Figure 2.19. Hypothetic transition state for our reaction based on Moody's Paper[8]

After collecting all the results, some questions occurred as they were contradictory to the previous literature. Thus these results cannot simply be explained using a mechanism similar to the corresponding diazo reaction published by Moody et al.[8] First of all, zinc chloride provides more aldol product **3a** and less insertion product **10** than rhodium acetate. If our reaction mechanism is the same as Moody's, the transition state **C** should form (**Figure 2.14.**). In this case, zinc is much more Lewis acidic than rhodium, which will greatly reduce the reactivity of the following aldol reaction. Therefore, if following the same mechanism, zinc chloride should give a higher insertion product yield but a lower aldol product yield than rhodium. This hypothesis was consistent with the room temperature reaction, but under reflux conditions, zinc gave a higher aldol product yield but a lower insertion product yield compared with rhodium. Therefore, our mechanism is different from Moody's.

Since zinc is a Lewis acid and has a high affinity to oxygen, it is reasonable to believe that zinc coordinates with the carbonyl group in **2a**. Such binding activated the

carbonyl group, leading to the formation of aldol product **3a**. It seems to be acceptable that a 20 mol% zinc catalyst can be quenched with stronger coordinators such as benzylamine, boc amide, and pyridine. However, Zinc can have coordination numbers of 4, 5, and 6. Tmbox is a bidentate ligand, thus zinc should not be quenched with a 1:1 TmBox ligand (**Figure 2.20.a**). In addition, changing bromine and chlorine from the para position to the ortho position greatly decreased yield and led to degradation (**Figure 2.20.c**). Such results cannot be simply explained by electronic effects. Lastly, moving free alcohol from enynals to aminoketones results in no product being formed.

These results suggest that other than election effects, the position of substitution is an important factor. Notably, the 0% yield of 2- hydroxymethyl and amino-chalcone were different from simply quenching the Zinc catalysts (**Figure 2.20.b and d**). Degradation of enynal suggests the formation of carbenoid species, but this carbenoid did not eventually convert to the corresponding product.

Clearly, these comparisons showed the restriction lies in the aminoketone counterpart. It is reasonable to believe that the structural difference in different aminoketones caused different results in this reaction. Considering Zinc can have coordination numbers of 4, 5, and 6. When aminoketones are treated as ligands. Most of the amino ketones other than amino-chalcone can be considered as bidentate

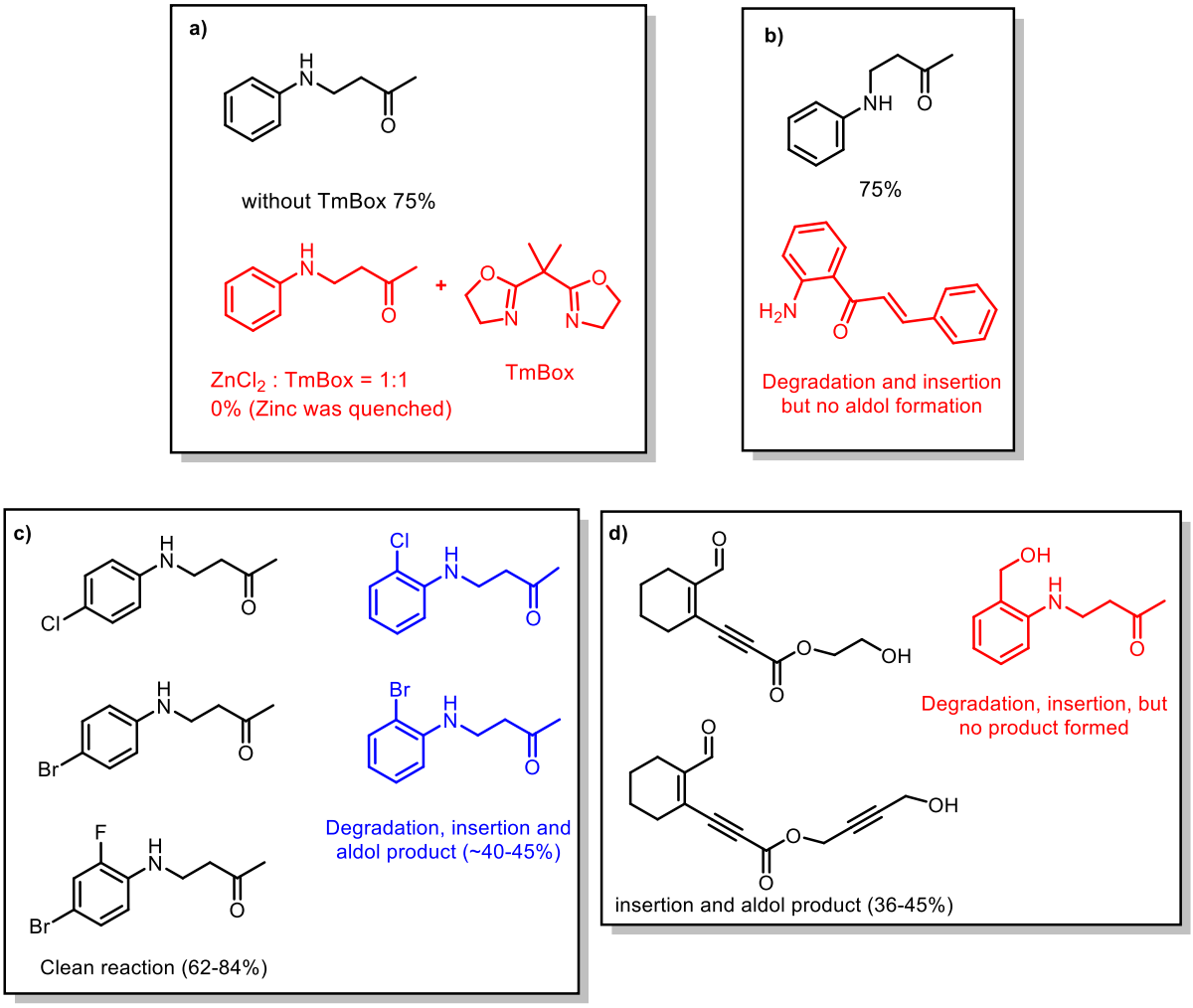

Figure 2.20. Comparison between different groups. a) TmBox quenched $ZnCl_2$. b) free bidentate ligand (black) vs planer bidentate ligand (red). c) bidentate ligands (black) vs tridentate ligands (blue). d) free alcohol on enynal (black) vs free alcohol on aminoketone (red).

ligands. 2-Floro-4-Bromo in this case is still considered as a bidentate ligand due to fluorine's high electronegativity and low coordination ability. 2- Hydroxymethyl is a strong tridentate ligand, which gave 0% yield. 2-Bromo and 2-Chloro are somewhat between the bidentate ligand and tridentate ligand. Bromine and Chlorine have weak coordination with Zinc which alters the binding. Therefore, the reaction yields were decreased, and

degradation was increased. While amino-chalcone itself is a bidentate ligand, the conjugation of amine and ketone moieties also altered the binding towards zinc, leading to no production of the final product.

The coordination effect can also explain why TmBox completely quenches the zinc catalyst. Tmbox itself is a bidentate ligand. Together with aminoketone and 2 Chlorine counter anions, these ligands completely shielded the zinc cation, thus Zinc cation had no access to the enynal molecule.

Other than that, there is some functional group tolerance issue. Namely, 4-methoxybenzene. Replacing 4-OMe with 4-OTBS doubled product yield. These results cannot be simply explained with electron effects. The major difference between OTBS and OMe groups is the stereo bulkiness. It is also well-known that zinc binds to diethyl ether. It is more likely that Zinc binds to the Methoxy ether more easily which eventually tears the molecule apart. While the OTBS group slows down the degradation process.

2.10. Proposed reaction mechanism

Therefore, I propose the following mechanism (**Figure 2.21.**). The zinc-aminoketone complex initially activates alkyne in **1a**, allowing the lone pair electrons on oxygen to form the five-member ring. After the formation of the C-Zn bond, the electrons of zinc back push to quench the charge on oxygen, forming the furyl-carbenoid. Then The nitrogen is transferred to the carbenoid to form intermediate **B**. 1,2-proton transfer of intermediate **B** will form the insertion byproduct. On the other hand, the further electron transfer to oxygen leads to the enol form of ester. Zinc chloride is also transferred together with the electrons. Throughout this transfer, zinc chloride keeps its coordination with

oxygen, which leads to the cis geometry of the intermediate. Then, intramolecular aldol reaction, followed by proton transfer generates aldol product. Similarly, the amino chalcone has a conjugated structure, which stopped nitrogen insertion as well as changing the intermediate geometries. The carbonyl group must be twisted outside of the phenyl plane in intermediate **D**. Only amino chalcone is not favored in this geometry due to conjugation, while other aminoketones don't have such an issue. Thus, it gave degradation and the insertion product only.

This mechanism explained some questions mentioned previously. First, zinc chloride gave a higher insertion product yield but a lower aldol product yield than rhodium acetate at RT, but it was the opposite under reflux conditions. The heating granted **B** more energy to overcome the energetic barrier between **B** and **C**, which leads to high production of aldol. On the other hand, at RT, the Lewis acidity of zinc reduced the aldol product. Second, degradation and low or even 0% yield were observed with tridentate ligands. Tridentate ligands have higher binding energy than bidentate ligands. Such binding reduced nitrogen insertion from **A** to **B**. As carbenes are unstable intermediates, degradation happens under heating conditions if nitrogen is not inserted. Thirdly, the amino chalcone has a planer geometry due to the conjugation effect, which causes difficulties in the formation of **B**, **C**, and **D**, where the carbonyl needs to be twisted out against the amine group. Thus, only degradation happened together with some insertion product, but no formation of aldol products. Lastly, the coordination also explains the chemoselectivity of the reaction. Presumably, nitrogen is a better nucleophile than oxygen, so nitrogen is always inserted into carbene. The free alcohol, however, protonated intermediate **B**, generating insertion products and decreasing the yield for aldol products.

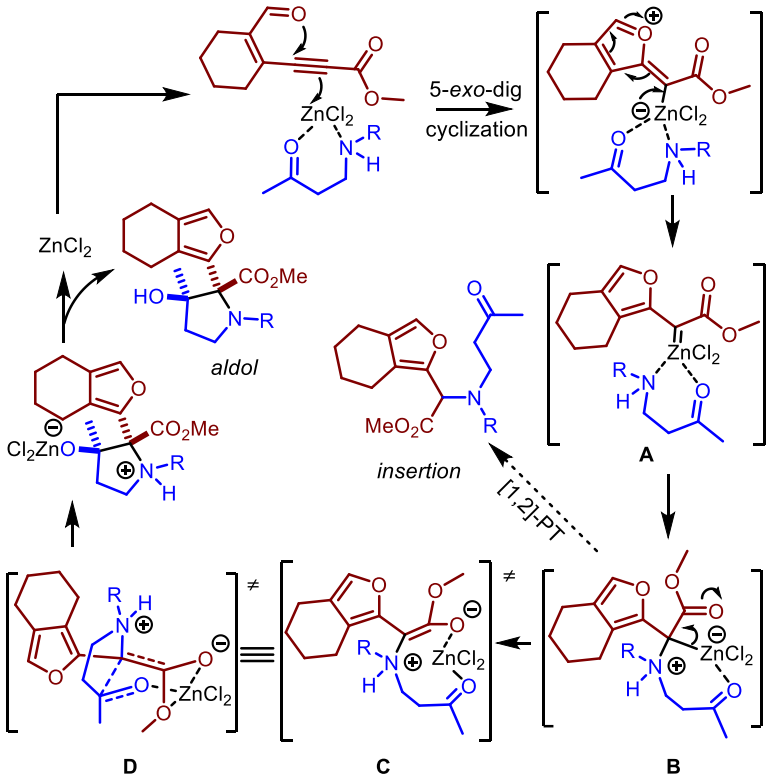

Figure 2.21. Proposed reaction mechanism including coordination between zinc and aminoketones and formation of important intermediates.

However, there are still some questions not fully answered. For example, only enynals with ester functionality produced aldol products, but ketone and amide generated Micheal addition and insertion products respectively. Both ketone and amide should have similar capabilities to generate intermediate **C** and **D**, but they did not. There could be energetic differences between different functional groups in these intermediates. If that is true, then computational modeling may give evidence for this explanation. In addition, there are reactivity differences between diazos and enynals. Namely, when comparing boc-amide-ketone with amino-ketones, boc-amide-ketone **2r** was completely inert with enynal unreacted under both zinc and rhodium catalysis. Based on the literature, diazos reacted with the same boc-amide-ketone **2r**, yielding the corresponding aldol product. But

the enynal **1a** and **2r** were both unreacted in my case. As mentioned in previous sections, furan group is more electron rich than benzene, which make furyl carbene less reactive but more selective than phenyl carben.[30] Therefore, modifying enynal to control the electron density of the forming furan moiety may allow different substrates such as boc-amide-ketone **2r** to participate in such cascade reaction. Further investigation into enyn-al/-one chemistry is needed to prove this hypothesis.

2.11. Conclusion and future directions.

A novel methodology for synthesizing furyl-pyrrolidine is developed using enynal as a carbene precursor under Earth-abundant zinc catalysis. However, there are still questions unsolved. First, while the experimental results are consistent with the proposed mechanism, there is no direct evidence of aminoketone binding to zinc catalysts. Computational modeling can be done to validate the hypothesis. Secondly, different reactivity between enynals and diazo compounds was observed. Lastly, only enynal with ester groups but not ketone or amide groups generated the final product. These two questions are still in doubt. Further investigation of these three questions may reveal more insight into enyn-al/-one chemistry.

In addition, this work focused on the illustration of the possibility of enynal in cascade reactions. Initially, the cyclohexane ring in the enynals molecules is used to stabilize the compounds. However, acyclic enyn-als/ -ones are known for O-H and N-H insertion similar as cyclic enynals.[7, 33] Possibly, acyclic enyn-als/ -ones have the same potential as cyclic enyn-als/-ones. Therefore, acyclic enyn-als/-ones could be synthesized to further expand the substrate scope.

Lastly, post modification of the aldol product could help further utilizing this furyl-pyrrolidine scaffold. Since alkenes and alkynes are well tolerated in this reaction, olefine metathesis and click chemistry can be applied to the product to ligate other counterparts and functionalities.

2.12. REFERENCES FOR CHAPTER 2

1. Saito, I.; Takayama, M.; Sugiyama, H.; Nakatani, K.; Tsuchida, A.; Yamamoto, M., Photoinduced DNA cleavage via electron transfer: demonstration that guanine residues located 5'to guanine are the most electron-donating sites. *J. Am. Chem. Soc.* **1995,** *117* (23), 6406-6407.

2. Nakatani, K.; Higashida, N.; Saito, I., Highly efficient photochemical generation of o-Quinone methide from Mannich bases of phenol derivatives. *Tetrahedron Lett.* **1997,** *38* (28), 5005-5008.

3. Miki, K.; Yokoi, T.; Nishino, F.; Ohe, K.; Uemura, S., Synthesis of 2-pyranylidene or (2-furyl)carbene–chromium complexes from conjugated enyne carbonyl compounds with Cr(CO)5(THF). *J. Organomet. Chem.* **2002,** *645* (1), 228-234.

4. Miki, K.; Yokoi, T.; Nishino, F.; Kato, Y.; Washitake, Y.; Ohe, K.; Uemura, S., Catalytic Cyclopropanation of Alkenes via (2-Furyl)carbene Complexes from 1-Benzoyl-cis-1-buten-3-yne with Transition Metal Compounds. *J. Org. Chem.* **2004,** *69* (5), 1557-1564.

5. Miki, K.; Kato, Y.; Uemura, S.; Ohe, K., Catalytic Nucleophilic Addition Reaction to (2-Furyl) carbene Intermediates Generated from Carbonyl–Ene–Ynes. *Bull. Chem. Soc. Jpn.* **2008,** *81* (9), 1158-1165.

6. Vicente, R.; González, J.; Riesgo, L.; González, J.; López, L. A., Catalytic Generation of Zinc Carbenes from Alkynes: Zinc-Catalyzed Cyclopropanation and Si H Bond Insertion Reactions. *Angew. Chem. Int. Ed.* **2012,** *51* (32), 8063-8067.

7. González, J.; González, J.; Pérez-Calleja, C.; López, L. A.; Vicente, R., Zinc-Catalyzed Synthesis of Functionalized Furans and Triarylmethanes from Enynones and

Alcohols or Azoles: Dual X H Bond Activation by Zinc. *Angew. Chem. Int. Ed.* **2013,** *52* (22), 5853-5857.

8. Nicolle, S. M.; Lewis, W.; Hayes, C. J.; Moody, C. J., Stereoselective Synthesis of Functionalized Pyrrolidines by the Diverted N− H Insertion Reaction of Metallocarbenes with β-Aminoketone Derivatives. *Angew. Chem. Int. Ed.* **2016,** *55* (11), 3749-3753.

9. Jing, C. C.; Xing, D.; Gao, L. X.; Li, J.; Hu, W. H., Divergent Synthesis of Multisubstituted Tetrahydrofurans and Pyrrolidines via Intramolecular Aldol-type Trapping of Onium Ylide Intermediates. *Chem-Eur J* **2015,** *21* (52), 19202-19207.

10. Liu, K.; Zhu, C.; Min, J.; Peng, S.; Xu, G.; Sun, J., Stereodivergent Synthesis of N-Heterocycles by Catalyst-Controlled, Activity-Directed Tandem Annulation of Diazo Compounds with Amino Alkynes. *Angew. Chem. Int. Ed.* **2015,** *54* (44), 12962-12967.

11. Chinthapally, K.; Massaro, N. P.; Ton, S.; Gardner, E. D.; Sharma, I., Trapping rhodium vinylcarbenoids with aminochalcones for the synthesis of medium-sized azacycles. *Tetrahedron Lett.* **2019,** *60* (46), 151253.

12. Hunter, A. C.; Almutwalli, B.; Bain, A. I.; Sharma, I., Trapping rhodium carbenoids with aminoalkynes for the synthesis of diverse N-heterocycles. *Tetrahedron* **2018,** *74* (38), 5451-5457.

13. Xia, Y.; Zhang, Y.; Wang, J. B., Catalytic Cascade Reactions Involving Metal Carbene Migratory Insertion. *ACS Catal.* **2013,** *3* (11), 2586-2598.

14. Xu, X. F.; Han, X. C.; Yang, L. P.; Hu, W. H., Highly Diastereoselective Synthesis of Fully Substituted Tetrahydrofurans by a One-Pot Cascade Reaction of Aryldiazoacetates with Allyl Alcohols. *Chem-Eur J* **2009,** *15* (46), 12604-12607.

15. Hashimoto, Y.; Itoh, K.; Kakehi, A.; Shiro, M.; Suga, H., Diastereoselective Synthesis of Tetrahydrofurans by Lewis Acid Catalyzed Intermolecular Carbenoid–Carbonyl Reaction–Cycloaddition Sequences: Unusual Diastereoselectivity of Lewis Acid Catalyzed Cycloadditions. *J. Org. Chem.* **2013,** *78* (12), 6182-6195.

16. Nicolle, S. M.; Lewis, W.; Hayes, C. J.; Moody, C. J., Stereoselective Synthesis of Highly Substituted Tetrahydrofurans through Diverted Carbene O H Insertion Reaction. *Angew. Chem. Int. Ed.* **2015,** *54* (29), 8485-8489.

17. Shibano, M.; Kitagawa, S.; Nakamura, S.; AKAZAWA, N.; KUSANO, G., Studies on the constituents of Broussonetia species. II. Six new pyrrolidine alkaloids, broussonetine A, B, E, F and broussonetinine A and B, as inhibitors of glycosidases from Broussonetia kazinoki Sieb. *Chem. Pharm. Bull.* **1997,** *45* (4), 700-705.

18. Biard, J.; Guyot, S.; Roussakis, C.; Verbist, J.; Vercauteren, J.; Weber, J.; Boukef, K., Lepadiformine, a new marine cytotoxic alkaloid from Clavelina lepadiformis Müller. *Tetrahedron Lett.* **1994,** *35* (17), 2691-2694.

19. Han, X.; Widenhoefer, R. A., Gold(I)-Catalyzed Intramolecular Hydroamination of Alkenyl Carbamates. *Angew. Chem. Int. Ed.* **2006,** *45* (11), 1747-1749.

20. Pandey, G.; Banerjee, P.; Gadre, S. R., Construction of Enantiopure Pyrrolidine Ring System via Asymmetric [3+2]-Cycloaddition of Azomethine Ylides. *Chem. Rev.* **2006,** *106* (11), 4484-4517.

21. Feula, A.; Dhillon, S. S.; Byravan, R.; Sangha, M.; Ebanks, R.; Hama Salih, M. A.; Spencer, N.; Male, L.; Magyary, I.; Deng, W.-P.; Müller, F.; Fossey, J. S., Synthesis of azetidines and pyrrolidines via iodocyclisation of homoallyl amines and exploration of activity in a zebrafish embryo assay. *Org. Biomol. Chem.* **2013,** *11* (31), 5083-5093.

22. Jing, C.; Xing, D.; Qian, Y.; Shi, T.; Zhao, Y.; Hu, W., Diversity-Oriented Three-Component Reactions of Diazo Compounds with Anilines and 4-Oxo-Enoates. *Angew. Chem. Int. Ed.* **2013,** *52* (35), 9289-9292.

23. Liu, K.; Zhu, C.; Min, J.; Peng, S.; Xu, G.; Sun, J., Stereodivergent Synthesis of N-Heterocycles by Catalyst-Controlled, Activity-Directed Tandem Annulation of Diazo Compounds with Amino Alkynes. *Angew. Chem. Int. Ed.* **2015,** *54* (44), 12962-12967.

24. Jing, C.; Xing, D.; Gao, L.; Li, J.; Hu, W., Divergent Synthesis of Multisubstituted Tetrahydrofurans and Pyrrolidines via Intramolecular Aldol-type Trapping of Onium Ylide Intermediates. *Chem-Eur J* **2015,** *21* (52), 19202-7.

25. Hong, K.; Shu, J.; Dong, S.; Zhang, Z.; He, Y.; Liu, M.; Huang, J.; Hu, W.; Xu, X., Asymmetric Three-Component Reaction of Enynal with Alcohol and Imine as An Expeditious Track to Afford Chiral α-Furyl-β-amino Carboxylate Derivatives. *ACS Catal.* **2022,** *12* (22), 14185-14193.

26. Kato, Y.; Miki, K.; Nishino, F.; Ohe, K.; Uemura, S., Doyle− Kirmse reaction of allylic sulfides with diazoalkane-free (2-furyl) carbenoid transfer. *Org. Lett.* **2003,** *5* (15), 2619-2621.

27. Wang, D.; Gao, S., Sonogashira coupling in natural product synthesis. *Org. Chem. Front.* **2014,** *1* (5), 556-566.

28. Schilz, M.; Plenio, H., A guide to Sonogashira cross-coupling reactions: the influence of substituents in aryl bromides, acetylenes, and phosphines. *J. Org. Chem.* **2012,** *77* (6), 2798-2807.

29. Sonogashira, K.; Tohda, Y.; Hagihara, N., A convenient synthesis of acetylenes: catalytic substitutions of acetylenic hydrogen with bromoalkenes, iodoarenes and bromopyridines. *Tetrahedron Lett.* **1975,** *16* (50), 4467-4470.

30. Davies, H. M.; Denton, J. R., Application of donor/acceptor-carbenoids to the synthesis of natural products. *Chem. Soc. Rev.* **2009,** *38* (11), 3061-3071.

31. Clayden, J.; Greeves, N.; Warren, S., *Organic chemistry*. Oxford University Press, USA: 2012.

32. Jiang, R.; Li, D.-H.; Jiang, J.; Xu, X.-P.; Chen, T.; Ji, S.-J., Green, efficient and practical Michael addition of arylamines to α,β-unsaturated ketones. *Tetrahedron* **2011,** *67* (20), 3631-3637.

33. Vicente, R.; González, J.; Riesgo, L.; González, J.; López, L. A., Catalytic Generation of Zinc Carbenes from Alkynes: Zinc-Catalyzed Cyclopropanation and Si H Bond Insertion Reactions. *Angew. Chem.* **2012,** *124* (32), 8187-8191.

2.13. EXPERIMENTAL SECTION FOR CHAPTER 2

Reagents

Reagents and solvents were obtained from Sigma-Aldrich (www.sigma-aldrich.com), Chem-Impex (www.chemimpex.com) or Acros Organics (www.fishersci.com) and used without further purification unless otherwise indicated. Dry solvents (acetonitrile) were obtained from Acros Organics (www.fishersci.com), and dichloromethane was distilled over CaH_2 under N_2 unless otherwise indicated. THF purchased from Sigma-Aldrich was distilled over Na metal with benzophenone indicator. Chlorobenzene was obtained from Sigma-Aldrich.

Reactions

All reactions were performed in flame-dried glassware under positive N_2 pressure with magnetic stirring unless otherwise noted. Liquid reagents and solutions were transferred thru rubber septa via syringes flushed with N_2 prior to use.

Chromatography

TLC was performed on 0.25 mm E. Merck silica gel 60 F254 plates and visualized under UV light (254 nm) or by staining with potassium permanganate ($KMnO_4$), cerium ammonium molybdenate (CAM), phosphomolybdic acid (PMA), and ninhydrin. Silica flash chromatography was performed on Sorbtech 230–400 mesh silica gel 60.

Analytical Instrumentation

NMR spectra were recorded on a Varian VNMRS 300, 400, 500 and 600 MHz NMR spectrometer in $CDCl_3$ unless otherwise indicated. Chemical shifts are expressed in ppm

relative to solvent signals: $CDCl_3$ (^1H, 7.26 ppm, ^{13}C, 77.16 ppm), CD_3OD(^1H, 3.34 ppm, ^{13}C, 49.00 ppm); coupling constants are expressed in Hz. NMR spectra were processed using Mnova (www.mestrelab.com/software/mnova-nmr). Mass spectra were obtained at the OU Analytical Core Facility on an Agilent 6538 High-Mass-Resolution QTOF Mass Spectrometer and an Agilent 1290 UPLC.

Nomenclature

N.B.: Atom numbers shown in chemical structures herein correspond to IUPAC nomenclature, which was used to name each compound.

PUBLICATION AND CONTRIBUTIONS STATEMENT

The research presented in this chapter was published in Organic Chemistry Frontiers. **2023** .**DOI**: 10.1039/D3QO01354E as first author. Materials synthesized by Chenxin will be reported within.

2.13.1. General Procedure 1 for the Synthesis of Enynals (1b-1f)

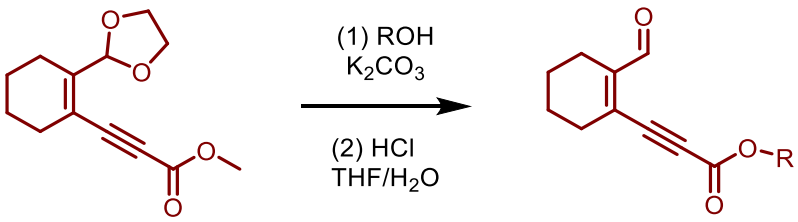

Methyl 3-(2-(1,3-dioxolan-2-yl)cyclohex-1-en-1-yl)propiolate was synthesized following the reported procedure.[1] To a suspension of Na_2CO_3 (1.2 mmol, 2 equiv.) in DMF (2 ml) was added methyl 3-(2-(1,3-dioxolan-2-yl)cyclohex-1-en-1-yl)propiolate (0.6 mmol, 1 equiv.) and alcohol (6 mmol, 10 equiv.). The mixture was heated at 60 °C overnight. The reaction was separated by ether and water. The aqueous phase was extracted with ether

twice. The combined organic phase was washed with brine and dried over Na_2SO_4. After solvent being removed, the remaining oil was dissolved in THF (3 ml). To this solution, HCl (35%, 0.8 ml) and water (2.2 ml) was added. The reaction was stirred at 0 °C for 1.5 h. After completion, the reaction was extracted with EtOAc, washed with water, brine and dried over Na_2SO_4. The organic layer was concentrated and purified by column chromatography eluting with 1:20 ethyl acetate:hexanes gradient to 1:5 ethyl acetate:hexanes to furnish pure enynals **1b-1f**.

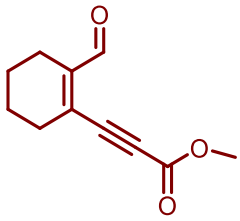

Methyl 3-(2-formylcyclohex-1-en-1-yl)propiolate (1a). Synthesized following the reported procedure. (450 mg, 62% yield.) Characterization data was in accordance with previous reports.[1]

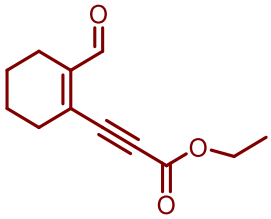

Ethyl 3-(2-formylcyclohex-1-en-1-yl)propiolate (1b). Synthesized using general procedure 1. (75mg, 61% yield.) Characterization data was in accordance with previous reports.[2]

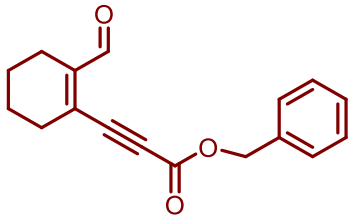

Benzyl 3-(2-formylcyclohex-1-en-1-yl)propiolate (1c). Synthesized following the reported procedure. (64 mg, 40% yield.) Characterization data was in accordance with previous reports.[3]

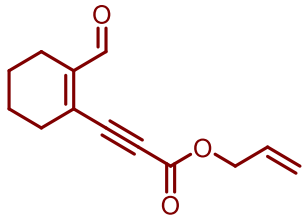

Allyl 3-(2-formylcyclohex-1-en-1-yl)propiolate (1d). Synthesized using general procedure 1. (61 mg, 45% yield). Characterization data was in accordance with previous reports. [2]

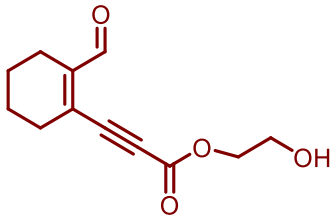

2-Hydroxyethyl 3-(2-formylcyclohex-1-en-1-yl)propiolate (1e). Synthesized using general procedure 1. Yellow oil, (64 mg, 48% yield). **TLC**: R_f 0.52 (ethyl acetate/hexanes = 3: 2). **^{1}H NMR** ($CDCl_3$, 400 MHz) δ 10.15 (s, 1H), 4.36 (s, 0H), 3.90 (s, 0H), 2.46 (d, J = 2.6 Hz, 3H), 2.38 – 2.22 (m, 4H), 1.78 – 1.64 (m, 10H). **^{13}C NMR** ($CDCl_3$, 125 MHz): δ 191.69, 191.66, 153.51, 148.14, 135.77, 87.96, 82.93, 67.75, 60.80, 31.33, 22.46, 21.66, 20.71. **HRMS** (ESI) *m/z* calcd for $C_{12}H_{14}O_4Na$ ([M+Na]$^+$) 245.0790; found 245.0789.

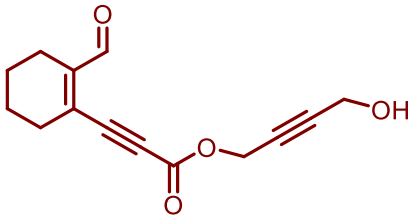

2-Butyne-1,4-diol 3-(2-formylcyclohex-1-en-1-yl)propiolate (1f). Synthesized using general procedure 1. Yellow oil, (38mg, 26%). **TLC**: R_f 0.69 (ethyl acetate/hexanes = 3: 2). **^{1}H NMR** ($CDCl_3$, 400 MHz) δ 10.15 (s, 1H), 4.85 (t, J = 1.9 Hz, 2H), 4.33 (dt, J = 6.2, 1.8 Hz, 2H), 2.45 (dq, J = 6.1, 2.7 Hz, 2H), 2.31 (dq, J = 5.9, 2.7 Hz, 2H), 1.76 – 1.61 (m, 4H).**^{13}C NMR** ($CDCl_3$, 100 MHz δ 191.64, 152.66, 148.46, 135.60, 87.48, 86.24, 83.41, 78.72, 53.95, 51.18, 31.27, 22.48, 21.67, 20.71. **HRMS** (ESI) *m/z* calcd for $C_{14}H_{14}O_4Na$ ($[M+Na]^+$) 269.0790; found 269.0778.

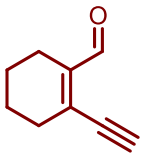

2-ethynylcyclohex-1-ene-1-carbaldehyde (1g). Synthesized following the reported procedure. (3.7 g, 70% yield.) Characterization data was in accordance with previous reports.[1]

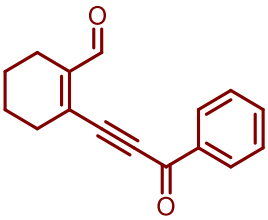

2-(3-oxo-3-phenylprop-1-yn-1-yl)cyclohex-1-ene-1-carbaldehyde (1h). Synthesized following the reported procedure. (450 mg, 75% yield.) Characterization data was in accordance with previous reports. [1]

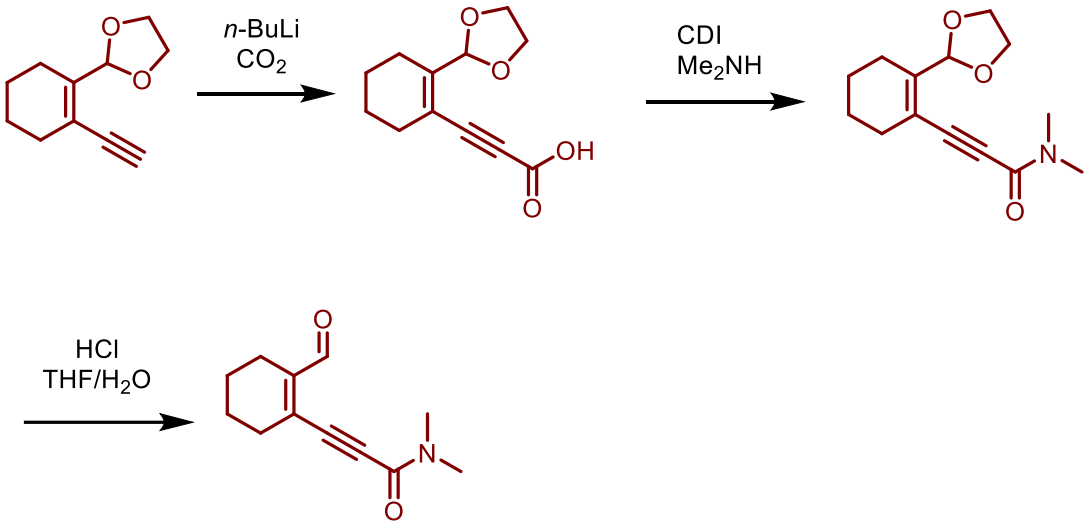

3-(2-formylcyclohex-1-en-1-yl)-N,N-dimethylpropiolamide (1i). 2-(2-ethynylcyclohex-1-en-1-yl)-1,3-dioxolane was synthesized following the reported procedure.[1] To 2-(2-ethynylcyclohex-1-en-1-yl)-1,3-dioxolane (200 mg, 1.1 mmol) in THF was added *n*-butyl Lithium (1.1 mmol) at -20 °C. After 20 min, the mixture was warmed to RT. Then CO2 was bubbled into the solution for 2 h. Solution was washed by EtOAc. The aqueous layer was acidified by phosphoric acid and extracted by EtOAc. The organic layer was dried over Na_2SO_4. After solvent being removed, the remaining oil was dissolved in acetonitrile. CDI (1 mmol) was added at 40 °C and stirred for 2 h. Then the mixture was cooled to RT and added with dimethylamine (2 mmol) in THF solution and stirred for overnight. The reaction mixture was filtered through silica plug. After solvent being removed, the remaining oil was dissolved in THF (3 ml). To this solution, HCl (35%, 0.8 ml) and water (2.2 ml) was added. The reaction was stirred at 0 ° for 1.5 h. After completion, the reaction was extracted with EtOAc, washed with water, brine and dried over Na_2SO_4. The organic layer was concentrated and purified by column chromatography eluting with 1:5 ethyl acetate:hexanes to furnish pure enynal **1h**. Yellow oil (45 mg, overall 20% yield after 3 steps) **TLC**: R_f 0.12 (ethyl acetate/hexanes = 2: 3). **^{1}H NMR** ($CDCl_3$, 400 MHz) δ 10.16

(s, 1H), 3.22 (s, 3H), 3.02 (s, 3H), 2.47 (dq, *J* = 6.0, 2.8 Hz, 2H), 2.30 (dt, *J* = 6.0, 3.0 Hz, 2H), 1.80 – 1.61 (m, 4H). **^{13}C NMR** ($CDCl_3$, 100 MHz) δ 191.85, 153.97, 146.08, 137.17, 89.76, 86.54, 38.45, 34.39, 31.75, 22.35, 21.79, 20.86. **MS** (ESI) *m/z* calcd for $C_{12}H_{16}NO_2$ ($[M+H]^+$) 206.1; found 206.1.

2.13.2. General Procedure 2 for the Synthesis of Beta-Arylaminoketones (2)

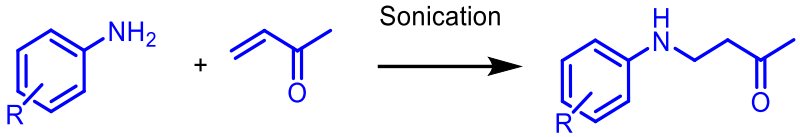

Aminoketones (2). Aminoketones were synthesized following a modified literature procedure.[4] Methyl vinyl ketone (1.2 mmol, 1.2 equiv.) and substituted aniline (1 mmol, 1 equiv.) were mixed in an eppendorf tube for overnight sonication. The product was directly purified by column chromatography, eluting with 1:9 ethyl acetate:hexanes gradient to 3:7 ethyl acetate:hexanes to furnish pure aminoketones **2a-2j**.

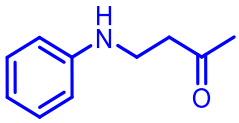

4-(Phenylamino)butan-2-one (2a). Synthesized using general procedure 2. (99 mg, 66% yield). Characterization data was in accordance with previous reports. [5]

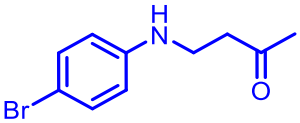

4-((4-Bromophenyl)amino)butan-2-one (2b). Synthesized using general procedure 2. (110 mg, 45% yield). Characterization data was in accordance with previous reports. [6]

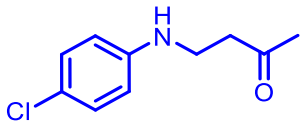

4-((4-Chlorophenyl)amino)butan-2-one (2c). Synthesized using general procedure 2. (110 mg, 45% yield.) Characterization data was in accordance with previous reports.[7]

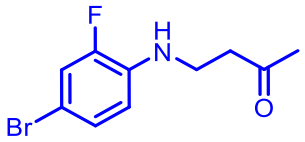

4-((4-Bromo-2-fluorophenyl)amino)butan-2-one(2d). Synthesized using general procedure 2. Yellow oil (123 mg, 53% yield). **TLC**: R_f 0.53 (ethyl acetate/hexanes = 1:1). **^{1}H NMR** ($CDCl_3$, 400 MHz) δ 7.16 – 7.06 (m, 2H), 6.56 (t, J = 8.7 Hz, 1H), 4.19 (s, 1H), 3.41 (t, J = 6.2 Hz, 2H), 2.76 (t, J = 6.2 Hz, 2H), 2.18 (s, 3H). **^{13}C NMR** ($CDCl_3$, 100 MHz) δ 207.52, 151.47 (d, J = 243.5 Hz), 135.58 (d, J = 11.5 Hz), 127.54 (d, J = 3.5 Hz), 118.16 (d, J = 21.9 Hz), 113.01 (d, J = 3.8 Hz), 107.38 (d, J = 8.8 Hz).42.52, 38.01, 30.50. **HRMS** (ESI) We were unable to obtain accurate HRMS data for this compound.

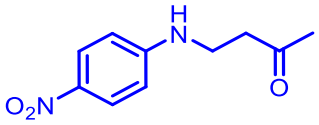

4-((4-Nitrophenyl)amino)butan-2-one (2e). Synthesized following the reported procedure. (61 mg, 29% yield). Characterization data was in accordance with previous reports.[8]

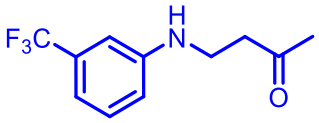

4-((3-(Trifluoromethyl)phenyl)amino)butan-2-one (2f). Synthesized using general procedure 2. (140 mg, 61% yield). Characterization data was in accordance with previous reports. [9]

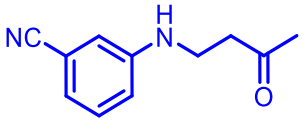

3-((3-Oxobutyl)amino)benzonitrile (2g). Synthesized using general procedure 2. Yellow solid (110 mg 46% yield). **TLC**: R_f 0.20 (ethyl acetate/hexanes = 3:7). **^{1}H NMR** ($CDCl_3$, 400 MHz) δ 7.20 (tq, J = 6.5, 2.1 Hz, 1H), 6.99 – 6.90 (m, 1H), 6.77 (qd, J = 2.8, 1.4 Hz, 2H), 4.32 (s, 1H), 3.38 (ddt, J = 8.0, 6.0, 2.4 Hz, 2H), 2.79 – 2.70 (m, 2H), 2.18 (s, 3H). **^{13}C NMR** ($CDCl_3$, 100 MHz) δ 207.84, 148.05, 130.02, 120.86, 119.53, 117.53, 114.82, 112.92, 42.13, 37.91, 30.40. **HRMS** (ESI) *m/z* calcd for $C_{11}H_{12}N_2ONa$ ([M+Na]$^+$) 211.0847; found 211.0847.

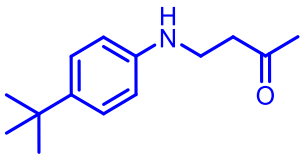

4-[[4-(1,1-Dimethylethyl)phenyl]amino]butan-2-one (2h). Synthesized using general procedure 2. (149 mg, 68% yield). Characterization data was in accordance with previous reports.[9]

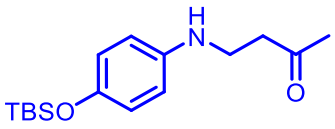

4-((4-((Tert-butyldimethylsilyl)oxy)phenyl)amino)butan-2-one (2i). Synthesized using general procedure 2. Yellow solid (153 mg 45% yield). **TLC**: R_f 0.20 (ethyl acetate/hexanes = 3:7). **^{1}H NMR** ($CDCl_3$, 500 MHz) 6.77 – 6.67 (m, 2H), 6.53 (dt, J = 12.7, 5.3 Hz, 2H), 3.35 (tt, J = 6.2, 1.2 Hz, 2H), 2.74 (q, J = 6.5 Hz, 2H), 2.17 (s, 3H), 0.96 (s, 9H), 0.15 (s, 6H). **^{13}C NMR** ($CDCl_3$, 125 MHz) δ δ 208.40, 147.94, 142.13, 120.86, 114.62, 42.83, 39.67, 30.47, 25.89, 18.32, -4.33. **HRMS** (ESI) *m/z* calcd $C_{16}H_{28}NO_2Si$ ($[M+H]^+$) 294.1889; found 294.1893.

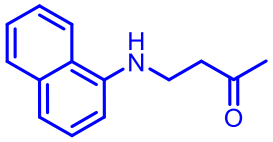

4-(Naphthalen-1-ylamino)butan-2-one (2j). Synthesized using general procedure 2. (105 mg, 49% yield). Characterization data was in accordance with previous reports.[4]

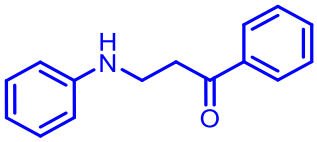

1-phenyl-3-(phenylamino)propan-1-one (2k)). Synthesized following the reported procedure. (112 mg, 43% yield). Characterization data was in accordance with previous reports.[10]

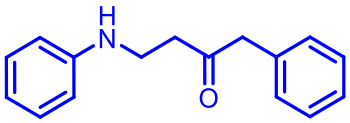

1-phenyl-4-(phenylamino)butan-2-one (2l). Synthesized using general procedure 2. Yellow oil (110 mg, 48% yield). **TLC**: R_f 0.53 (ethyl acetate/hexanes = 1: 4). **^{1}H NMR** ($CDCl_3$, 400 MHz) δ 7.38 – 7.27 (m, 3H), 7.17 (ddd, *J* = 13.8, 7.1, 1.8 Hz, 4H), 6.70 (t, *J* = 7.4 Hz, 1H), 6.55 (d, *J* = 8.1 Hz, 2H), 3.91 (s, 1H), 3.70 (s, 2H), 3.38 (t, *J* = 6.1 Hz, 2H), 2.76 (t, *J* = 6.1 Hz, 2H). **^{13}C NMR** ($CDCl_3$, 100 MHz,) δ 207.96, 147.70, 133.89, 129.56, 129.42, 128.96, 127.32, 117.75, 113.13, 50.67, 41.03, 38.59. **MS** (ESI) *m/z* calcd for $C_{16}H_{18}NO$ ($[M+H]^+$) 240.1; found 240.1.

2.13.3. General Procedure 3 for the Synthesis of Furyl Pyrrolidines (3)

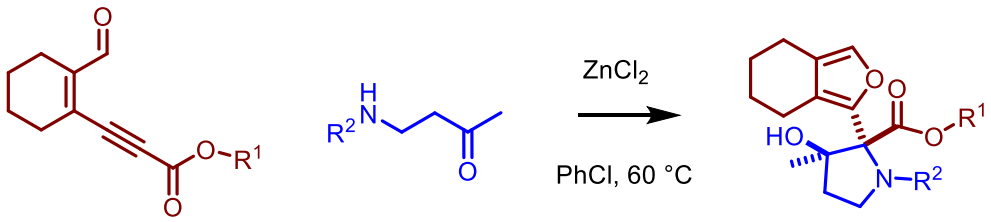

To a 5.0 mL RB flask equipped with a magnetic stir bar was added $ZnCl_2$ (10 µmol, 0.2 equiv.). A solution of amino ketone (50 µmol, 1 equiv.) in chlorobenzene (1 ml) was added. Lastly, the enynal (85 µmol, 1.7 equiv.) in chlorobenzene (0.5 ml) was added via syringe pump over 4 h at 60 °C. Reaction was monitored by TLC. After completion, the reaction mixture was directly purified by column chromatography 1:9 ethyl acetate:hexanes gradient to 1:4 ethyl acetate:hexanes to Furyl Pyrrolidines **3a**-**3j** and **5a**-**5e**.

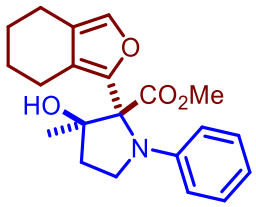

Methyl 3-hydroxy-3-methyl-1-phenyl-2-(4,5,6,7-tetrahydroisobenzofuran-1-yl)pyrrolidine-2-carboxylate (3a). Synthesized using general procedure 3. Yellow solid. (75% NMR yield using 1,3,5-trimethoxybenzene as reference.) **TLC**: R_f 0.33 (ethyl acetate/hexanes = 3:7). **^{1}H NMR** ($CDCl_3$, 400 MHz): δ 7.18 (s, 1H), 7.12 (dd, J = 8.6, 7.2 Hz, 2H), 6.69 (t, J = 7.3 Hz, 1H), 6.49 (d, J = 8.1 Hz, 2H), 3.71 (m, 4H), 3.67 – 3.55 (m, 1H), 2.66 (s, 1H), 2.48 (q, J = 6.5, 6.1 Hz, 2H), 2.38 – 1.92 (m, 4H), 1.72 – 1.40 (m, 4H), 1.12 (s, 3H). **^{13}C NMR** ($CDCl_3$, 100 MHz δ 171.14, 146.91, 143.66, 136.74, 128.66, 122.57, 120.23, 117.18, 113.38, 86.03, 77.36, 52.44, 48.09, 37.16, 24.17, 23.57, 22.82, 21.90, 20.48. **HRMS** (ESI) *m/z* calcd for $C_{21}H_{25}NO_4Na$ ($[M+Na]^+$) 378.1682; found 378.1673.

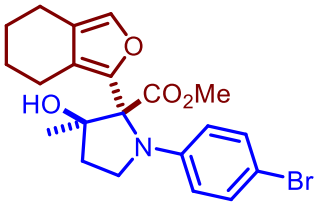

Methyl 1-(4-bromophenyl)-3-hydroxy-3-methyl-2-(4,5,6,7-tetrahydroisobenzofuran-1-yl)pyrrolidine-2-carboxylate (3b). Synthesized using general procedure 3. Yellow solid. (84% NMR yield using 1,3,5-trimethoxybenzene as reference.) **TLC**: R_f 0.45 (ethyl acetate/hexanes = 2:3). **^{1}H NMR** ($CDCl_3$, 400 MHz): 7.22 – 7.13 (m, 3H), 6.35 (d, J = 9.1 Hz, 2H), 3.72 (d, J = 1.3 Hz, 4H), 3.54 (td, J = 8.6, 4.1 Hz, 1H), 2.62 (s, 1H), 2.47 (d, J = 5.9 Hz, 2H), 2.23 (ddt, J = 12.8, 9.6, 4.5 Hz, 2H), 2.16 – 1.99 (m, 2H), 1.66 – 1.42 (m,

4H), 1.14 (d, J = 1.4 Hz, 3H). **^{13}C NMR** ($CDCl_3$, 100 MHz) δ 170.54, 145.92, 143.05, 136.87, 131.28, 122.65, 120.27, 115.04, 109.24, 86.10, 77.36, 52.49, 48.18, 37.20, 24.07, 23.53, 22.76, 21.93, 20.43.**HRMS** (ESI) *m/z* calcd for $C_{21}H_{25}BrNO_4$ ($[M+H]^+$) 434.0967; found 434.0971.

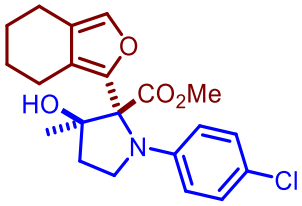

Methyl 1-(4-chlorophenyl)-3-hydroxy-3-methyl-2-(4,5,6,7-tetrahydroisobenzofuran-1-yl)pyrrolidine-2-carboxylate (3c). Synthesized using general procedure 3. Colourless oil. (62% NMR yield using 1,3,5-trimethoxybenzene as reference.) **TLC**: R_f 0.39 (ethyl acetate/hexanes = 3:7). **^{1}H NMR** ($CDCl_3$, 400 MHz): δ 7.17 (s, 1H), 7.13 – 6.97 (m, 2H), 6.52 – 6.31 (m, 2H), 3.72 (m, 4H), 3.55 (td, J = 8.6, 4.1 Hz, 1H), 2.58 (s, 1H), 2.48 (d, J = 5.7 Hz, 2H), 2.31 – 2.03 (m, 4H), 1.74 – 1.41 (m, 4H), 1.14 (s, 3H). **^{13}C NMR** ($CDCl_3$, 100 MHz) δ 170.66, 145.53, 143.16, 136.88, 128.46, 122.67, 121.99, 120.29, 114.53, 86.11, 77.36, 52.50, 48.27, 37.21, 24.12, 23.54, 22.78, 21.93, 20.44. **HRMS** (ESI) *m/z* calcd for $C_{21}H_{25}ClNO_4$ ($[M+H]^+$) 390.14723; found 390.1455.

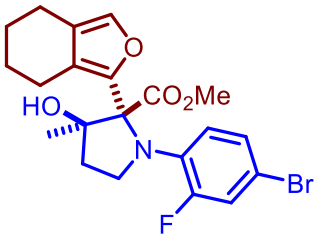

Methyl 1-(4-bromo-2-fluorophenyl)-3-hydroxy-3-methyl-2-(4,5,6,7-tetrahydroisobenzofuran-1-yl)pyrrolidine-2-carboxylate (3d). Synthesized using general procedure 3. Colourless oil. (80% NMR yield using 1,3,5-trimethoxybenzene as reference.) **TLC**: R_f 0.38 (ethyl acetate/hexanes = 2:3). **^{1}H NMR** ($CDCl_3$, 500 MHz): δ 7.16 (s, 1H), 7.09 (dd, J = 13.1, 2.3 Hz, 1H), 6.95 (dd, J = 8.8, 2.3 Hz, 1H), 6.38 (t, J = 9.1 Hz, 1H), 3.89 (ddt, J = 11.4, 7.9, 3.9 Hz, 1H), 3.74 (s, 3H), 3.68 (tt, J = 8.7, 4.2 Hz, 1H), 2.60 (s, 1H), 2.56 – 2.47 (m, 2H), 2.29 – 2.16 (m, 2H), 2.19 – 2.04 (m, 2H), 1.69 – 1.50 (m, 4H), 1.19 (s, 3H). **^{13}C NMR** ($CDCl_3$, 125 MHz) δ 170.40, 143.95, 137.80, 136.45, 126.80, 126.78, 122.59, 119.69, 119.49, 84.99, 77.26, 52.37, 50.17, 50.10, 36.89, 23.63, 23.43, 22.63, 20.30. **HRMS** (ESI) *m/z* calcd for $C_{21}H_{23}BrFNO_4Na$ ($[M+Na]^+$) 474.0692; found 474.0696.

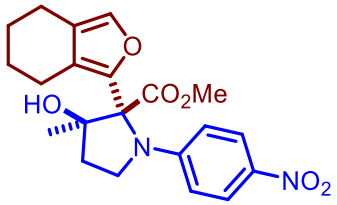

Methyl 3-hydroxy-3-methyl-1-(4-nitrophenyl)-2-(4,5,6,7-tetrahydroisobenzofuran-1-yl)pyrrolidine-2-carboxylate (3e). Synthesized using general procedure 3. Colourless oil. (81% NMR yield using 1,3,5-trimethoxybenzene as reference.) **TLC**: R_f 0.34 (ethyl acetate/hexanes = 2:3). **^{1}H NMR** ($CDCl_3$, 400 MHz) : δ 8.01 (d, 2H), 7.15 (s, 1H), 6.44 (d, J = 8.9 Hz, 2H), 3.87 (dt, J = 9.5, 8.2 Hz, 1H), 3.76 (s, 3H), 3.74 – 3.55 (m, 1H), 2.62 – 2.35 (m, 2H), 2.31 – 2.08 (m, 4H), 1.59 – 1.49 (m, 4H), 1.24 (s, 3H). **^{13}C NMR** ($CDCl_3$, 100 MHz) δ 169.07, 151.98, 141.78, 138.42, 138.10, 137.16, 125.32, 122.88, 112.70, 86.22, 77.36, 52.73, 48.53, 37.32, 23.94, 23.47, 22.66, 22.16, 20.36. **HRMS** (ESI) *m/z* calcd for $C_{21}H_{25}N_2O_6$ ($[M+H]^+$) 401.1713; found 401.1720.

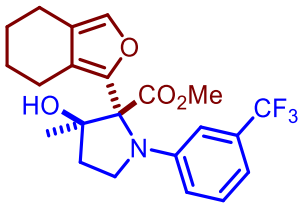

Methyl 3-hydroxy-3-methyl-2-(4,5,6,7-tetrahydroisobenzofuran-1-yl)-1-(3-(trifluoromethyl)phenyl)pyrrolidine-2-carboxylate (3f). Synthesized using general procedure 3. Colourless oil. (72% NMR yield using 1,3,5-trimethoxybenzene as reference.) **TLC**: R_f 0.45 (ethyl acetate/hexanes = 2:3). **^{1}H NMR** ($CDCl_3$, 400 MHz): δ 7.22 – 7.08 (m, 2H), 6.91 (d, J = 7.6 Hz, 1H), 6.71 (t, J = 2.0 Hz, 1H), 6.59 (dd, J = 8.4, 2.5 Hz, 1H), 3.80 (q, J = 8.2 Hz, 1H), 3.73 (s, 3H), 3.61 (dt, J = 9.2, 6.0 Hz, 1H), 2.58 (s, 1H), 2.54 – 2.39 (m, 2H), 2.35 – 2.19 (m, 3H), 2.12 (s, 1H), 1.70 – 1.45 (m, 4H), 1.20 (s, 3H). **^{13}C NMR** ($CDCl_3$, 100 MHz) δ 170.20, 146.95, 142.66, 136.86, 130.72 (q, J = 31.5 Hz), 128.78, 124.59 (d, J = 272.4 Hz), 122.61, 120.52, 116.61, 113.55, 109.98, 86.09, 77.36, 52.48, 48.24, 37.30, 23.91, 23.50, 22.75, 22.16, 20.42. **HRMS** (ESI) *m/z* calcd for $C_{22}H_{25}F_3NO_4$ ($[M+H]^+$) 424.17358; found 424.1721.

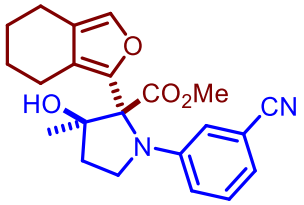

Methyl 1-(3-cyanophenyl)-3-hydroxy-3-methyl-2-(4,5,6,7-tetrahydroisobenzofuran-1-yl)pyrrolidine-2-carboxylate (3g). Synthesized using general procedure 3. Colourless oil. (71% NMR yield using 1,3,5-trimethoxybenzene as reference.) **TLC**: R_f 0.29 (ethyl acetate/hexanes = 2:3). **^{1}H NMR** ($CDCl_3$, 400 MHz): δ 7.15 (t, J = 8.0 Hz, 2H), 6.95 (d, J = 7.5 Hz, 1H), 6.70 (s, 1H), 6.64 (dd, J = 8.5, 2.3 Hz, 1H), 3.75 (s, 4H), 3.57 (dt, J = 9.2, 5.9 Hz, 1H), 2.55 – 2.40 (m, 3H), 2.33 – 2.15 (m, 3H), 2.13 – 2.00 (m, 1H), 1.69 – 1.49

(m, 4H), 1.20 (s, 3H). **^{13}C NMR** ($CDCl_3$, 100 MHz) δ 169.80, 147.02, 142.21, 137.06, 129.14, 122.74, 120.52, 120.47, 119.91, 117.82, 116.38, 112.23, 86.15, 77.36, 52.61, 48.13, 42.01, 37.28, 23.89, 23.49, 22.72, 22.16, 20.36. **HRMS** (ESI) *m/z* calcd for $C_{22}H_{25}N_2O_4$ ($[M+H]^+$) 381.1815; found 381.1800.

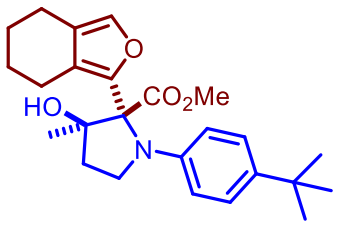

Methyl 1-(4-(tert-butyl)phenyl)-3-hydroxy-3-methyl-2-(4,5,6,7-tetrahydroisobenzofuran-1-yl)pyrrolidine-2-carboxylate (3h). Synthesized using general procedure 3. Colourless oil. (52% NMR yield using 1,3,5-trimethoxybenzene as reference.) **TLC**: R_f 0.50 (ethyl acetate/hexanes = 2:3). **^{1}H NMR** ($CDCl_3$, 400 MHz): δ 7.22 – 6.99 (m, 3H), 6.50 – 6.29 (m, 2H), 3.73 (s, 4H), 3.58 (dt, J = 8.7, 4.4 Hz, 1H), 2.74 (s, 1H), 2.48 (q, J = 6.1, 5.5 Hz, 2H), 2.26 (dt, J = 14.1, 5.5 Hz, 2H), 2.17 – 2.00 (m, 2H), 1.64 – 1.47 (m, 4H), 1.24 (s, 9H), 1.11 (s, 3H). **^{13}C NMR** ($CDCl_3$, 100 MHz) δ 171.32, 144.39, 143.84, 139.61, 136.56, 125.38, 122.49, 120.24, 113.08, 85.97, 77.36, 52.42, 48.08, 37.26, 33.87, 31.74, 31.63, 24.04, 23.58, 22.87, 22.00, 20.49. **HRMS** (ESI) *m/z* calcd for $C_{25}H_{28}N_2O_4$ ($[M+H]^+$) 406.20185; found 406.2009.

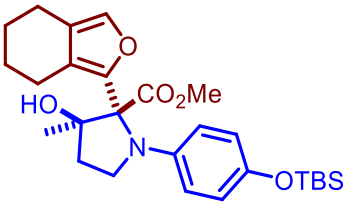

Methyl 1-(4-((tert-butyldimethylsilyl)oxy)phenyl)-3-hydroxy-3-methyl-2-(4,5,6,7-tetrahydroisobenzofuran-1-yl)pyrrolidine-2-carboxylate (3i). Synthesized using

general procedure 3. Colourless oil. (50% NMR yield using 1,3,5-trimethoxybenzene as reference.) **TLC**: R_f 0.45 (ethyl acetate/hexanes = 2:3). **^{1}H NMR** ($CDCl_3$, 400 MHz): δ 7.19 (s, 1H), 6.63 (d, J = 8.7 Hz, 2H), 6.37 (d, J = 8.5 Hz, 2H), 3.70 (m, 4H), 3.57 – 3.51 (m, 1H), 2.68 (s, 1H), 2.52 – 2.39 (m, 2H), 2.36 – 2.25 (m, 1H), 2.23 – 2.12 (m, 1H), 2.11 – 2.01 (m, 1H), 2.01 – 1.89 (m, 1H), 1.63-1.38 (m, 4H), 1.10 (s, 3H), 0.95 (s, 9H), 0.12 (s, 6H). **^{13}C NMR** ($CDCl_3$, 100 MHz) δ 171.52, 147.14, 144.00, 141.68, 136.68, 122.51, 120.26, 120.14, 114.44, 85.93, 77.36, 52.32, 48.51, 37.24, 25.89, 24.27, 23.54, 22.85, 21.80, 20.49, 18.34, -4.30. **HRMS** (ESI) *m/z* calcd for $C_{27}H_{40}N_2O_5Si$ ($[M+H]^+$) 486.2676; found 486.2694.

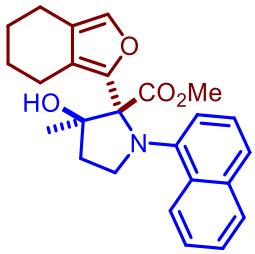

Methyl 3-hydroxy-3-methyl-1-(naphthalen-1-yl)-2-(4,5,6,7-tetrahydroisobenzofuran-1-yl)pyrrolidine-2-carboxylate (3j). Synthesized using general procedure 3. Gray solid. (76% NMR yield using 1,3,5-trimethoxybenzene as reference.) **TLC**: R_f 0.39 (ethyl acetate/hexanes = 2:3). **^{1}H NMR** ($CDCl_3$, 400 MHz):): δ 8.42 (d, J = 8.4 Hz, 1H), 7.78 (d, J = 8.1 Hz, 1H), 7.60 (d, J = 8.2 Hz, 1H), 7.47 (dt, J = 23.6, 6.8 Hz, 2H), 7.25 (d, J = 6.3 Hz, 1H), 7.17 (t, J = 7.8 Hz, 1H), 6.19 (d, J = 7.5 Hz, 1H), 3.78 – 3.70 (m, 1H), 3.49 (s, 3H), 3.36 – 3.27 (m, 2H), 2.75 (ddd, J = 13.3, 10.4, 6.2 Hz, 1H), 2.57 (q, J = 7.3, 6.5 Hz, 1H), 2.25 (ddd, J = 13.0, 8.7, 4.0 Hz, 1H), 2.08 (ddd, J = 16.3, 8.9, 5.3 Hz, 1H), 1.71 (dt, J = 16.0, 5.5 Hz, 1H), 1.66 – 1.52 (m, 3H), 1.50 (s, 3H), 1.38 – 1.23 (m, 2H). **^{13}C NMR** ($CDCl_3$, 100 MHz) δ 170.54, 144.09, 137.95, 136.59, 126.94, 126.92, 122.73, 119.83,

119.63, 85.13, 77.40, 52.51, 50.31, 50.24, 37.04, 23.78, 23.58, 22.77, 21.77, 20.45. **HRMS** (ESI) *m/z* calcd for $C_{27}H_{30}NO_4$ ([M+H]$^+$) 432.2169; found 432.2181.

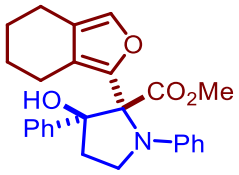

methyl (2R,3S)-3-hydroxy-1,3-diphenyl-2-(4,5,6,7-tetrahydroisobenzofuran-1-yl)pyrrolidine-2-carboxylate (3k). Synthesized using general procedure 3. Yellow solid. (32% NMR yield using 1,3,5-trimethoxybenzene as reference.) **TLC**: Rf 0.35 (ethyl acetate/hexanes = 1:4). **^{1}H NMR** ($CDCl_3$, 600 MHz) δ 7.25 – 7.18 (m, 3H), 7.17 – 7.11 (m, 4H), 6.86 (s, 1H), 6.72 (t, *J* = 7.4 Hz, 1H), 6.53 (d, *J* = 7.6 Hz, 2H), 4.04 (q, *J* = 8.3 Hz, 1H), 3.90 (d, *J* = 2.4 Hz, 1H), 3.82 (td, *J* = 8.8, 2.6 Hz, 1H), 3.74 (s, 3H), 2.70 (dt, *J* = 12.7, 8.8 Hz, 1H), 2.39 – 2.32 (m, 2H), 2.27 (ddd, *J* = 12.7, 7.2, 2.4 Hz, 1H), 2.20 – 2.07 (m, 1H), 1.47 – 1.31 (m, 4H), 1.23 – 1.16 (m, 1H). **^{13}C NMR** ($CDCl_3$, 100 MHz) δ 171.19, 146.88, 142.22, 140.14, 136.39, 128.83, 127.71, 127.54, 126.24, 122.55, 121.88, 117.60, 113.64, 88.08, 78.10, 77.48, 77.16, 76.84, 52.68, 48.67, 36.21, 23.64, 22.75, 22.15, 20.49. **MS** (ESI) *m/z* calcd for $C_{26}H_{18}NO_4$ ([M+H]$^+$) 418.2; found 418.0.

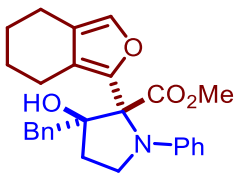

methyl (2R,3R)-3-benzyl-3-hydroxy-1-phenyl-2-(4,5,6,7-tetrahydroisobenzofuran-1-yl)pyrrolidine-2-carboxylate (3l). Synthesized using general procedure 3. Colourless oil. (40% NMR yield using 1,3,5-trimethoxybenzene as reference.) **TLC**: Rf 0.35 (ethyl acetate/hexanes = 1:4). **^{1}H NMR** ($CDCl_3$, 400 MHz) δ 7.27 (q, *J* = 6.8 Hz, 3H), 7.23 – 7.17

(m, 3H), 7.12 (t, *J* = 7.7 Hz, 2H), 6.69 (t, *J* = 7.2 Hz, 1H), 6.48 (d, *J* = 8.1 Hz, 2H), 3.74 (s, 3H), δ 3.69 (t, *J* = 8.1 Hz, 1H), 3.63 (dt, *J* = 8.8, 4.3 Hz, 1H)., 2.95 (d, *J* = 13.8 Hz, 1H), 2.58 – 2.41 (m, 2H), 2.41 – 2.30 (m, 3H), 2.24 – 2.11 (m, 2H), 1.89 (ddd, *J* = 11.9, 7.1, 3.6 Hz, 1H), 1.62 (q, *J* = 9.7, 8.1 Hz, 1H), 1.55 (m, 4H). **^{13}C NMR** ($CDCl_3$, 100 MHz) δ 170.50, 146.71, 143.06, 136.99, 130.65, 129.56, 128.57, 128.40, 126.89, 122.74, 120.87, 117.06, 113.42, 87.69, 77.36, 52.40, 47.95, 41.85, 34.62, 23.63, 22.82, 22.21, 20.51. **MS** (ESI) *m/z* calcd for $C_{27}H_{30}NO_4$ ($[M+H]^+$) 432.2; found 432.0.

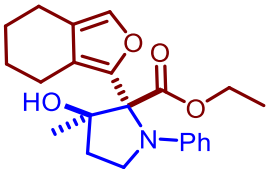

Ethyl 3-hydroxy-3-methyl-1-phenyl-2-(4,5,6,7-tetrahydroisobenzofuran-1-yl)pyrrolidine-2-carboxylate (3m). Synthesized using general procedure 3. Colourless oil. (51% NMR yield using 1,3,5-trimethoxybenzene as reference.) **TLC**: R_f 0.45 (ethyl acetate/hexanes = 2:3). **^{1}H NMR** ($CDCl_3$, 400 MHz): δ 7.18 (s, 1H), 7.11 (t, J = 2.3 Hz, 2H), 6.68 (t, J = 7.3 Hz, 1H), 6.51 (d, J = 8.9 Hz, 1H), 4.30 – 4.04 (m, 2H), 3.80 – 3.67 (m, 1H), 3.59 (td, J = 8.6, 4.5 Hz, 1H), 2.72 (s, 1H), 2.51 – 2.41 (m, 3H), 2.28 (ddd, J = 12.1, 7.6, 4.5 Hz, 2H), 2.17 – 1.98 (m, 2H), 1.48 (d, J = 5.3 Hz, 4H), 1.17 – 1.08 (m, 6H). **^{13}C NMR** ($CDCl_3$, 100 MHz) δ 170.49, 147.02, 143.87, 136.71, 128.54, 122.53, 120.17, 117.15, 113.53, 85.94, 76.64, 61.59, 48.08, 37.22, 24.26, 23.59, 22.85, 21.94, 20.49, 14.14. **HRMS** (ESI) *m/z* calcd for $C_{22}H_{28}NO_4$ ($[M+H]^+$) 370.20185; found 370.2009.

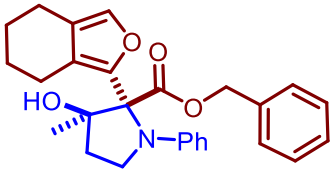

Benzyl 3-hydroxy-3-methyl-1-phenyl-2-(4,5,6,7-tetrahydroisobenzofuran-1-yl)pyrrolidine-2-carboxylate (3n). Synthesized using general procedure 3. Gray sold. (51% NMR yield using 1,3,5-trimethoxybenzene as reference.) **TLC**: R_f 0.52 (ethyl acetate/hexanes = 2:3). **^{1}H NMR** ($CDCl_3$, 600 MHz): δ 7.25 – 7.19 (m, 4H), 7.10 (t, J = 7.9 Hz, 2H), 7.06 (d, J = 6.5 Hz, 2H), 6.70 (t, J = 7.2 Hz, 1H), 6.51 (d, J = 8.0 Hz, 2H), 5.19 (d, J = 12.5 Hz, 1H), 5.10 (d, J = 12.6 Hz, 1H), 3.78 – 3.67 (m, 1H), 3.64 – 3.56 (m, 1H), 2.55 (s, 1H), 2.47 (dq, J = 16.7, 9.0, 8.0 Hz, 2H), 2.22 (d, J = 18.3 Hz, 2H), 2.11 – 1.94 (m, 2H), 1.67 – 1.34 (m, 4H), 1.12 (s, 3H). **^{13}C NMR** ($CDCl_3$, 150 MHz) δ 170.36, 147.03, 143.76, 136.80, 135.54, 128.71, 128.44, 128.21, 128.07, 122.59, 120.19, 117.26, 113.51, 86.17, 67.24, 48.08, 37.22, 24.31, 23.56, 22.83, 21.87, 20.49. **HRMS** (ESI) *m/z* calcd for $C_{27}H_{30}NO_4$ ($[M+H]^+$) 432.2169; found 432.2181.

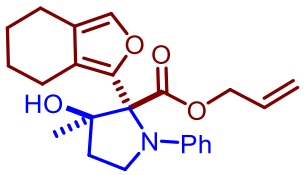

Allyl 3-hydroxy-3-methyl-1-phenyl-2-(4,5,6,7-tetrahydroisobenzofuran-1-yl)pyrrolidine-2-carboxylate (3o). Synthesized using general procedure 3. Colourless oil. (51% NMR yield using 1,3,5-trimethoxybenzene as reference.) **TLC**: R_f 0.50 (ethyl acetate/hexanes = 3:7). **^{1}H NMR** ($CDCl_3$, 400 MHz): δ 7.18 (s, 1H), 7.11 (t, J = 2.3 Hz, 2H), 6.68 (t, J = 7.3 Hz, 1H), 6.51 (d, J = 8.9 Hz, 1H), 4.30 – 4.04 (m, 2H), 3.80 – 3.67 (m, 1H), 3.59 (td, J = 8.6, 4.5 Hz, 1H), 2.72 (s, 1H), 2.51 – 2.41 (m, 3H), 2.28 (ddd, J = 12.1, 7.6, 4.5 Hz, 2H), 2.17 – 1.98 (m, 2H), 1.48 (d, J = 5.3 Hz, 4H), 1.17 – 1.08 (m, 6H). **^{13}C NMR** ($CDCl_3$, 100 MHz) δ 170.49, 147.02, 143.87, 136.71, 128.54, 122.53, 120.17, 117.15, 113.53, 85.94, 76.64, 61.59, 48.08, 37.22, 24.26, 23.59, 22.85, 21.94, 20.49, 14.14. **HRMS** (ESI) *m/z* calcd for $C_{22}H_{28}NO_4$ ($[M+H]^+$) 370.20185; found 370.2009.

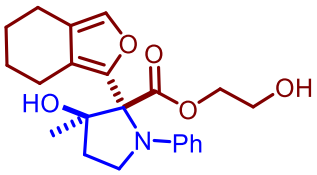

2-Hydroxyethyl 3-hydroxy-3-methyl-1-phenyl-2-(4,5,6,7-tetrahydroisobenzofuran-1-yl)pyrrolidine-2-carboxylate (3p). Synthesized using general procedure 3. Colourless oil. (45% NMR yield using 1,3,5-trimethoxybenzene as reference.) **TLC**: R_f 0.12 (ethyl acetate/hexanes = 2:3). **^{1}H NMR** (CD_3OD, 400 MHz): δ 7.17 (s, 1H), 7.01 (t, J = 7.8 Hz, 2H), 6.58 (t, J = 7.2 Hz, 1H), 6.41 (d, J = 8.1 Hz, 2H), 4.27 – 4.09 (m, 2H), 3.74 (q, J = 8.0, 7.5 Hz, 1H), 3.68 – 3.49 (m, 3H), 2.44 (d, J = 5.6 Hz, 2H), 2.30 – 2.04 (m, 4H), 1.51 (d, J = 41.6 Hz, 4H), 1.11 (s, 3H). **^{13}C NMR** (CD_3OD, 100 MHz) δ 171.07, 148.15, 145.16, 137.60, 129.19, 123.71, 120.87, 117.52, 114.23, 87.08, 78.43, 67.05, 60.68, 48.67, 38.85, 24.66, 24.35, 23.96, 23.24, 21.33. **HRMS** (ESI) *m/z* calcd for $C_{22}H_{28}NO_5$ ($[M+H]^+$) 386.1968; found 386.1978.

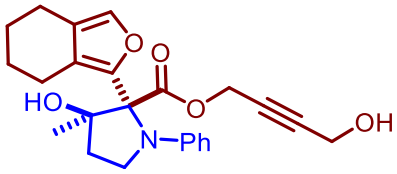

4-Hydroxybut-2-yn-1-yl 3-hydroxy-3-methyl-1-phenyl-2-(4,5,6,7-tetrahydroisobenzofuran-1-yl)pyrrolidine-2-carboxylate (3q). Synthesized using general procedure 3. Colourless oil. (36% NMR yield using 1,3,5-trimethoxybenzene as reference.) **TLC**: R_f 0.15 (ethyl acetate/hexanes = 2:3) **^{1}H NMR** ($CDCl_3$, 400 MHz): δ 7.19 (s, 1H), 7.13 (dd, J = 8.6, 7.2 Hz, 2H), 6.70 (dd, J = 8.0, 6.8 Hz, 1H), 6.57 – 6.43 (m, 2H), 4.76 (dt, J = 6.6, 1.9 Hz, 2H), 4.19 (s, 2H), 3.76 (q, J = 8.0 Hz, 1H), 3.62 (td, J = 8.6, 4.9 Hz, 1H), 2.65 (s, 1H), 2.59 – 2.45 (m, 2H), 2.37 – 2.22 (m, 2H), 2.17 – 2.00 (m, 2H), 1.78 – 1.66 (m, 4H), 1.55 – 1.46 (m, 3H), 1.11 (s, 3H). **^{13}C NMR** ($CDCl_3$, 100 MHz)): δ 169.96,

146.90, 143.40, 136.85, 128.65, 122.60, 120.36, 117.24, 113.62, 86.34, 85.21, 79.75, 77.36, 52.91, 51.13, 48.19, 37.12, 24.43, 23.54, 22.81, 21.91, 20.46. **HRMS** (ESI) *m/z* calcd for $C_{24}H_{28}NO_5$ ($[M+H]^+$) 410.19677; found 410.1977.

2.13.4. Synthesis of Insertion Product (10)

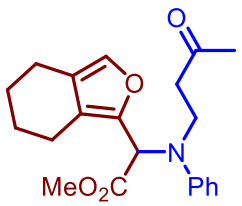

To a vial was added 4-(phenylamino)butan-2-one (50 μmol, 1 equiv.), the methyl 3-(2-formylcyclohex-1-en-1-yl)propiolate (85 μmol, 1.7 equiv.) and $Rh_2(OAc)_4$ (2.5 μmol, 0.05 equiv.). The reaction mixture was stirred for overnight at RT. The product was purified by flash chromatography 1:20 ethyl acetate:hexanes gradient to 1:9 ethyl acetate:hexanes to furnish insertion product (**4**) . Colourless oil. (23% NMR yield using 1,3,5-trimethoxybenzene as reference.) **TLC**: R_f 0.67 (ethyl acetate/hexanes = 3:7). **^{1}H NMR** ($CDCl_3$, 400 MHz):): δ 7.23 (d, J = 7.4 Hz, 2H), 7.14 (s, 1H), 6.79 (t, J = 7.3 Hz, 1H), 6.75 – 6.67 (m, 2H), 5.46 (s, 1H), 3.77 (s, 3H), 3.62 (dd, J = 15.3, 10.0, 5.1 Hz), 3.55 – 3.43 (m, 1H), 2.76 (dd, J = 15.7, 10.1, 5.4 Hz), 2.62 – 2.18 (m, 5H), 2.05 (s, 3H), 1.77 – 1.49 (m, 4H). **^{13}C NMR** ($CDCl_3$, 100 MHz)): δ 208.47, 171.02, 147.40, 141.72, 137.44, 129.58, 122.80, 121.66, 118.34, 113.63, 77.36, 59.23, 52.69, 42.19, 41.98, 30.47, 23.06, 23.01, 20.34, 20.21. **HRMS** (ESI) *m/z* calcd for $C_{21}H_{25}NO_4Na$ ($[M+Na]^+$) 378.1682; found 378.1675.

2.14. APPENDIX 1

Spectra Relevant to Chapter 2

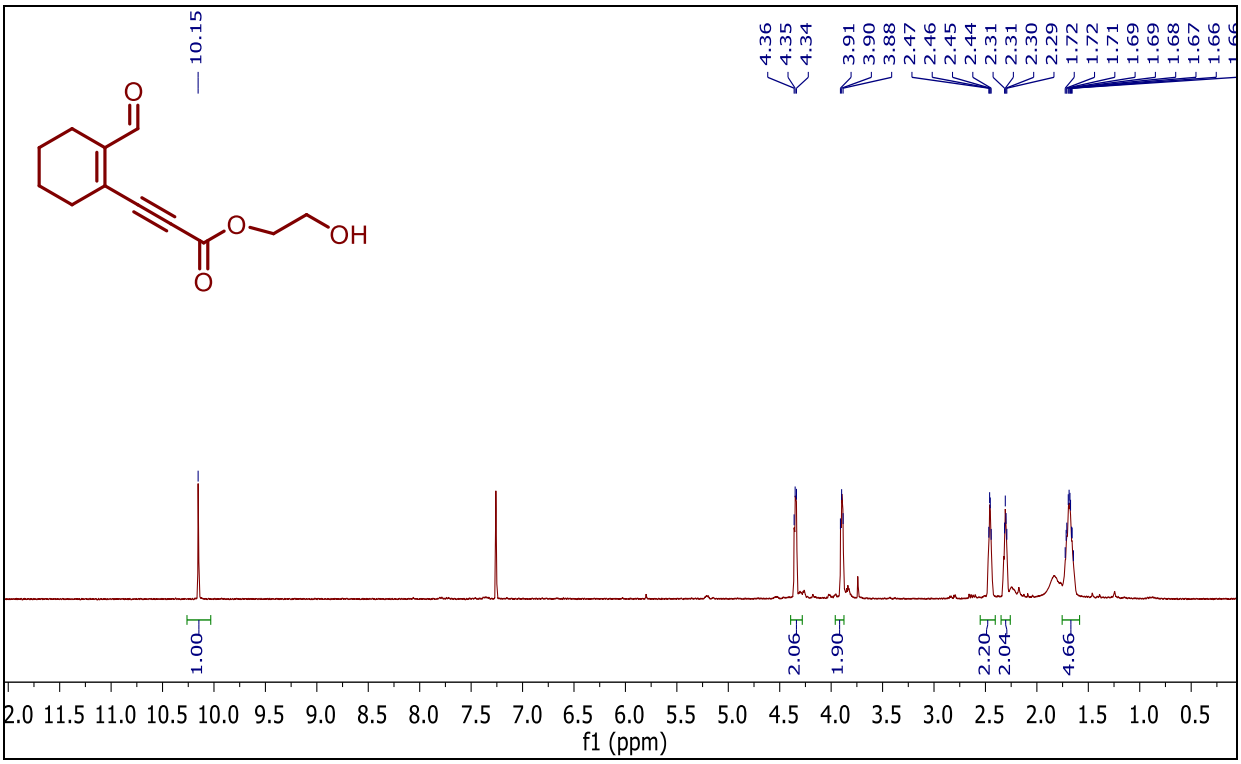
10.15
4.36
4.35
4.34
3.91
3.90
3.88
2.47
2.46
2.45
2.44
2.31
2.30
2.29
1.72
1.71
1.69
1.68
1.67
1.66
O
O
O
OH
1.00
2.06
1.90
2.20
2.04
4.66
2.0 11.5 11.0 10.5 10.0 9.5 9.0 8.5 8.0 7.5 7.0 6.5 6.0 5.5 5.0 4.5 4.0 3.5 3.0 2.5 2.0 1.5 1.0 0.5
f1 (ppm)

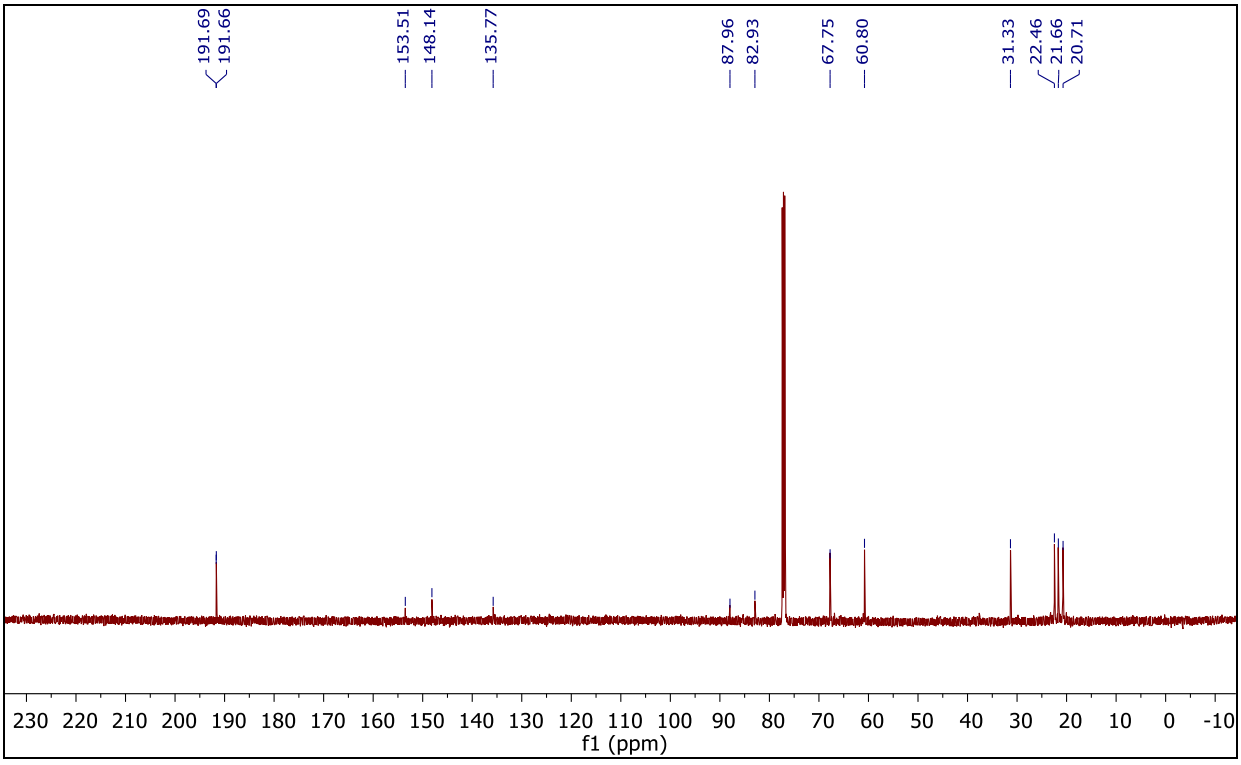
191.69
191.66
153.51
148.14
135.77
87.96
82.93
67.75
60.80
31.33
22.46
21.66
20.71
230 220 210 200 190 180 170 160 150 140 130 120 110 100 90 80 70 60 50 40 30 20 10 0 -10
f1 (ppm)

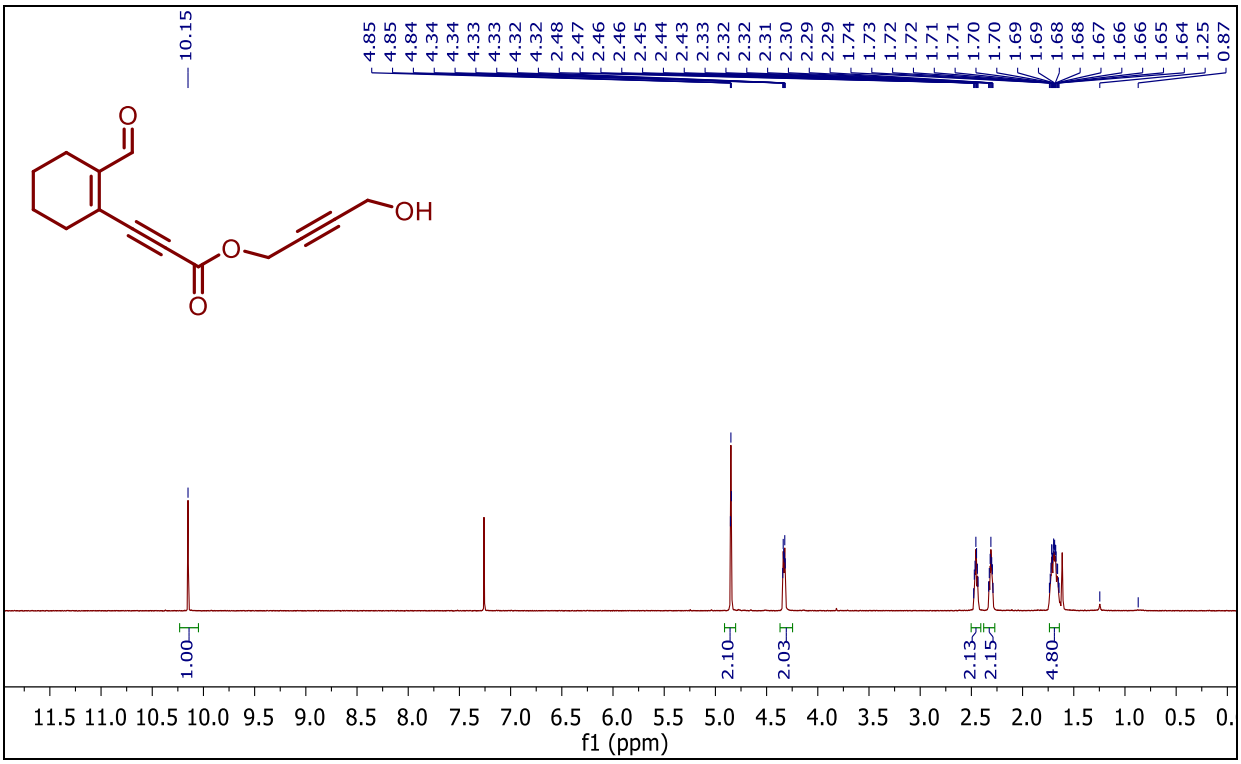
10.15
4.85
4.85
4.84
4.34
4.34
4.33
4.33
4.32
4.32
2.48
2.47
2.46
2.46
2.45
2.44
2.43
2.33
2.32
2.32
2.31
2.30
2.29
2.29
1.74
1.73
1.72
1.72
1.71
1.71
1.70
1.70
1.69
1.69
1.68
1.68
1.67
1.66
1.66
1.65
1.64
1.25
0.87
O
O
O
OH
1.00
2.10
2.03
2.13
2.15
4.80
11.5 11.0 10.5 10.0 9.5 9.0 8.5 8.0 7.5 7.0 6.5 6.0 5.5 5.0 4.5 4.0 3.5 3.0 2.5 2.0 1.5 1.0 0.5 0.
f1 (ppm)

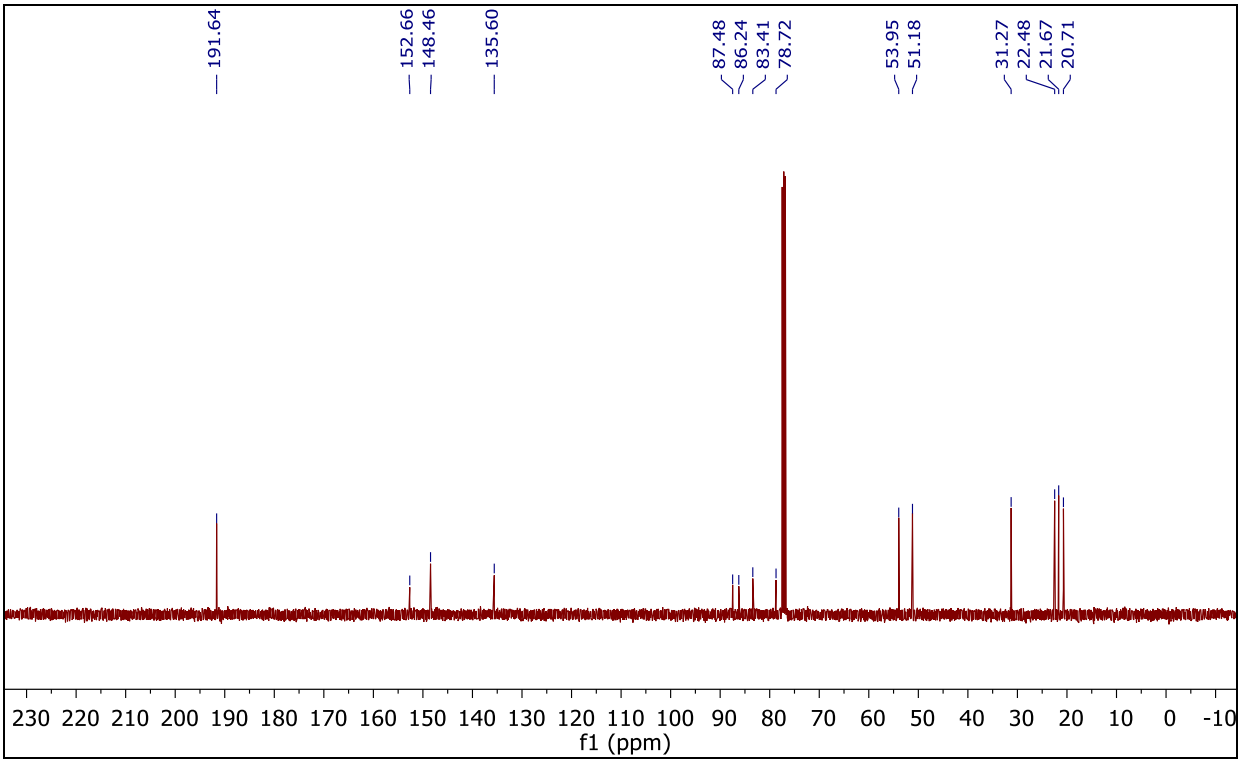
191.64
152.66
148.46
135.60
87.48
86.24
83.41
78.72
53.95
51.18
31.27
22.48
21.67
20.71
230 220 210 200 190 180 170 160 150 140 130 120 110 100 90 80 70 60 50 40 30 20 10 0 -10
f1 (ppm)

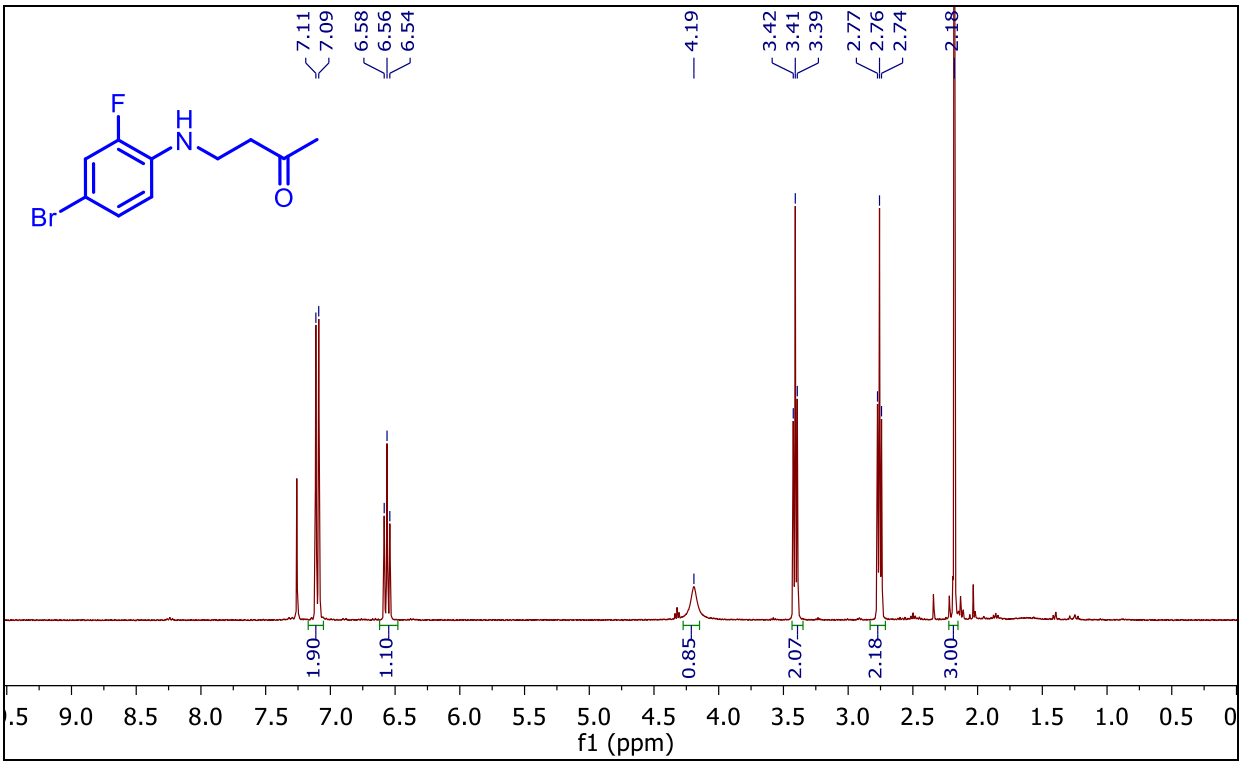
7.11
7.09
6.58
6.56
6.54
4.19
3.42
3.41
3.39
2.77
2.76
2.74
2.18
F
H
N
O
Br
1.90
1.10
0.85
2.07
2.18
3.00
f1 (ppm)

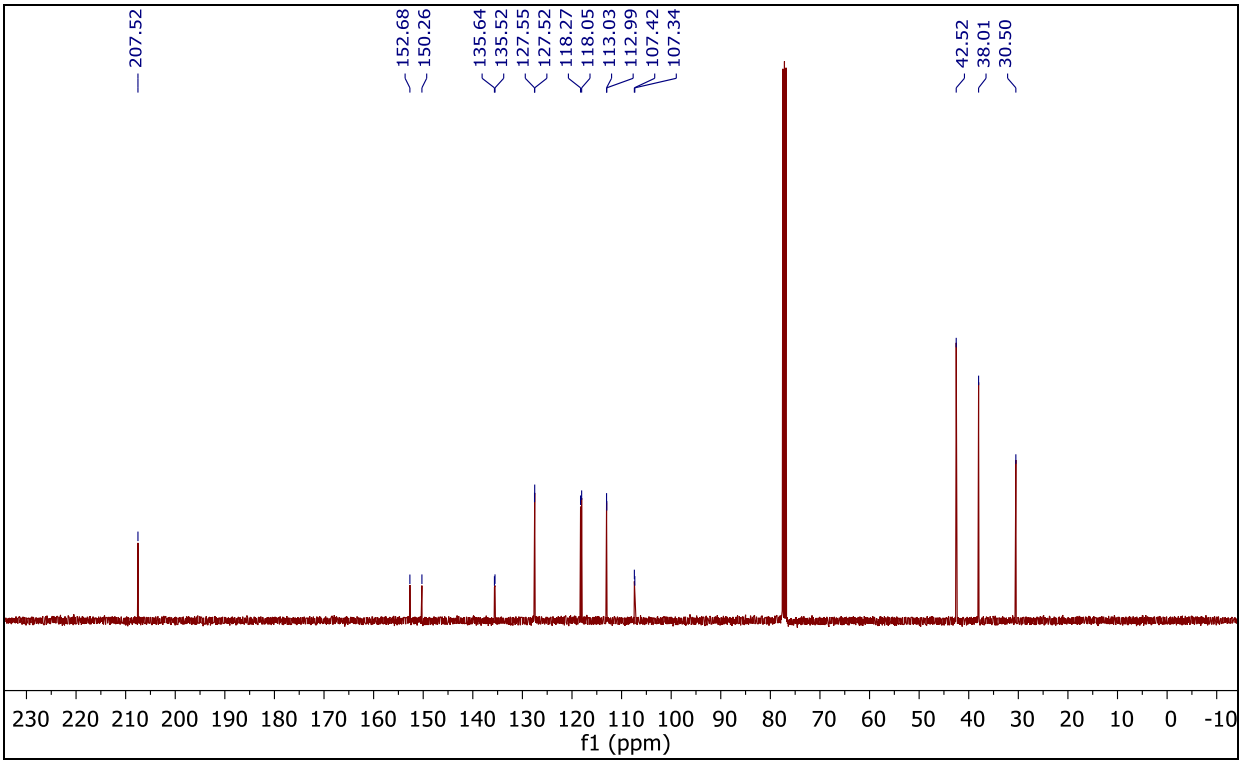
207.52
152.68
150.26
135.64
135.52
127.55
127.52
118.27
118.05
113.03
112.99
107.42
107.34
42.52
38.01
30.50
f1 (ppm)

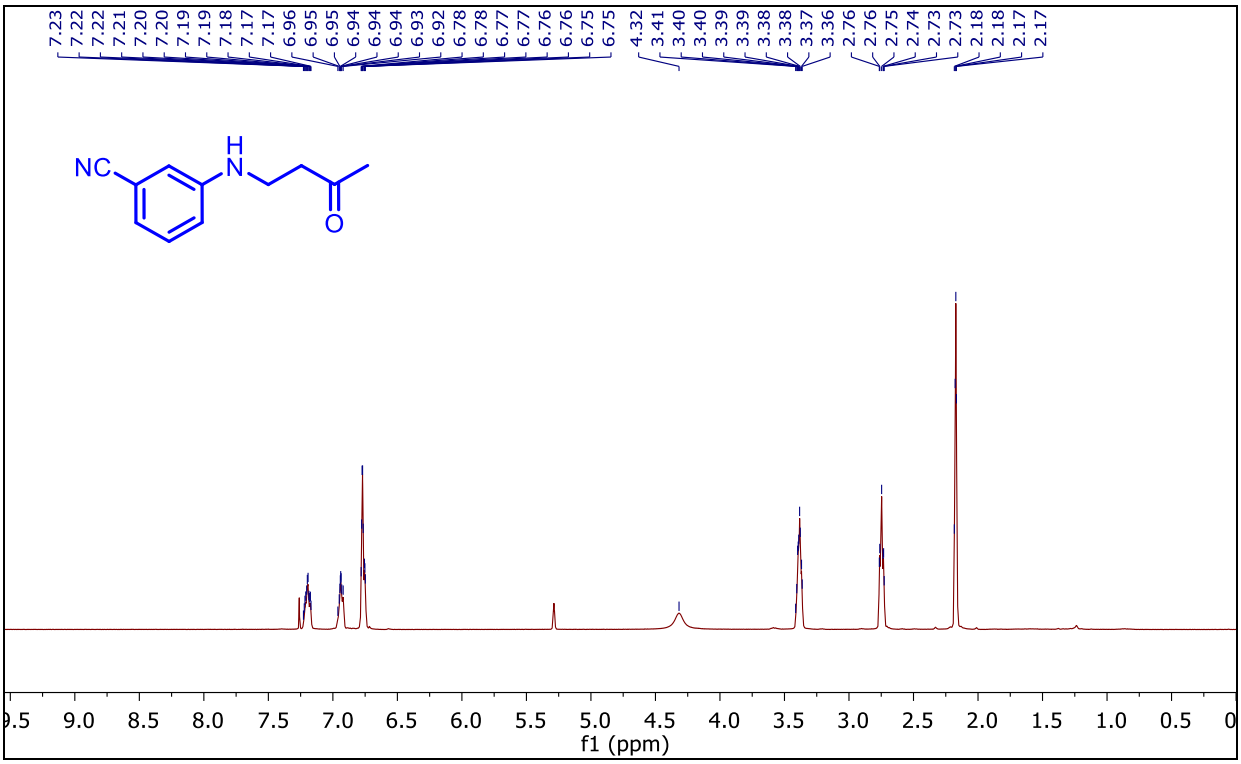
7.23 7.22 7.22 7.21 7.20 7.20 7.19 7.19 7.18 7.17 7.17 6.96 6.95 6.95 6.94 6.94 6.94 6.93 6.92 6.78 6.78 6.77 6.77 6.76 6.76 6.75 6.75
4.32 3.41 3.40 3.40 3.39 3.39 3.38 3.38 3.37 3.36
2.76 2.76 2.75 2.74 2.73 2.73 2.18 2.18 2.17 2.17
NC
H
N
O
9.5 9.0 8.5 8.0 7.5 7.0 6.5 6.0 5.5 5.0 4.5 4.0 3.5 3.0 2.5 2.0 1.5 1.0 0.5 0
f1 (ppm)

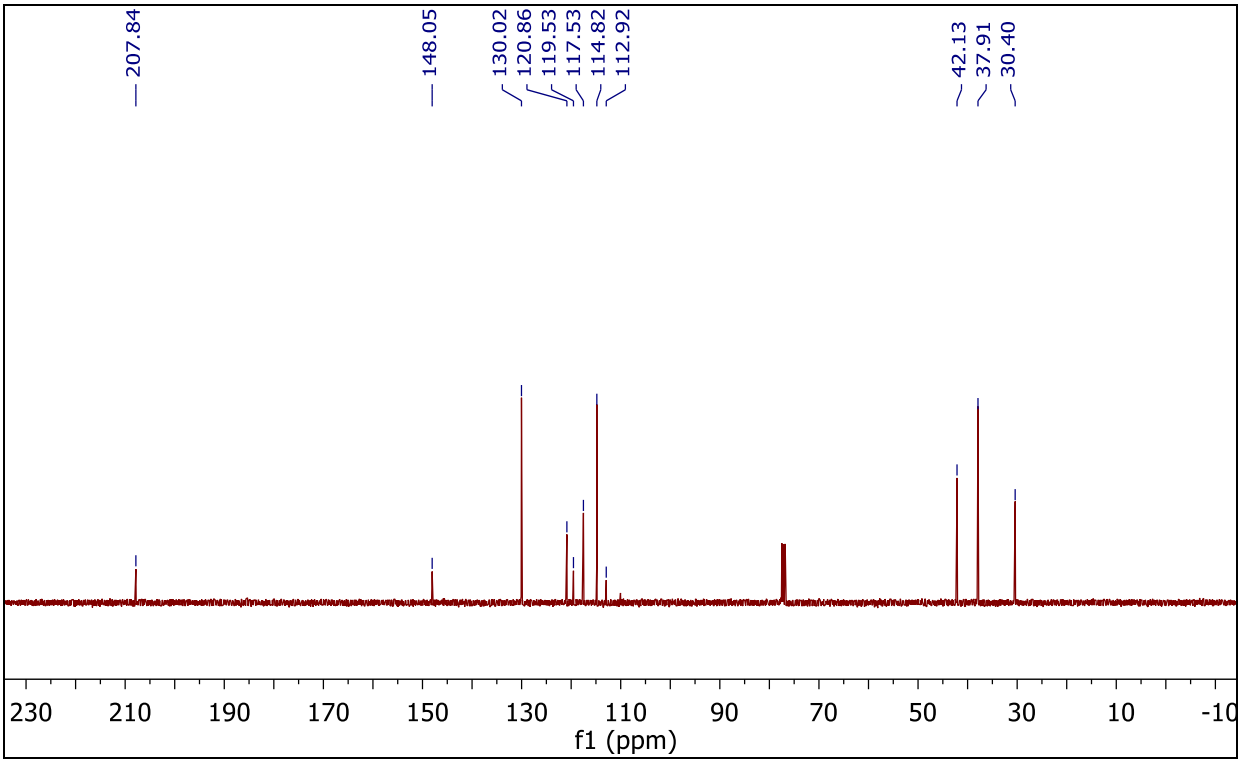
207.84
148.05
130.02
120.86
119.53
117.53
114.82
112.92
42.13
37.91
30.40
230 210 190 170 150 130 110 90 70 50 30 10 -10
f1 (ppm)

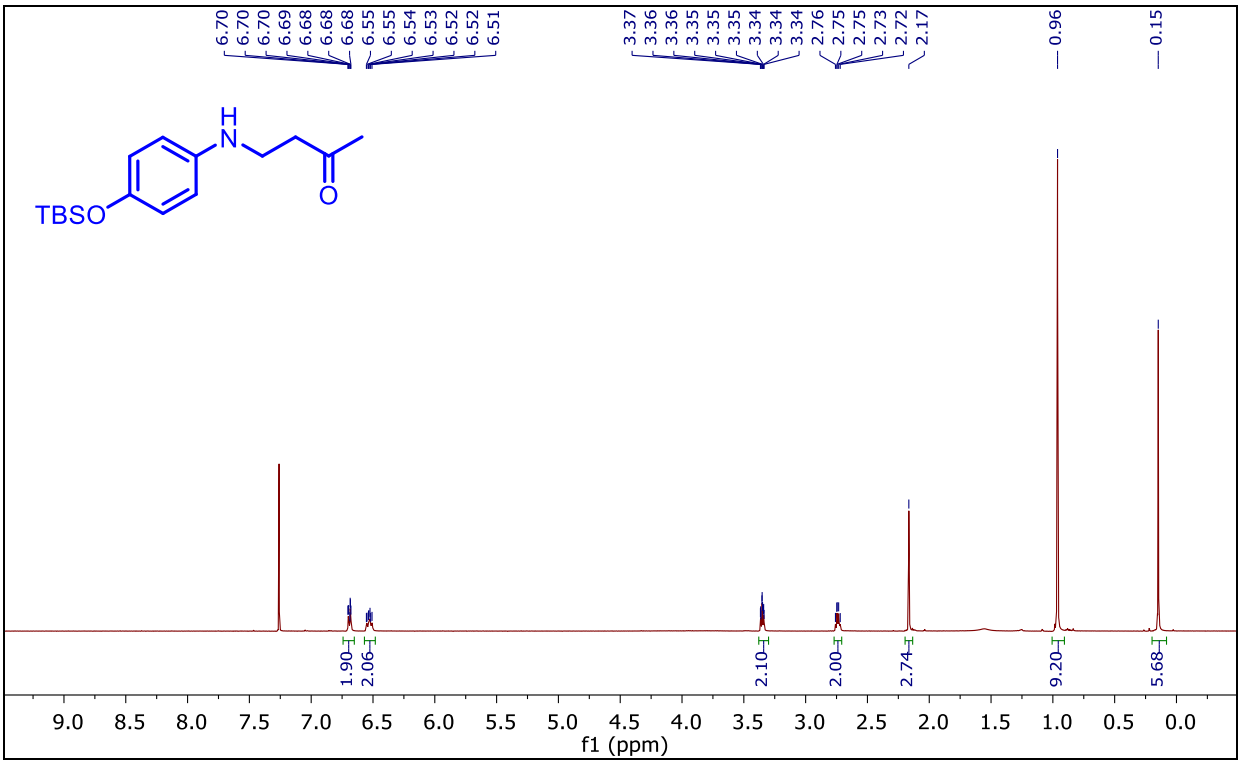
6.70
6.70
6.70
6.69
6.68
6.68
6.68
6.55
6.55
6.54
6.53
6.52
6.52
6.51
3.37
3.36
3.36
3.35
3.35
3.35
3.34
3.34
3.34
2.76
2.75
2.75
2.73
2.72
2.17
0.96
0.15
H
N
O
TBSO
1.90
2.06
2.10
2.00
2.74
9.20
5.68
9.0 8.5 8.0 7.5 7.0 6.5 6.0 5.5 5.0 4.5 4.0 3.5 3.0 2.5 2.0 1.5 1.0 0.5 0.0
f1 (ppm)

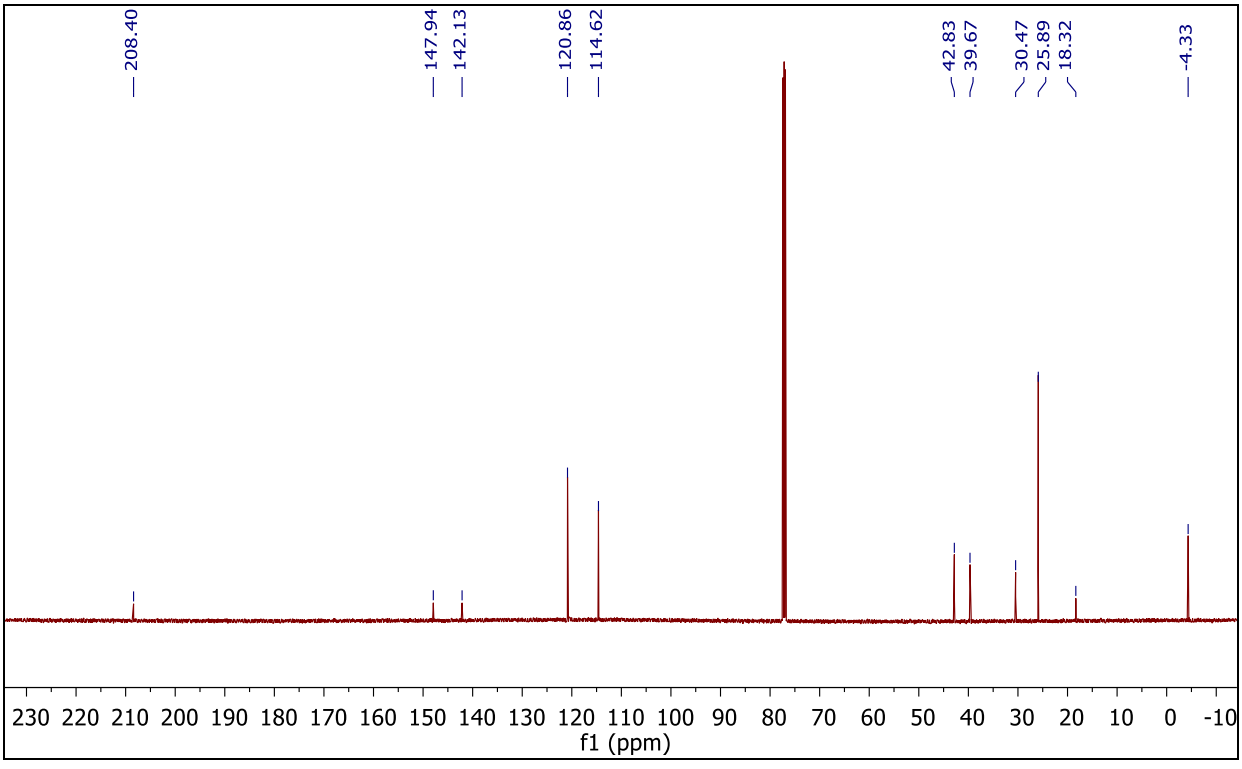
208.40
147.94
142.13
120.86
114.62
42.83
39.67
30.47
25.89
18.32
-4.33
230 220 210 200 190 180 170 160 150 140 130 120 110 100 90 80 70 60 50 40 30 20 10 0 -10
f1 (ppm)

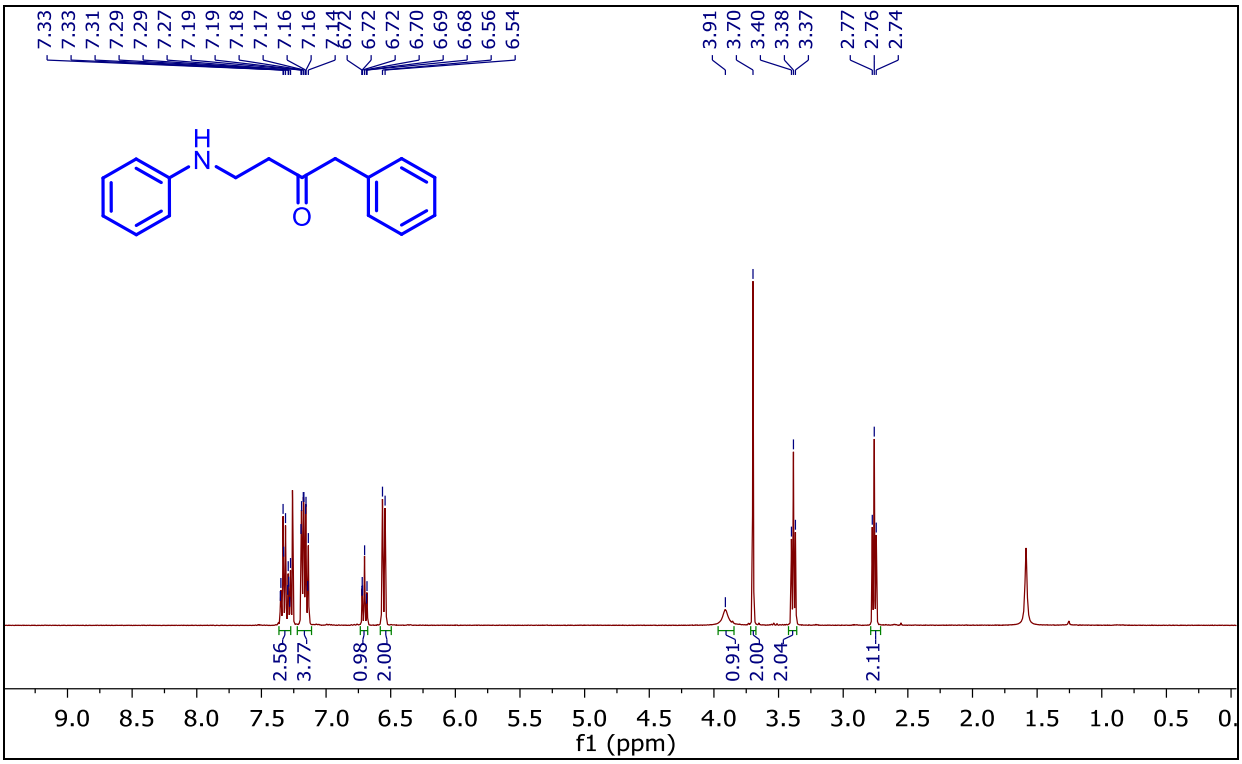
7.33
7.33
7.31
7.29
7.29
7.27
7.19
7.19
7.18
7.17
7.16
7.16
7.14
7.12
6.72
6.72
6.70
6.69
6.68
6.56
6.54
3.91
3.70
3.40
3.38
3.37
2.77
2.76
2.74
H
N
O
2.56
3.77
0.98
2.00
0.91
2.00
2.04
2.11
9.0 8.5 8.0 7.5 7.0 6.5 6.0 5.5 5.0 4.5 4.0 3.5 3.0 2.5 2.0 1.5 1.0 0.5 0.
f1 (ppm)

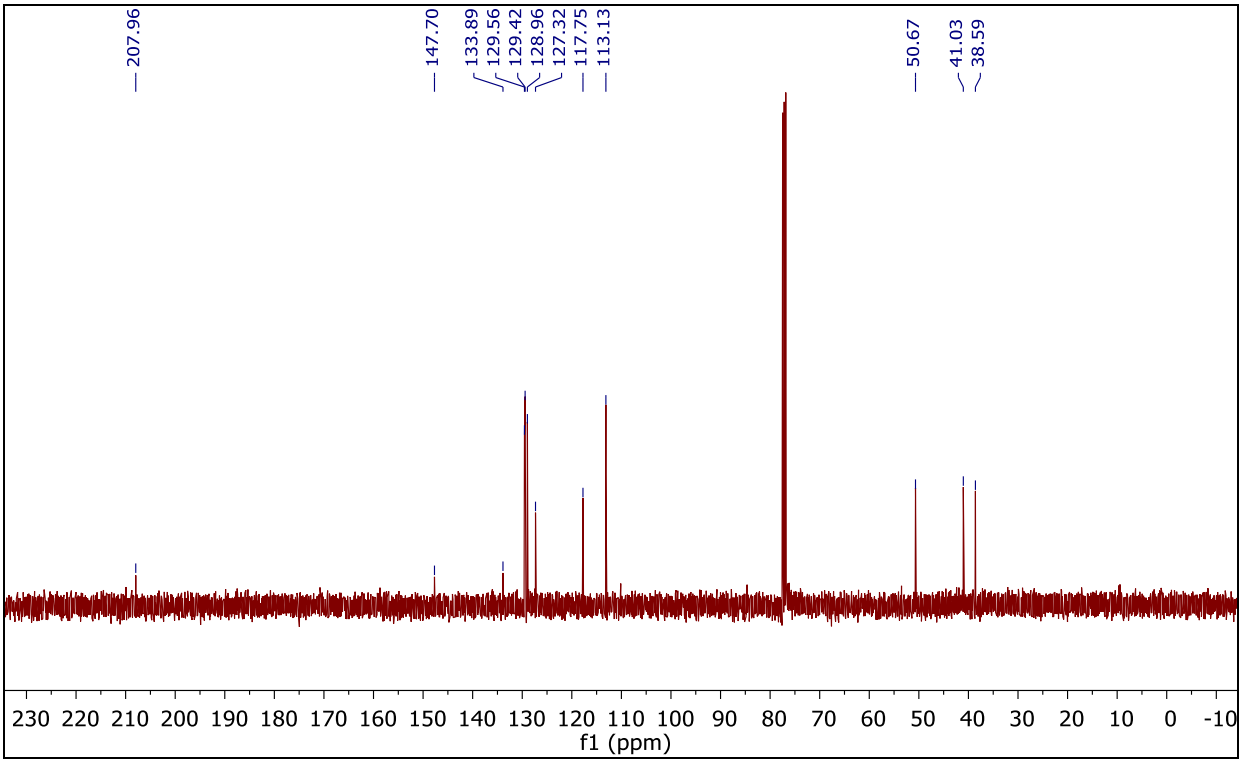
207.96
147.70
133.89
129.56
129.42
128.96
127.32
117.75
113.13
50.67
41.03
38.59
230 220 210 200 190 180 170 160 150 140 130 120 110 100 90 80 70 60 50 40 30 20 10 0 -10
f1 (ppm)

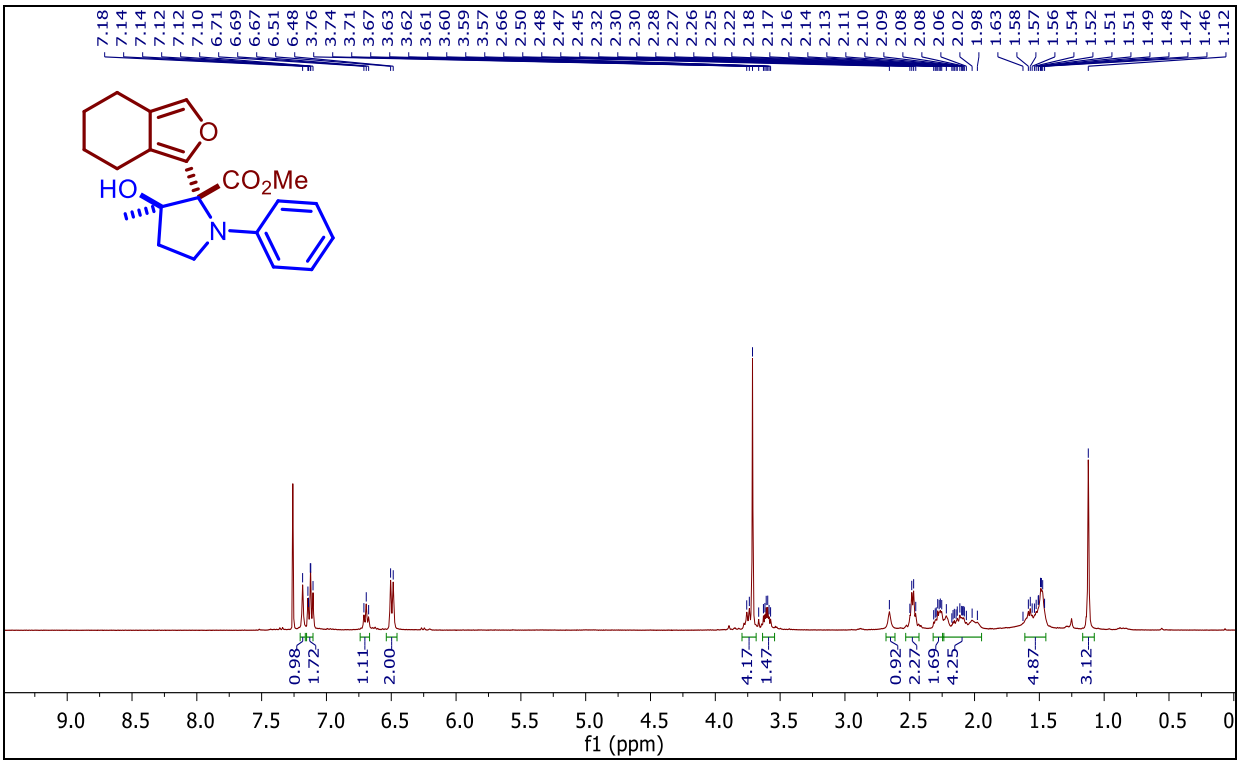
7.18 7.14 7.14 7.12 7.12 7.10 6.71 6.69 6.67 6.51 6.48 3.76 3.74 3.71 3.67 3.63 3.62 3.61 3.60 3.59 3.57 2.66 2.50 2.48 2.47 2.45 2.32 2.30 2.30 2.28 2.27 2.26 2.25 2.22 2.18 2.17 2.16 2.14 2.13 2.11 2.10 2.09 2.08 2.08 2.06 2.02 1.98 1.63 1.58 1.57 1.56 1.54 1.52 1.51 1.51 1.49 1.48 1.47 1.46 1.12
HO
CO2Me
N
O
0.98 1.72 1.11 2.00 4.17 1.47 0.92 2.27 1.69 4.25 4.87 3.12
9.0 8.5 8.0 7.5 7.0 6.5 6.0 5.5 5.0 4.5 4.0 3.5 3.0 2.5 2.0 1.5 1.0 0.5 0
f1 (ppm)

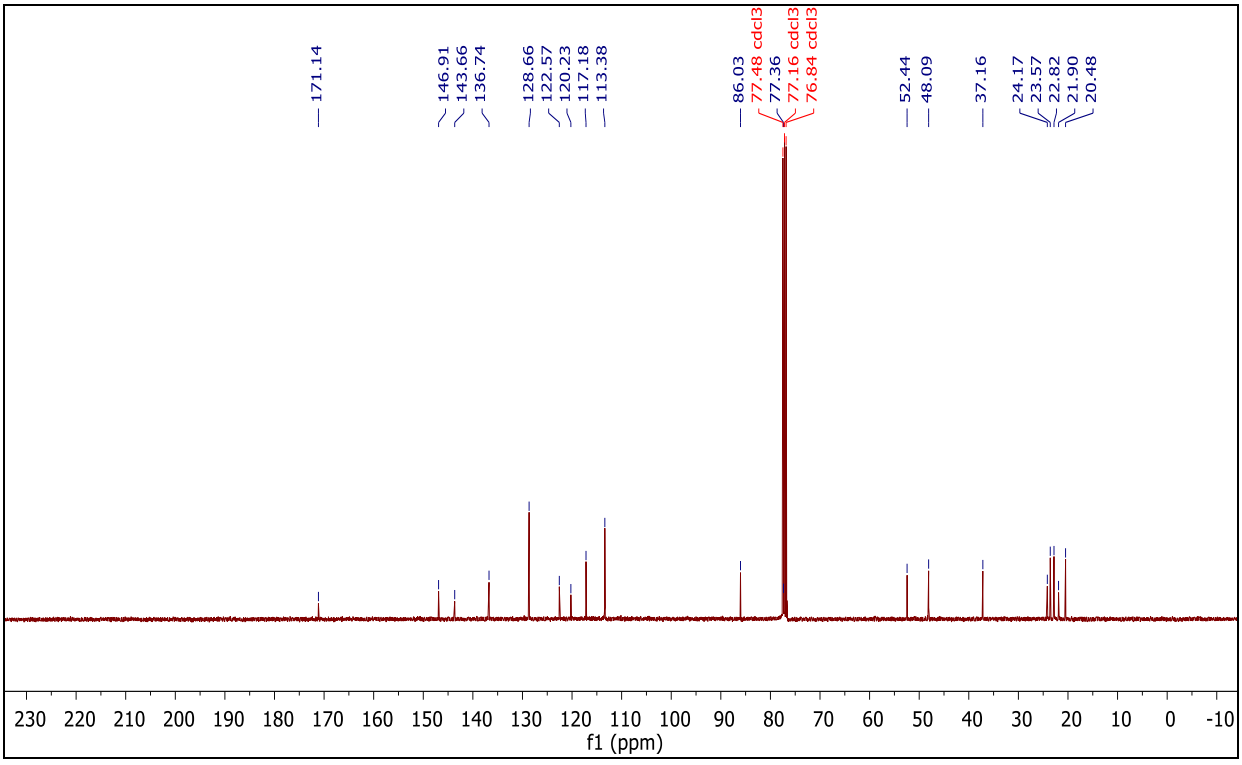
171.14
146.91 143.66 136.74
128.66 122.57 120.23 117.18 113.38
86.03
77.48 cdcl3 77.36 77.16 cdcl3 76.84 cdcl3
52.44 48.09
37.16
24.17 23.57 22.82 21.90 20.48
230 220 210 200 190 180 170 160 150 140 130 120 110 100 90 80 70 60 50 40 30 20 10 0 -10
f1 (ppm)

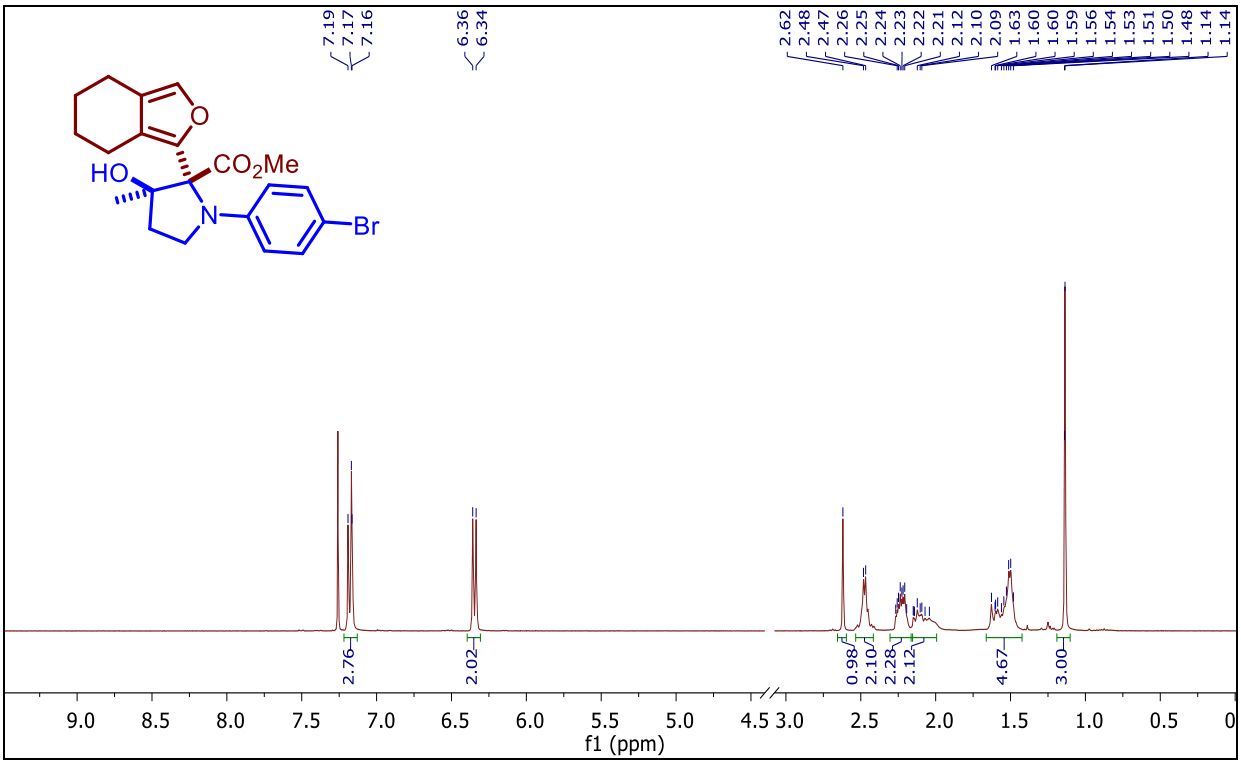
7.19
7.17
7.16
6.36
6.34
2.62
2.48
2.47
2.26
2.25
2.24
2.23
2.22
2.21
2.12
2.10
2.09
1.63
1.60
1.60
1.59
1.56
1.54
1.53
1.51
1.50
1.48
1.14
1.14
O
HO
CO2Me
N
Br
2.76
2.02
0.98
2.10
2.28
2.12
4.67
3.00
9.0
8.5
8.0
7.5
7.0
6.5
6.0
5.5
5.0
4.5
3.0
2.5
2.0
1.5
1.0
0.5
0
f1 (ppm)

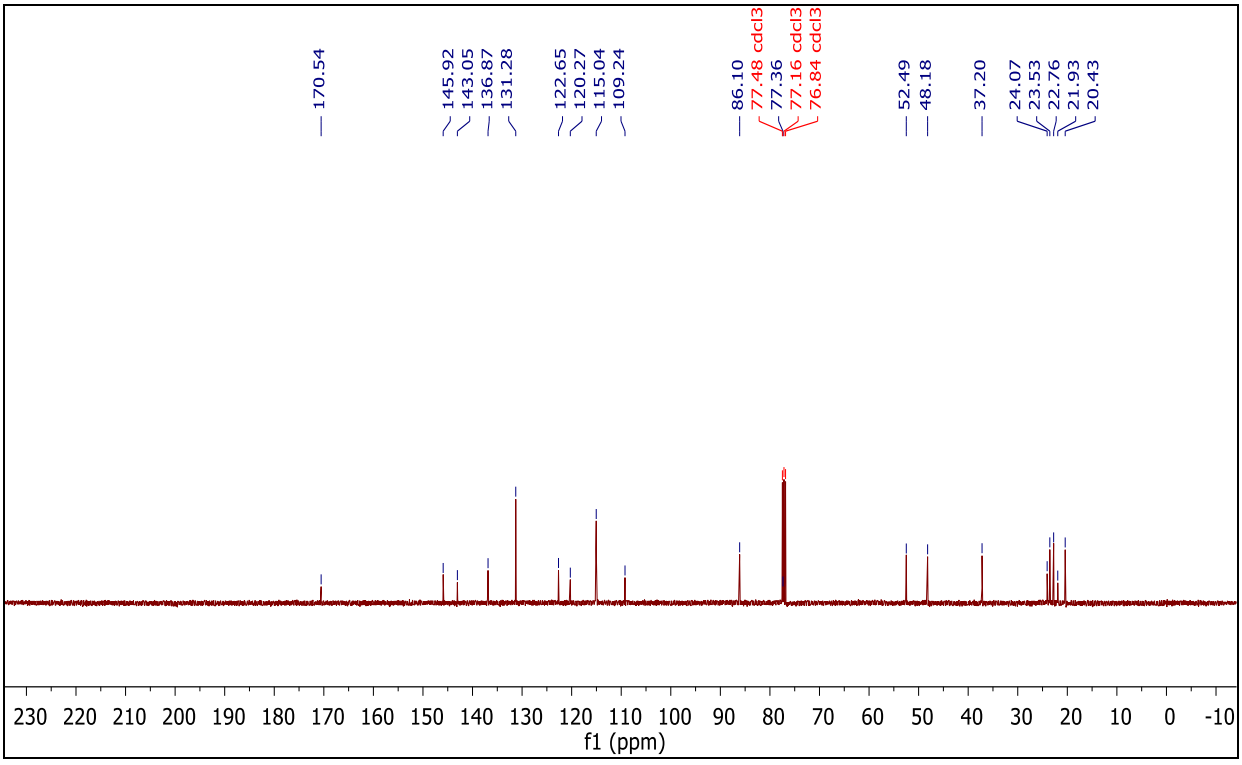
170.54
145.92
143.05
136.87
131.28
122.65
120.27
115.04
109.24
86.10
77.48 cdcl3
77.36
77.16 cdcl3
76.84 cdcl3
52.49
48.18
37.20
24.07
23.53
22.76
21.93
20.43
230
220
210
200
190
180
170
160
150
140
130
120
110
100
90
80
70
60
50
40
30
20
10
0
-10
f1 (ppm)

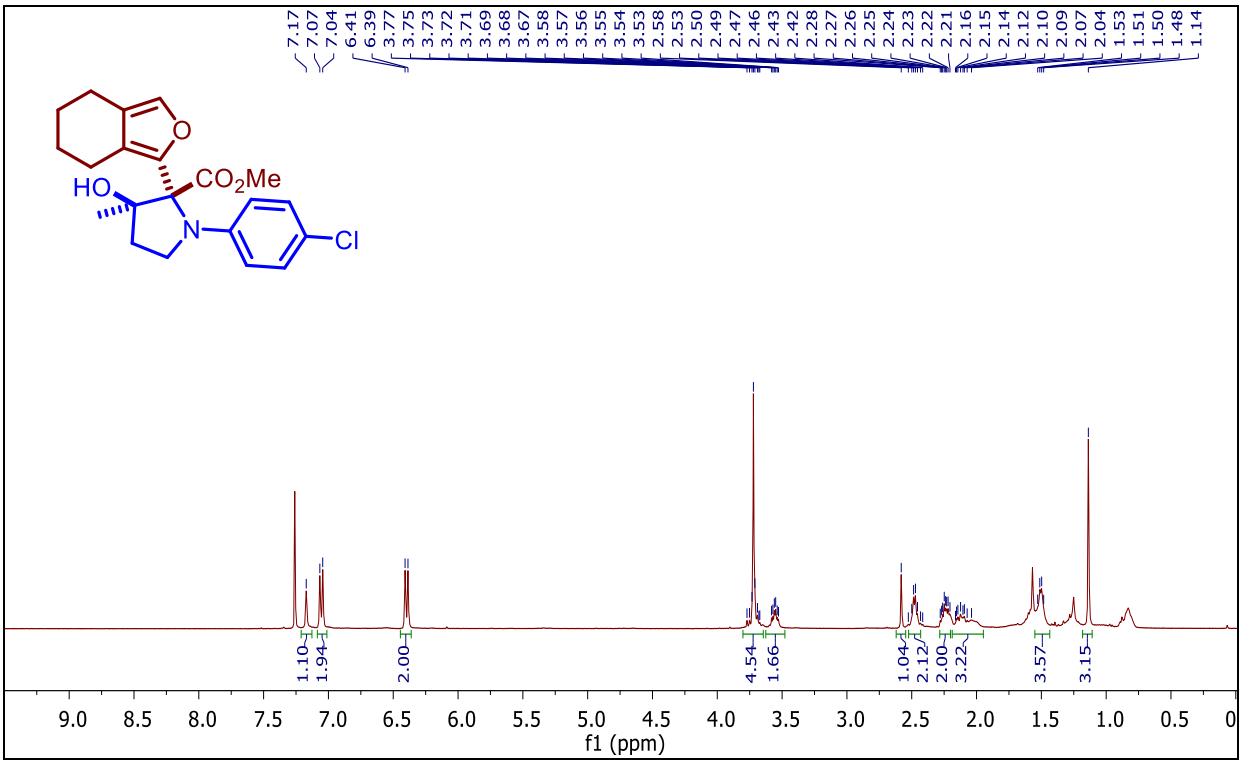
7.17 7.07 7.04 6.41 6.39 3.77 3.75 3.73 3.72 3.71 3.69 3.68 3.67 3.58 3.57 3.56 3.55 3.54 3.53 2.58 2.53 2.50 2.49 2.47 2.46 2.43 2.42 2.28 2.27 2.26 2.25 2.24 2.23 2.22 2.21 2.16 2.15 2.14 2.12 2.10 2.09 2.07 2.04 1.53 1.51 1.50 1.48 1.14
O
CO2Me
HO
N
Cl
1.10 1.94 2.00 4.54 1.66 1.04 2.12 2.00 3.22 3.57 3.15
9.0 8.5 8.0 7.5 7.0 6.5 6.0 5.5 5.0 4.5 4.0 3.5 3.0 2.5 2.0 1.5 1.0 0.5 0
f1 (ppm)

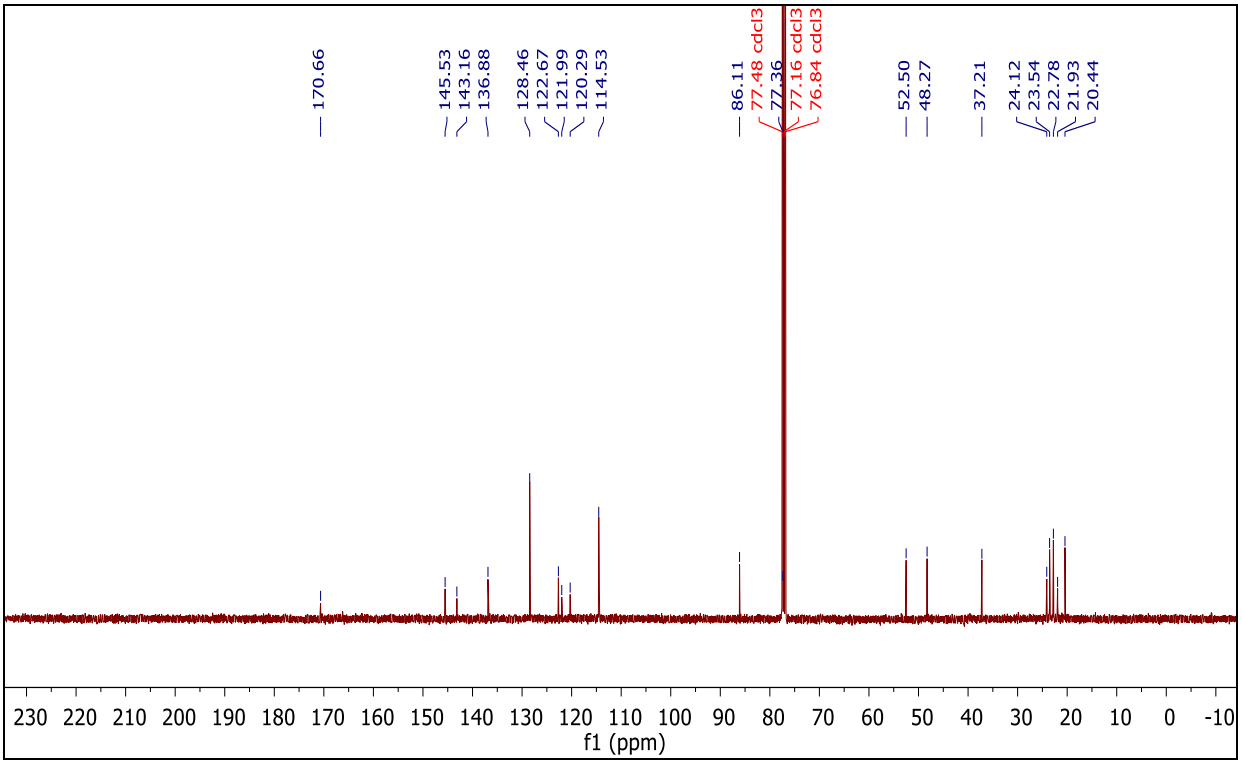
170.66
145.53 143.16 136.88 128.46 122.67 121.99 120.29 114.53
86.11 77.48 cdcl3 77.36 77.16 cdcl3 76.84 cdcl3
52.50 48.27 37.21 24.12 23.54 22.78 21.93 20.44
230 220 210 200 190 180 170 160 150 140 130 120 110 100 90 80 70 60 50 40 30 20 10 0 -10
f1 (ppm)

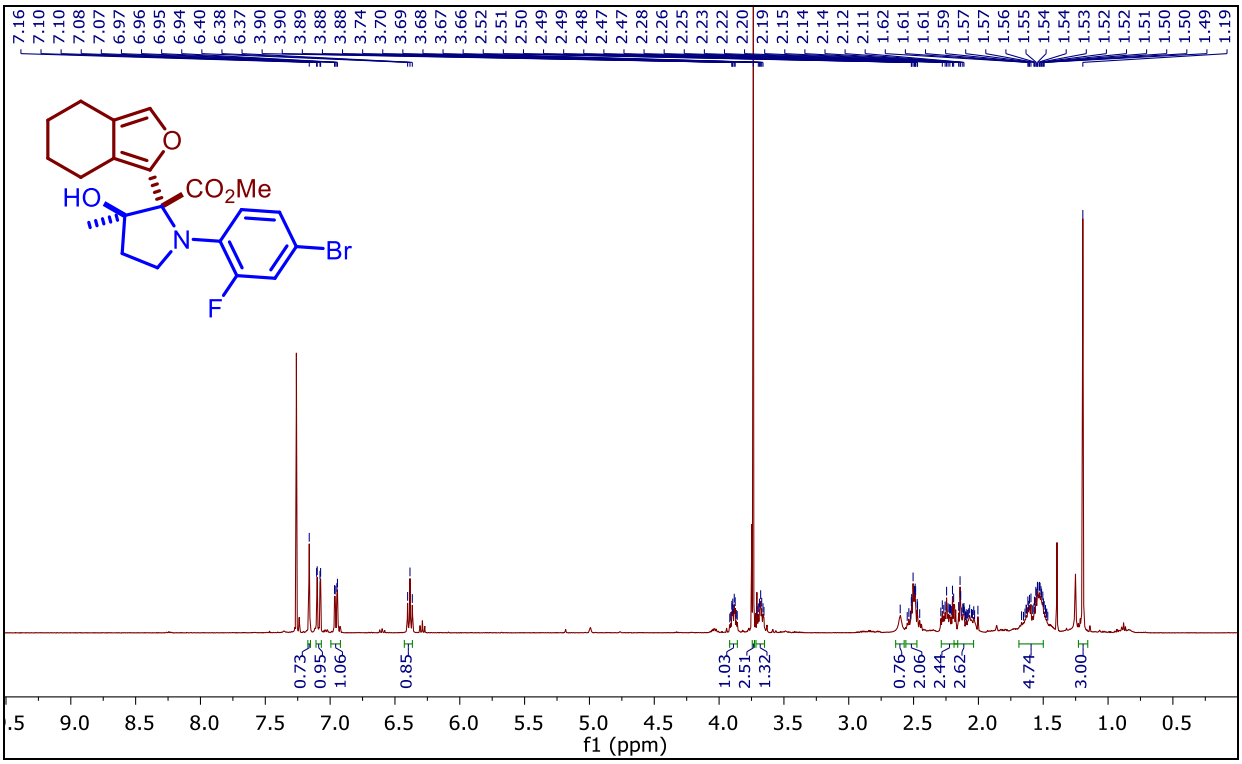
HO
CO2Me
N
Br
F
f1 (ppm)

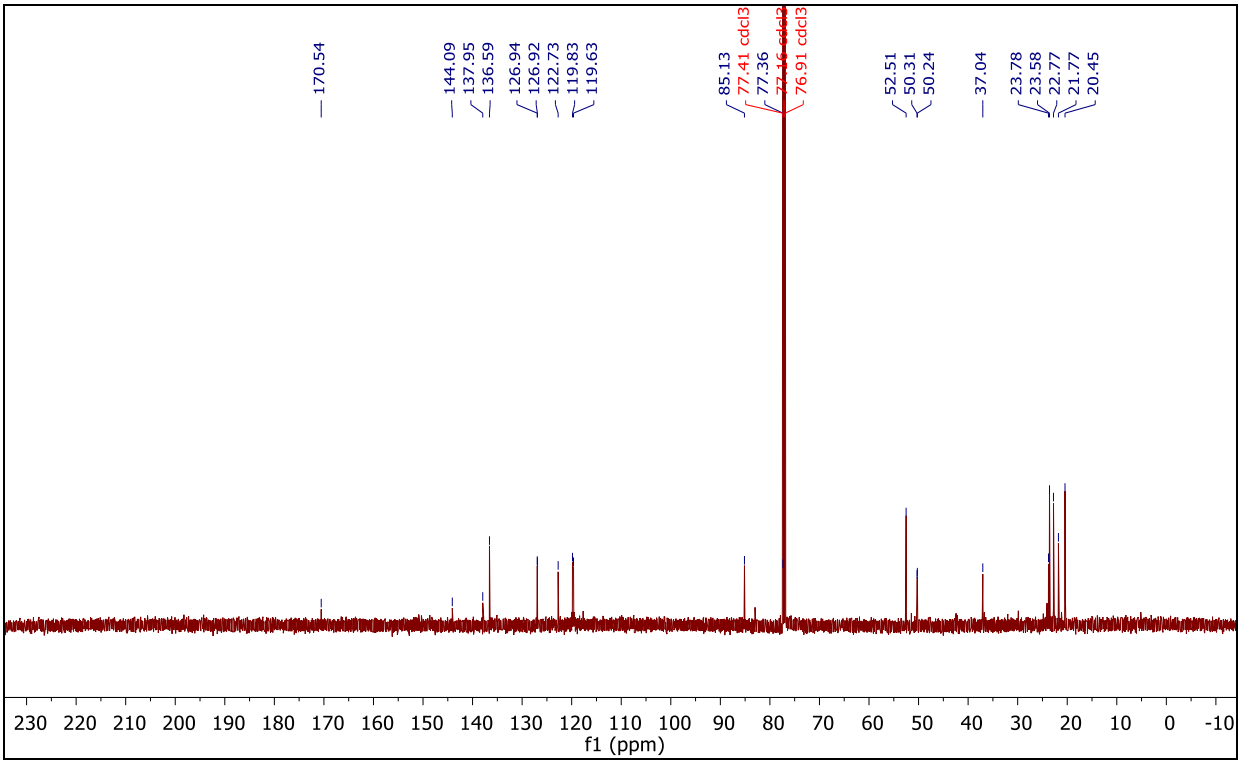
f1 (ppm)

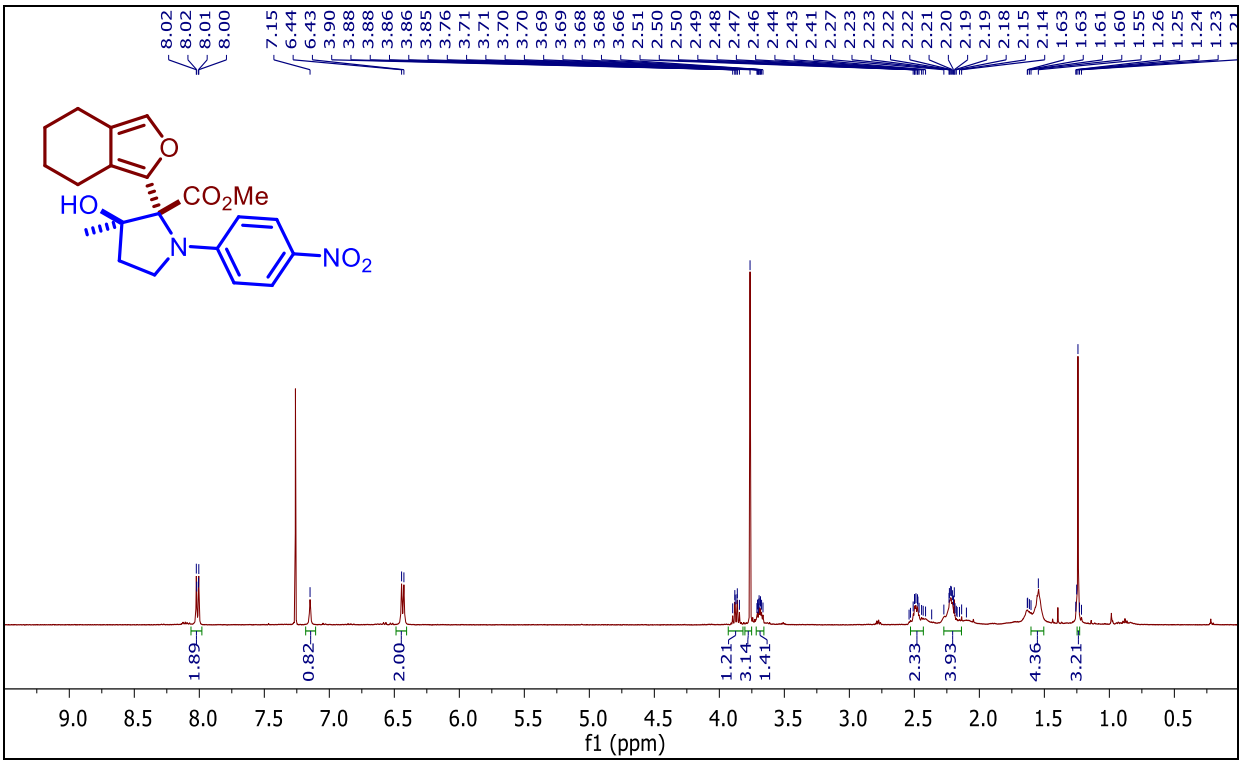
8.02 8.02 8.01 8.00 7.15 6.44 6.43 3.90 3.88 3.88 3.86 3.86 3.85 3.76 3.71 3.71 3.70 3.70 3.69 3.69 3.68 3.68 3.66 2.51 2.50 2.50 2.49 2.48 2.47 2.46 2.44 2.43 2.41 2.27 2.23 2.23 2.22 2.22 2.21 2.20 2.19 2.19 2.18 2.15 2.14 1.63 1.63 1.61 1.60 1.55 1.26 1.25 1.24 1.23
O
HO
CO2Me
N
NO2
1.89 0.82 2.00 1.21 3.14 1.41 2.33 3.93 4.36 3.21
9.0 8.5 8.0 7.5 7.0 6.5 6.0 5.5 5.0 4.5 4.0 3.5 3.0 2.5 2.0 1.5 1.0 0.5
f1 (ppm)

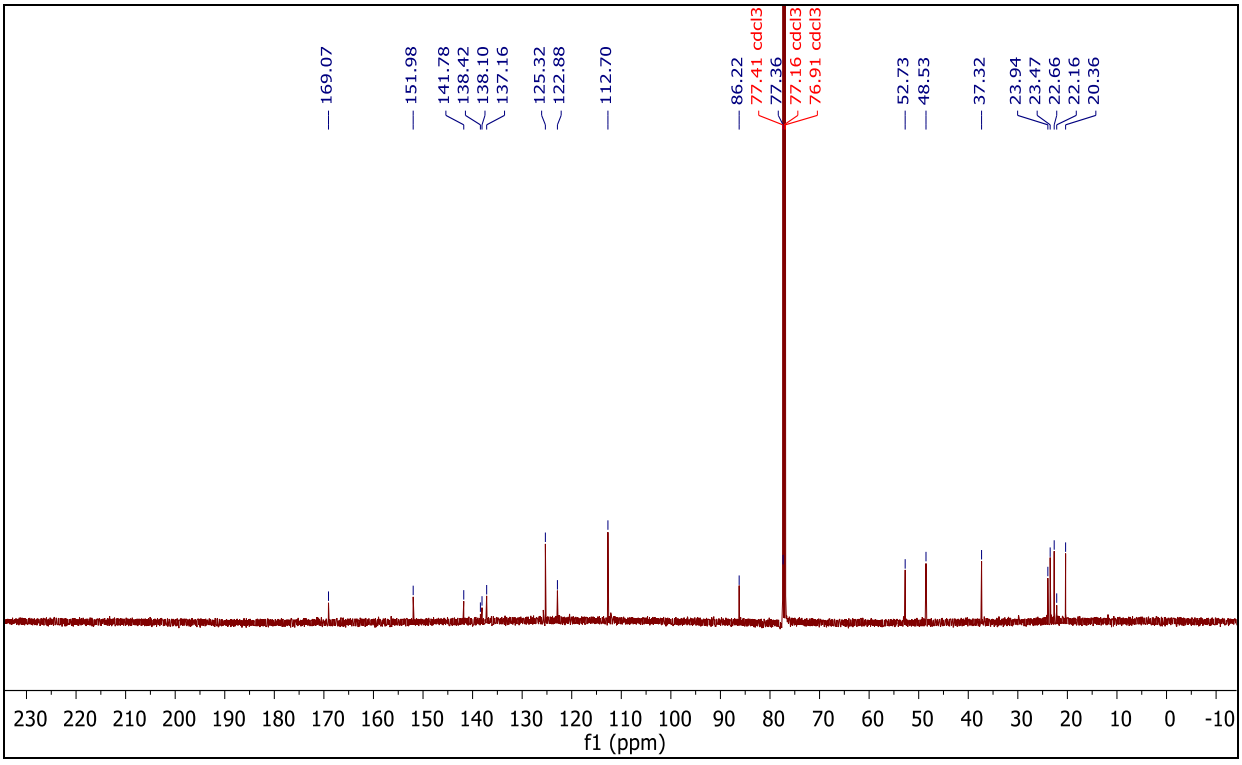
169.07 151.98 141.78 138.42 138.10 137.16 125.32 122.88 112.70 86.22 77.41 cdcl3 77.36 77.16 cdcl3 76.91 cdcl3 52.73 48.53 37.32 23.94 23.47 22.66 22.16 20.36
230 220 210 200 190 180 170 160 150 140 130 120 110 100 90 80 70 60 50 40 30 20 10 0 -10
f1 (ppm)

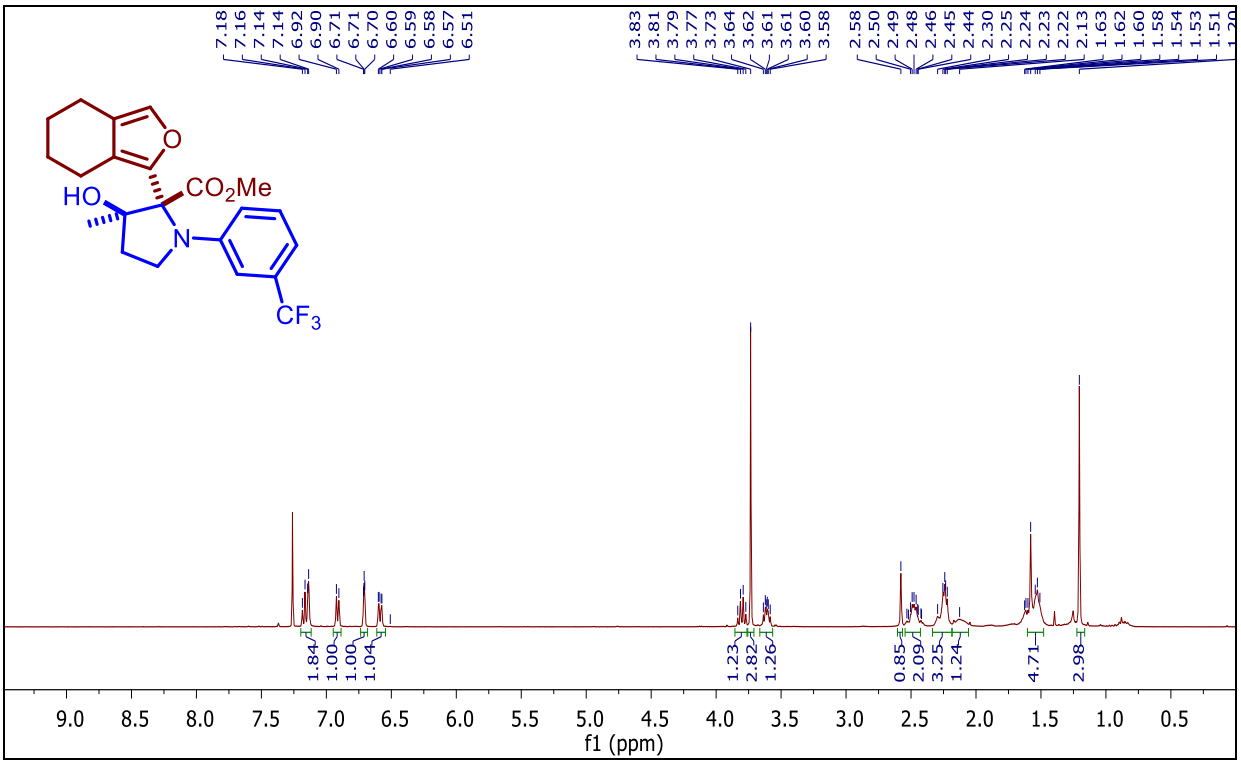
7.18 7.16 7.14 7.14 6.92 6.90 6.71 6.71 6.70 6.60 6.59 6.58 6.57 6.51
3.83 3.81 3.79 3.77 3.73 3.64 3.62 3.61 3.61 3.60 3.58
2.58 2.50 2.49 2.48 2.46 2.45 2.44 2.30 2.25 2.24 2.23 2.22 2.13 1.63 1.62 1.60 1.58 1.54 1.53 1.51
O
HO
CO2Me
N
CF3
1.84 1.00 1.00 1.04 1.23 2.82 1.26 0.85 2.09 3.25 1.24 4.71 2.98
9.0 8.5 8.0 7.5 7.0 6.5 6.0 5.5 5.0 4.5 4.0 3.5 3.0 2.5 2.0 1.5 1.0 0.5
f1 (ppm)

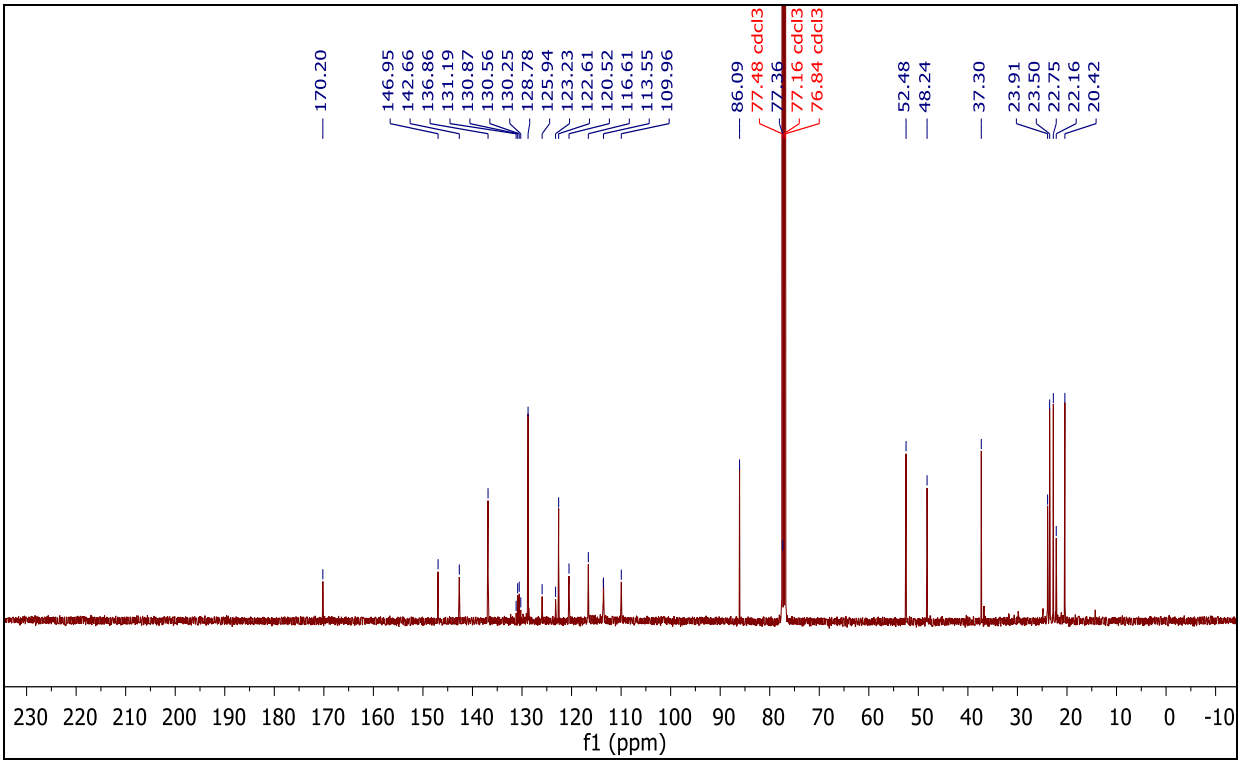
170.20
146.95 142.66 136.86 131.19 130.87 130.56 130.25 128.78 125.94 123.23 122.61 120.52 116.61 113.55 109.96
86.09
77.48 cdcl3 77.36 77.16 cdcl3 76.84 cdcl3
52.48 48.24 37.30 23.91 23.50 22.75 22.16 20.42
230 220 210 200 190 180 170 160 150 140 130 120 110 100 90 80 70 60 50 40 30 20 10 0 -10
f1 (ppm)

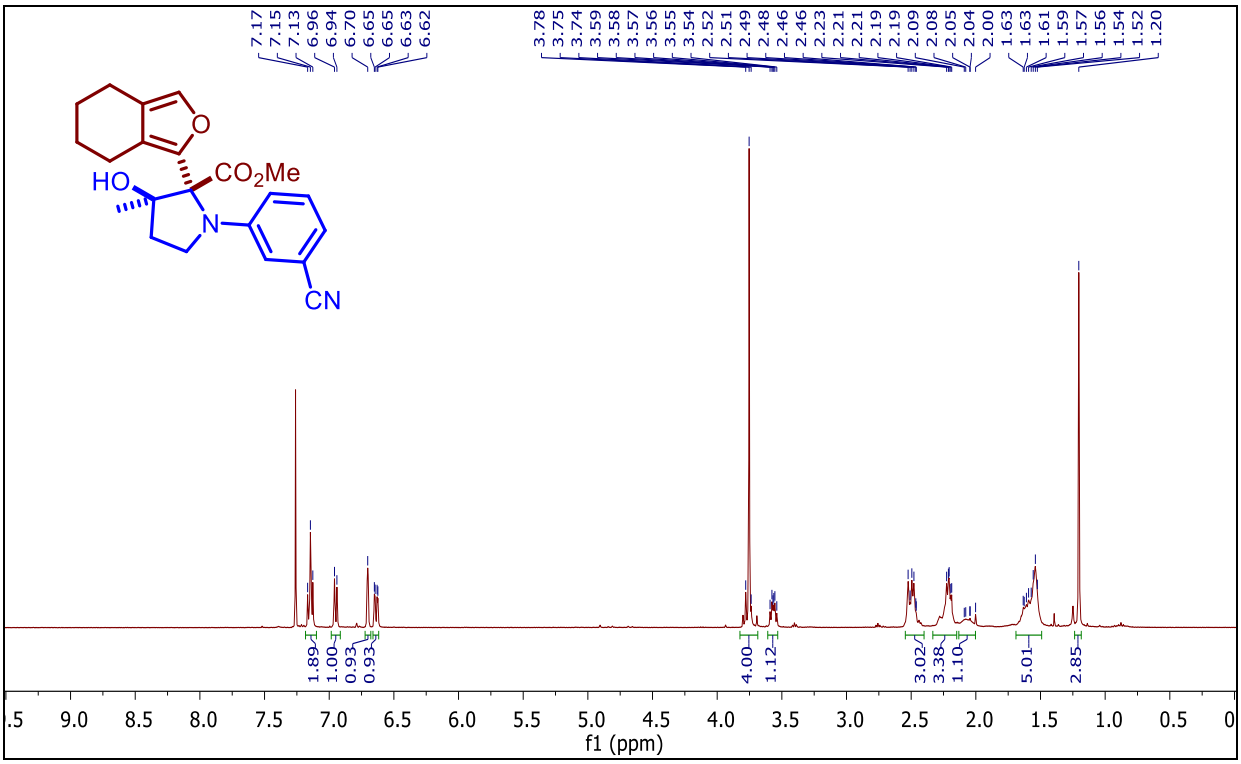
7.17
7.15
7.13
6.96
6.94
6.70
6.65
6.65
6.63
6.62
3.78
3.75
3.74
3.59
3.58
3.57
3.56
3.55
3.54
2.52
2.51
2.49
2.48
2.46
2.46
2.23
2.21
2.21
2.19
2.19
2.09
2.08
2.05
2.04
2.00
1.63
1.63
1.61
1.59
1.57
1.56
1.54
1.52
1.20
O
HO
CO2Me
N
CN
1.89
1.00
0.93
0.93
4.00
1.12
3.02
3.38
1.10
5.01
2.85
f1 (ppm)

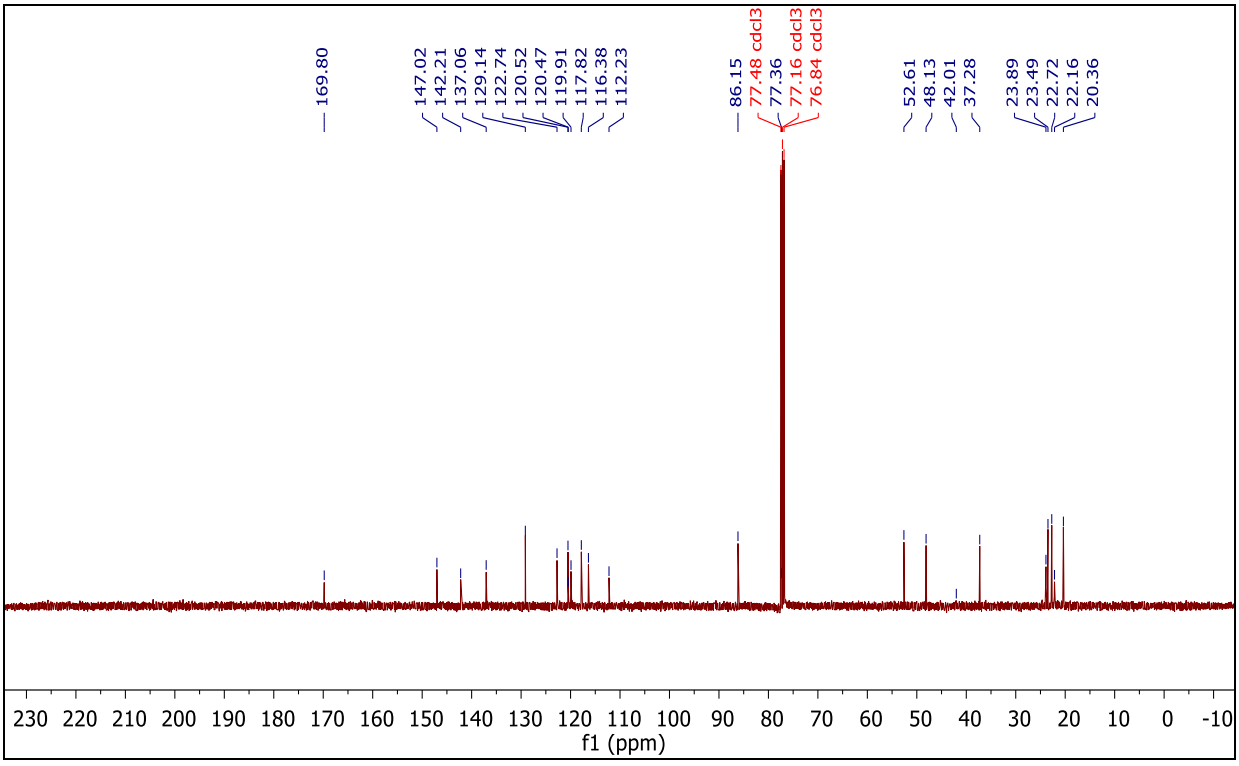
169.80
147.02
142.21
137.06
129.14
122.74
120.52
120.47
119.91
117.82
116.38
112.23
86.15
77.48 cdcl3
77.36
77.16 cdcl3
76.84 cdcl3
52.61
48.13
42.01
37.28
23.89
23.49
22.72
22.16
20.36
f1 (ppm)

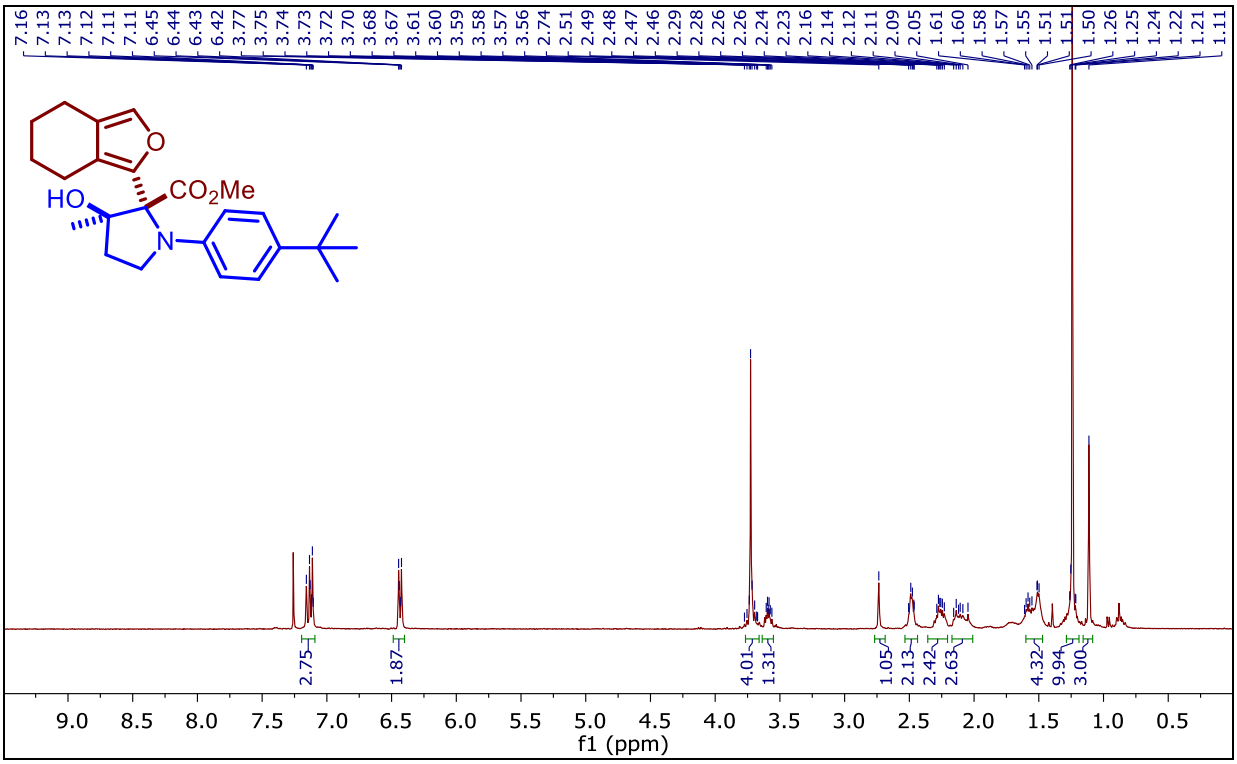
7.16 7.13 7.13 7.12 7.11 7.11 6.45 6.44 6.43 6.42 3.77 3.75 3.74 3.73 3.72 3.70 3.68 3.67 3.61 3.60 3.59 3.58 3.57 3.56 2.74 2.51 2.49 2.48 2.47 2.46 2.29 2.28 2.26 2.26 2.24 2.23 2.16 2.14 2.12 2.11 2.09 2.05 1.61 1.60 1.58 1.57 1.55 1.51 1.51 1.50 1.26 1.25 1.24 1.22 1.21 1.11
O
HO
CO2Me
N
2.75
1.87
4.01
1.31
1.05
2.13
2.42
2.63
4.32
9.94
3.00
9.0 8.5 8.0 7.5 7.0 6.5 6.0 5.5 5.0 4.5 4.0 3.5 3.0 2.5 2.0 1.5 1.0 0.5
f1 (ppm)

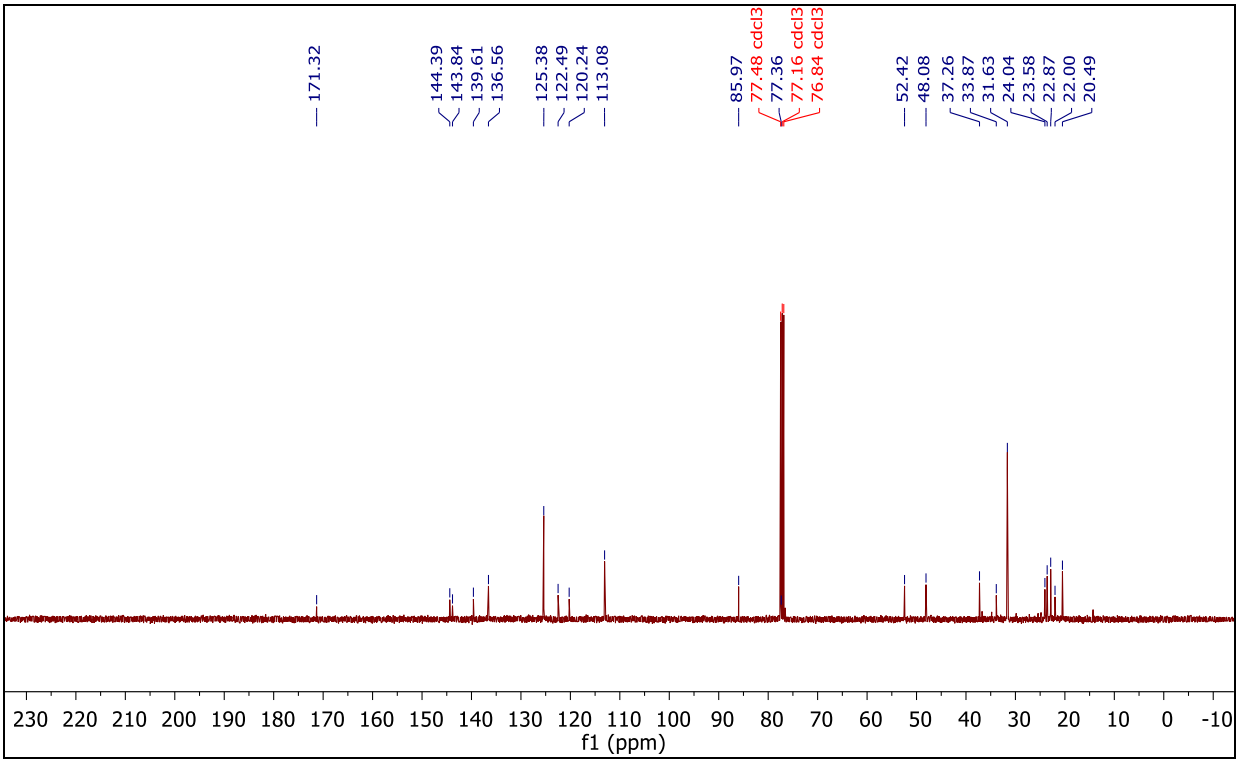
171.32
144.39
143.84
139.61
136.56
125.38
122.49
120.24
113.08
85.97
77.48 cdcl3
77.36
77.16 cdcl3
76.84 cdcl3
52.42
48.08
37.26
33.87
31.63
24.04
23.58
22.87
22.00
20.49
230 220 210 200 190 180 170 160 150 140 130 120 110 100 90 80 70 60 50 40 30 20 10 0 -10
f1 (ppm)

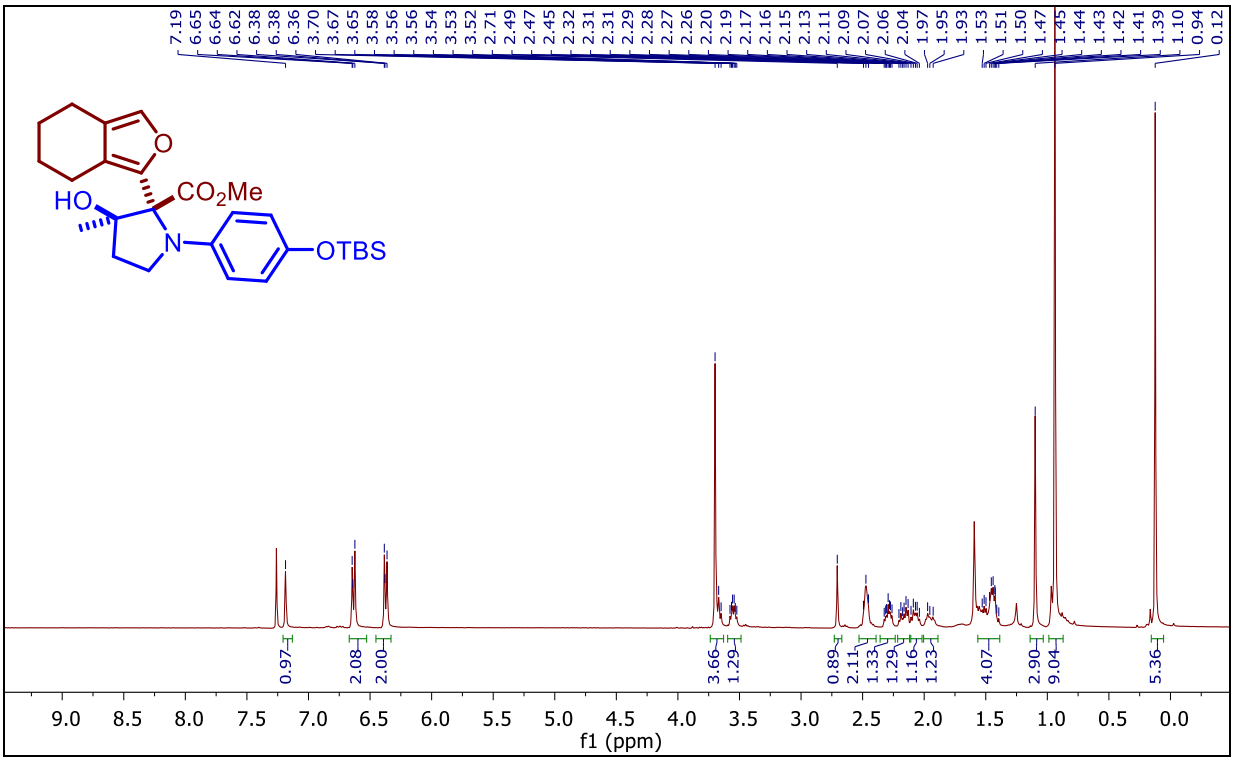
7.19 6.65 6.64 6.62 6.38 6.38 6.36 3.70 3.67 3.65 3.58 3.56 3.56 3.54 3.53 3.52 2.71 2.49 2.47 2.45 2.32 2.31 2.31 2.29 2.28 2.27 2.26 2.20 2.19 2.17 2.16 2.15 2.13 2.11 2.09 2.07 2.06 2.04 1.97 1.95 1.93 1.53 1.51 1.50 1.47 1.45 1.44 1.43 1.42 1.41 1.39 1.10 0.94 0.12
O
CO2Me
HO
N
OTBS
0.97 2.08 2.00 3.66 1.29 0.89 2.11 1.33 1.29 1.16 1.23 4.07 2.90 9.04 5.36
9.0 8.5 8.0 7.5 7.0 6.5 6.0 5.5 5.0 4.5 4.0 3.5 3.0 2.5 2.0 1.5 1.0 0.5 0.0
f1 (ppm)

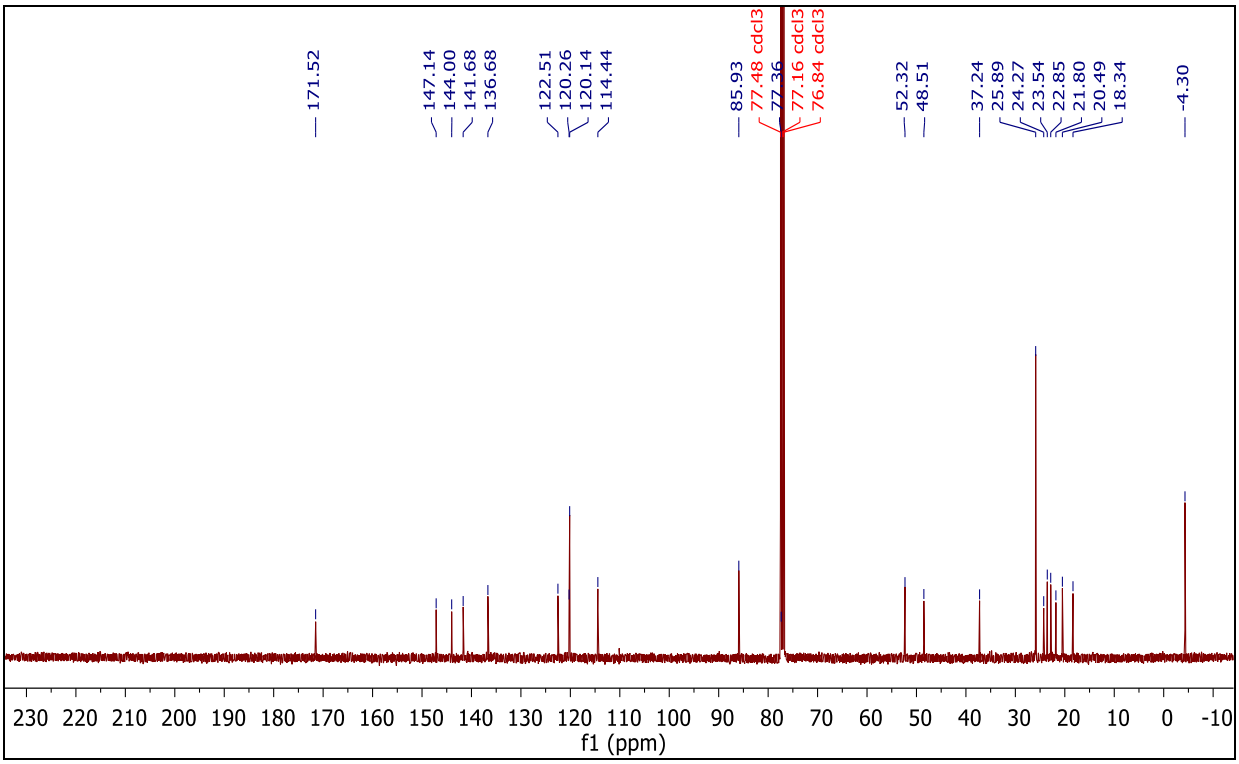
171.52
147.14 144.00 141.68 136.68
122.51 120.26 120.14 114.44
85.93 77.48 cdcl3 77.36 77.16 cdcl3 76.84 cdcl3
52.32 48.51
37.24 25.89 24.27 23.54 22.85 21.80 20.49 18.34
-4.30
230 220 210 200 190 180 170 160 150 140 130 120 110 100 90 80 70 60 50 40 30 20 10 0 -10
f1 (ppm)

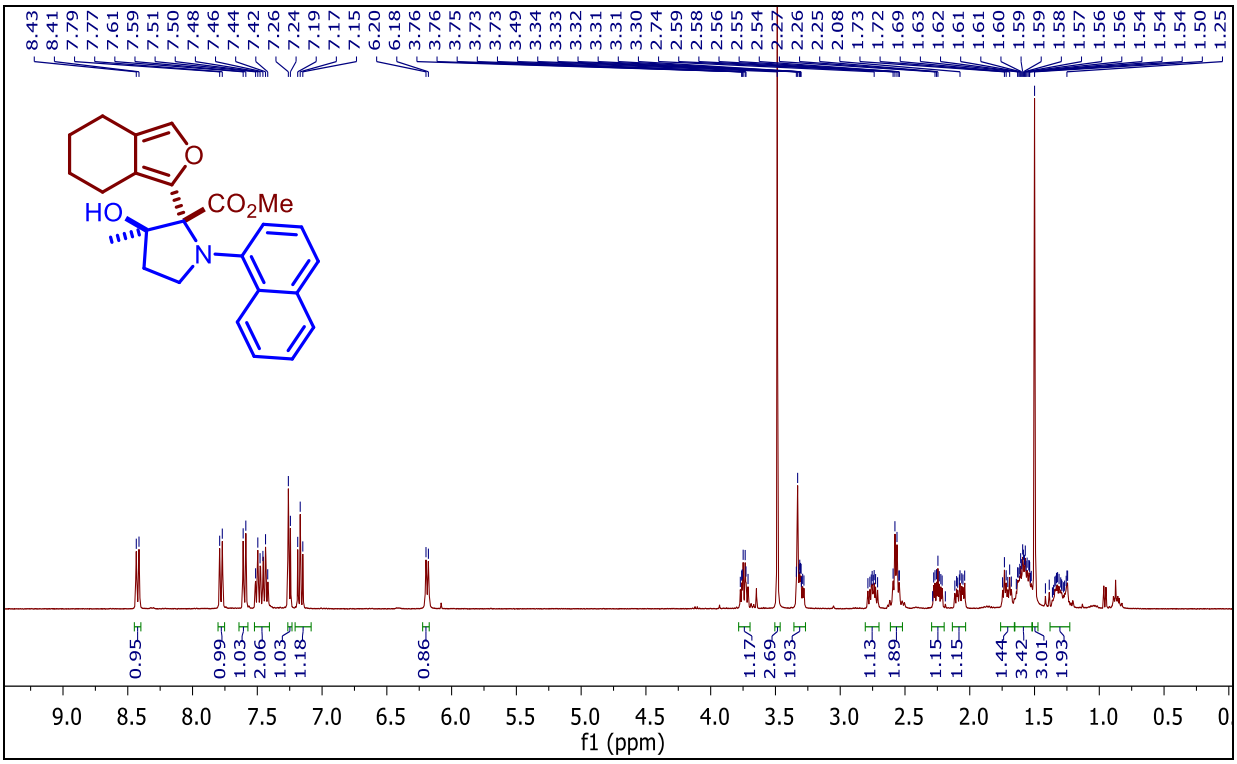
HO
CO2Me
N
O
f1 (ppm)

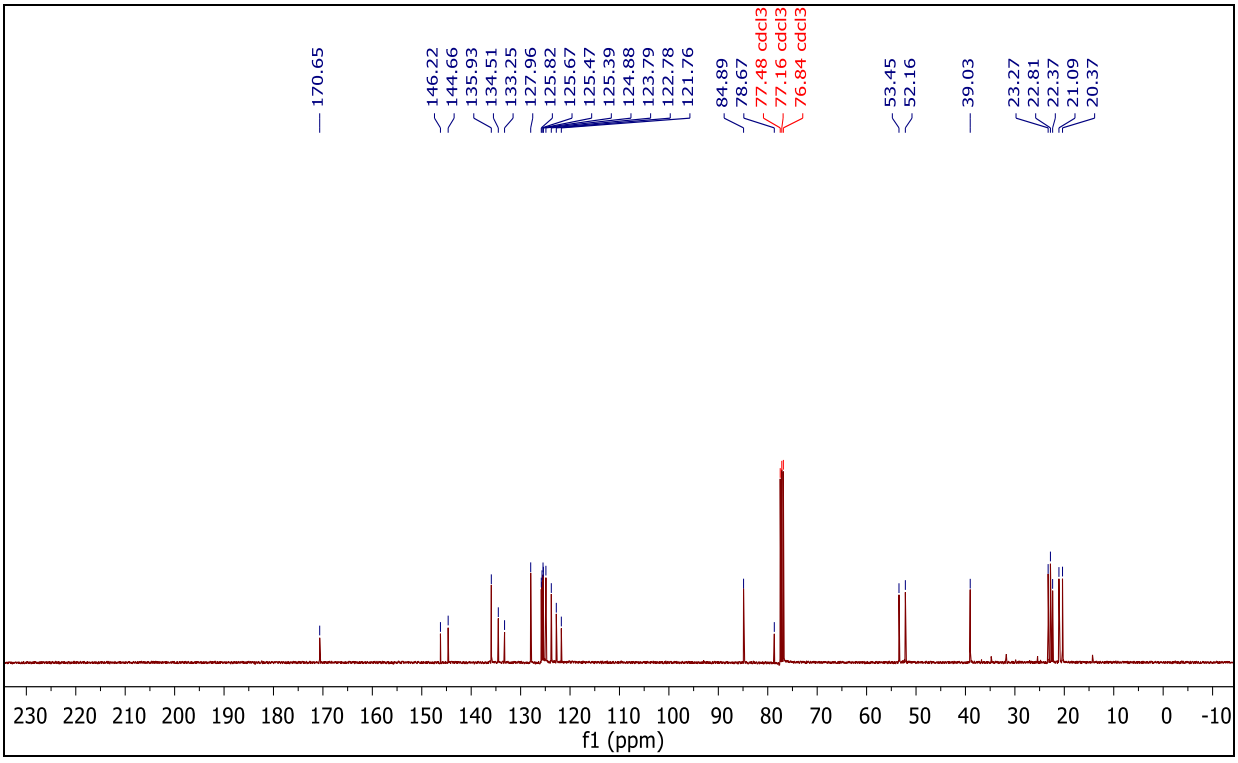
f1 (ppm)

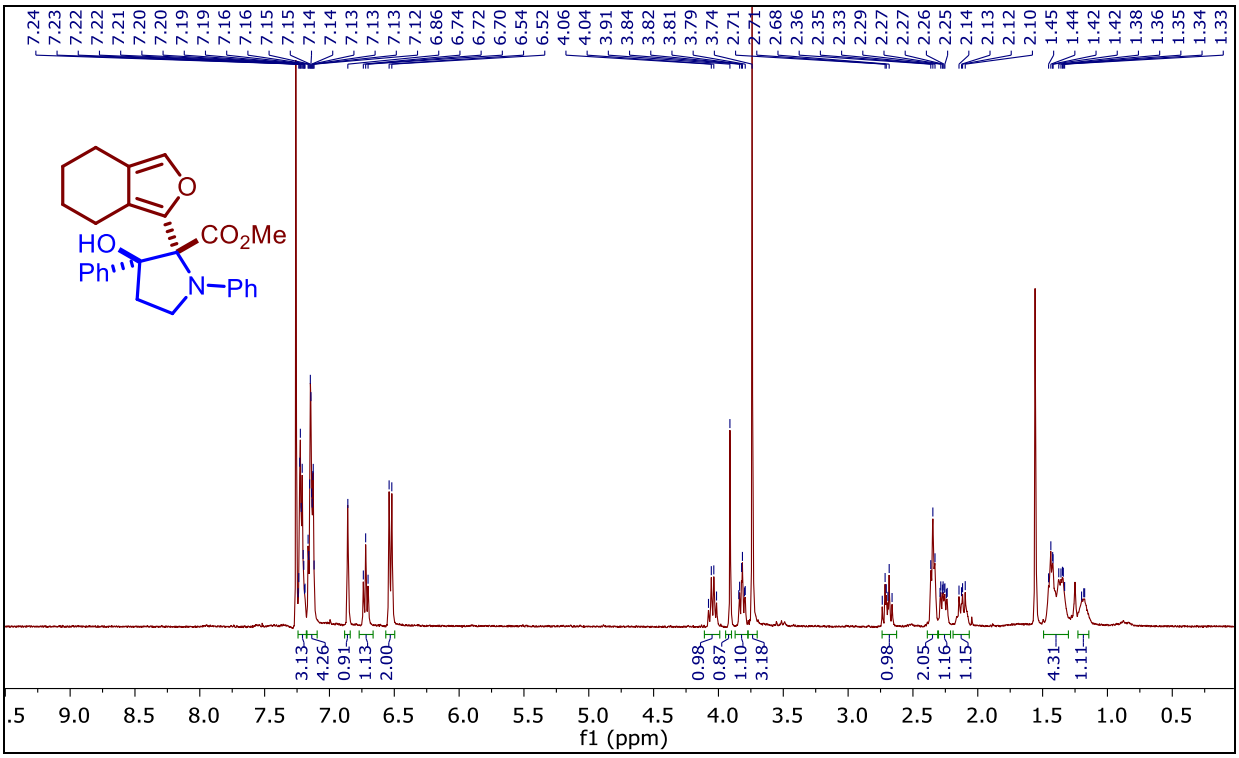
7.24 7.23 7.22 7.22 7.21 7.20 7.20 7.19 7.19 7.16 7.16 7.15 7.15 7.14 7.14 7.13 7.13 7.13 7.12 6.86 6.74 6.72 6.70 6.54 6.52
4.06 4.04 3.91 3.84 3.82 3.81 3.79 3.74 2.71 2.71 2.68 2.36 2.35 2.33 2.29 2.27 2.27 2.26 2.25 2.14 2.13 2.12 2.10
1.45 1.44 1.42 1.42 1.38 1.36 1.35 1.34 1.33
O
CO2Me
HO
Ph
N–Ph
3.13 4.26 0.91 1.13 2.00 0.98 0.87 1.10 3.18 0.98 2.05 1.16 1.15 4.31 1.11
.5 9.0 8.5 8.0 7.5 7.0 6.5 6.0 5.5 5.0 4.5 4.0 3.5 3.0 2.5 2.0 1.5 1.0 0.5
f1 (ppm)

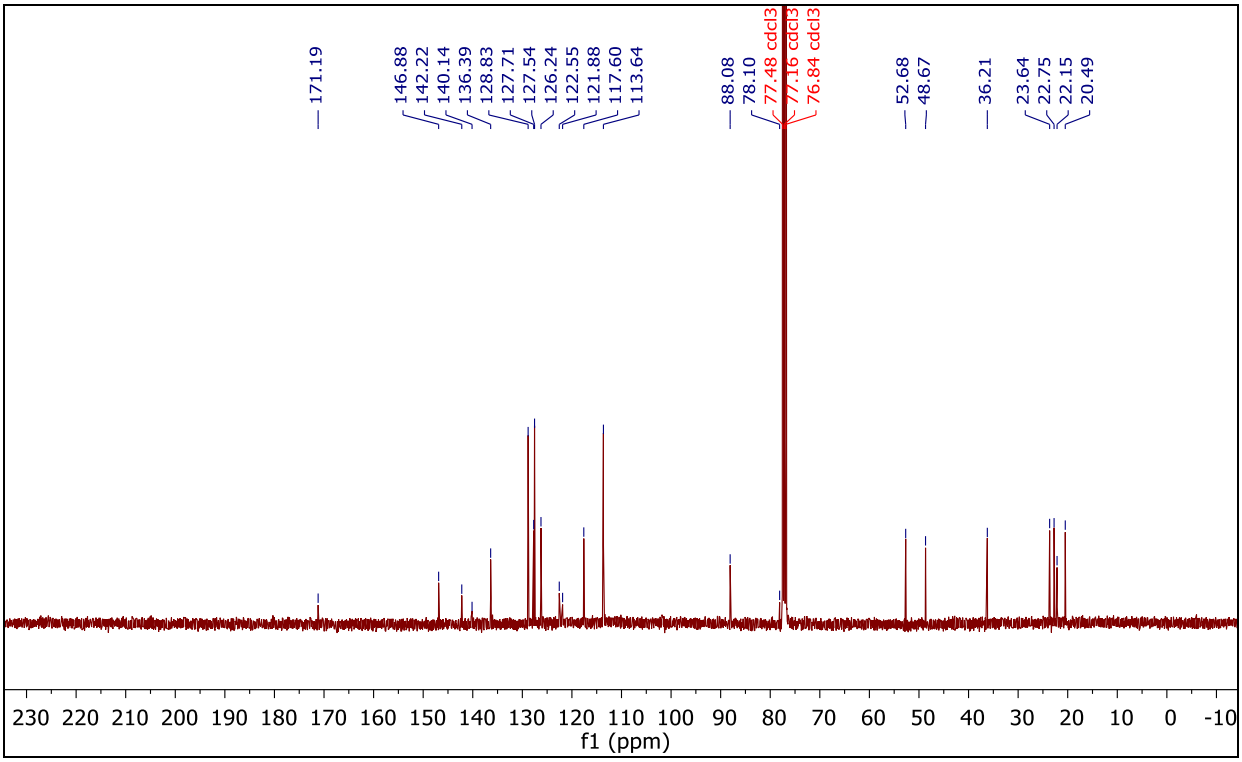
171.19
146.88 142.22 140.14 136.39 128.83 127.71 127.54 126.24 122.55 121.88 117.60 113.64
88.08 78.10 77.48 cdcl3 77.16 cdcl3 76.84 cdcl3
52.68 48.67 36.21 23.64 22.75 22.15 20.49
230 220 210 200 190 180 170 160 150 140 130 120 110 100 90 80 70 60 50 40 30 20 10 0 -10
f1 (ppm)

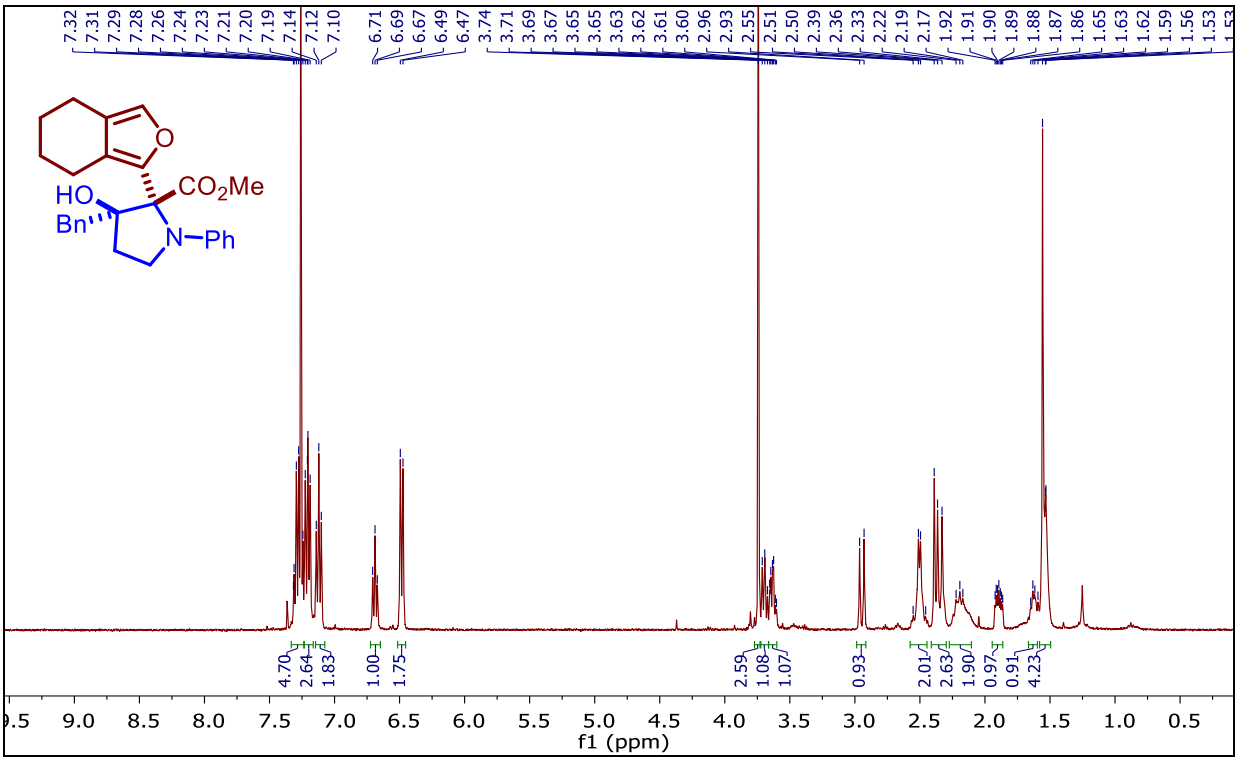
HO
Bn
CO2Me
N–Ph
f1 (ppm)

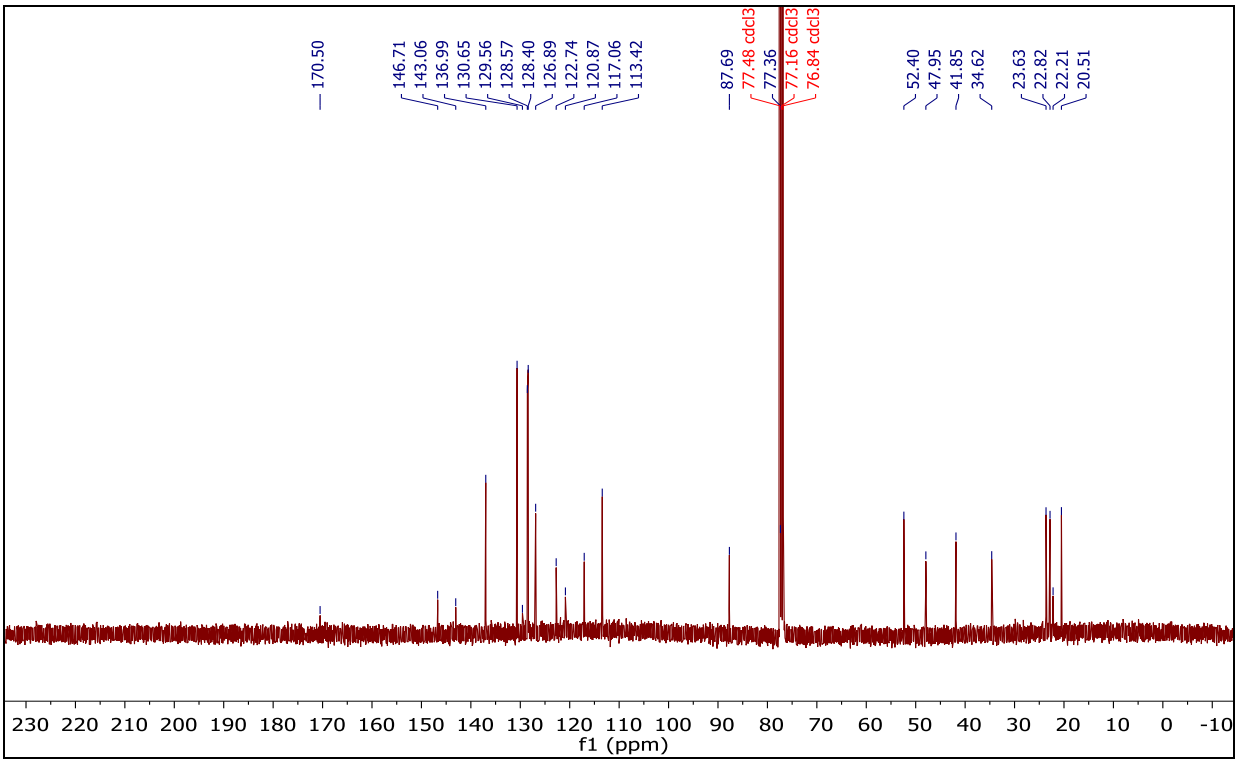
f1 (ppm)

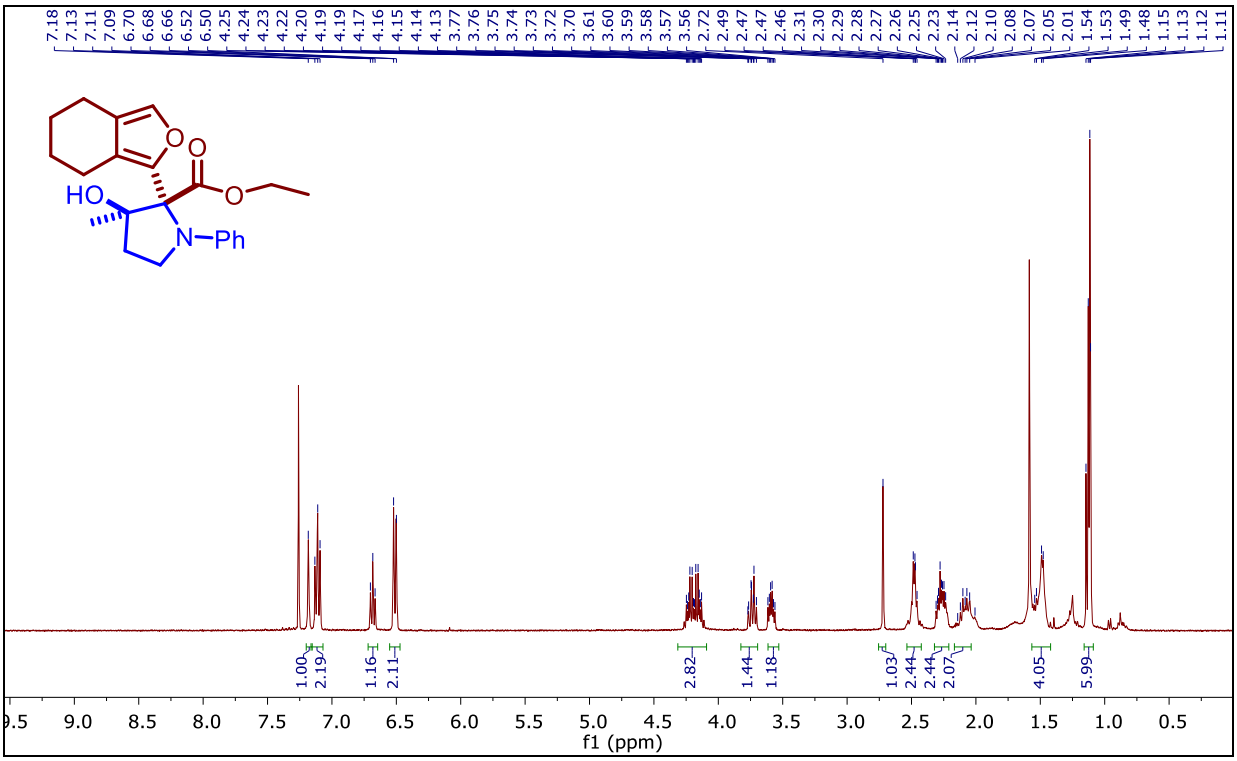
HO
O
O
O
N–Ph
f1 (ppm)

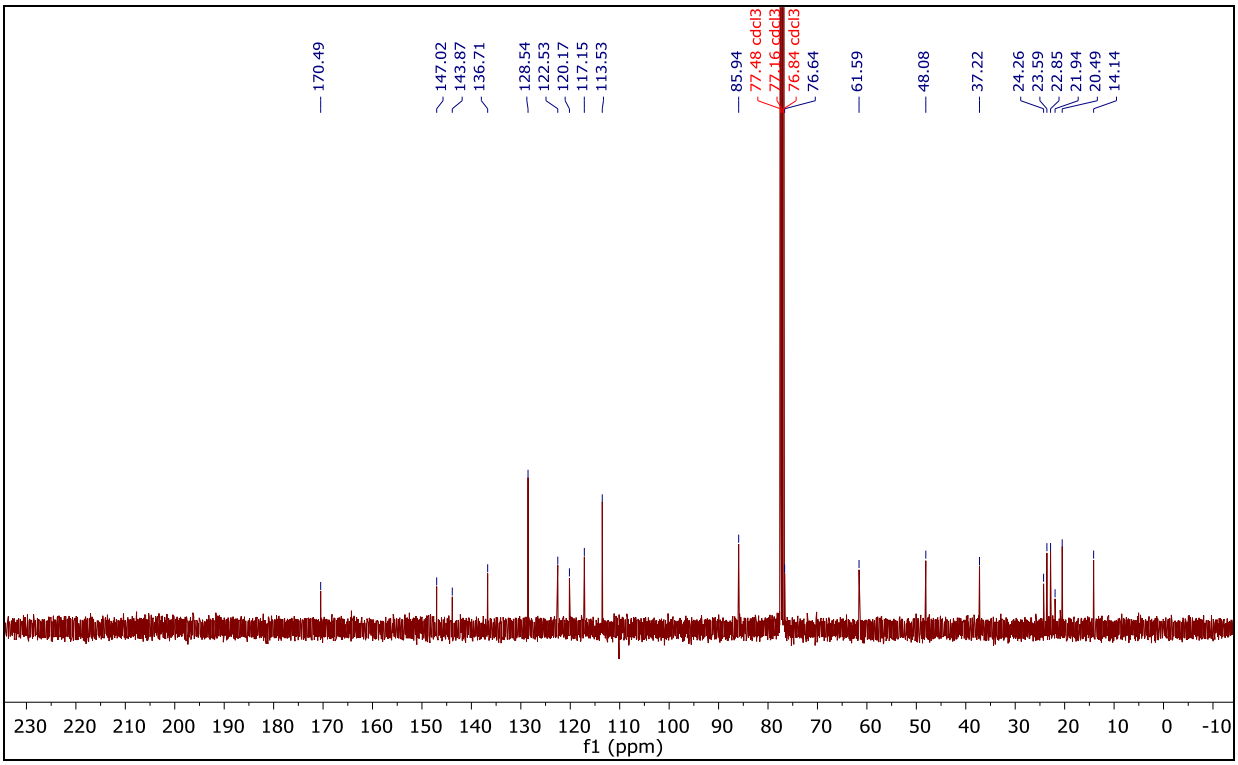
170.49
147.02
143.87
136.71
128.54
122.53
120.17
117.15
113.53
85.94
77.48 cdcl3
77.16 cdcl3
76.84 cdcl3
76.64
61.59
48.08
37.22
24.26
23.59
22.85
21.94
20.49
14.14
f1 (ppm)

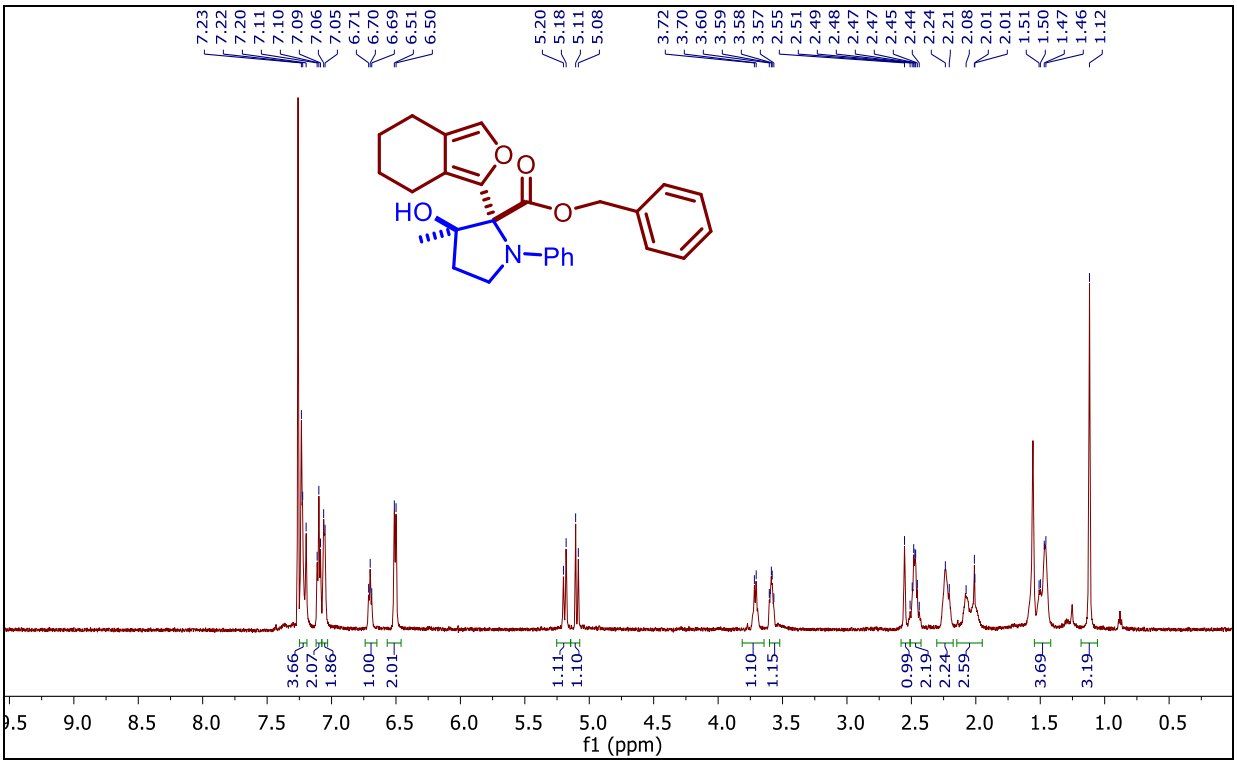
7.23 7.22 7.20 7.11 7.10 7.09 7.06 7.05 6.71 6.70 6.69 6.51 6.50
5.20 5.18 5.11 5.08
3.72 3.70 3.60 3.59 3.58 3.57 2.55 2.51 2.49 2.48 2.47 2.47 2.45 2.44 2.24 2.21 2.08 2.01 2.01 1.51 1.50 1.47 1.46 1.12
HO
O
O
O
N–Ph
3.66 2.07 1.86 1.00 2.01 1.11 1.10 1.10 1.15 0.99 2.19 2.24 2.59 3.69 3.19
f1 (ppm)

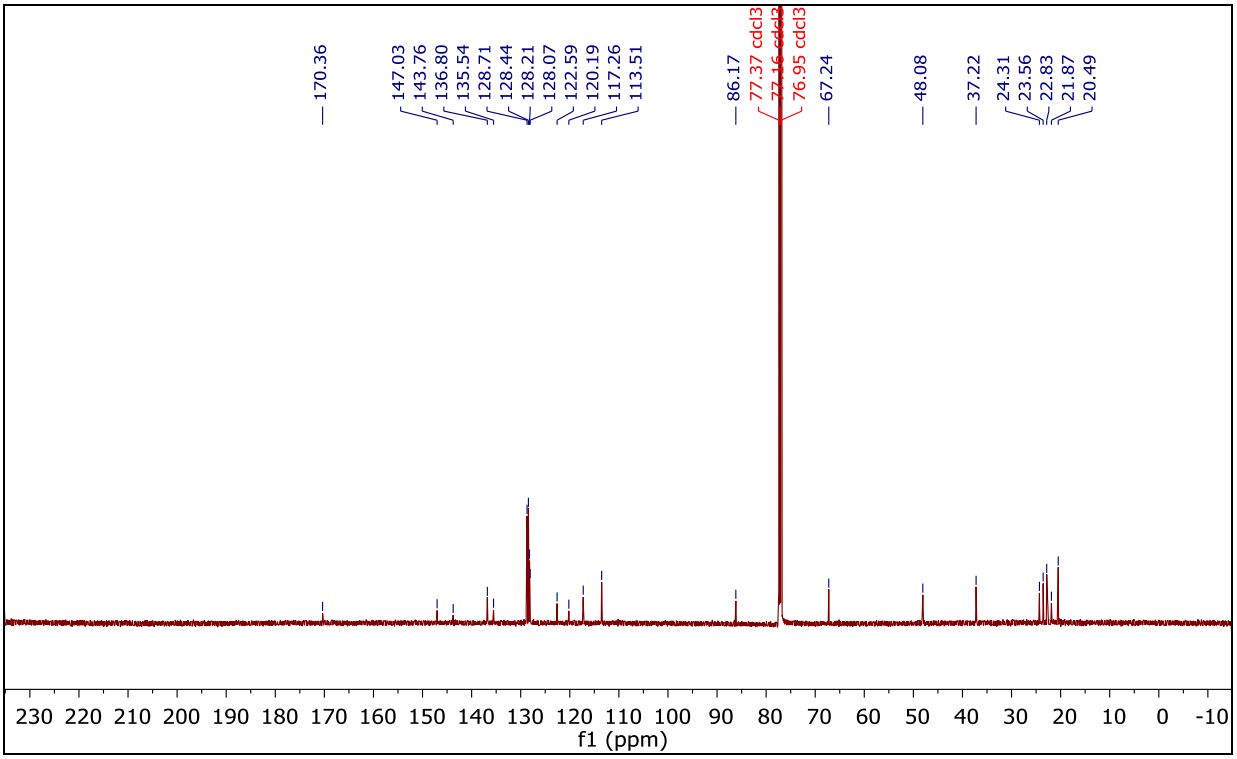
170.36
147.03 143.76 136.80 135.54 128.71 128.44 128.21 128.07 122.59 120.19 117.26 113.51
86.17
77.37 cdcl3
77.16 cdcl3
76.95 cdcl3
67.24
48.08
37.22
24.31 23.56 22.83 21.87 20.49
f1 (ppm)

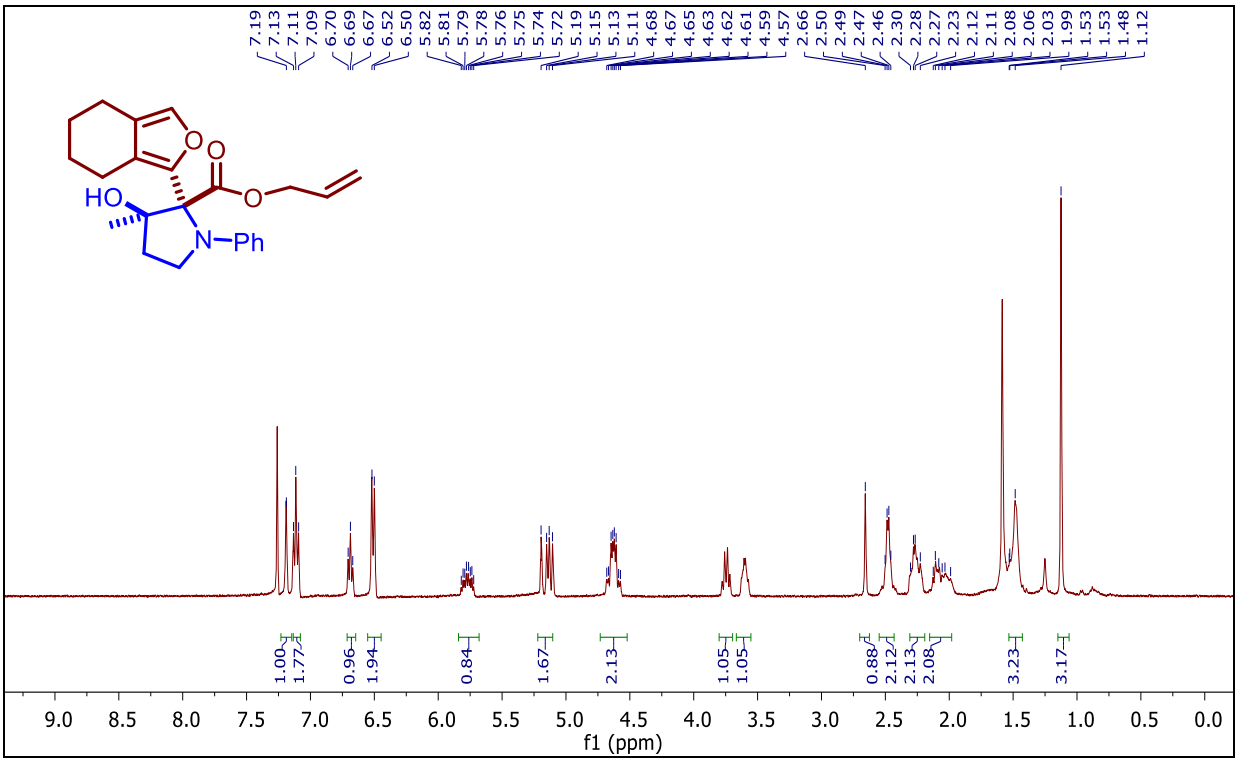
7.19 7.13 7.11 7.09 6.70 6.69 6.67 6.52 6.50 5.82 5.81 5.79 5.78 5.76 5.75 5.74 5.72 5.19 5.15 5.13 5.11 4.68 4.67 4.65 4.63 4.62 4.61 4.59 4.57 2.66 2.50 2.49 2.47 2.46 2.30 2.28 2.27 2.23 2.12 2.11 2.08 2.06 2.03 1.99 1.53 1.53 1.48 1.12
HO
O
O
O
N–Ph
1.00 1.77 0.96 1.94 0.84 1.67 2.13 1.05 1.05 0.88 2.12 2.13 2.08 3.23 3.17
9.0 8.5 8.0 7.5 7.0 6.5 6.0 5.5 5.0 4.5 4.0 3.5 3.0 2.5 2.0 1.5 1.0 0.5 0.0
f1 (ppm)

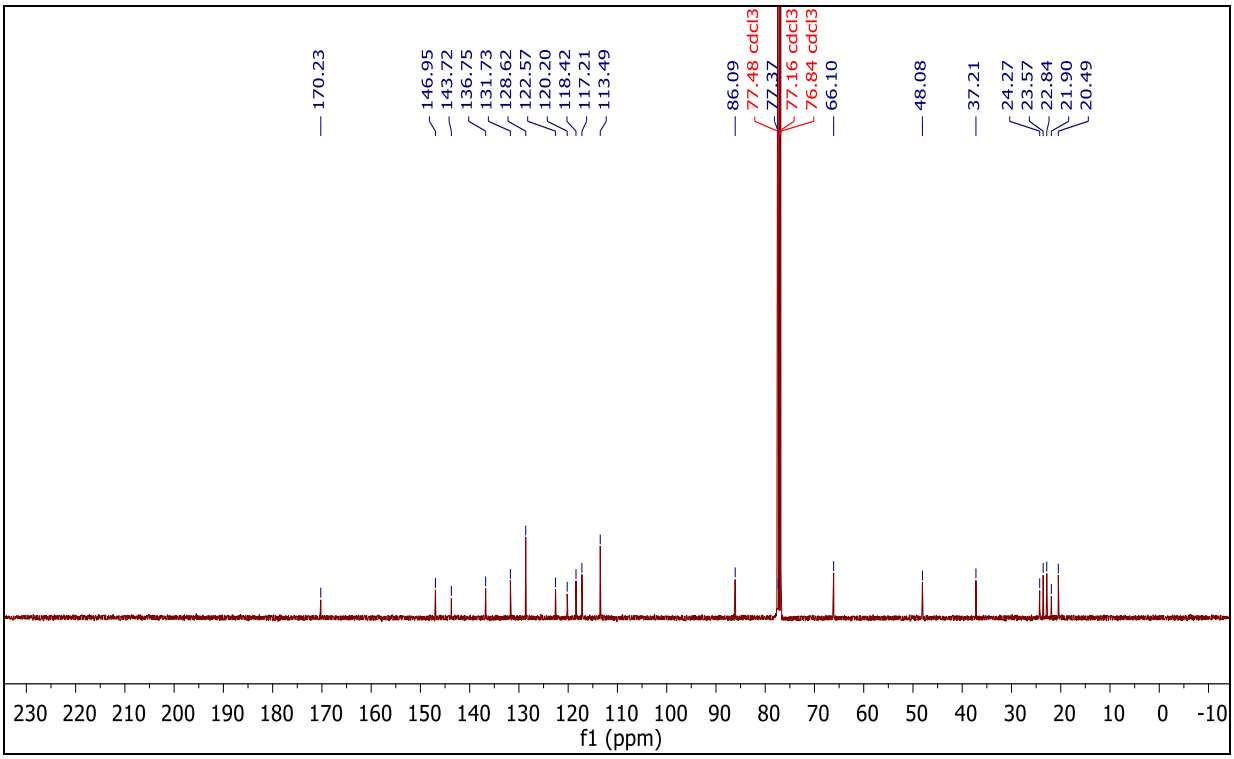
170.23
146.95 143.72 136.75 131.73 128.62 122.57 120.20 118.42 117.21 113.49
86.09
77.48 cdcl3 77.37 77.16 cdcl3 76.84 cdcl3
66.10
48.08
37.21
24.27 23.57 22.84 21.90 20.49
230 220 210 200 190 180 170 160 150 140 130 120 110 100 90 80 70 60 50 40 30 20 10 0 -10
f1 (ppm)

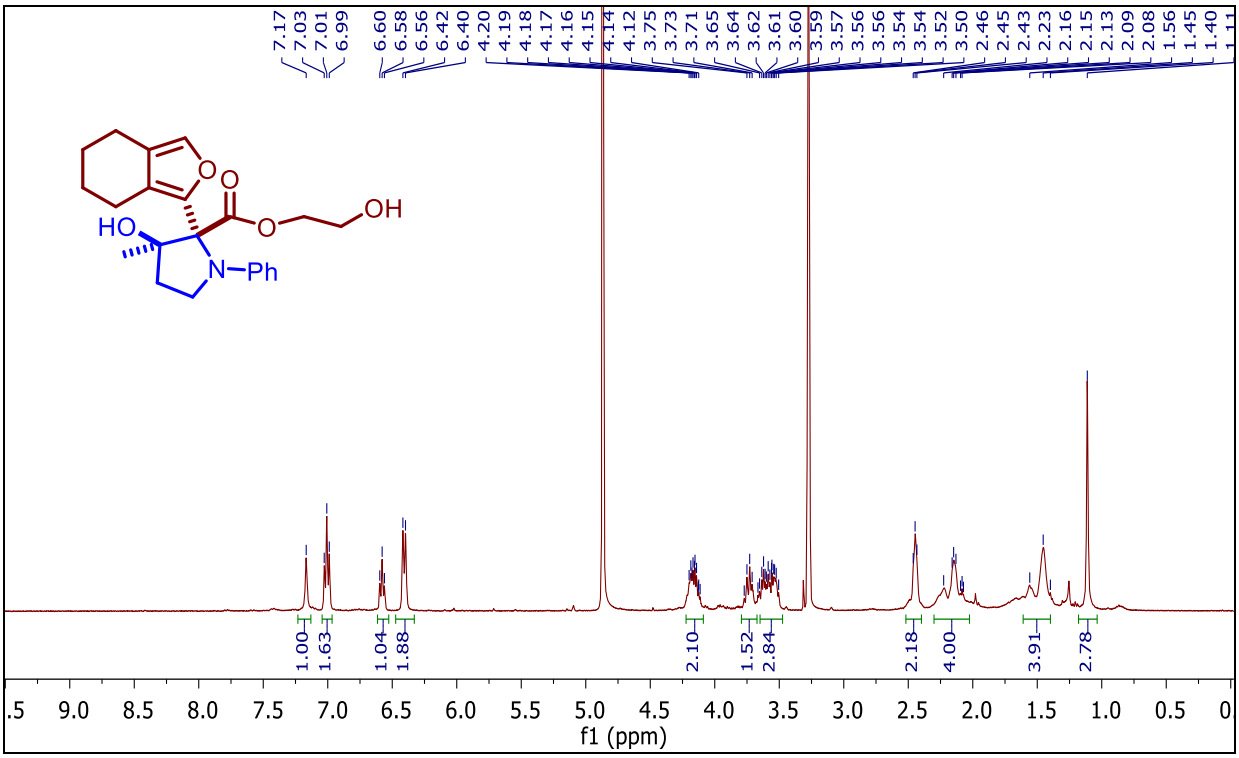
7.17
7.03
7.01
6.99
6.60
6.58
6.56
6.42
6.40
4.20
4.19
4.18
4.17
4.16
4.15
4.14
4.12
3.75
3.73
3.71
3.65
3.64
3.62
3.61
3.60
3.59
3.57
3.56
3.56
3.54
3.54
3.52
3.50
2.46
2.45
2.43
2.23
2.16
2.15
2.13
2.09
2.08
1.56
1.45
1.40
O
O
HO
O
OH
N–Ph
1.00
1.63
1.04
1.88
2.10
1.52
2.84
2.18
4.00
3.91
2.78
f1 (ppm)

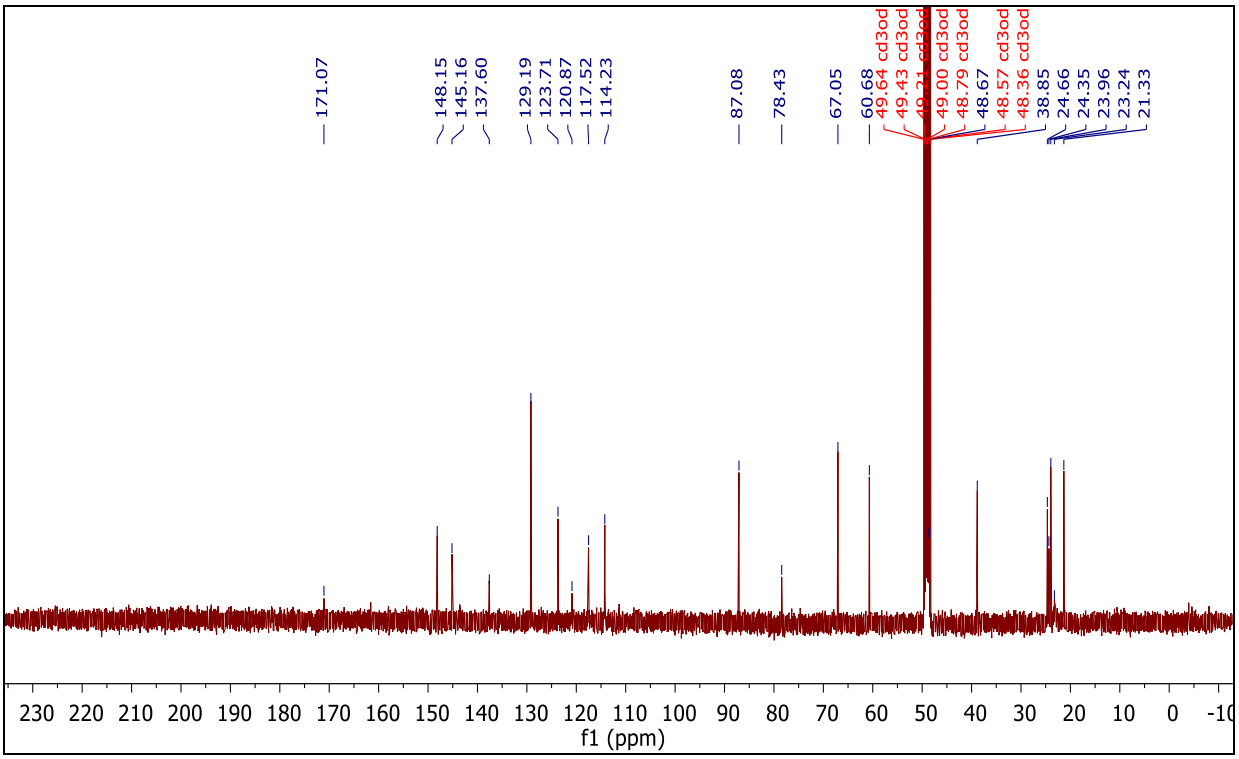
171.07
148.15
145.16
137.60
129.19
123.71
120.87
117.52
114.23
87.08
78.43
67.05
60.68
49.64 cd3od
49.43 cd3od
49.21 cd3od
49.00 cd3od
48.79 cd3od
48.67
48.57 cd3od
48.36 cd3od
38.85
24.66
24.35
23.96
23.24
21.33
f1 (ppm)

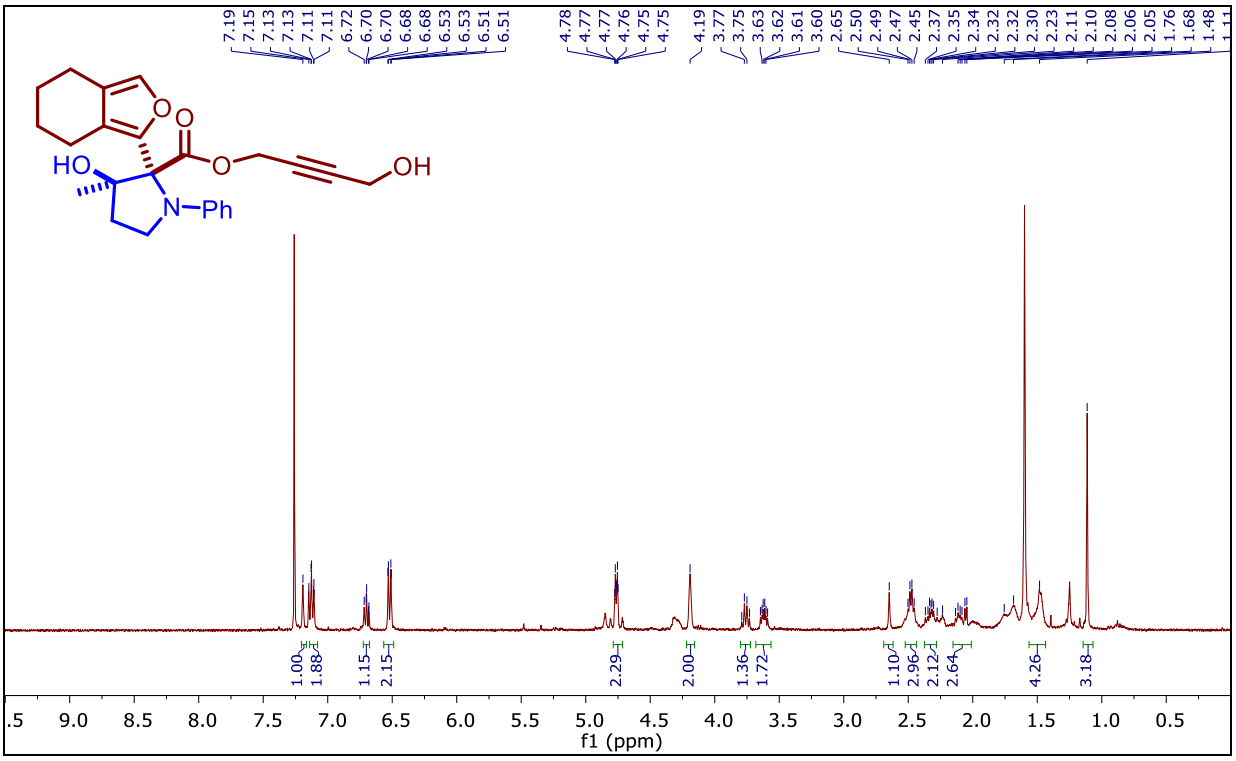
7.19 7.15 7.13 7.13 7.11 7.11 6.72 6.70 6.70 6.68 6.68 6.53 6.53 6.51 6.51
4.78 4.77 4.77 4.76 4.75 4.75 4.19 3.77 3.75 3.63 3.62 3.61 3.60
2.65 2.50 2.49 2.47 2.45 2.37 2.35 2.34 2.32 2.32 2.30 2.23 2.11 2.10 2.08 2.06 2.05 1.76 1.68 1.48
HO
O
O
O
OH
N–Ph
1.00 1.88 1.15 2.15 2.29 2.00 1.36 1.72 1.10 2.96 2.12 2.64 4.26 3.18
f1 (ppm)

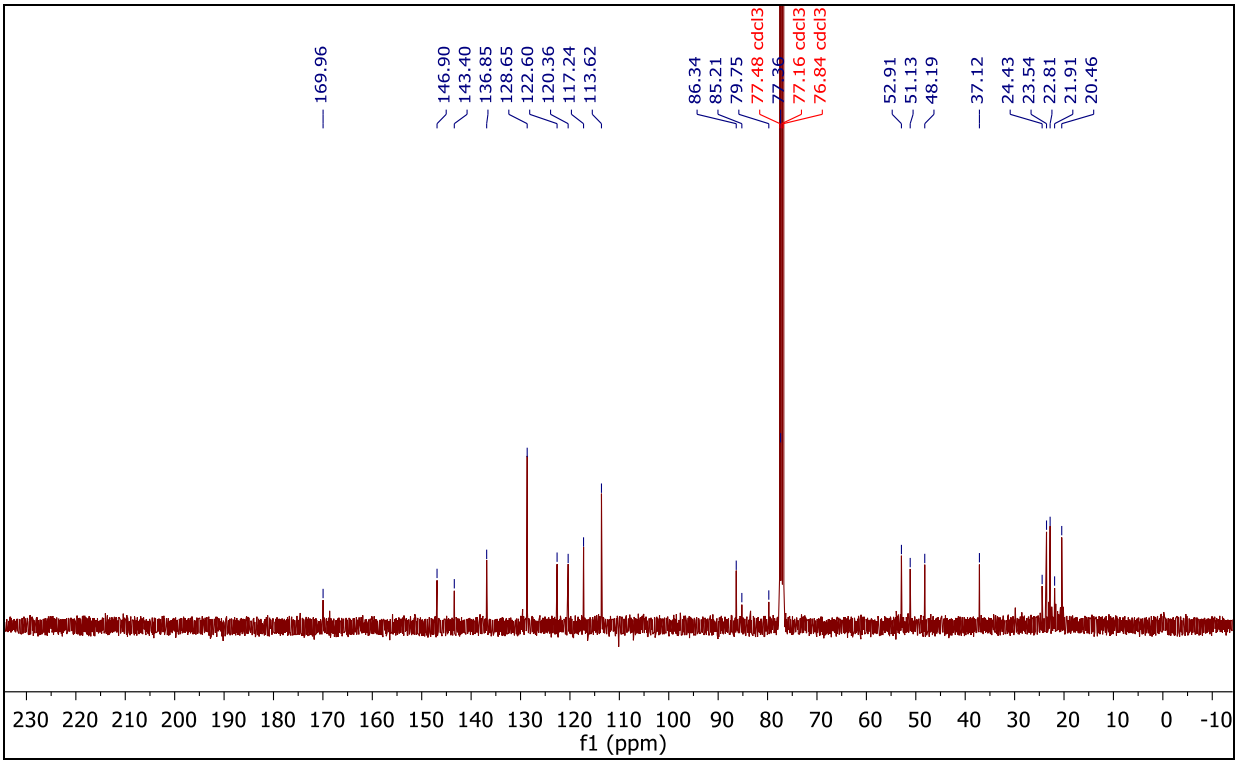
169.96
146.90 143.40 136.85 128.65 122.60 120.36 117.24 113.62
86.34 85.21 79.75 77.48 cdcl3 77.36 77.16 cdcl3 76.84 cdcl3
52.91 51.13 48.19
37.12
24.43 23.54 22.81 21.91 20.46
f1 (ppm)

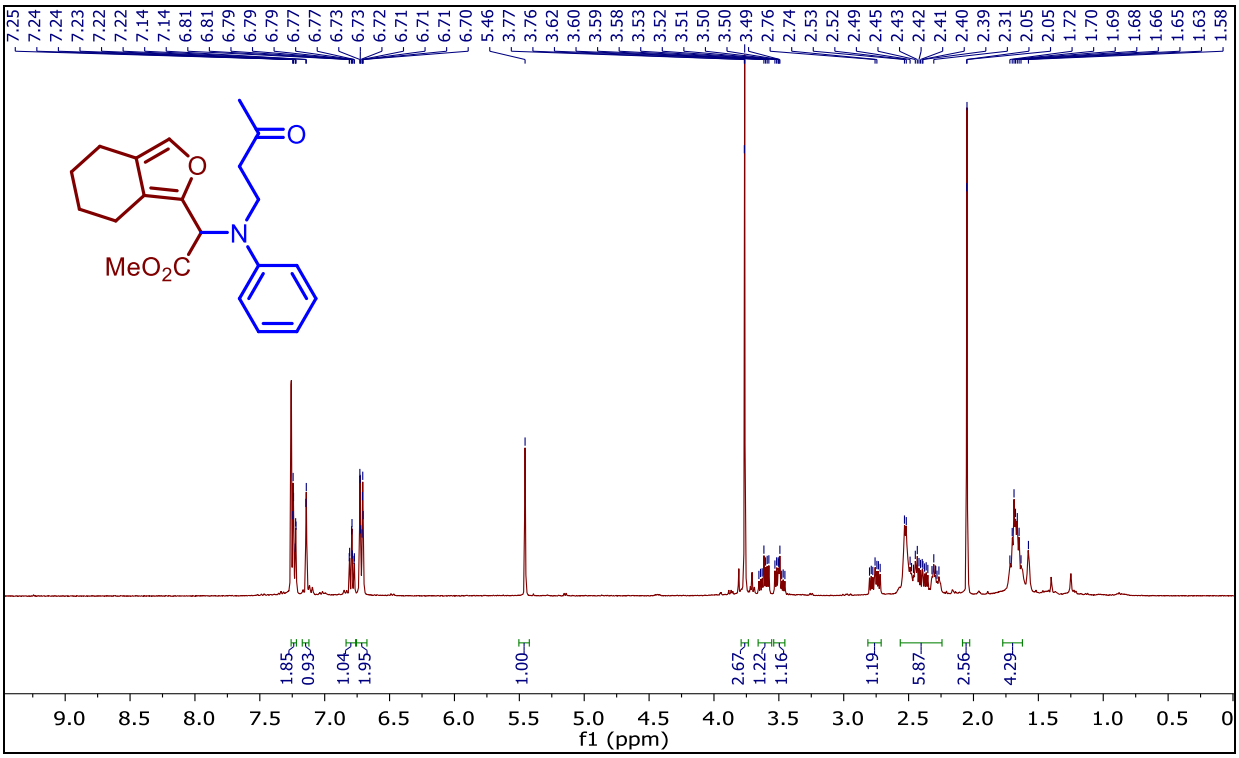
7.25 7.24 7.24 7.23 7.22 7.22 7.14 7.14 6.81 6.81 6.79 6.79 6.79 6.77 6.77 6.73 6.73 6.72 6.71 6.71 6.71 6.70 5.46 3.77 3.76 3.62 3.60 3.59 3.58 3.53 3.52 3.51 3.50 3.50 3.49 2.76 2.74 2.53 2.52 2.49 2.45 2.43 2.42 2.41 2.40 2.39 2.31 2.05 2.05 1.72 1.70 1.69 1.68 1.66 1.65 1.63 1.58
O
O
N
MeO2C
1.85 0.93 1.04 1.95 1.00 2.67 1.22 1.16 1.19 5.87 2.56 4.29
9.0 8.5 8.0 7.5 7.0 6.5 6.0 5.5 5.0 4.5 4.0 3.5 3.0 2.5 2.0 1.5 1.0 0.5 0
f1 (ppm)

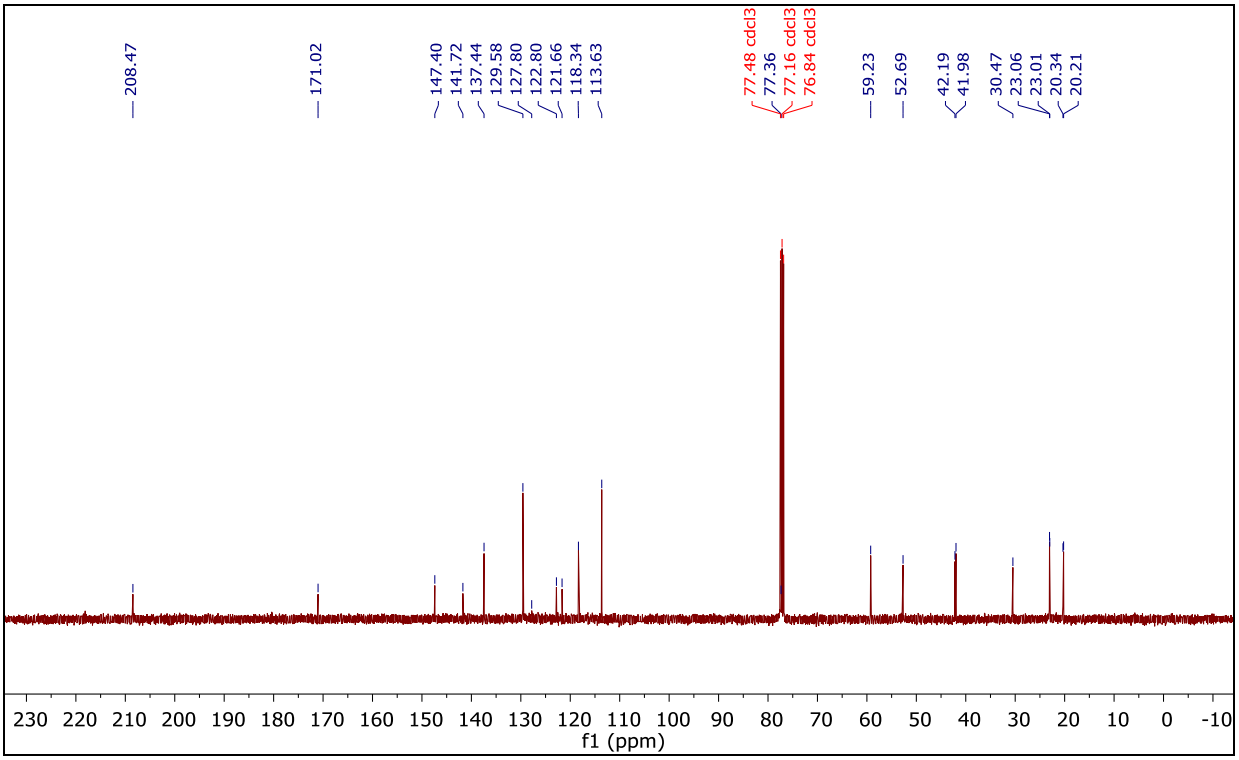
208.47
171.02
147.40 141.72 137.44 129.58 127.80 122.80 121.66 118.34 113.63
77.48 cdcl3 77.36 77.16 cdcl3 76.84 cdcl3
59.23 52.69 42.19 41.98 30.47 23.06 23.01 20.34 20.21
230 220 210 200 190 180 170 160 150 140 130 120 110 100 90 80 70 60 50 40 30 20 10 0 -10
f1 (ppm)

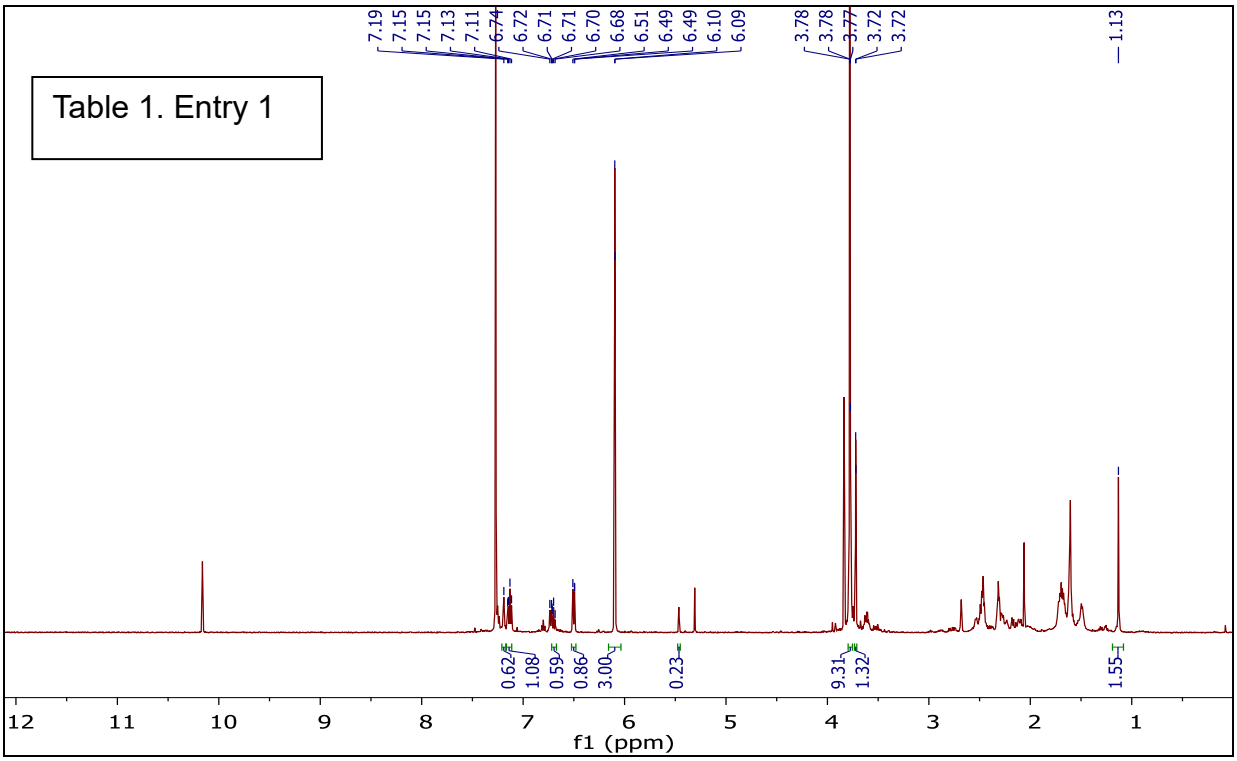
Table 1. Entry 1
7.19
7.15
7.15
7.13
7.11
6.74
6.72
6.71
6.71
6.70
6.68
6.51
6.49
6.49
6.10
6.09
3.78
3.78
3.77
3.72
3.72
1.13
0.62
1.08
0.59
0.86
3.00
0.23
9.31
1.32
1.55
12
11
10
9
8
7
6
5
4
3
2
1
f1 (ppm)

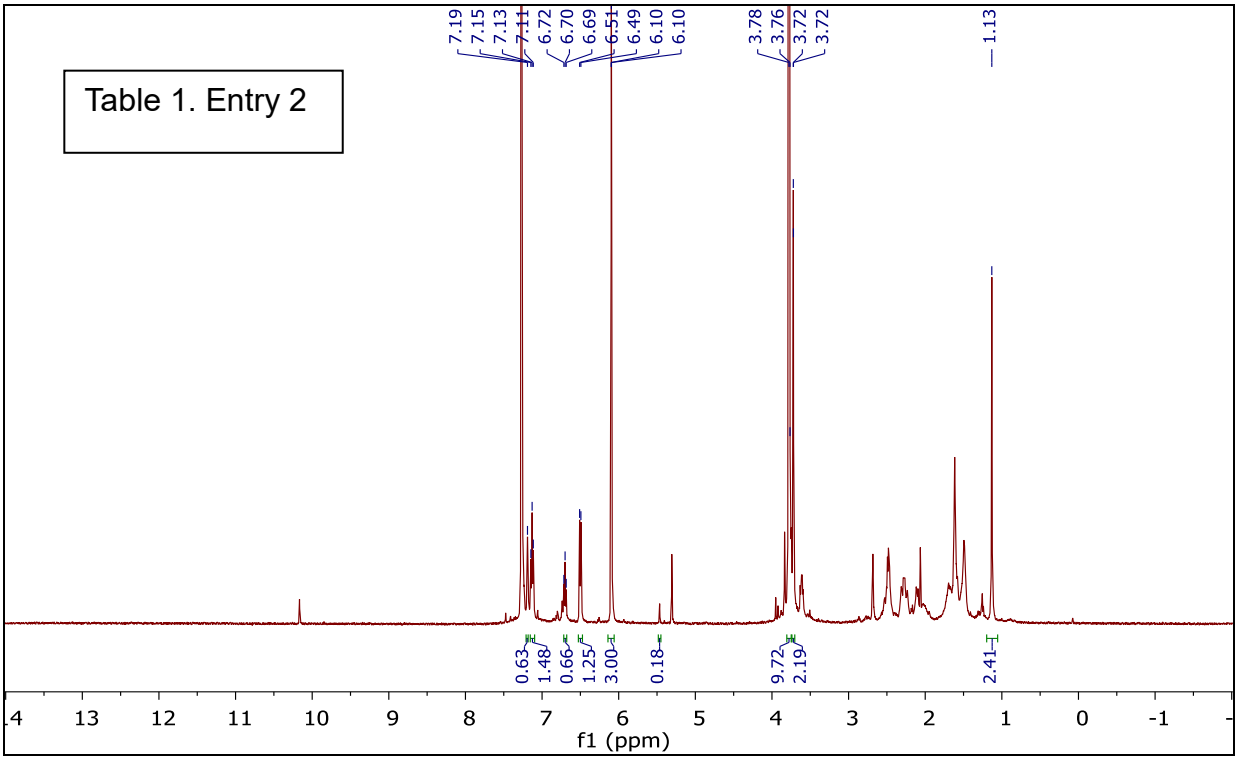
Table 1. Entry 2
7.19
7.15
7.13
7.11
6.72
6.70
6.69
6.51
6.49
6.10
6.10
3.78
3.76
3.72
3.72
1.13
0.63
1.48
0.66
1.25
3.00
0.18
9.72
2.19
2.41
13
12
11
10
9
8
7
6
5
4
3
2
1
0
-1
f1 (ppm)

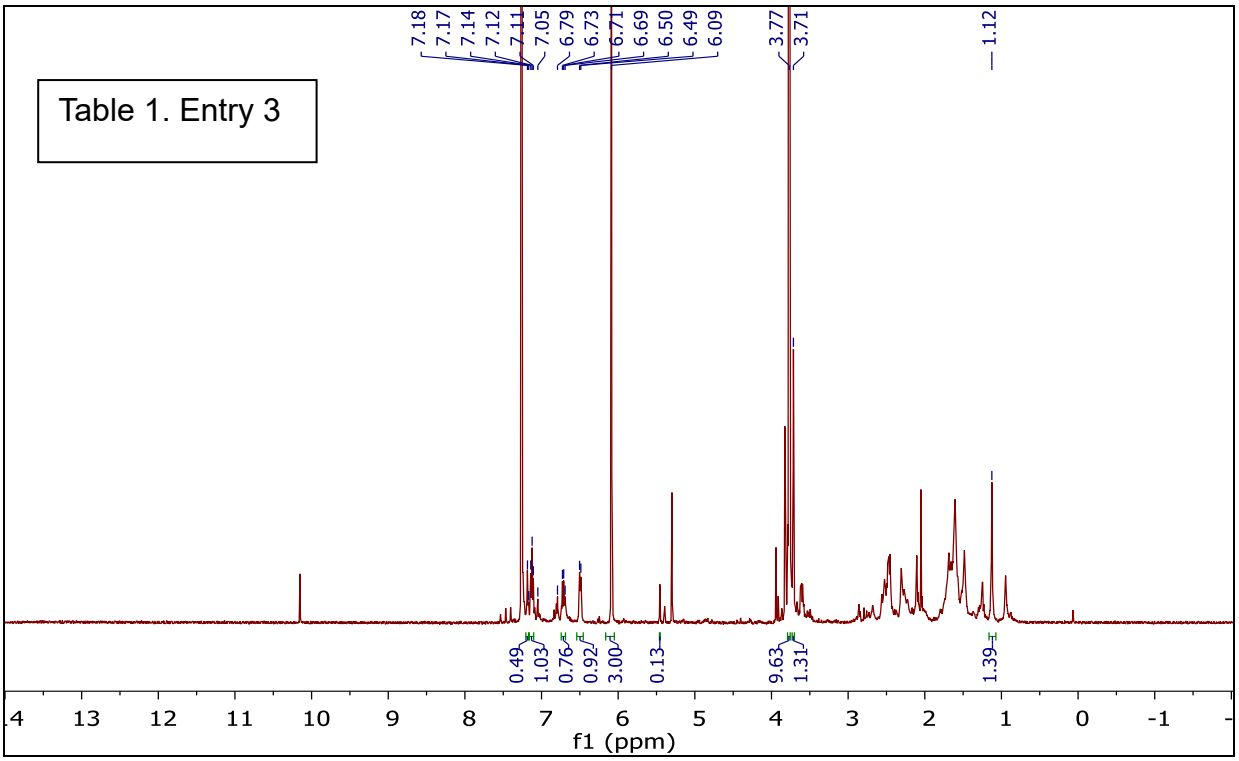
Table 1. Entry 3
7.18
7.17
7.14
7.12
7.11
7.05
6.79
6.73
6.71
6.69
6.50
6.49
6.09
3.77
3.71
1.12
0.49
1.03
0.76
0.92
3.00
0.13
9.63
1.31
1.39
f1 (ppm)

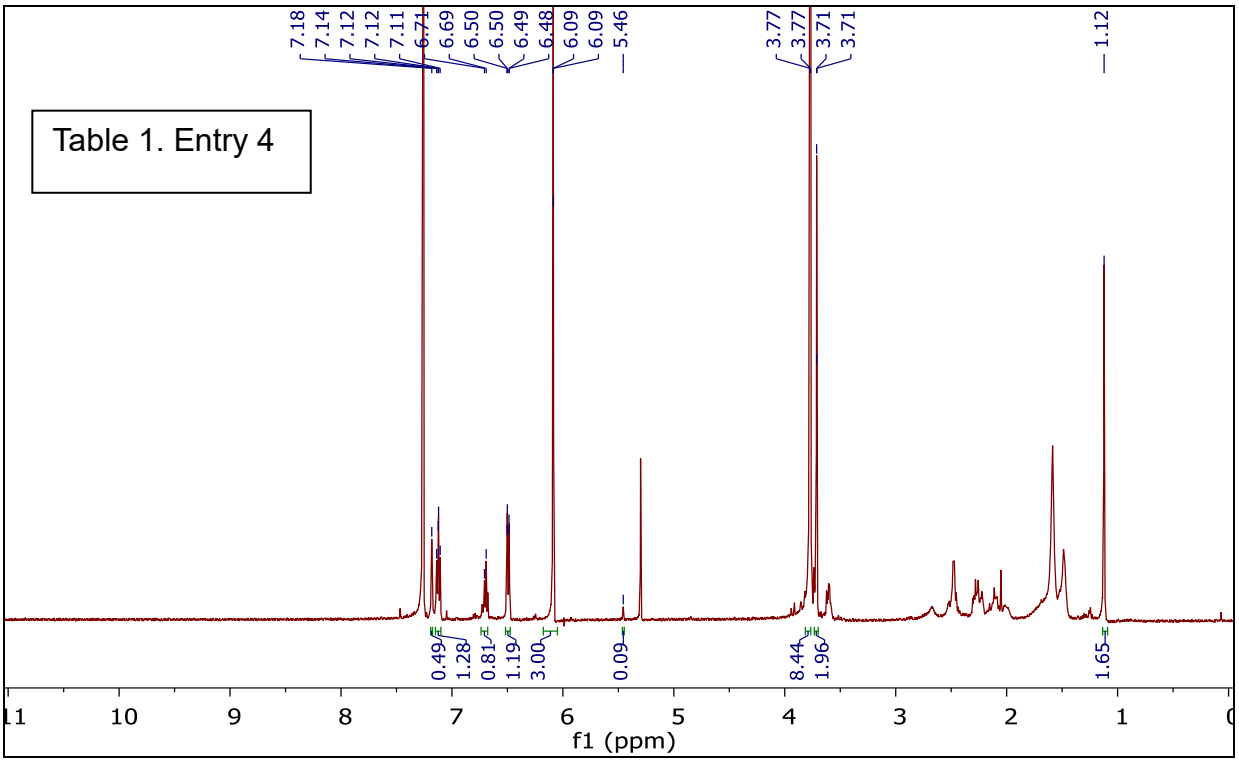
Table 1. Entry 4
7.18
7.14
7.12
7.12
7.11
6.71
6.69
6.50
6.50
6.49
6.48
6.09
6.09
5.46
3.77
3.77
3.71
3.71
1.12
0.49
1.28
0.81
1.19
3.00
0.09
8.44
1.96
1.65
f1 (ppm)

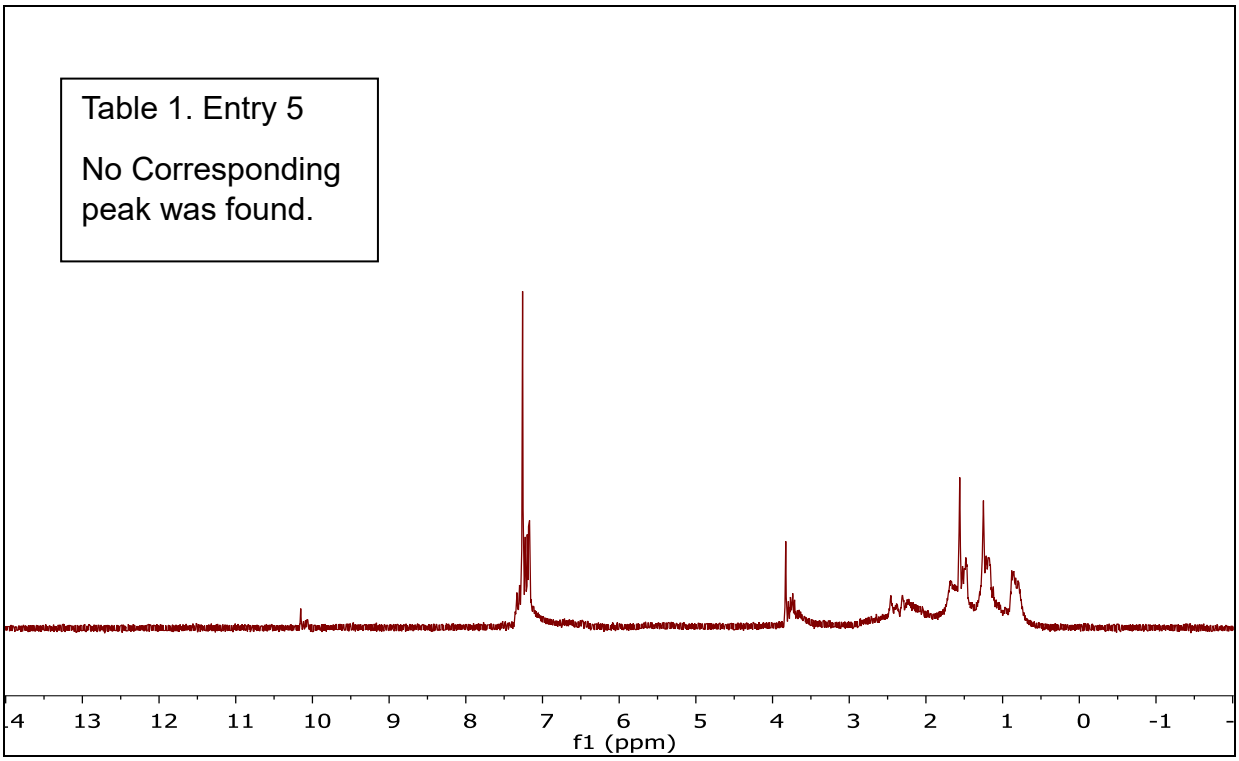
Table 1. Entry 5
No Corresponding peak was found.
f1 (ppm)

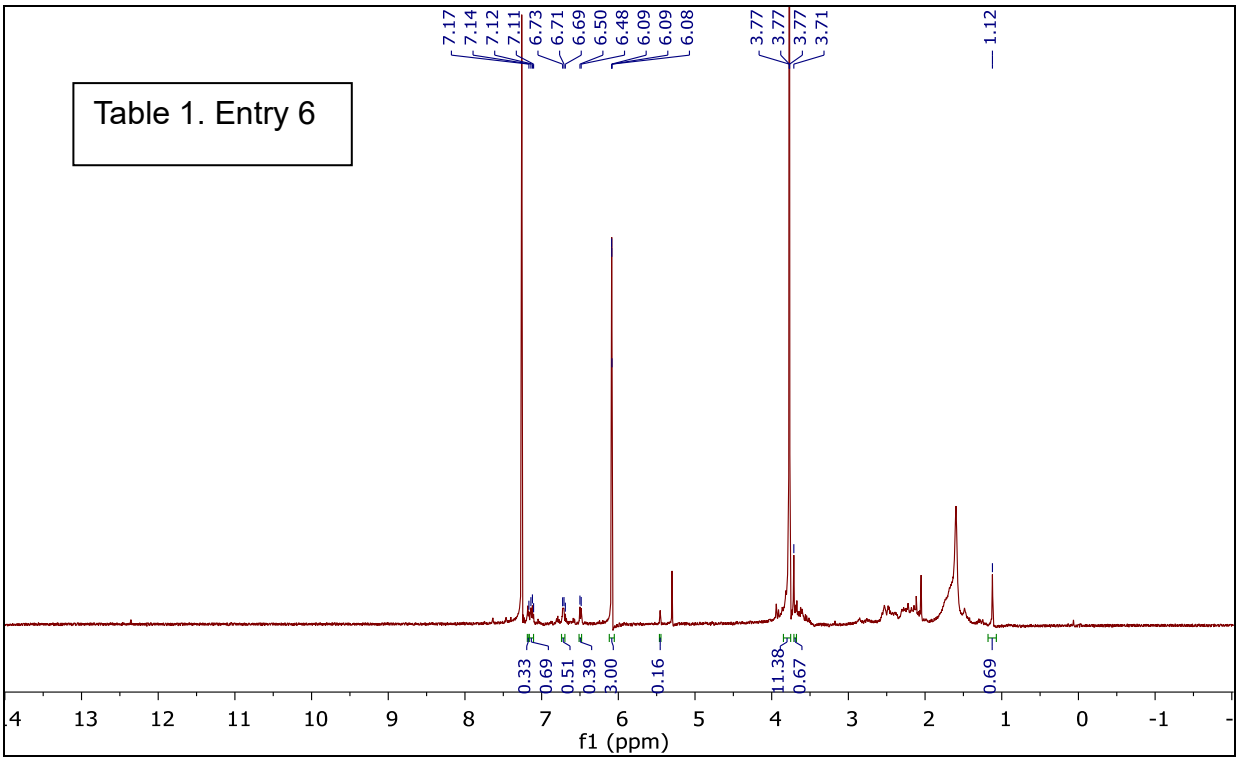
Table 1. Entry 6
7.17
7.14
7.12
7.11
6.73
6.71
6.69
6.50
6.48
6.09
6.09
6.08
3.77
3.77
3.77
3.71
1.12
0.33
0.69
0.51
0.39
3.00
0.16
11.38
0.67
0.69
f1 (ppm)

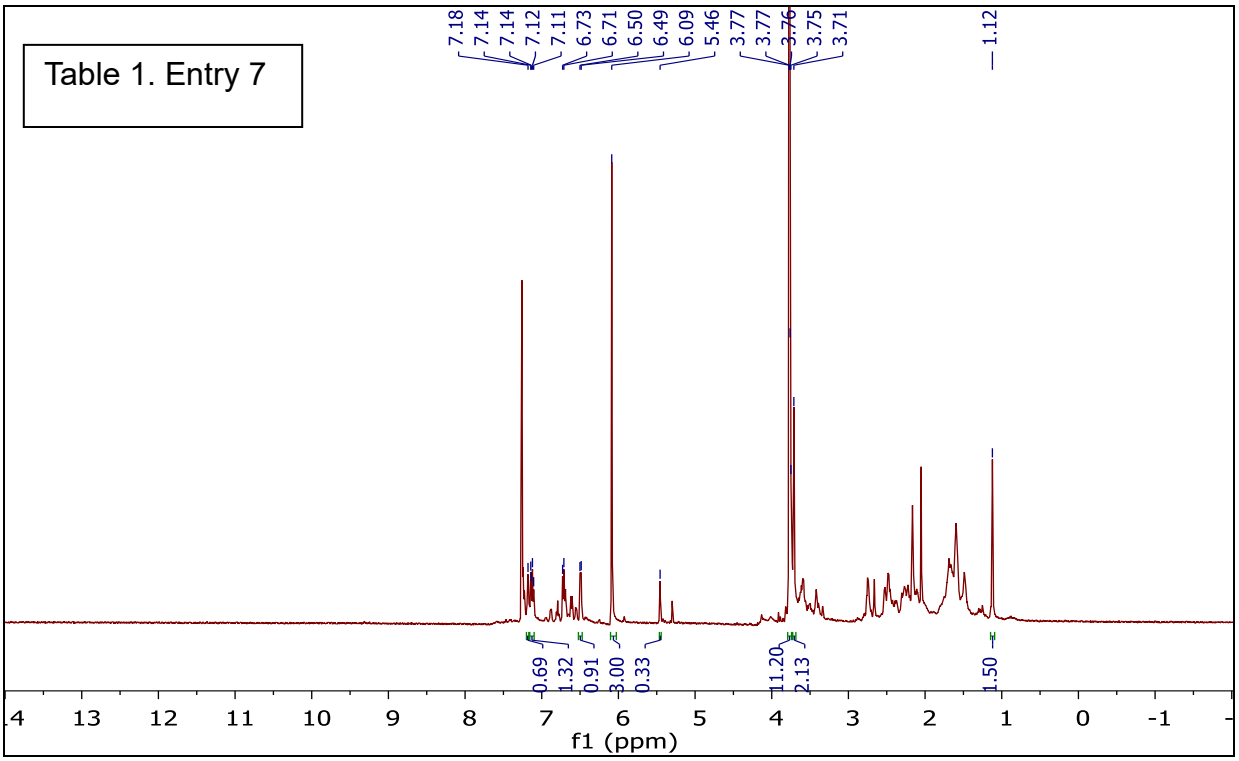
Table 1. Entry 7
7.18
7.14
7.14
7.12
7.11
6.73
6.71
6.50
6.49
6.09
5.46
3.77
3.77
3.76
3.75
3.71
1.12
0.69
1.32
0.91
3.00
0.33
11.20
2.13
1.50
f1 (ppm)

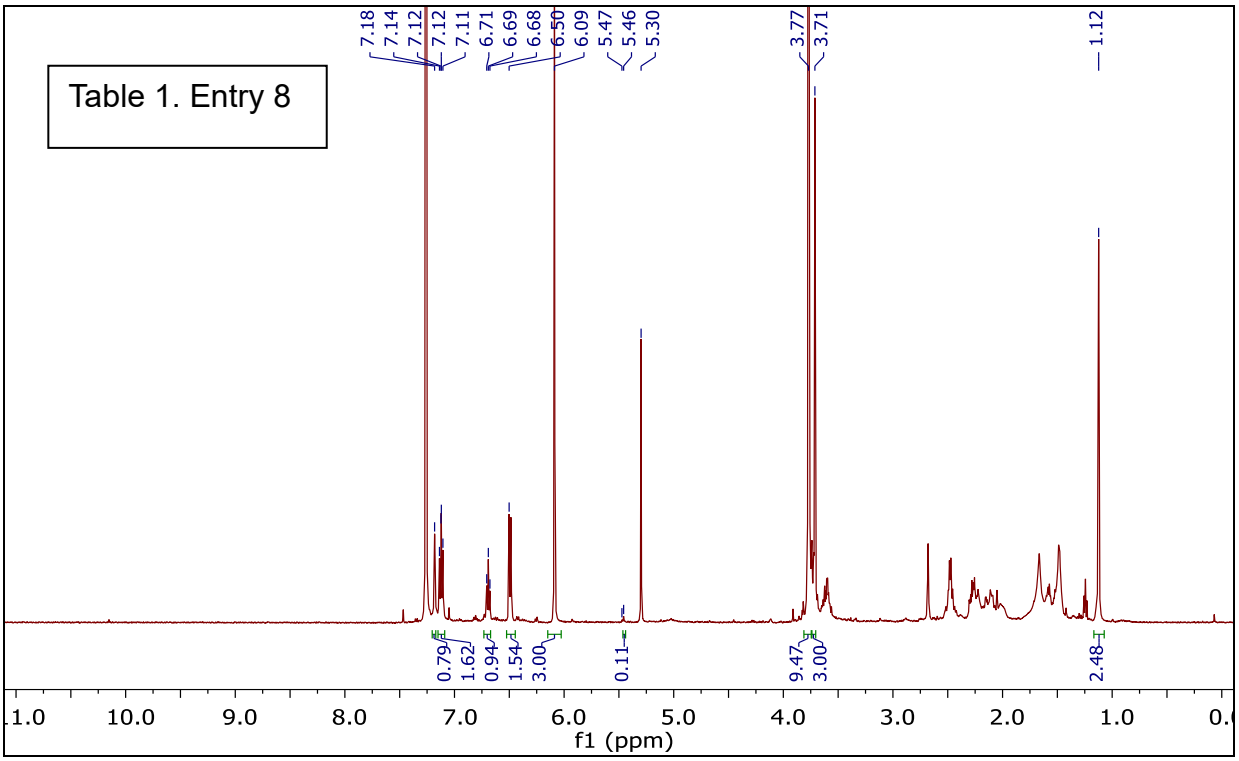
Table 1. Entry 8
7.18
7.14
7.12
7.12
7.11
6.71
6.69
6.68
6.50
6.09
5.47
5.46
5.30
3.77
3.71
1.12
0.79
1.62
0.94
1.54
3.00
0.11
9.47
3.00
2.48
f1 (ppm)

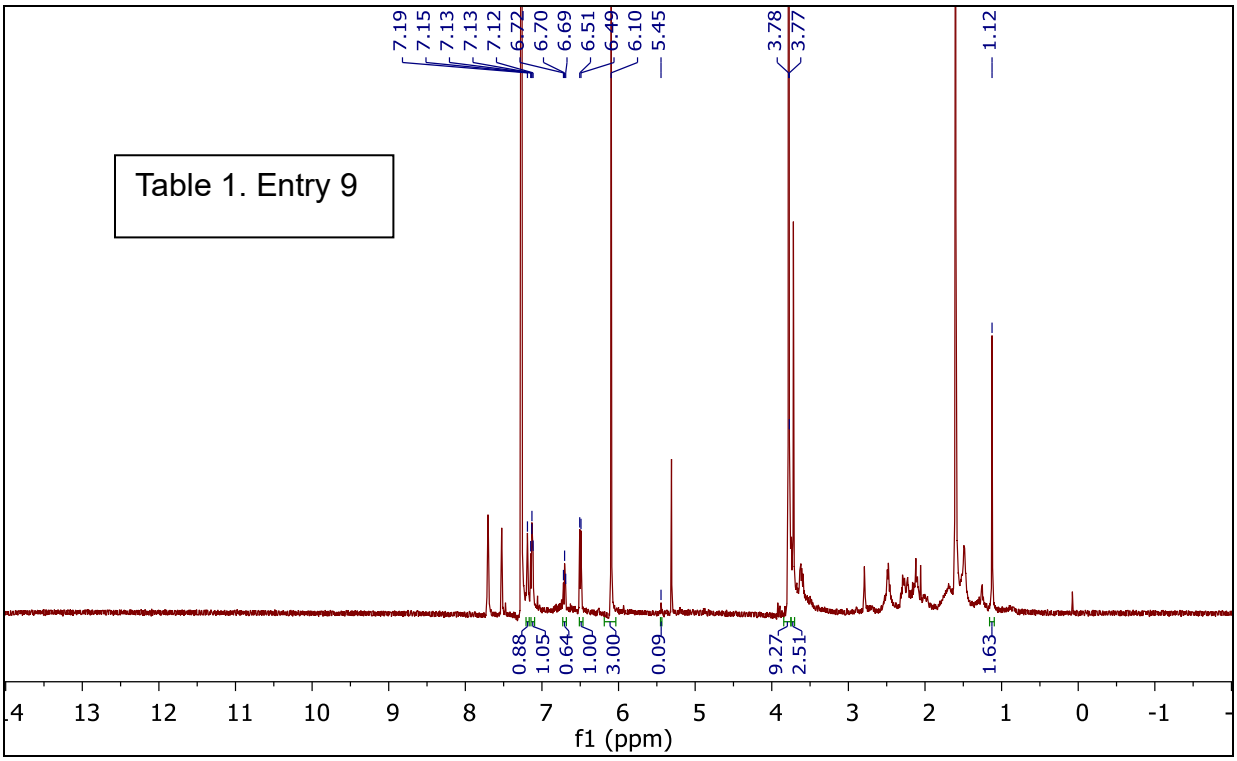
Table 1. Entry 9
7.19
7.15
7.13
7.13
7.12
6.72
6.70
6.69
6.51
6.49
6.10
5.45
3.78
3.77
1.12
0.88
1.05
0.64
1.00
3.00
0.09
9.27
2.51
1.63
f1 (ppm)

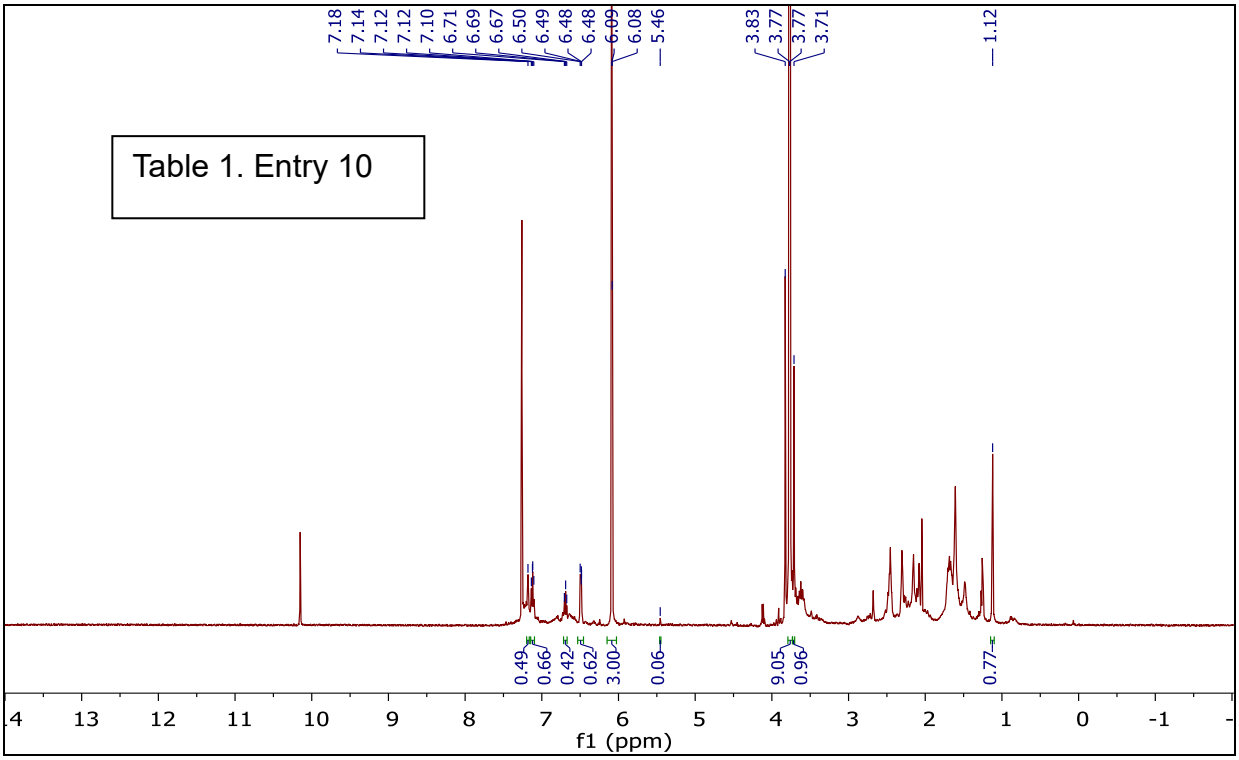
Table 1. Entry 10
7.18
7.14
7.12
7.12
7.10
6.71
6.69
6.67
6.50
6.49
6.48
6.48
6.09
6.08
5.46
3.83
3.77
3.77
3.71
1.12
0.49
0.66
0.42
0.62
3.00
0.06
9.05
0.96
0.77
f1 (ppm)

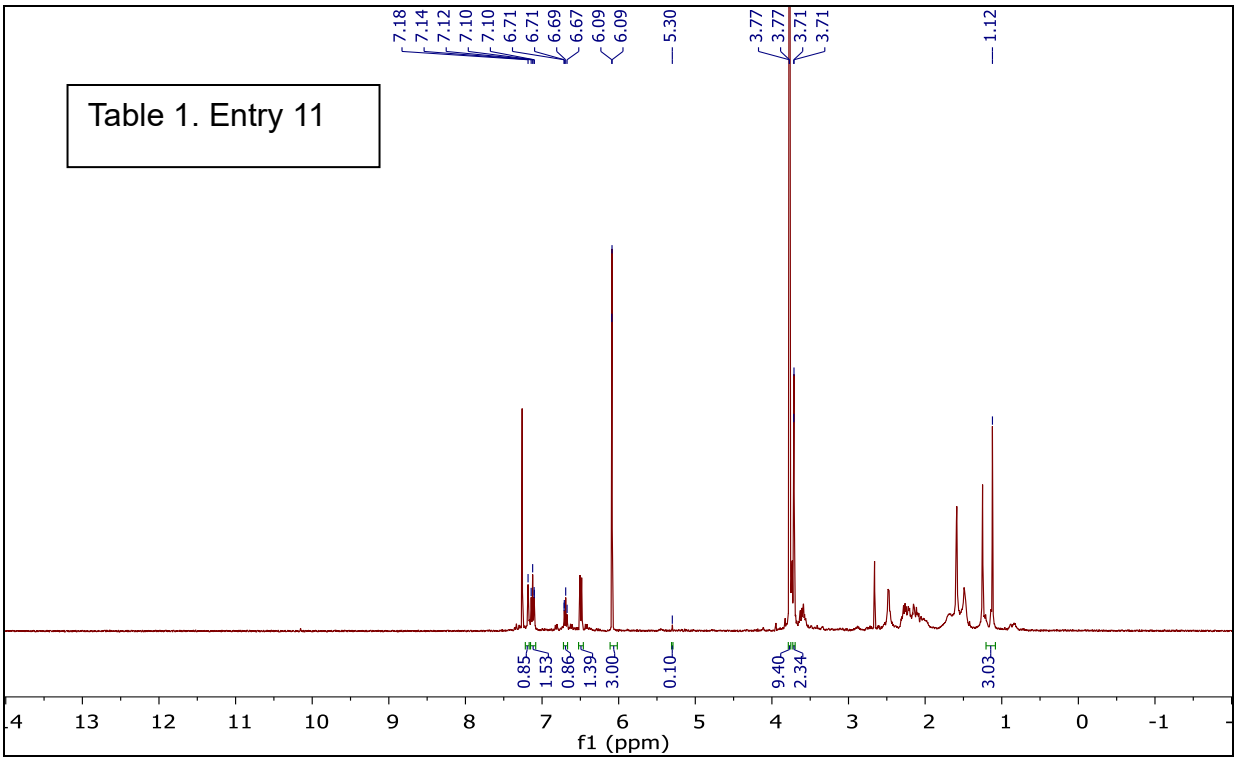
Table 1. Entry 11
7.18
7.14
7.12
7.10
7.10
6.71
6.71
6.69
6.67
6.09
6.09
5.30
3.77
3.77
3.71
3.71
1.12
0.85
1.53
0.86
1.39
3.00
0.10
9.40
2.34
3.03
f1 (ppm)

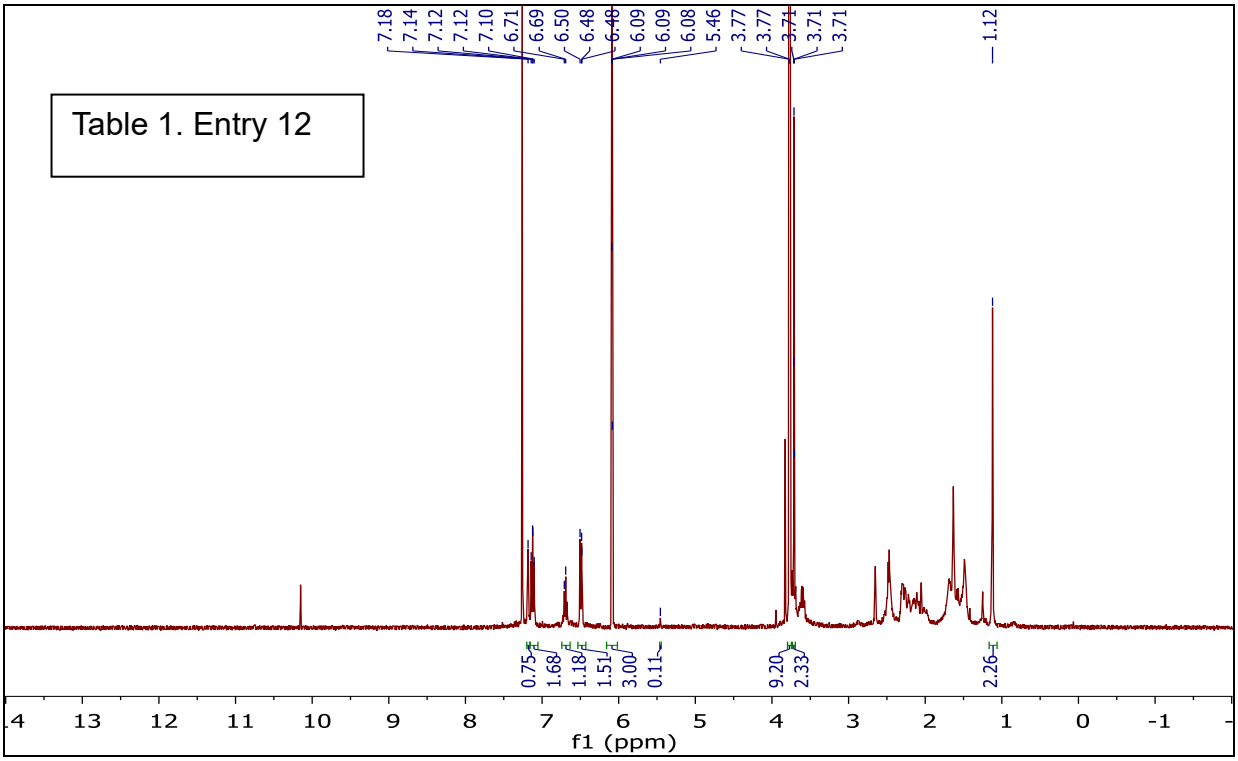
Table 1. Entry 12
7.18
7.14
7.12
7.12
7.10
6.71
6.69
6.50
6.48
6.48
6.09
6.09
6.08
5.46
3.77
3.77
3.71
3.71
3.71
1.12
0.75
1.68
1.18
1.51
3.00
0.11
9.20
2.33
2.26
f1 (ppm)

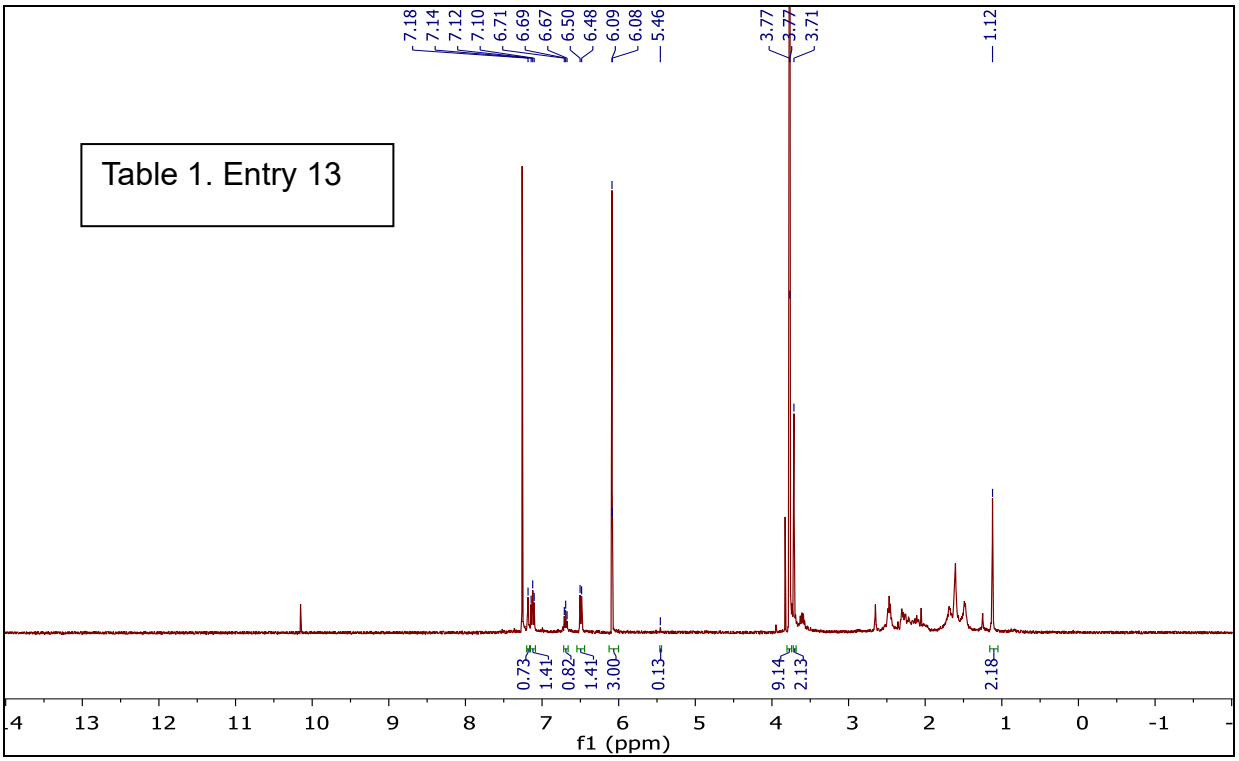
Table 1. Entry 13
7.18
7.14
7.12
7.10
6.71
6.69
6.67
6.50
6.48
6.09
6.08
5.46
3.77
3.77
3.71
1.12
0.73
1.41
0.82
1.41
3.00
0.13
9.14
2.13
2.18
f1 (ppm)

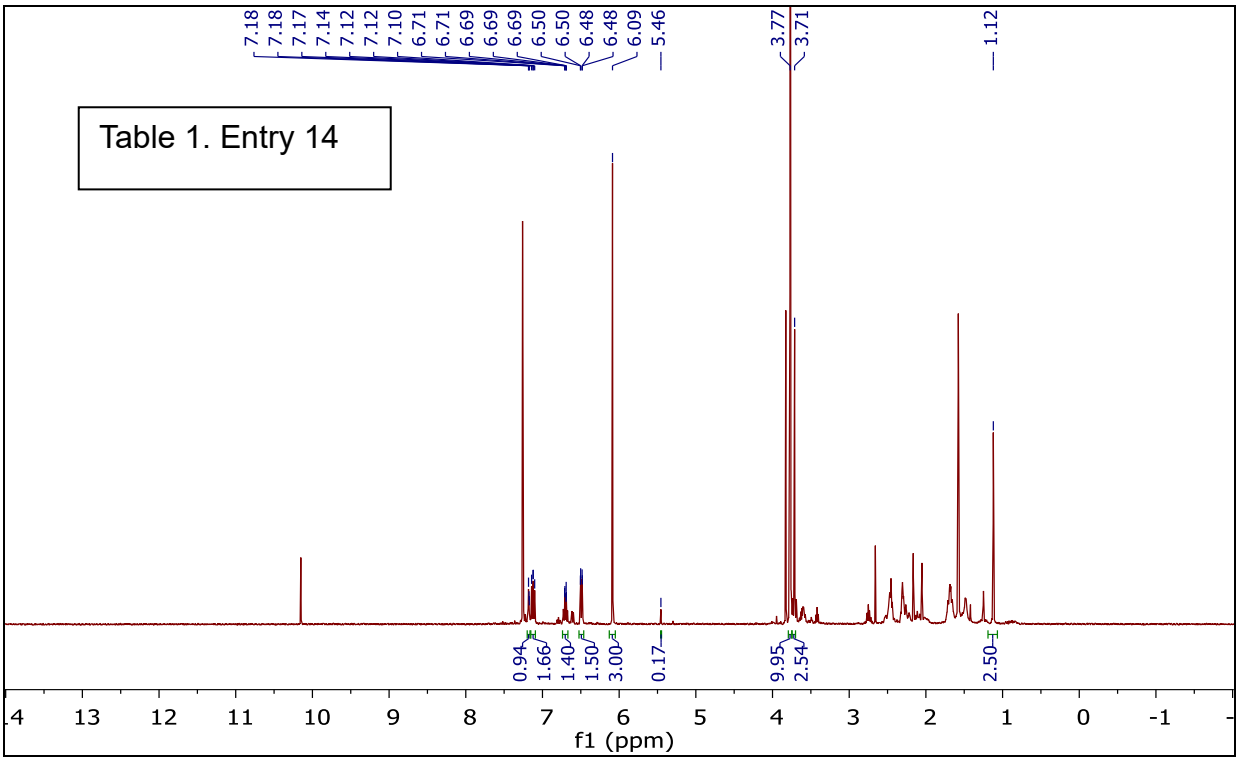
Table 1. Entry 14
7.18
7.18
7.17
7.14
7.12
7.12
7.10
6.71
6.71
6.69
6.69
6.69
6.50
6.50
6.48
6.48
6.09
5.46
3.77
3.71
1.12
0.94
1.66
1.40
1.50
3.00
0.17
9.95
2.54
2.50
f1 (ppm)

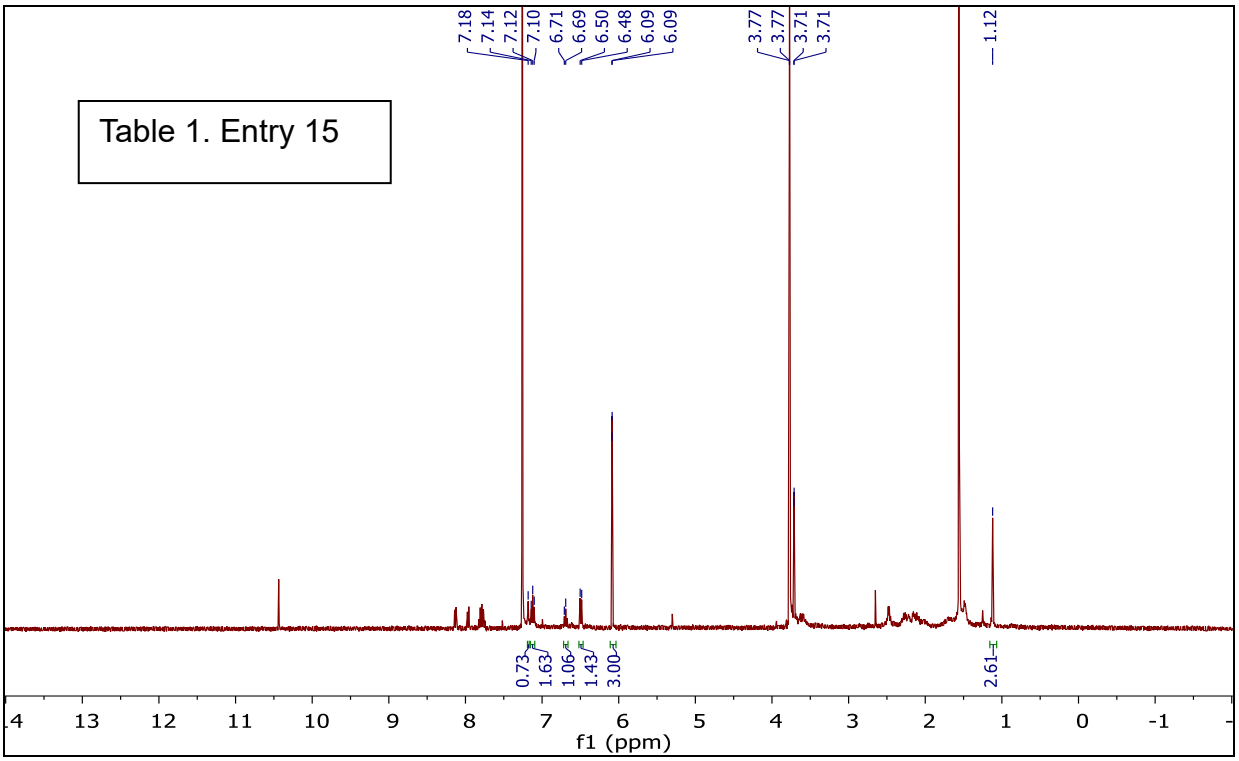
Table 1. Entry 15
7.18
7.14
7.12
7.10
6.71
6.69
6.50
6.48
6.09
6.09
3.77
3.77
3.71
3.71
1.12
0.73
1.63
1.06
1.43
3.00
2.61
f1 (ppm)

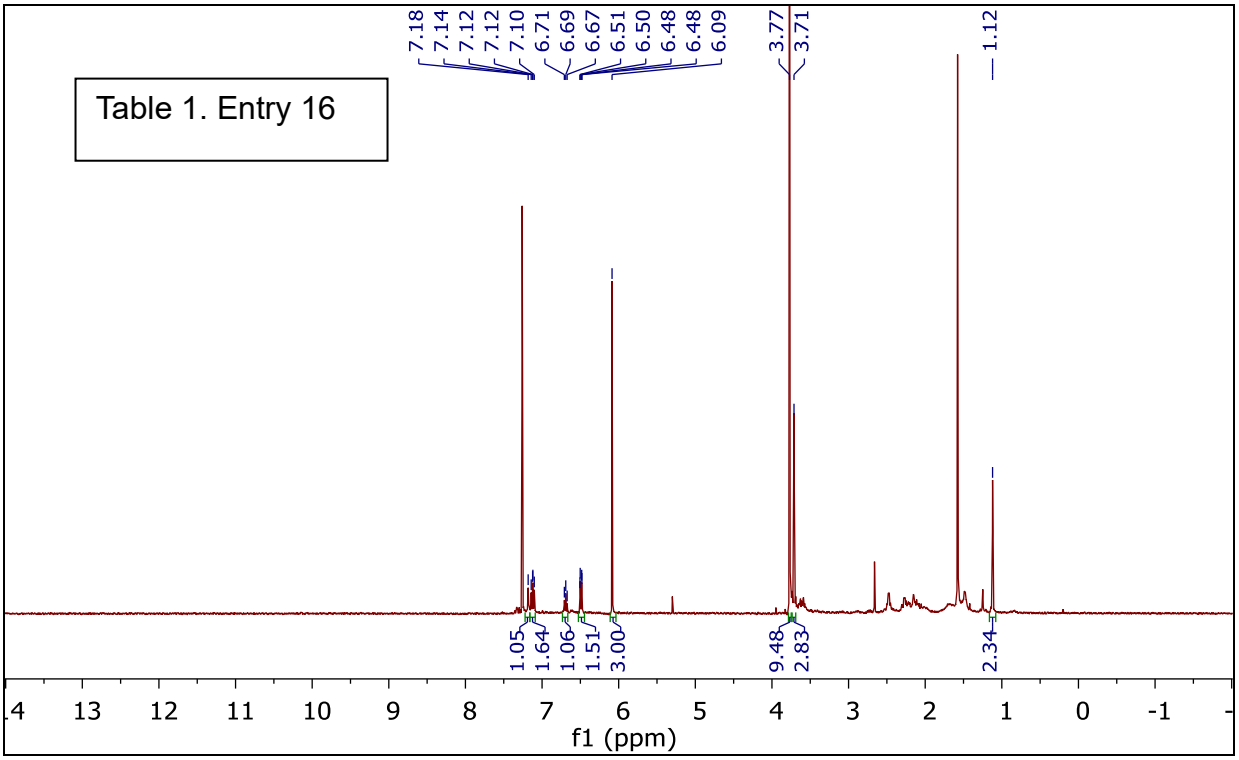
Table 1. Entry 16
7.18
7.14
7.12
7.12
7.10
6.71
6.69
6.67
6.51
6.50
6.48
6.48
6.09
3.77
3.71
1.12
1.05
1.64
1.06
1.51
3.00
9.48
2.83
2.34
f1 (ppm)

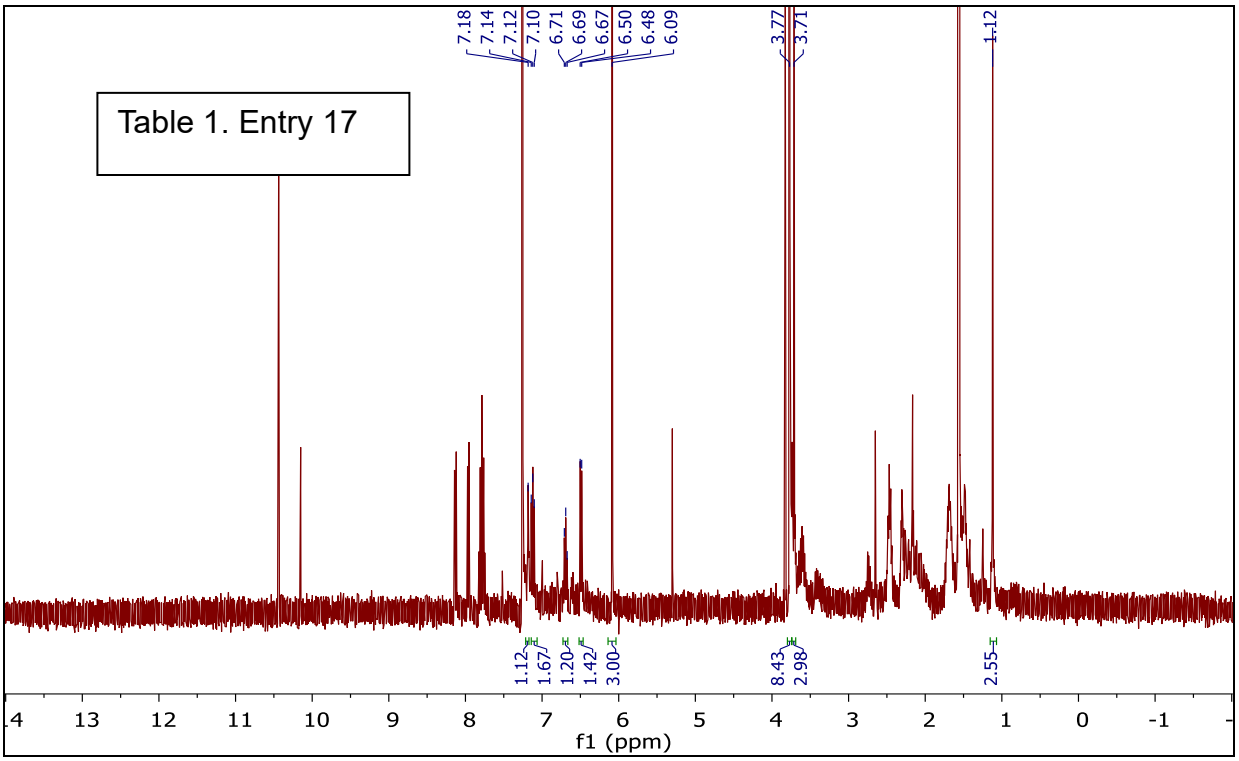
Table 1. Entry 17
7.18
7.14
7.12
7.10
6.71
6.69
6.67
6.50
6.48
6.09
3.77
3.71
1.12
1.12
1.67
1.20
1.42
3.00
8.43
2.98
2.55
f1 (ppm)

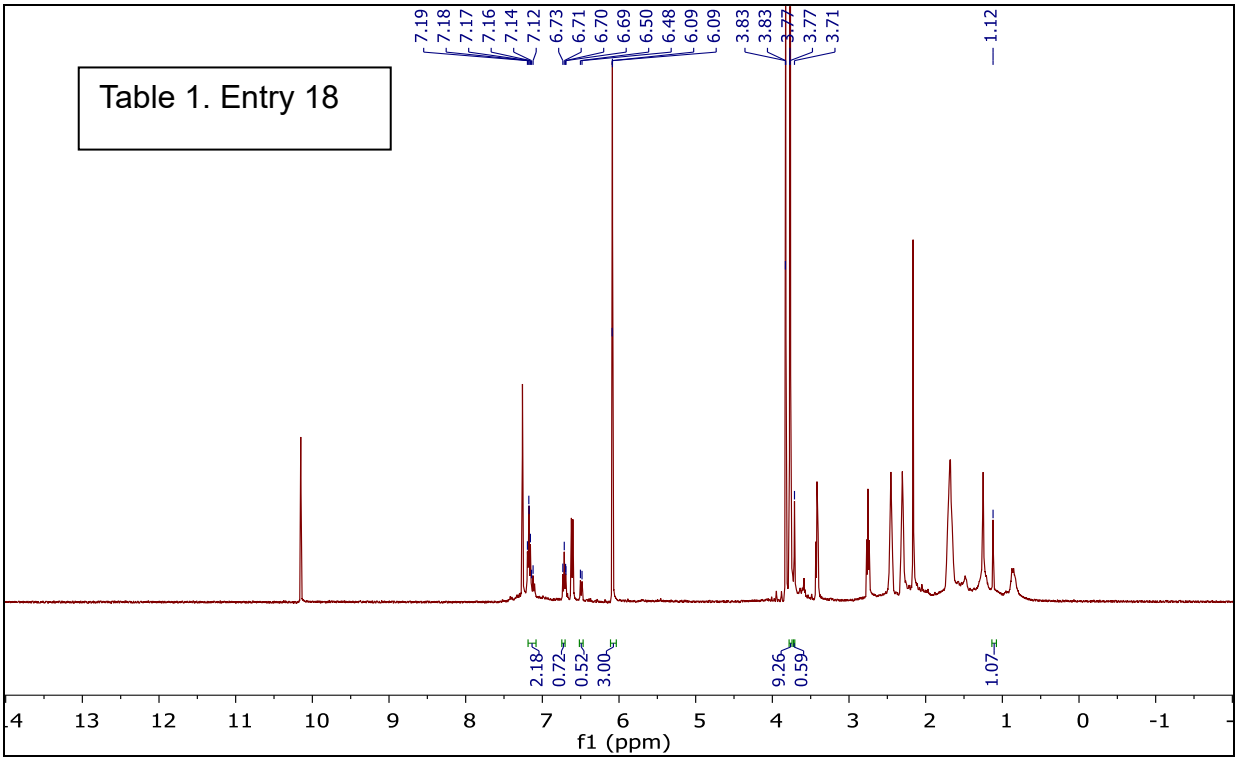
Table 1. Entry 18
7.19
7.18
7.17
7.16
7.14
7.12
6.73
6.71
6.70
6.69
6.50
6.48
6.09
6.09
3.83
3.83
3.77
3.77
3.71
1.12
2.18
0.72
0.52
3.00
9.26
0.59
1.07
f1 (ppm)

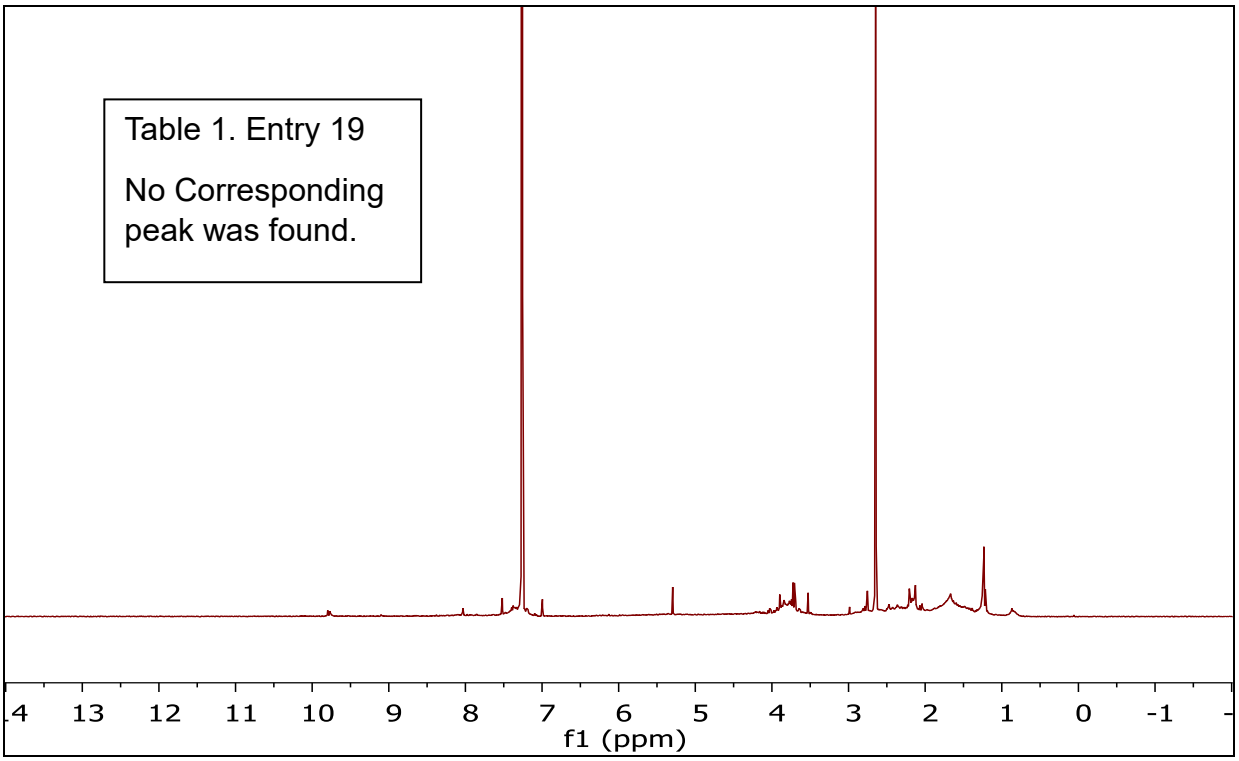
Table 1. Entry 19
No Corresponding peak was found.
13 12 11 10 9 8 7 6 5 4 3 2 1 0 -1
f1 (ppm)

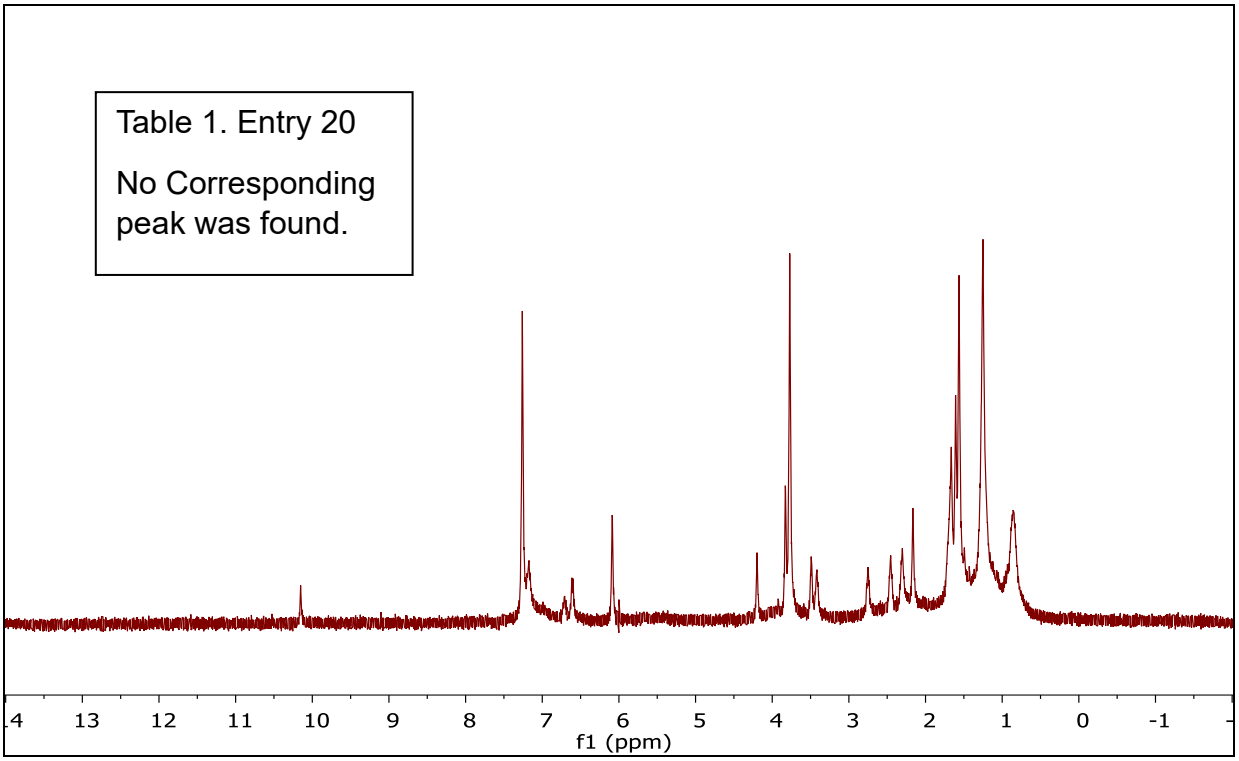
Table 1. Entry 20
No Corresponding peak was found.
13 12 11 10 9 8 7 6 5 4 3 2 1 0 -1
f1 (ppm)

X-Ray Diffraction Data for 3b (BG-CO-05)

CCDC 2285842

Formula: C21 H24 Br N O4

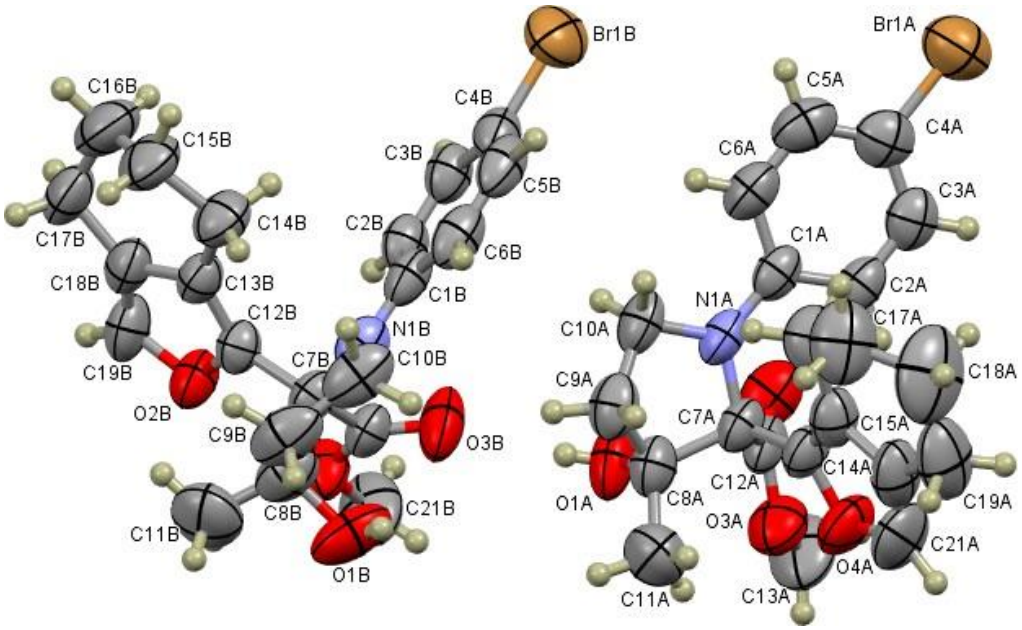

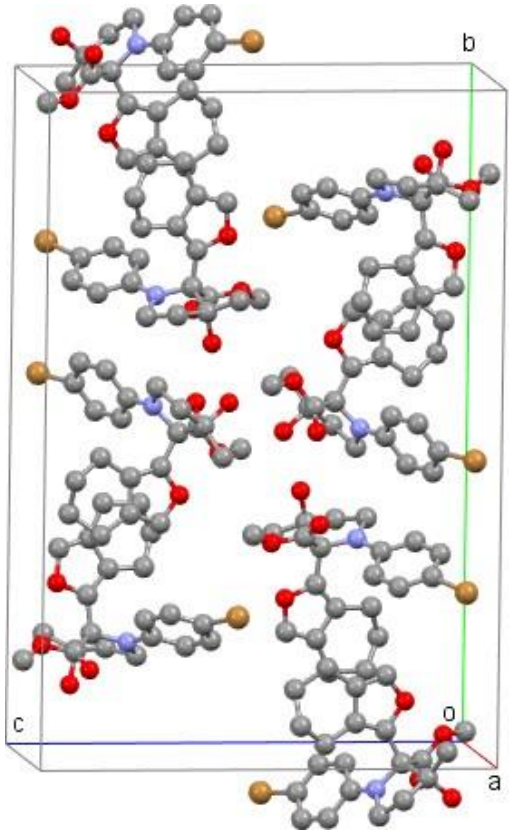

Table 1. Crystal data and structure refinement for BG-CO-05.

Empirical formula	C21 H24 Br N O4	
Formula weight	434.32	
Crystal system	monoclinic	
Space group	*P*2**1**/*c*	
Unit cell dimensions	*a* = 8.1671(2) Å	= 90°
	b = 26.8544(6) Å	= 91.4034(8)°
	c = 18.1446(5) Å	= 90°
Volume	3978.33(17) Å^3	
Z, Z'	8, 1	
Density (calculated)	1.450 Mg/m^3	
Wavelength	0.71073 Å	
Temperature	100(2) K	
F(000)	1792	
Absorption coefficient	2.093 mm^{-1}	
Absorption correction	semi-empirical from equivalents	
Max. and min. transmission	0.7454 and 0.6379	
Theta range for data collection	2.246 to 26.389°	
Reflections collected	69735	
Independent reflections	8148 [R(int) = 0.0610]	
Data / restraints / parameters	8148 / 36 / 507	
wR(*F*^{2} all data)	*wR*2 = 0.1041	
R(*F* obsd data)	*R*1 = 0.0393	
Goodness-of-fit on *F*^{2}	1.003	
Observed data [I > 2 (I)]	5833	
Largest and mean shift / s.u	0.002 and 0.000	
Largest diff. peak and hole	0.543 and -0.613 e/Å^3	

$wR2 = \{ [w(F_o^2 - F_c^2)^2] / [w(F_o^2)^2] \}^{1/2}$

$R1 = ||F_o| - |F_c|| / |F_o|$

Table 2. Atomic coordinates and equivalent isotropic displacement parameters for BG-CO-05. U(eq) is defined as one third of the trace of the orthogonalized U_{ij} tensor.

	x	y	z	U(eq)
Br(1A)	-0.20072(5)	.73275(2)	91177(2)	06589(12)
O(1A)	0.4714(3)	.60791(7)	59708(13)	0530(6)
O(2A)	0.1154(3)	.64398(7)	61266(12)	0526(5)
O(3A)	0.2479(3)	.67554(8)	51713(11)	0535(5)
O(4A)	0.3690(3)	.76246(7)	55788(12)	0537(5)
N(1A)	0.3570(3)	.67458(8)	71279(12)	0376(5)
C(1A)	0.2296(3)	.68843(9)	75639(15)	0352(6)
C(2A)	0.0965(3)	.71787(10)	73104(16)	0395(6)
C(3A)	-0.0279(4)	.73077(10)	77677(17)	0430(7)
C(4A)	-0.0254(4)	.71553(11)	84940(17)	0461(7)
C(5A)	0.1036(4)	.68725(11)	87622(17)	0495(7)
C(6A)	0.2281(4)	.67369(10)	83064(16)	0437(7)
C(7A)	0.3745(3)	.68717(9)	63498(15)	0363(6)
C(8A)	0.5321(3)	.65678(10)	61392(16)	0423(7)
C(9A)	0.6300(3)	.65615(11)	68590(17)	0456(7)
C(10A)	0.5025(3)	.64937(10)	74392(16)	0424(7)
C(11A)	0.6256(4)	.67715(14)	5499(2)	0645(9)
C(12A)	0.2292(4)	.66624(10)	58817(15)	0398(6)
C(13A)	0.1185(5)	.65863(15)	4670(2)	0725(11)
C(14A)	0.3958(3)	.74302(9)	62713(16)	0391(6)
C(15A)	0.4395(3)	.77985(10)	67507(17)	0408(6)
C(16A)	0.4820(4)	.78036(10)	75610(18)	0507(8)
C(17A)	0.5696(7)	.82765(11)	7783(3)	0685(15)
C(17')	0.472(4)	.82937(14)	7953(5)	068(2)
C(18A)	0.4937(6)	.87382(12)	7468(3)	0858(13)
C(19A)	0.4771(5)	.87526(11)	6649(2)	0660(10)
C(20A)	0.4390(4)	.82517(10)	6329(2)	0504(8)
C(21A)	0.3976(5)	.81248(11)	5636(2)	0629(10)
Br(1B)	0.34468(5)	.56025(2)	96800(2)	06148(12)
O(1B)	1.0232(3)	.54237(9)	60044(13)	0642(7)
O(2B)	0.9273(2)	.40272(6)	69898(10)	0418(5)
O(3B)	0.6744(3)	.52911(8)	64606(12)	0603(6)
O(4B)	0.7736(2)	.45871(7)	60203(10)	0457(5)
N(1B)	0.9059(3)	.53376(8)	75829(13)	0401(5)
C(1B)	0.7758(3)	.54029(9)	80394(15)	0369(6)
C(2B)	0.6469(3)	.50581(9)	80690(15)	0382(6)

C(3B)	0.5214(3)	**0.51195(9)**	0.85516(15)	0.0395(6)
C(4B)	0.5192(4)	**0.55282(10)**	0.90139(15)	0.0426(7)
C(5B)	0.6428(4)	**0.58764(10)**	0.89939(16)	0.0457(7)
C(6B)	0.7693(4)	**0.58147(10)**	0.85126(16)	0.0443(7)
C(7B)	0.9202(3)	**0.49438(9)**	0.70352(14)	0.0345(6)
C(8B)	1.0767(4)	**0.51038(12)**	0.65900(17)	0.0491(7)
C(9B)	1.1738(4)	**0.53904(13)**	0.71772(18)	0.0563(9)
C(10B)	1.0487(4)	**0.56680(11)**	0.76099(18)	0.0523(8)
C(11B)	1.1688(4)	**0.46812(14)**	0.6241(2)	0.0696(10)
C(12B)	0.9430(3)	**0.44469(9)**	0.74181(14)	0.0332(6)
C(13B)	0.9908(3)	**0.43176(9)**	0.81158(15)	0.0350(6)
C(14B)	1.0218(4)	**0.46200(11)**	0.88012(16)	0.0474(7)
C(15B)	1.1080(4)	**0.43155(12)**	0.94026(17)	0.0560(8)
C(16B)	1.0351(5)	**0.38053(13)**	0.94869(19)	0.0622(9)
C(17B)	1.0487(4)	**0.34846(11)**	0.88010(17)	0.0503(8)
C(18B)	1.0028(3)	**0.37834(10)**	0.81257(16)	0.0399(6)
C(19B)	0.9636(4)	**0.36303(10)**	0.74388(18)	0.0470(7)
C(20B)	0.7740(3)	**0.49645(9)**	0.64812(15)	0.0364(6)
C(21B)	0.6484(4)	**0.45903(15)**	0.54463(19)	0.0698(11)

Table 3. Bond lengths [Å] and angles [°] for BG-CO-05

Br(1A)-C(4A)	1.904(3)	C(16A)-H(16A)	0.9900
O(1A)-C(8A)	1.433(3)	C(16A)-H(16B)	0.9900
O(1A)-H(1A)	0.78(4)	C(16A)-H(16E)	0.9900
O(2A)-C(12A)	1.200(3)	C(16A)-H(16F)	0.9900
O(3A)-C(12A)	1.325(3)	C(17A)-C(18A)	1.494(4)
O(3A)-C(13A)	1.451(4)	C(17A)-H(17A)	0.9900
O(4A)-C(21A)	1.367(4)	C(17A)-H(17B)	0.9900
O(4A)-C(14A)	1.373(3)	C(17')-C(18A)	1.496(5)
N(1A)-C(1A)	1.374(4)	C(17')-H(17E)	0.9900
N(1A)-C(7A)	1.462(3)	C(17')-H(17F)	0.9900
N(1A)-C(10A)	1.468(3)	C(18A)-C(19A)	1.489(6)
C(1A)-C(6A)	1.405(4)	C(18A)-H(18A)	0.9900
C(1A)-C(2A)	1.412(4)	C(18A)-H(18B)	0.9900
C(2A)-C(3A)	1.372(4)	C(18A)-H(18C)	0.9900
C(2A)-H(2A)	0.9500	C(18A)-H(18D)	0.9900
C(3A)-C(4A)	1.379(4)	C(19A)-C(20A)	1.495(4)
C(3A)-H(3A)	0.9500	C(19A)-H(19A)	0.9900
C(4A)-C(5A)	1.378(4)	C(19A)-H(19B)	0.9900
C(5A)-C(6A)	1.375(4)	C(20A)-C(21A)	1.337(5)
C(5A)-H(5A)	0.9500	C(21A)-H(21A)	0.9500
C(6A)-H(6A)	0.9500	Br(1B)-C(4B)	1.902(3)
C(7A)-C(14A)	1.517(3)	O(1B)-C(8B)	1.427(4)
C(7A)-C(12A)	1.548(4)	O(1B)-H(1B)	0.76(4)
C(7A)-C(8A)	1.579(4)	O(2B)-C(19B)	1.370(3)
C(8A)-C(11A)	1.509(4)	O(2B)-C(12B)	1.373(3)
C(8A)-C(9A)	1.515(4)	O(3B)-C(20B)	1.196(3)
C(9A)-C(10A)	1.510(4)	O(4B)-C(20B)	1.314(3)
C(9A)-H(9AA)	0.9900	O(4B)-C(21B)	1.442(3)
C(9A)-H(9AB)	0.9900	N(1B)-C(1B)	1.375(4)
C(10A)-H(10A)	0.9900	N(1B)-C(7B)	1.458(3)
C(10A)-H(10B)	0.9900	N(1B)-C(10B)	1.465(3)
C(11A)-H(11A)	0.9800	C(1B)-C(6B)	1.402(4)
C(11A)-H(11B)	0.9800	C(1B)-C(2B)	1.404(4)
C(11A)-H(11C)	0.9800	C(2B)-C(3B)	1.374(4)
C(13A)-H(13A)	0.9800	C(2B)-H(2B)	0.9500
C(13A)-H(13B)	0.9800	C(3B)-C(4B)	1.382(4)
C(13A)-H(13C)	0.9800	C(3B)-H(3B)	0.9500
C(14A)-C(15A)	1.359(4)	C(4B)-C(5B)	1.377(4)
C(15A)-C(20A)	1.438(4)	C(5B)-C(6B)	1.379(4)
C(15A)-C(16A)	1.502(4)	C(5B)-H(5B)	0.9500
C(16A)-C(17')	1.499(5)	C(6B)-H(6B)	0.9500
C(16A)-C(17A)	1.507(4)	C(7B)-C(12B)	1.514(3)

C(7B)-C(20B)	1.543(4)	C(14B)-H(14A)	0.9900
C(7B)-C(8B)	1.588(4)	C(14B)-H(14B)	0.9900
C(8B)-C(11B)	1.510(5)	C(15B)-C(16B)	1.503(5)
C(8B)-C(9B)	1.521(4)	C(15B)-H(15A)	0.9900
C(9B)-C(10B)	1.502(5)	C(15B)-H(15B)	0.9900
C(9B)-H(9BA)	0.9900	C(16B)-C(17B)	1.520(5)
C(9B)-H(9BB)	0.9900	C(16B)-H(16C)	0.9900
C(10B)-H(10C)	0.9900	C(16B)-H(16D)	0.9900
C(10B)-H(10D)	0.9900	C(17B)-C(18B)	1.505(4)
C(11B)-H(11D)	0.9800	C(17B)-H(17C)	0.9900
C(11B)-H(11E)	0.9800	C(17B)-H(17D)	0.9900
C(11B)-H(11F)	0.9800	C(18B)-C(19B)	1.344(4)
C(12B)-C(13B)	1.361(4)	C(19B)-H(19C)	0.9500
C(13B)-C(18B)	1.438(4)	C(21B)-H(21B)	0.9800
C(13B)-C(14B)	1.502(4)	C(21B)-H(21C)	0.9800
C(14B)-C(15B)	1.522(4)	C(21B)-H(21D)	0.9800

C(8A)-O(1A)-H(1A)	106(3)	C(14A)-C(7A)-C(8A)	113.1(2)
C(12A)-O(3A)-C(13A)	116.8(3)	C(12A)-C(7A)-C(8A)	107.3(2)
C(21A)-O(4A)-C(14A)	106.3(2)	O(1A)-C(8A)-C(11A)	110.3(3)
C(1A)-N(1A)-C(7A)	125.9(2)	O(1A)-C(8A)-C(9A)	110.3(2)
C(1A)-N(1A)-C(10A)	121.4(2)	C(11A)-C(8A)-C(9A)	113.7(3)
C(7A)-N(1A)-C(10A)	112.4(2)	O(1A)-C(8A)-C(7A)	104.2(2)
N(1A)-C(1A)-C(6A)	120.0(2)	C(11A)-C(8A)-C(7A)	115.5(2)
N(1A)-C(1A)-C(2A)	123.5(2)	C(9A)-C(8A)-C(7A)	102.3(2)
C(6A)-C(1A)-C(2A)	116.5(3)	C(10A)-C(9A)-C(8A)	104.1(2)
C(3A)-C(2A)-C(1A)	121.3(3)	C(10A)-C(9A)-H(9AA)	110.9
C(3A)-C(2A)-H(2A)	119.3	C(8A)-C(9A)-H(9AA)	110.9
C(1A)-C(2A)-H(2A)	119.3	C(10A)-C(9A)-H(9AB)	110.9
C(2A)-C(3A)-C(4A)	120.6(3)	C(8A)-C(9A)-H(9AB)	110.9
C(2A)-C(3A)-H(3A)	119.7	H(9AA)-C(9A)-H(9AB)	108.9
C(4A)-C(3A)-H(3A)	119.7	N(1A)-C(10A)-C(9A)	104.0(2)
C(5A)-C(4A)-C(3A)	119.6(3)	N(1A)-C(10A)-H(10A)	111.0
C(5A)-C(4A)-Br(1A)	120.2(2)	C(9A)-C(10A)-H(10A)	111.0
C(3A)-C(4A)-Br(1A)	120.1(2)	N(1A)-C(10A)-H(10B)	111.0
C(6A)-C(5A)-C(4A)	120.2(3)	C(9A)-C(10A)-H(10B)	111.0
C(6A)-C(5A)-H(5A)	119.9	H(10A)-C(10A)-H(10B)	109.0
C(4A)-C(5A)-H(5A)	119.9	C(8A)-C(11A)-H(11A)	109.5
C(5A)-C(6A)-C(1A)	121.7(3)	C(8A)-C(11A)-H(11B)	109.5
C(5A)-C(6A)-H(6A)	119.1	H(11A)-C(11A)-H(11B)	109.5
C(1A)-C(6A)-H(6A)	119.1	C(8A)-C(11A)-H(11C)	109.5
N(1A)-C(7A)-C(14A)	109.5(2)	H(11A)-C(11A)-H(11C)	109.5
N(1A)-C(7A)-C(12A)	110.7(2)	H(11B)-C(11A)-H(11C)	109.5
C(14A)-C(7A)-C(12A)	113.3(2)	O(2A)-C(12A)-O(3A)	124.3(3)
N(1A)-C(7A)-C(8A)	102.3(2)	O(2A)-C(12A)-C(7A)	124.6(3)
O(3A)-C(12A)-C(7A)	111.1(2)	C(17')-C(18A)-H(18C)	105.6
O(3A)-C(13A)-H(13A)	109.5	C(19A)-C(18A)-H(18D)	105.6

O(3A)-C(13A)-H(13B)	109.5	C(17')-C(18A)-H(18D)	105.6
H(13A)-C(13A)-H(13B)	109.5	H(18C)-C(18A)-H(18D)	106.1
O(3A)-C(13A)-H(13C)	109.5	C(18A)-C(19A)-C(20A)	112.2(3)
H(13A)-C(13A)-H(13C)	109.5	C(18A)-C(19A)-H(19A)	109.2
H(13B)-C(13A)-H(13C)	109.5	C(20A)-C(19A)-H(19A)	109.2
C(15A)-C(14A)-O(4A)	110.0(2)	C(18A)-C(19A)-H(19B)	109.2
C(15A)-C(14A)-C(7A)	133.5(3)	C(20A)-C(19A)-H(19B)	109.2
O(4A)-C(14A)-C(7A)	116.5(2)	H(19A)-C(19A)-H(19B)	107.9
C(14A)-C(15A)-C(20A)	106.1(3)	C(21A)-C(20A)-C(15A)	106.4(3)
C(14A)-C(15A)-C(16A)	133.1(2)	C(21A)-C(20A)-C(19A)	129.8(3)
C(20A)-C(15A)-C(16A)	120.7(3)	C(15A)-C(20A)-C(19A)	123.8(3)
C(17')-C(16A)-C(15A)	117.3(6)	C(20A)-C(21A)-O(4A)	111.2(3)
C(15A)-C(16A)-C(17A)	111.4(3)	C(20A)-C(21A)-H(21A)	124.4
C(15A)-C(16A)-H(16A)	109.3	O(4A)-C(21A)-H(21A)	124.4
C(17A)-C(16A)-H(16A)	109.3	C(8B)-O(1B)-H(1B)	108(3)
C(15A)-C(16A)-H(16B)	109.3	C(19B)-O(2B)-C(12B)	106.6(2)
C(17A)-C(16A)-H(16B)	109.3	C(20B)-O(4B)-C(21B)	116.5(2)
H(16A)-C(16A)-H(16B)	108.0	C(1B)-N(1B)-C(7B)	125.4(2)
C(17')-C(16A)-H(16E)	108.0	C(1B)-N(1B)-C(10B)	121.9(2)
C(15A)-C(16A)-H(16E)	108.0	C(7B)-N(1B)-C(10B)	112.6(2)
C(17')-C(16A)-H(16F)	108.0	N(1B)-C(1B)-C(6B)	120.7(3)
C(15A)-C(16A)-H(16F)	108.0	N(1B)-C(1B)-C(2B)	122.0(2)
H(16E)-C(16A)-H(16F)	107.2	C(6B)-C(1B)-C(2B)	117.2(3)
C(18A)-C(17A)-C(16A)	114.0(3)	C(3B)-C(2B)-C(1B)	121.1(2)
C(18A)-C(17A)-H(17A)	108.7	C(3B)-C(2B)-H(2B)	119.4
C(16A)-C(17A)-H(17A)	108.7	C(1B)-C(2B)-H(2B)	119.4
C(18A)-C(17A)-H(17B)	108.7	C(2B)-C(3B)-C(4B)	120.2(3)
C(16A)-C(17A)-H(17B)	108.7	C(2B)-C(3B)-H(3B)	119.9
H(17A)-C(17A)-H(17B)	107.6	C(4B)-C(3B)-H(3B)	119.9
C(18A)-C(17')-C(16A)	114.4(5)	C(5B)-C(4B)-C(3B)	120.2(3)
C(18A)-C(17')-H(17E)	108.7	C(5B)-C(4B)-Br(1B)	120.5(2)
C(16A)-C(17')-H(17E)	108.7	C(3B)-C(4B)-Br(1B)	119.3(2)
C(18A)-C(17')-H(17F)	108.7	C(4B)-C(5B)-C(6B)	119.7(3)
C(16A)-C(17')-H(17F)	108.7	C(4B)-C(5B)-H(5B)	120.1
H(17E)-C(17')-H(17F)	107.6	C(6B)-C(5B)-H(5B)	120.1
C(19A)-C(18A)-C(17A)	115.5(4)	C(5B)-C(6B)-C(1B)	121.5(3)
C(19A)-C(18A)-C(17')	126.8(5)	C(5B)-C(6B)-H(6B)	119.2
C(19A)-C(18A)-H(18A)	108.4	C(1B)-C(6B)-H(6B)	119.2
C(17A)-C(18A)-H(18A)	108.4	N(1B)-C(7B)-C(12B)	109.7(2)
C(19A)-C(18A)-H(18B)	108.4	N(1B)-C(7B)-C(20B)	110.1(2)
C(17A)-C(18A)-H(18B)	108.4	C(12B)-C(7B)-C(20B)	114.5(2)
H(18A)-C(18A)-H(18B)	107.5	N(1B)-C(7B)-C(8B)	103.3(2)
C(19A)-C(18A)-H(18C)	105.6	C(12B)-C(7B)-C(8B)	112.4(2)
C(20B)-C(7B)-C(8B)	106.2(2)	C(15B)-C(14B)-H(14B)	109.3
O(1B)-C(8B)-C(11B)	106.7(3)	H(14A)-C(14B)-H(14B)	108.0
O(1B)-C(8B)-C(9B)	111.2(2)	C(16B)-C(15B)-C(14B)	112.7(3)
C(11B)-C(8B)-C(9B)	114.7(3)	C(16B)-C(15B)-H(15A)	109.1

O(1B)-C(8B)-C(7B)	107.8(2)	C(14B)-C(15B)-H(15A)	109.1
C(11B)-C(8B)-C(7B)	115.2(2)	C(16B)-C(15B)-H(15B)	109.1
C(9B)-C(8B)-C(7B)	101.1(2)	C(14B)-C(15B)-H(15B)	109.1
C(10B)-C(9B)-C(8B)	105.5(3)	H(15A)-C(15B)-H(15B)	107.8
C(10B)-C(9B)-H(9BA)	110.6	C(15B)-C(16B)-C(17B)	113.3(3)
C(8B)-C(9B)-H(9BA)	110.6	C(15B)-C(16B)-H(16C)	108.9
C(10B)-C(9B)-H(9BB)	110.6	C(17B)-C(16B)-H(16C)	108.9
C(8B)-C(9B)-H(9BB)	110.6	C(15B)-C(16B)-H(16D)	108.9
H(9BA)-C(9B)-H(9BB)	108.8	C(17B)-C(16B)-H(16D)	108.9
N(1B)-C(10B)-C(9B)	103.5(2)	H(16C)-C(16B)-H(16D)	107.7
N(1B)-C(10B)-H(10C)	111.1	C(18B)-C(17B)-C(16B)	110.1(2)
C(9B)-C(10B)-H(10C)	111.1	C(18B)-C(17B)-H(17C)	109.6
N(1B)-C(10B)-H(10D)	111.1	C(16B)-C(17B)-H(17C)	109.6
C(9B)-C(10B)-H(10D)	111.1	C(18B)-C(17B)-H(17D)	109.6
H(10C)-C(10B)-H(10D)	109.0	C(16B)-C(17B)-H(17D)	109.6
C(8B)-C(11B)-H(11D)	109.5	H(17C)-C(17B)-H(17D)	108.2
C(8B)-C(11B)-H(11E)	109.5	C(19B)-C(18B)-C(13B)	106.2(2)
H(11D)-C(11B)-H(11E)	109.5	C(19B)-C(18B)-C(17B)	129.9(3)
C(8B)-C(11B)-H(11F)	109.5	C(13B)-C(18B)-C(17B)	123.9(3)
H(11D)-C(11B)-H(11F)	109.5	C(18B)-C(19B)-O(2B)	110.9(2)
H(11E)-C(11B)-H(11F)	109.5	C(18B)-C(19B)-H(19C)	124.6
C(13B)-C(12B)-O(2B)	109.7(2)	O(2B)-C(19B)-H(19C)	124.6
C(13B)-C(12B)-C(7B)	132.9(2)	O(3B)-C(20B)-O(4B)	123.7(3)
O(2B)-C(12B)-C(7B)	117.1(2)	O(3B)-C(20B)-C(7B)	124.2(3)
C(12B)-C(13B)-C(18B)	106.5(2)	O(4B)-C(20B)-C(7B)	112.1(2)
C(12B)-C(13B)-C(14B)	132.2(2)	O(4B)-C(21B)-H(21B)	109.5
C(18B)-C(13B)-C(14B)	121.3(2)	O(4B)-C(21B)-H(21C)	109.5
C(13B)-C(14B)-C(15B)	111.6(2)	H(21B)-C(21B)-H(21C)	109.5
C(13B)-C(14B)-H(14A)	109.3	O(4B)-C(21B)-H(21D)	109.5
C(15B)-C(14B)-H(14A)	109.3	H(21B)-C(21B)-H(21D)	109.5
C(13B)-C(14B)-H(14B)	109.3	H(21C)-C(21B)-H(21D)	109.5

Table 4. Anisotropic displacement parameters ($Å^2 \times 10^3$) for **3b**. The anisotropic displacement factor exponent takes the form:

$-2\pi^2[h^2 a^{*2} U_{11} + ... + 2 h k a^* b^* U_{12}]$

	U_{11}	U_{22}	U_{33}	U_{23}	U_{13}	U_{12}
Br(1A)	66(1)	66(1)	66(1)	-5(1)	15(1)	1(1)
O(1A)	59(1)	32(1)	67(2)	-7(1)	-23(1)	2(1)
O(2A)	57(1)	41(1)	59(1)	4(1)	-14(1)	.3(1)
O(3A)	63(1)	56(1)	40(1)	0(1)	-12(1)	6(1)
O(4A)	77(2)	34(1)	50(1)	14(1)	-3(1)	3(1)
N(1A)	43(1)	31(1)	38(1)	8(1)	-10(1)	2(1)
C(1A)	42(2)	24(1)	39(2)	4(1)	-9(1)	6(1)
C(2A)	45(2)	31(1)	42(2)	6(1)	-9(1)	4(1)
C(3A)	44(2)	31(1)	54(2)	1(1)	-5(1)	5(1)
C(4A)	50(2)	37(2)	52(2)	-1(1)	5(1)	.0(1)
C(5A)	61(2)	44(2)	43(2)	8(1)	-3(2)	.0(2)
C(6A)	49(2)	38(2)	44(2)	10(1)	-8(1)	3(1)
C(7A)	43(2)	27(1)	39(2)	5(1)	-6(1)	1(1)
C(8A)	45(2)	31(1)	50(2)	1(1)	-5(1)	4(1)
C(9A)	40(2)	40(2)	56(2)	0(1)	-13(1)	2(1)
C(10A)	43(2)	34(1)	49(2)	5(1)	-16(1)	3(1)
C(11A)	59(2)	71(2)	65(2)	7(2)	13(2)	1(2)
C(12A)	50(2)	29(1)	40(2)	2(1)	-10(1)	9(1)
C(13A)	80(3)	82(3)	53(2)	-12(2)	-33(2)	6(2)
C(14A)	46(2)	28(1)	43(2)	9(1)	0(1)	3(1)
C(15A)	38(2)	28(1)	56(2)	4(1)	3(1)	2(1)
C(16A)	53(2)	38(2)	61(2)	-5(1)	-5(2)	8(1)
C(17A)	65(3)	46(2)	93(3)	-11(2)	-16(3)	.1(2)
C(17')	64(5)	47(3)	92(4)	-15(3)	-14(4)	9(4)
C(18A)	97(3)	36(2)	123(3)	-14(2)	-24(3)	7(2)
C(19A)	62(2)	30(2)	107(3)	0(2)	12(2)	1(2)
C(20A)	48(2)	28(1)	76(2)	9(2)	9(2)	1(1)
C(21A)	84(3)	32(2)	73(3)	20(2)	7(2)	4(2)
Br(1B)	81(1)	51(1)	52(1)	-11(1)	10(1)	3(1)
O(1B)	89(2)	54(1)	49(1)	20(1)	-13(1)	26(1)
O(2B)	51(1)	31(1)	43(1)	2(1)	-10(1)	4(1)
O(3B)	75(2)	46(1)	59(1)	-5(1)	-24(1)	7(1)
O(4B)	50(1)	46(1)	40(1)	-7(1)	-15(1)	2(1)
N(1B)	46(1)	28(1)	46(1)	1(1)	-7(1)	.0(1)
C(1B)	48(2)	24(1)	38(2)	3(1)	-14(1)	0(1)

C(2B)	46(2)	24(1)	44(2)	-4(1)	-7(1)	1(1)
C(3B)	47(2)	27(1)	44(2)	-1(1)	-9(1)	1(1)
C(4B)	56(2)	35(2)	36(2)	-1(1)	-7(1)	10(1)
C(5B)	71(2)	26(1)	39(2)	-5(1)	-17(2)	5(1)
C(6B)	62(2)	25(1)	45(2)	-1(1)	-18(2)	-4(1)
C(7B)	38(1)	28(1)	38(2)	5(1)	-5(1)	-4(1)
C(8B)	47(2)	50(2)	50(2)	15(1)	-3(1)	-12(1)
C(9B)	46(2)	64(2)	58(2)	21(2)	-9(2)	-21(2)
C(10B)	59(2)	44(2)	53(2)	10(1)	-16(2)	-24(2)
C(11B)	53(2)	77(3)	80(3)	10(2)	24(2)	-3(2)
C(12B)	33(1)	28(1)	39(2)	1(1)	-4(1)	-1(1)
C(13B)	34(1)	32(1)	39(2)	9(1)	-1(1)	0(1)
C(14B)	57(2)	47(2)	38(2)	4(1)	-9(1)	1(1)
C(15B)	69(2)	60(2)	39(2)	10(2)	-10(2)	6(2)
C(16B)	67(2)	69(2)	51(2)	26(2)	-1(2)	2(2)
C(17B)	48(2)	45(2)	57(2)	22(2)	-3(1)	5(1)
C(18B)	35(1)	37(1)	48(2)	11(1)	-1(1)	3(1)
C(19B)	50(2)	29(1)	62(2)	7(1)	-7(2)	5(1)
C(20B)	40(2)	30(1)	39(2)	7(1)	-3(1)	3(1)
C(21B)	68(2)	89(3)	51(2)	-17(2)	-30(2)	22(2)

Table 5. Hydrogen coordinates and isotropic displacement parameters for BG-CO-05.

	x	y	z	U(eq)
H(1A)	0.540(4)	5894(13)	10(2)	0.064
H(2A)	0.093028	728979	81315	0.047
H(3A)	-0.116604	750367	58260	0.052
H(5A)	0.106573	677071	26382	0.059
H(6A)	0.315462	653833	49889	0.052
H(9AA)	0.709340	628273	86994	0.055
H(9AB)	0.690123	687831	93312	0.055
H(10A)	0.480303	613614	52435	0.051
H(10B)	0.538358	664899	91099	0.051
H(11A)	0.554801	677106	05480	0.097
H(11B)	0.721869	656281	41637	0.097
H(11C)	0.660814	711281	60918	0.097
H(13A)	0.018998	678046	75085	0.109
H(13B)	0.096442	623302	75917	0.109
H(13C)	0.152760	663113	15998	0.109
H(16A)	0.552703	751420	68300	0.061
H(16B)	0.380459	777231	84438	0.061
H(16E)	0.408165	756738	80797	0.061
H(16F)	0.594934	767446	62767	0.061
H(17A)	0.571815	830196	32704	0.082
H(17B)	0.684414	825586	62218	0.082
H(17E)	0.364814	831775	18953	0.082
H(17F)	0.558007	830182	34905	0.082
H(18A)	0.383467	877755	67562	0.103
H(18B)	0.560339	902734	63203	0.103
H(18C)	0.416208	899139	64843	0.103
H(18D)	0.604776	886706	58687	0.103
H(19A)	0.580436	887731	44288	0.079
H(19B)	0.388692	898804	50487	0.079
H(21A)	0.389173	835249	23667	0.076
H(1B)	1.032(5)	5693(15)	14(2)	0.077
H(2B)	0.646393	477760	74987	0.046
H(3B)	0.435897	488012	56753	0.047
H(5B)	0.640914	615800	31052	0.055
H(6B)	0.853969	605686	50148	0.053
H(9BA)	1.236849	515921	50046	0.068
H(9BB)	1.250864	562490	94718	0.068

H(10C)	1.087738	0.572295	0.812429	0.063
H(10D)	1.022812	0.599384	0.737989	0.063
H(11D)	1.098841	0.452223	0.586268	0.104
H(11E)	1.199670	0.443596	0.661928	0.104
H(11F)	1.267740	0.481108	0.601371	0.104
H(14A)	0.916246	0.474400	0.898511	0.057
H(14B)	1.090174	0.491200	0.868093	0.057
H(15A)	1.225203	0.428187	0.928475	0.067
H(15B)	1.101373	0.449560	0.987696	0.067
H(16C)	0.918001	0.383989	0.960688	0.075
H(16D)	1.090995	0.363435	0.990573	0.075
H(17C)	1.162404	0.336109	0.876205	0.060
H(17D)	0.975151	0.319319	0.883749	0.060
H(19C)	0.961294	0.329211	0.728517	0.056
H(21B)	0.673919	0.433870	0.507512	0.105
H(21C)	0.644055	0.491976	0.521424	0.105
H(21D)	0.542115	0.451469	0.565917	0.105

Table 6. Torsion angles [°] for BG-CO-05.

C(7A)-N(1A)-C(1A)-C(6A)	180.0(2)
C(10A)-N(1A)-C(1A)-C(6A)	-7.1(4)
C(7A)-N(1A)-C(1A)-C(2A)	-0.8(4)
C(10A)-N(1A)-C(1A)-C(2A)	172.2(2)
N(1A)-C(1A)-C(2A)-C(3A)	-179.9(2)
C(6A)-C(1A)-C(2A)-C(3A)	-0.7(4)
C(1A)-C(2A)-C(3A)-C(4A)	0.6(4)
C(2A)-C(3A)-C(4A)-C(5A)	0.2(4)
C(2A)-C(3A)-C(4A)-Br(1A)	-178.9(2)
C(3A)-C(4A)-C(5A)-C(6A)	-0.9(4)
Br(1A)-C(4A)-C(5A)-C(6A)	178.3(2)
C(4A)-C(5A)-C(6A)-C(1A)	0.8(4)
N(1A)-C(1A)-C(6A)-C(5A)	179.3(3)
C(2A)-C(1A)-C(6A)-C(5A)	0.0(4)
C(1A)-N(1A)-C(7A)-C(14A)	65.3(3)
C(10A)-N(1A)-C(7A)-C(14A)	-108.2(2)
C(1A)-N(1A)-C(7A)-C(12A)	-60.3(3)
C(10A)-N(1A)-C(7A)-C(12A)	126.2(2)
C(1A)-N(1A)-C(7A)-C(8A)	-174.5(2)
C(10A)-N(1A)-C(7A)-C(8A)	12.1(3)
N(1A)-C(7A)-C(8A)-O(1A)	84.0(2)
C(14A)-C(7A)-C(8A)-O(1A)	-158.4(2)
C(12A)-C(7A)-C(8A)-O(1A)	-32.7(3)
N(1A)-C(7A)-C(8A)-C(11A)	-154.9(3)
C(14A)-C(7A)-C(8A)-C(11A)	-37.3(3)
C(12A)-C(7A)-C(8A)-C(11A)	88.4(3)
N(1A)-C(7A)-C(8A)-C(9A)	-30.9(3)
C(14A)-C(7A)-C(8A)-C(9A)	86.8(3)
C(12A)-C(7A)-C(8A)-C(9A)	-147.5(2)
O(1A)-C(8A)-C(9A)-C(10A)	-71.6(3)
C(11A)-C(8A)-C(9A)-C(10A)	164.0(3)
C(7A)-C(8A)-C(9A)-C(10A)	38.8(3)
C(1A)-N(1A)-C(10A)-C(9A)	-162.1(2)
C(7A)-N(1A)-C(10A)-C(9A)	11.7(3)
C(8A)-C(9A)-C(10A)-N(1A)	-31.7(3)
C(13A)-O(3A)-C(12A)-O(2A)	1.9(4)
C(13A)-O(3A)-C(12A)-C(7A)	-179.0(2)
N(1A)-C(7A)-C(12A)-O(2A)	2.0(4)
C(14A)-C(7A)-C(12A)-O(2A)	-121.5(3)
C(8A)-C(7A)-C(12A)-O(2A)	113.0(3)
N(1A)-C(7A)-C(12A)-O(3A)	-177.2(2)
C(14A)-C(7A)-C(12A)-O(3A)	59.4(3)

C(8A)-C(7A)-C(12A)-O(3A)	-66.2(3)
C(21A)-O(4A)-C(14A)-C(15A)	0.2(3)
C(21A)-O(4A)-C(14A)-C(7A)	-179.0(3)
N(1A)-C(7A)-C(14A)-C(15A)	18.4(4)
C(12A)-C(7A)-C(14A)-C(15A)	142.5(3)
C(8A)-C(7A)-C(14A)-C(15A)	-95.0(4)
N(1A)-C(7A)-C(14A)-O(4A)	-162.7(2)
C(12A)-C(7A)-C(14A)-O(4A)	-38.5(3)
C(8A)-C(7A)-C(14A)-O(4A)	83.9(3)
O(4A)-C(14A)-C(15A)-C(20A)	0.3(3)
C(7A)-C(14A)-C(15A)-C(20A)	179.3(3)
O(4A)-C(14A)-C(15A)-C(16A)	179.8(3)
C(7A)-C(14A)-C(15A)-C(16A)	-1.2(6)
C(14A)-C(15A)-C(16A)-C(17')	-161.0(12)
C(20A)-C(15A)-C(16A)-C(17')	18.4(12)
C(14A)-C(15A)-C(16A)-C(17A)	162.9(4)
C(20A)-C(15A)-C(16A)-C(17A)	-17.6(5)
C(15A)-C(16A)-C(17A)-C(18A)	45.2(6)
C(15A)-C(16A)-C(17')-C(18A)	-25(2)
C(16A)-C(17A)-C(18A)-C(19A)	-56.9(7)
C(16A)-C(17')-C(18A)-C(19A)	18(3)
C(17A)-C(18A)-C(19A)-C(20A)	35.6(5)
C(17')-C(18A)-C(19A)-C(20A)	-1.5(14)
C(14A)-C(15A)-C(20A)-C(21A)	-0.7(4)
C(16A)-C(15A)-C(20A)-C(21A)	179.7(3)
C(14A)-C(15A)-C(20A)-C(19A)	178.7(3)
C(16A)-C(15A)-C(20A)-C(19A)	-0.9(5)
C(18A)-C(19A)-C(20A)-C(21A)	171.6(4)
C(18A)-C(19A)-C(20A)-C(15A)	-7.6(5)
C(15A)-C(20A)-C(21A)-O(4A)	0.8(4)
C(19A)-C(20A)-C(21A)-O(4A)	-178.5(3)
C(14A)-O(4A)-C(21A)-C(20A)	-0.7(4)
C(7B)-N(1B)-C(1B)-C(6B)	-175.6(2)
C(10B)-N(1B)-C(1B)-C(6B)	5.0(4)
C(7B)-N(1B)-C(1B)-C(2B)	6.2(4)
C(10B)-N(1B)-C(1B)-C(2B)	-173.2(3)
N(1B)-C(1B)-C(2B)-C(3B)	177.2(2)
C(6B)-C(1B)-C(2B)-C(3B)	-1.1(4)
C(1B)-C(2B)-C(3B)-C(4B)	0.7(4)
C(2B)-C(3B)-C(4B)-C(5B)	0.0(4)
C(2B)-C(3B)-C(4B)-Br(1B)	-179.7(2)
C(3B)-C(4B)-C(5B)-C(6B)	-0.3(4)
Br(1B)-C(4B)-C(5B)-C(6B)	179.4(2)
C(4B)-C(5B)-C(6B)-C(1B)	-0.1(4)
N(1B)-C(1B)-C(6B)-C(5B)	-177.5(3)

C(2B)-C(1B)-C(6B)-C(5B)	0.8(4)
C(1B)-N(1B)-C(7B)-C(12B)	-69.3(3)
C(10B)-N(1B)-C(7B)-C(12B)	110.2(2)
C(1B)-N(1B)-C(7B)-C(20B)	57.7(3)
C(10B)-N(1B)-C(7B)-C(20B)	-122.9(2)
C(1B)-N(1B)-C(7B)-C(8B)	170.7(2)
C(10B)-N(1B)-C(7B)-C(8B)	-9.8(3)
N(1B)-C(7B)-C(8B)-O(1B)	-88.3(3)
C(12B)-C(7B)-C(8B)-O(1B)	153.5(2)
C(20B)-C(7B)-C(8B)-O(1B)	27.6(3)
N(1B)-C(7B)-C(8B)-C(11B)	152.7(3)
C(12B)-C(7B)-C(8B)-C(11B)	34.6(4)
C(20B)-C(7B)-C(8B)-C(11B)	-91.4(3)
N(1B)-C(7B)-C(8B)-C(9B)	28.5(3)
C(12B)-C(7B)-C(8B)-C(9B)	-89.7(3)
C(20B)-C(7B)-C(8B)-C(9B)	144.4(2)
O(1B)-C(8B)-C(9B)-C(10B)	76.7(3)
C(11B)-C(8B)-C(9B)-C(10B)	-162.1(3)
C(7B)-C(8B)-C(9B)-C(10B)	-37.5(3)
C(1B)-N(1B)-C(10B)-C(9B)	166.1(2)
C(7B)-N(1B)-C(10B)-C(9B)	-13.4(3)
C(8B)-C(9B)-C(10B)-N(1B)	32.2(3)
C(19B)-O(2B)-C(12B)-C(13B)	1.1(3)
C(19B)-O(2B)-C(12B)-C(7B)	176.0(2)
N(1B)-C(7B)-C(12B)-C(13B)	-18.6(4)
C(20B)-C(7B)-C(12B)-C(13B)	-143.1(3)
C(8B)-C(7B)-C(12B)-C(13B)	95.7(3)
N(1B)-C(7B)-C(12B)-O(2B)	167.9(2)
C(20B)-C(7B)-C(12B)-O(2B)	43.5(3)
C(8B)-C(7B)-C(12B)-O(2B)	-77.8(3)
O(2B)-C(12B)-C(13B)-C(18B)	-1.1(3)
C(7B)-C(12B)-C(13B)-C(18B)	-174.9(3)
O(2B)-C(12B)-C(13B)-C(14B)	-178.3(3)
C(7B)-C(12B)-C(13B)-C(14B)	7.9(5)
C(12B)-C(13B)-C(14B)-C(15B)	-167.9(3)
C(18B)-C(13B)-C(14B)-C(15B)	15.3(4)
C(13B)-C(14B)-C(15B)-C(16B)	-44.7(4)
C(14B)-C(15B)-C(16B)-C(17B)	62.4(4)
C(15B)-C(16B)-C(17B)-C(18B)	-44.7(4)
C(12B)-C(13B)-C(18B)-C(19B)	0.7(3)
C(14B)-C(13B)-C(18B)-C(19B)	178.3(3)
C(12B)-C(13B)-C(18B)-C(17B)	-178.5(3)
C(14B)-C(13B)-C(18B)-C(17B)	-1.0(4)
C(16B)-C(17B)-C(18B)-C(19B)	-163.9(3)
C(16B)-C(17B)-C(18B)-C(13B)	15.2(4)

C(13B)-C(18B)-C(19B)-O(2B)	0.0(3)
C(17B)-C(18B)-C(19B)-O(2B)	179.1(3)
C(12B)-O(2B)-C(19B)-C(18B)	-0.6(3)
C(21B)-O(4B)-C(20B)-O(3B)	2.7(4)
C(21B)-O(4B)-C(20B)-C(7B)	-175.7(3)
N(1B)-C(7B)-C(20B)-O(3B)	7.7(4)
C(12B)-C(7B)-C(20B)-O(3B)	132.0(3)
C(8B)-C(7B)-C(20B)-O(3B)	-103.4(3)
N(1B)-C(7B)-C(20B)-O(4B)	-173.9(2)
C(12B)-C(7B)-C(20B)-O(4B)	-49.6(3)
C(8B)-C(7B)-C(20B)-O(4B)	75.0(3)

Table 7. Hydrogen bonds for BG-CO-05 [Å and °].

D-H...A	d(D-H)	d(H...A)	d(D...A)	<(DHA)
O(1A)-H(1A)...O(3B)	0.78(4)	2.05(4)	2.819(3)	166(4)
C(11A)-H(11A)...O(3A)	0.98	2.52	3.127(4)	119.9
C(21A)-H(21A)...Br(1B)#1	0.95	3.00	3.853(3)	149.9
O(1B)-H(1B)...O(2A)#2	0.76(4)	2.12(4)	2.838(3)	157(4)
C(21B)-H(21B)...O(1A)#3	0.98	2.48	3.268(4)	137.0

Symmetry transformations used to generate equivalent atoms: #1 x, -y+3/2, z-1/2 #2 x+1, y, z #3 -x+1, -y+1, -z+1

2.15. REFERENCES FOR CHAPTER 2 EXPERIMENTALS

1. Kato, Y.; Miki, K.; Nishino, F.; Ohe, K.; Uemura, S., Doyle−Kirmse Reaction of Allylic Sulfides with Diazoalkane-Free (2-Furyl)carbenoid Transfer. *Org. Lett.* **2003,** *5* (15), 2619-2621.

2. Sämann, C.; Schade, M. A.; Yamada, S.; Knochel, P., Functionalized Alkenylzinc Reagents Bearing Carbonyl Groups: Preparation by Direct Metal Insertion and Reaction with Electrophiles. *Angew. Chem. Int. Ed.* **2013,** *52* (36), 9495-9499.

3. Hong, K.; Shu, J.; Dong, S.; Zhang, Z.; He, Y.; Liu, M.; Huang, J.; Hu, W.; Xu, X., Asymmetric Three-Component Reaction of Enynal with Alcohol and Imine as An Expeditious Track to Afford Chiral α-Furyl-β-amino Carboxylate Derivatives. *ACS Catal.* **2022,** *12* (22), 14185-14193.

4. Jiang, R.; Li, D.-H.; Jiang, J.; Xu, X.-P.; Chen, T.; Ji, S.-J., Green, efficient and practical Michael addition of arylamines to α,β-unsaturated ketones. *Tetrahedron* **2011,** *67* (20), 3631-3637.

5. Monrad, R. N.; Madsen, R., Ruthenium-catalysed synthesis of 2-and 3-substituted quinolines from anilines and 1, 3-diols. *Org. Biomol. Chem.* **2011,** *9* (2), 610-615.

6. Phippen, C. B.; Beattie, J. K.; McErlean, C. S., “On-water” conjugate additions of anilines. *Chem. Commun.* **2010,** *46* (43), 8234-8236.

7. De, K.; Legros, J.; Crousse, B.; Bonnet-Delpon, D., Solvent-promoted and-controlled aza-Michael reaction with aromatic amines. *J. Org. Chem.* **2009,** *74* (16), 6260-6265.

8. Ouyang, L.; Huang, J.; Li, J.; Qi, C.; Wu, W.; Jiang, H., Palladium-catalyzed oxidative amination of homoallylic alcohols: sequentially installing carbonyl and amino groups along an alkyl chain. *Chem. Commun.* **2017,** *53* (75), 10422-10425.

9. Miao, C.; Jiang, L.; Ren, L.; Xue, Q.; Yan, F.; Shi, W.; Li, X.; Sheng, J.; Kai, S., Iodine-catalyzed coupling of β-hydroxyketones with aromatic amines to form β-aminoketones and Benzo[h]quinolones. *Tetrahedron* **2019,** *75* (14), 2215-2228.

10. Barbero, M.; Cadamuro, S.; Dughera, S., O-Benzenedisulfonimide as a reusable Brønsted acid catalyst for hetero-Michael reactions. *Synth. Commun.* **2013,** *43* (5), 758-767.

CHAPTER 3

Efforts towards the synthesis of collybolide and its analogues

3.1. Introduction

3.1.1. Opioids

3.1.1.1. Discovery and Development of Opioids

Opioid is a modern term for all chemicals that bind to opioid receptors. The genesis and evolution of opioids as a cornerstone in pain management is a topic of remarkable depth and historical significance.[1-3] The origin of opioids can be traced back to thousands of years ago. Opium is one of the most famous natural sources of opioids. This potent sap extracted from the seed pods of the Papaver somniferum (opium poppy), has a storied history that dates back to the ancient civilizations of Mesopotamia. Its application began over 5,000 years ago, with its first known cultivation by the Sumerians who referred to it as the "joy plant."[3] From there, its use spread to various cultures and regions, including the Assyrians, the Egyptians, the Greeks, and the Romans, each incorporating opium into their medicinal and ritualistic practices. With the development of chemistry and pharmacology, more than 20 alkaloids were identified in opium.[4] These alkaloids and their derivatives are called opiates, the old term for drugs derived from opium in pharmacology.[4]

In the mid-19th century, the invention of the syringe allowed general pain management and injection of opiates in surgery.[2] However, the need for pain management development was not addressed until the 20th century. Both world wars dramatically stimulated this need due to many soldiers with appalling wounds and chronic pain. Since the 20th century, the term "opioid" was coined to describe both natural and synthetic substances that act on opioid receptors in the brain to produce morphine-like effects.[5] The development of these synthetic opioids was propelled by the need for better pain management tools with fewer side effects and reduced addiction risks.[6] Drugs such as methadone[7], developed in the 1930s, and later buprenorphine[8], were milestones in this area.

Methadone, a synthetic opioid with a unique pharmacological profile, has played a complex role in both pain management and addiction treatment since its development in Germany in the late 1930s.[9] Originally synthesized by chemists Gustav Ehrhart and Max Bockmühl at IG Farben in search of an analgesic with less potential for addiction than morphine, methadone was introduced to the United States in 1947.[10] As a potent analgesic, methadone is effective in the treatment of chronic pain, particularly due to its long half-life and oral bioavailability[7], which provides prolonged pain relief. Its pharmacokinetic properties set it apart from other opioids, offering steady-state pain control and making it a vital option for patients with chronic, severe pain. Parallel to its role in pain management, methadone has been a cornerstone in the treatment of opioid dependency. It is most widely recognized for its use in Medication-Assisted Treatment (MAT) for heroin and other opioid addictions.[11] Methadone maintenance therapy helps to mitigate withdrawal symptoms and cravings, a major breakthrough in the field of addiction

medicine. By activating opioid receptors at a slower pace and with less intensity, methadone provides a stable, controlled level of the drug in the bloodstream, which can prevent the euphoria associated with other opioids, reduce withdrawal symptoms, and decrease the desire for opioids.[9]

Buprenorphine represents a significant advancement in the pharmacological treatment of opioid addiction and is also utilized in the management of pain. Developed in the 1960s by the British company Reckitt & Colman, buprenorphine was first marketed in the 1970s.[8] As a medication, it has a unique profile that stems from its action as a partial agonist at the mu-opioid receptor and an antagonist at the kappa-opioid receptor.[12] The use of buprenorphine in opioid substitution therapy is a critical aspect of its application. It helps to reduce withdrawal symptoms and cravings in individuals addicted to opioids, facilitating a smoother transition in the recovery process. Buprenorphine's efficacy in decreasing the use of illicit opioids, coupled with a lower level of physical dependence and a milder withdrawal profile upon cessation, has established it as a cornerstone in the treatment of opioid dependence.[13] Furthermore, buprenorphine's sublingual formulation, which avoids first-pass metabolism, allows for effective outpatient treatment, thereby increasing accessibility and compliance among patients. In some regions, buprenorphine is combined with naloxone to deter intravenous misuse, promoting its safe use.[13]

3.1.2. Opioid receptors

Both opiates and opioids helped significantly in identifying opioid receptors and their functions. Beckett and Casy proposed the interaction between opioids and relevant receptors in 1954.[14] Goldstein et al. proposed that radiolabeling ligands could be used to

confirm the existence of the relevant receptors in 1971.[15] Today it is widely accepted that opioid receptors are G protein-coupled receptors (GPCRs). After a ligand binds to the receptor, the receptor undergoes conformational changes to allow intracellular coupling of heterotrimeric G proteins to the C terminus of the receptor. The G_{α} subunit dissociates from the $G_{\beta\gamma}$ subunit. The releasing of $G_{\beta\gamma}$ subunit inhibits adenylyl cyclase and reduces cAMP, decreasing the conductance of voltage-gated Ca^{2+} channels or opening and rectifying K^{+} channels. All three opioid receptors can modulate pre- and postsynaptic Ca^{2+} channels, and inhibit Ca^{2+} influx, which reduces the excitability of neurons, decreasing the release of pronociceptive neuropeptides. Activation of opioid receptors also inhibits Na+ channels, Hyperpolarization-activated nonselective cation channels (Ih channels), transient receptor potential vanilloid-1 (TRPV1) channels, and acid-sensing ion channels (ASICs) in dorsal root ganglion (DRG) neurons. This inhibition decreases the transmission of nociceptive stimuli at all levels of the neuraxis, blocking pain signals.[16]

Soon after the usage of radiolabeling ligands in this area, three opioid-binding sites were identified in the central nervous system. In 1976, Martin and coworkers proved the actions of opioid agonists, antagonists, and mixed agonist-antagonists on multiple opioid receptors.[17] Thus, three main types of opioid receptors, the mu, delta, and kappa receptors, were identified. Although there are other types of receptors, such as sigma, epsilon, and orphanin, that were proposed, they are not considered "classical" opioid receptors.[18]

The key differences between mu, delta, and kappa opioid receptors lie in distribution, ligand selectivity, functional effects, and side effects. The opioid system is intricately designed with different receptors, each playing a unique role in modulating pain

and other physiological responses. Among these, the mu-opioid receptors (MORs) are predominantly located presynaptically in areas like the periaqueductal gray region and the superficial dorsal horn of the spinal cord. These receptors exhibit a strong affinity for mu-selective opioids, with morphine being a classic example.[19] When MORs are activated, they bring about robust analgesic effects. However, this pain relief is often accompanied by side effects such as pronounced respiratory depression, euphoria, and a notable potential for abuse and dependence. In contrast, delta opioid receptors (DORs) are primarily expressed in the basal ganglia and the neocortical areas of the brain.[20] They have a preference for delta-selective opioids, with enkephalins being key ligands.[21] While DOR activation does result in pain relief and other opioid-like effects, these are generally less potent than those mediated by MOR. Thus, the balance of therapeutic benefits to side effects may be slightly better with DOR-targeted therapies. Lastly, the kappa opioid receptors (KORs) mainly reside in the brain and spinal cord. These receptors are selective for kappa-specific opioids, dynorphins being a prime example. The activation of KORs does produce analgesia, but it's distinct from MOR and DOR in terms of side effects. Specifically, KOR-mediated effects often manifest as dysphoria, sedation, and other side effects that many patients find distressing.[22-23] Understanding the nuanced roles and effects of these receptors is pivotal for developing opioids that can effectively alleviate pain while minimizing undesirable side effects.[24]

3.1.2.1. Opioid receptor agonists, partial agonists, and antagonists

Currently, based on their action at these opioid receptors, opioids are classified into agonists, partial agonists, and antagonists. Agonists like morphine, which was the first alkaloid isolated from opium by Friedrich Sertürner in 1805,[25] activate the opioid

receptors to provide pain relief but also have a high potential for abuse and addiction. Heroin, synthesized later in the 19th century, was initially marketed as a non-addictive alternative to morphine; however, it soon became evident that it was highly addictive, even more so than morphine itself.

The class of mixed agonist-antagonists was developed in an attempt to provide pain relief while reducing the risk of abuse. Nalorphine, synthesized in 1954[26], exemplifies this category by acting as an antagonist at the mu-opioid receptor, which is primarily responsible for opioids' addictive properties, while acting as an agonist at the kappa receptor, which can also mediate analgesia.[27] However, the analgesic effect of nalorphine was insufficient for it to be a standalone painkiller, and its historical significance lies in its role as an antidote to opioid overdose, paving the way for future development of opioid antagonists.[28]

The discovery of naloxone, discovered in 1960,[29] marked a pivotal moment in the management of opioid overdose. As a pure opioid antagonist, naloxone has no agonist activity and does not produce analgesia or euphoria. It works by competitively binding to opioid receptors, thereby displacing opioids like heroin or morphine, reversing their effects, and preventing further interaction with the receptors. This makes naloxone an essential life-saving tool in the context of opioid overdoses.[30]

The history and development of these opioid categories reflect the ongoing challenge in the medical and pharmaceutical fields: to create medications that can effectively relieve pain without introducing the risk of abuse and dependency. While significant advances have been made, the perfect balance in opioid pharmacotherapy

remains elusive, underlining the complexity of targeting a receptor system that is intertwined with critical physiological functions and behaviors.[18]

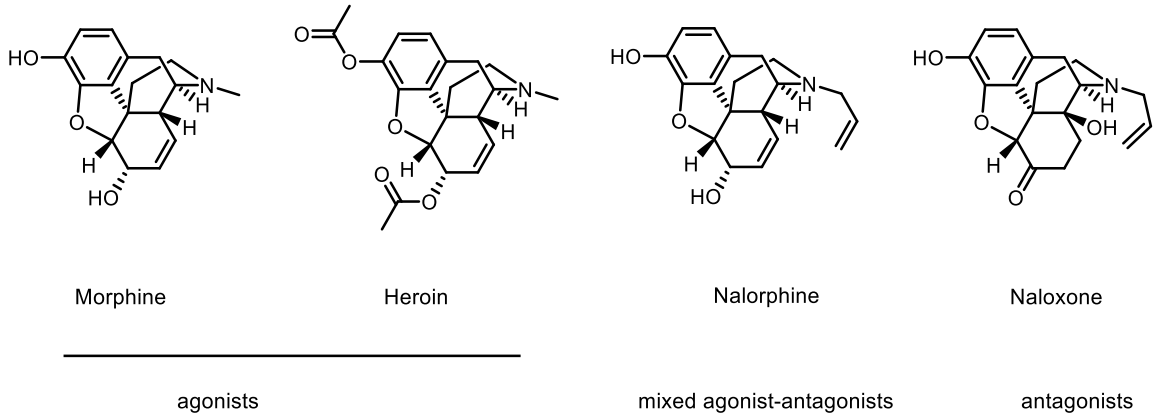

Figure 3.1. Examples of opioid receptor agonists, partial agonists, and antagonists

3.1.3. The key challenge in the opioid development

The development of opioids for medical use is deeply intertwined with the issue of abuse, which remains a persistent and formidable challenge in the field of pain management. The therapeutic benefit of opioids is their potent analgesic effect, making them invaluable in the treatment of acute and chronic pain. However, their ability to produce euphoria, along with their pain-relieving properties, can lead to misuse, abuse, and addiction, creating a public health dilemma of considerable proportions.[6, 31] During an opioid overdose, the respiratory system can be depressed. Slowed or stopped breathing can be fatal.

The alarming rise in opioid-related overdoses has emerged as a major public health concern, especially in the United States. According to the Centers for Disease Control and Prevention (CDC), the year 2021 saw an unprecedented number of fatalities attributed to this crisis, with approximately 80,411 individuals succumbing to opioid

overdoses.[32] This staggering statistic underscores the pressing need for a comprehensive and multidimensional response. One crucial aspect of addressing this crisis is the development of safer opioid formulations. The opioids currently available in the market have a narrow therapeutic window, meaning there is a fine line between a dose that provides pain relief and a dose that can result in an overdose. Furthermore, many opioids have a high potential for misuse and addiction, making their widespread prescription a potential hazard. Given the complexities of pain management and the genuine needs of chronic pain patients, simply curbing the prescription of opioids may not be a viable solution. Instead, the medical and scientific communities are urged to innovate and develop better opioids – drugs that can offer effective pain relief without the associated risks of addiction, misuse, or fatal overdose. This could involve opioids that have a different mechanism of action, opioids that are formulated to deter abuse, or drugs that can modulate the opioid receptors in a way that maximizes analgesic effects while minimizing euphoria, which often leads to misuse.

3.2. Selective Kappa Opioid Receptor Agonist Provides New Potentials to Drug Development

As mentioned in previous sections, kappa opioid receptor (κOR) agonists exhibit properties that make them candidates for the treatment of addiction, pain, and pruritus, and potentially as pain relievers with a lower risk of misuse. Their antipruritic effects are notable, and they have been shown to counteract the impact of psychostimulants.[23, 31, 33] Despite these benefits, the clinical application of κOR agonists is complicated by adverse effects such as anxiety, diuresis, stress, dysphoric reactions, and psychotomimetic experiences.[23] Moreover, the κOR system's activation has been linked to the risk of

relapse in substance abuse, posing a significant challenge in utilizing these agonists for treating addiction.[22]

Recent research has drawn a connection between the unwanted dysphoric outcomes of κOR agonists and the non-G-protein-mediated activation of the p38 MAPK pathway, shedding light on the complex pharmacodynamics at play.[34] These insights have prompted the pursuit of κOR agonists that preferentially activate G-protein-coupled pathways, which could minimize these negative side effects. Consequently, there is a focused effort to discover new κOR ligands or molecular frameworks that could serve as innovative therapeutic options. These novel agents could potentially address a spectrum of conditions where κOR plays a pivotal role, thus advancing the field of targeted opioid receptor modulation.[33, 35]

3.2.1. Salvinorin A

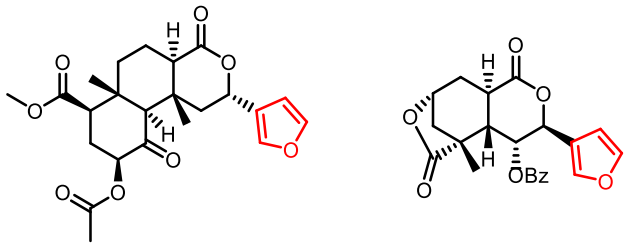

Figure 3.2. Salvinorin A and collybolide as two examples of selective κOR ligands

Salvinorin A (Sal A) is a non-nitrogenous diterpene extracted from the Mexican mint *Salvia divinorum*. Sal A has been reported to be a hallucinogen, but its mechanism of action was unclear for years until Roth et al. reported Sal A to be a selective κ opioid agonist.[36] The discovery of Sal A being a κ agonist is striking because it was the first

opioid agonist without nitrogen atoms in the molecule. Until this discovery, a positively charged nitrogen atom was considered essential to have a high affinity to opioid receptors.[37] This finding suggested the mechanism of action of Sal A was different from all known opioids at that time. Sal A was also the first natural product identified to be a selective κ opioid agonist. Research suggests that dysphoric effects of the kappa-opioid receptor (κOR) agonists result from the activation of the p38 MAPK pathway.[38] This pathway is separate from the G protein pathway, which causes a sedation effect. G protein-biased kappa agonists were hypothesized to have antipruritic effects with fewer side effects.

3.2.2. Collybolide

Collybolide was first isolated from the fungus *Collybia maculate* in 1974. It shares a similar furyl-d-lactone core with Sal A. *In vitro*, collybolide preferentially induced phosphorylation of Akt over ERK, which is a sign of G protein-biased kappa opioid agonists. In male C57BL/6 mice, antinociception in a tail-flick assay and the reduced chloroquine-induced itch were observed after intraperitoneal injection of collybolide. Collybolide produced a pain relief effect without sedation. However, aversion in a CPA paradigm and mild norbinaltorphimine reversible anxiety were observed.[39]

3.2.3. Total synthesis of salvinorin A and collybolide

Early studies suggested the desired analgesic effect resulted from the activation of the G protein-dependent pathway, while undesired side effects resulted from the activation of the G protein-independent pathway (euphoria -mu/depression -kappa). This result was not reproduced by recent studies. The current hypothesis is that both desired

and undesired effects are G protein-dependent. However, the behavioral effects of the opioid receptors are not fully understood. Biased receptor agonists are still valuable for mechanical studies.[40]

The total synthesis of Salvinorin A, due to its complex structure, is a significant challenge in the field of organic chemistry. As a trans-neoclerodane diterpenoid, it presents a unique and intricate scaffold for synthetic chemists to construct, one that demands a deep understanding of chemical reactions and stereochemical control. Several research groups have achieved the total synthesis of Salvinorin A. For example, Nozawa et al. published a twenty-step synthetic route starting from optically pure Wieland−Miescher ketone.[41] As mentioned in previous sections, lithiation of furan was used for furan installation at a late stage of the total synthesis.

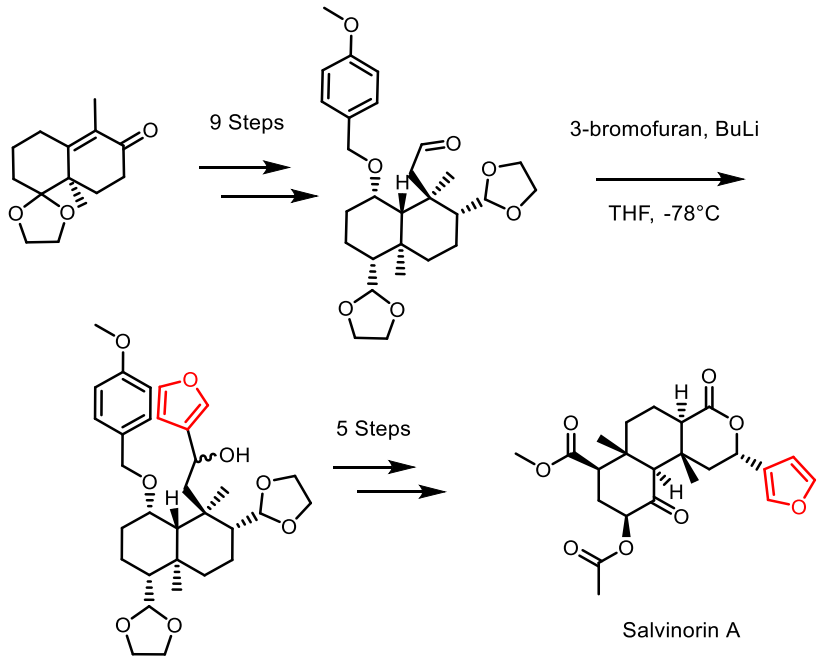

Figure 3.3. Total synthesis of Sal A by Nozawa *et al.*[41] Furan is installed by lithiation of furan at a late stage.

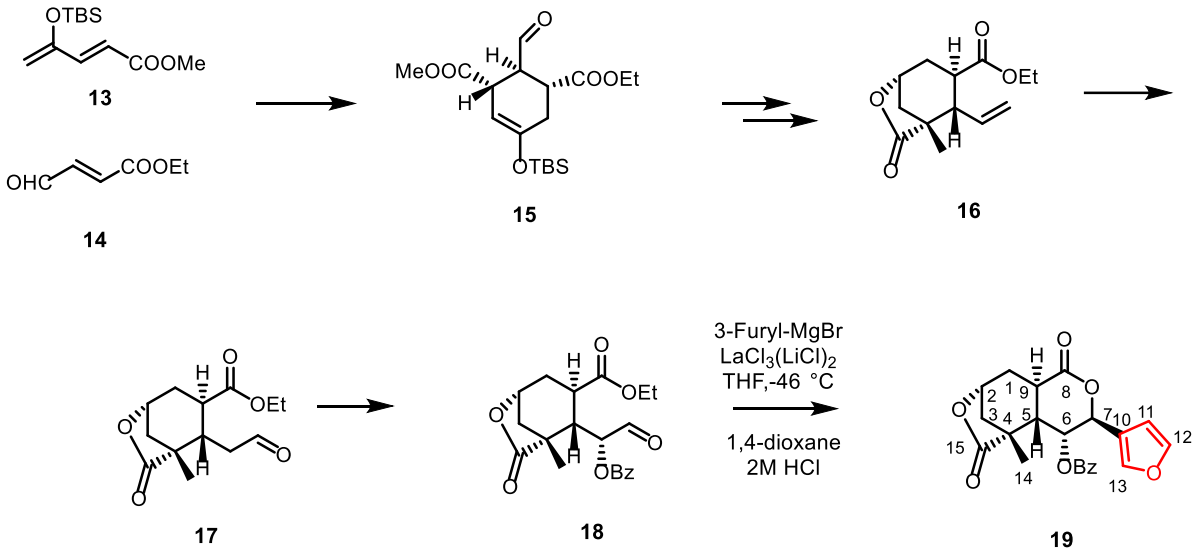

Figure 3.4. Total synthesis of Collybolide.[42] Furan is installed by modified Grignard reaction of furan at the last step

Total synthesis of Collybolide was achieved by Shevick et al. in 2022.[42] They started from two small molecules and performed an asymmetric Diels–Alder reaction. In 9 steps, the bicyclic substructure was achieved. In further four steps, they achieved Collybolide via aldehyde intermediates. There were two major challenges in this synthetic route. The Benzoyl ester on C6 carbon must be installed without a hydroxyl intermediate. A hydroxyl group on C6 carbon will cyclize with C15, breaking the original lactone substructure in collybolide. This challenge was overcome by using a N-tert-butyl-Obenzoylhydroxylammonium salt developed by the Tomkinson group. The alpha position of the aldehyde was directly converted to a benzoyl ester via a [3,3]-sigmatropic rearrangement. The other challenge was the installation of furan. While nucleophilic addition to an aldehyde has been widely used in organic synthesis, in this case, none of the furyl lithium, furyl magnesium halides, or furyl titanium reagents was able to install furan moiety into the molecule. The organolanthanum converted the final intermediate

into collybolide and 7-epi- collybolide (1:1.25). 7-epi- collybolide was converted into collybolide via acidic epimerization. These two steps gave a 42% yield.[42]

3.3. Efforts synthesis of salvinorin A and collybolide

3.3.1 Total synthesis of collybolide, a novel retrosynthetic route

In organic synthesis, the formation of a carbon-oxygen is usually easier than the formation of a carbon-carbon bond. Similar to Shevick *et al.*[42], the furyl lactone would be the last ring to be closed. Conversely, the remaining ester can be used for cyclization of the six-member ring, and the lactone was readily available from natural products. Hence, the lactone was set to be the first ring to be synthesized in the tricyclic core.

As mentioned earlier, the late-stage installation of furan was troublesome in this route, and the yield was low. Therefore, a novel retrosynthesis of collybolide was proposed. The furan moiety should be initially installed into the molecule in an early stage to avoid problems caused by the late-stage installation of furan.

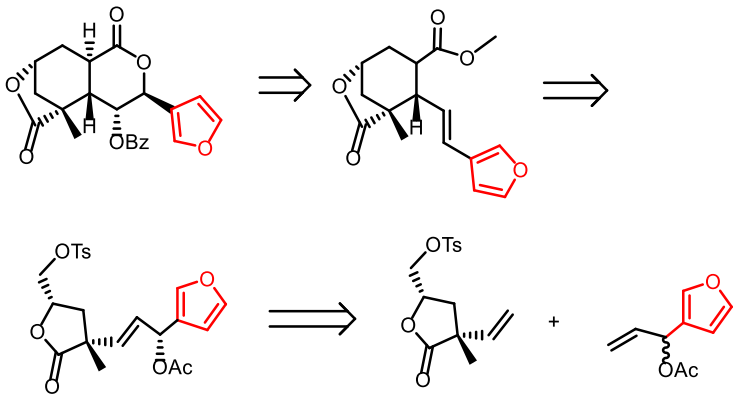

Figure 3.5. Retrosynthesis of collybolide. The lift lactone ring will be the base of the molecule. The intermediate will bear furan, undergoing two cyclization steps to make collybolide.

3.3.2. Formation of lactone moiety

During the formation of the lactone moiety, the installation of the methyl group was the most challenging part. Steric hindrance and stereoselectivity are two major concerns. In the Shevick paper, the methyl group was fused into the molecule using methyl copper. Methyllithium or methylmagnesium bromide, in combination with Cu(I) salts, failed to provide methylation. Pyrophoric trimethylaluminum was used in combination with Copper(II) trifluoromethane-sulfonate, yielding 64% product with 3.6:1 diastereoselectivity.

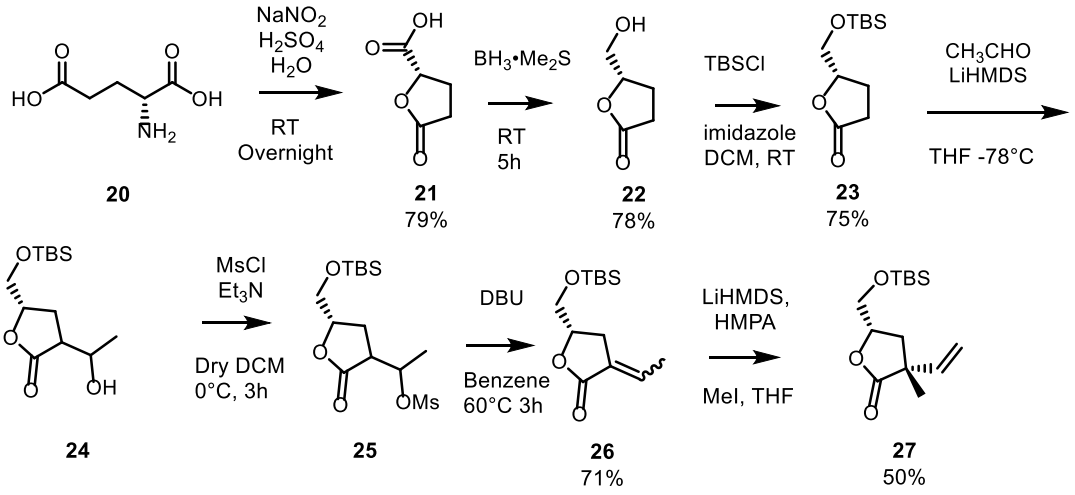

Figure 3.6. Synthesis of lactone intermediates **23** and further functionalize it with alkene group followed by methylation. **27** is the intermediate prepared for the Grubbs reaction.

The natural product glutamic acid was used as the starting material and the chiral source. Lactone **23** was synthesized from D-glutamic acid according to the published method with a good yield (75-79%) after three steps.[43] D-Glutamic acid was the chiral source of the branch on the lactone substructure. The mechanism of the cyclization was the formation of diazo and being self-attacked by the acidic sidechain. After the cyclization

of lactone, the remaining acid functional group was reduced to alcohol and followed by tert-butyldimethylsilyl (TBS) protection.

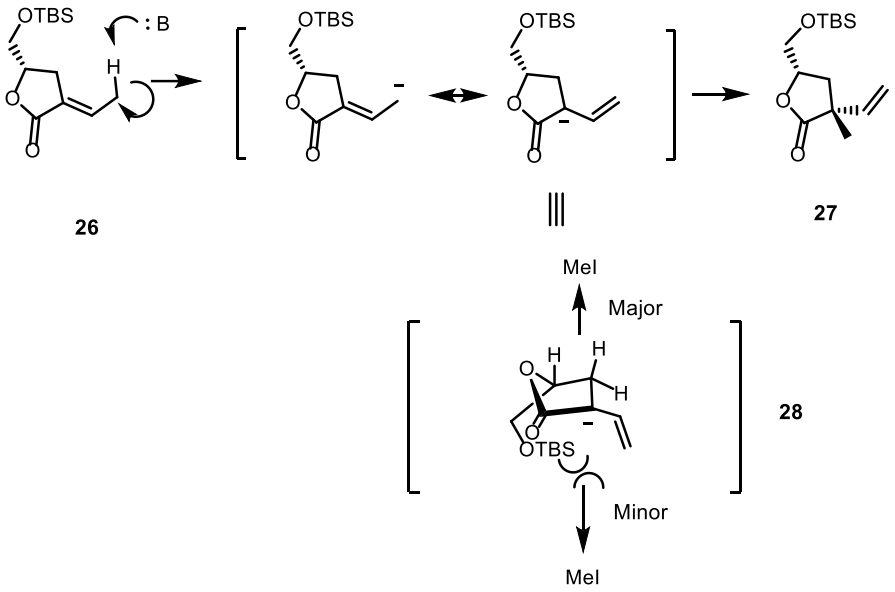

Figure 3.7. Proposed mechanism of installation of the methyl group onto the lactone **26**.

After the TBS protection of alcohol, lactone **23** was deprotonated by LiHMDS and performed a nucleophilic addition to acetaldehyde. The new alcohol group was first converted to methanesulfonyl (Ms) ester **25**, followed by the elimination of alcohol-produced ethylidene lactone **26**. This ethylidene lactone underwent further γ-deprotonation by LiHMDS, generating a conjugated anion. The α anion resonance structure was favored due to the neighboring ketone attacking methyl iodide to form product **27**. The OTBS group blocked the bottom phase, making the top phase adduct stereo-selectively favored. The installation of the methyl group yielded 50% of the product with 5:2 stereoselectivity. To be noted, while this result seemed to be less yielded and less selective than the corresponding methylation step in the Shevick paper[42], we did not

use any chiral catalyst to achieve the lactone ring. Considering their usage of a chiral catalyst in the first step of their synthesis, our design is overall beneficial.

3.3.3. Installation of furan

To install the furan, the first attempt was olefin metathesis with a well-known Grubbs catalyst. In organic chemistry, olefin metathesis is a powerful tool to form a new carbon-carbon double bond. Olefin metathesis is often used in cross-coupling and ring closure.[44-45] Two alkenes can undergo metathesis in the presence of certain catalysts. One of the most common catalyst families for olefin metathesis is Grubbs catalysts, which is named after their developer Robert H. Grubbs.[46] Olefin metathesis has the advantage of high selectivity, mild reaction conditions, and functional-group compatibility over other existing methods, such as Wittig Reaction.[47] In this case, the formation of a new carbon-carbon double bond would fuse the furan moiety into the intermediate molecule, and the double bond will be used in further synthesis of the bicyclic core.

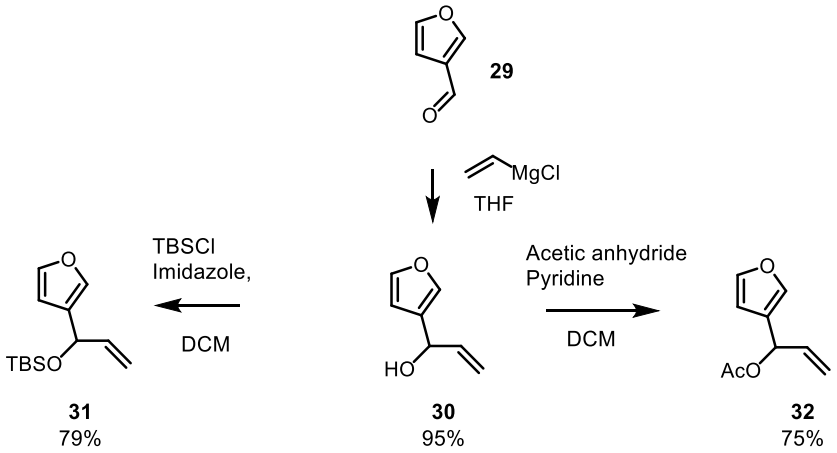

Figure 3.8. Synthesis of the furan moieties for the Grubbs reaction via the reported method.[48-50]

Allyl furan intermediates were synthesized via the reported method.[48-50] 3-Furaldehyde **29** was treated with allyl magnesium chloride, yielding allyl alcohol **30** with almost quantitative yield (95%). Other than free alcohol, acetic and TBS ester was synthesized with good yield (75 and 79%) separately. However, the olefin metathesis reaction did not occur under Grubbs catalysis with these three allyl furan intermediates. Another commercial reagent, crotonaldehyde, was tested as an alternative approach. The furan moiety could be added to the aldehyde as many works mentioned previously. However, this alternative approach did not produce the designed intermediate **36**. In these experiments, only dimerization of furyl starting materials was observed. The lactone **27** remained unreacted. These results were attributed to the stereo hindrance from the lactone ring and the neighboring methyl group. Thus, olefin metathesis catalyzed by the Grubbs reagent was proven not suitable for this synthetic route.

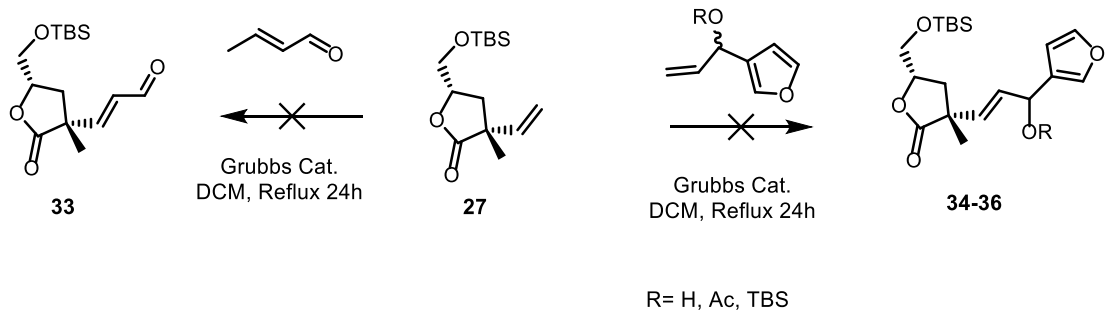

Figure 3.9. Attempts for Grubbs reaction to fuse lactone **27** and furan moieties did not yield the expected products.

In the previous design, lactone **23** was added to acetaldehyde. Since it was difficult to add furan moiety after this step, the furan moiety in this step must be fused into the intermediate molecule in this step. To achieve this goal, aldehyde **41** was synthesized. Furic acid **37** was activated by dicyclohexylcarbodiimide (DCC), coupled with Meldrum's

acid. The intermediate was isolated and heated with methanol, yielding beta-keto ester. The carbonyl group in **38** was protected by ethylene glycol, forming beta-ketal ester **39**.

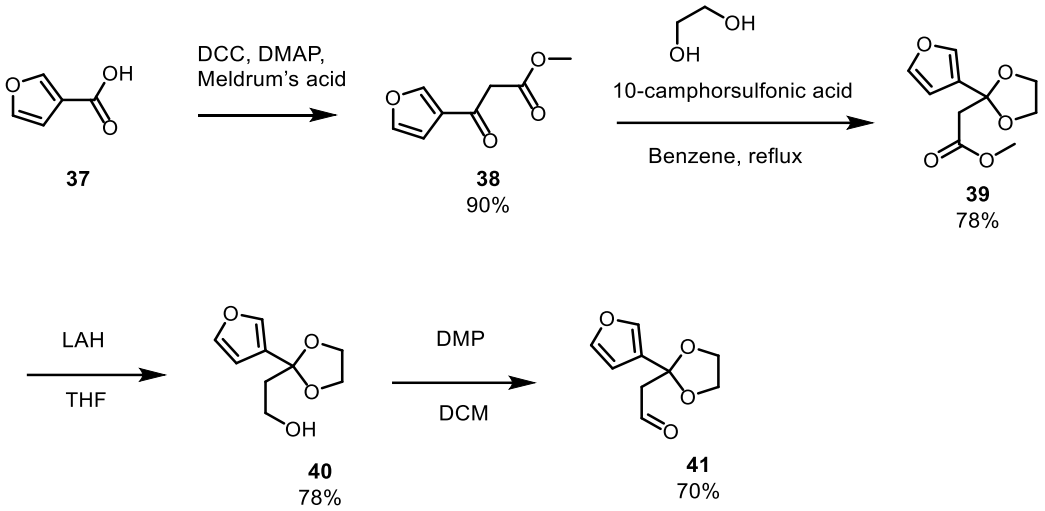

Figure 3.10. Synthesis of furyl aldehyde **41** for aldol reaction to fuse furan moiety into the intermediate.

The addition of lactone **23** to aldehyde **41** was successful. Further elimination and methylation followed the exact procedure to produce lactone **27**. Degradation was observed during the elimination step, leading to an overall 33% yield after 3 steps. Following methylation of **44** to **45** gave better results compared with **27**. In this case, the stereoselectivity of methylation to form **44** was much higher than lactone **26**. Only one isomer was identified and isolated after the reaction. The mechanism is the same as the reaction shown in **Figure 3.7**. But in this case, the extra bulk from the furyl substructure further blocks the bottom phase, forcing the attack on the top phase. Thus, after the furan moiety was successfully installed into the intermediate molecule, the methyl group was also installed with the correct geometry.

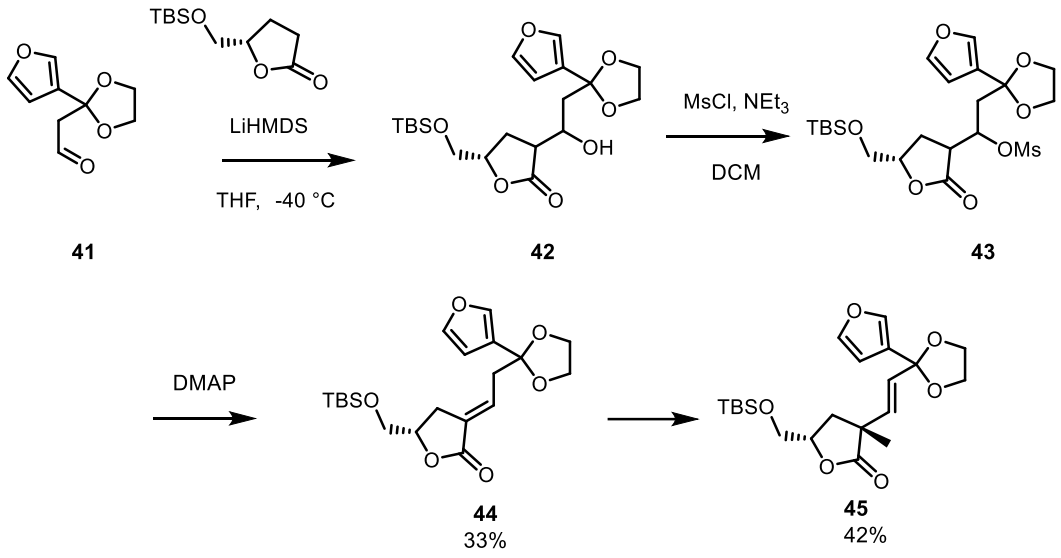

Figure 3.11. Ligation of Furan and lactone moieties and installation of methyl group.

To confirm the importance of furan moiety in this route, a similar route without furan moiety was used as a comparison. Acetal aldehyde **49** was synthesized via the reported method.[51] However, the nucleophilic addition to this aldehyde under the exact same condition with the formation of **42** did not produce the desired product **50**. These results suggested that the furan moiety participated in the reaction by removing the acetal proton, which was critical in this reaction.

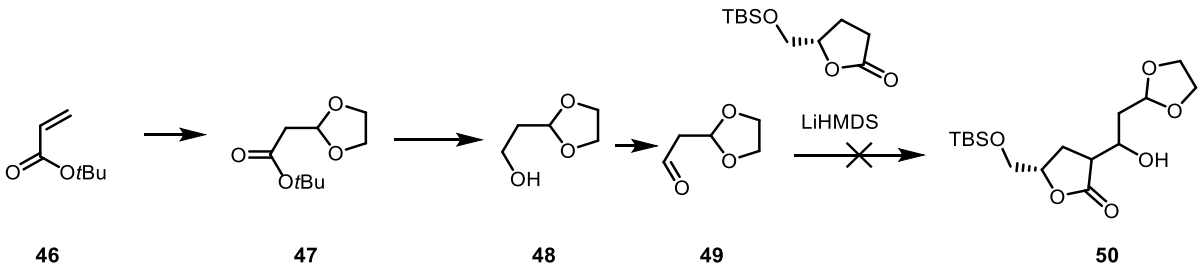

Figure 3.12. Control experiment without furan moiety led to no aldol reaction

3.3.4. Formation of the bicyclic core of collybolide

As it was designed in retrosynthesis, the next step is to generate the six-member carbon ring to form the bicyclic core of collybolide. Two new carbon-carbon bonds need to be formed, one with C1 and one with C5. The presence of beta-ketal alkene and OTBS group in the intermediate provided a possibility to close the six-member carbon ring in one step. From compound **45**, **53** can be easily achieved. In compound **53**, α,β-unsaturated carbonyl can accept carbon nucleophiles undergoing Michael addition. Additionally, 4-methylbenzenesulfonate (OTs) is a good leaving group, and it can form a carbon-carbon bond via a Substitution Nucleophilic biomolecular (S_N2) reaction. Thus, we select dimethyl malonate, which can be easily deprotonated twice, serving as a nucleophile for both Michael addition and the Sn2 reaction. Due to the difference in reaction rate, the first step was expected to be Michael addition, and the methyl group was expected to hinder the top phase addition. Intermediate **55** would regenerate malonic anion via proton transfer, followed by S_N2 reaction, kicking out the OTs group and forming the ring. The OTBS group was first deprotected into free alcohol and then converted into an OTs group. Ketal was deprotected under acidic conditions. Compound **49** was easily obtained after three steps with an overall 80% yield. Unfortunately, when treating **53** with malonate under basic conditions, the molecule fragmented instead of following the designed mechanism.

Since the one-pot strategy did not work out, stepwise cyclization was attempted. The OTs group in **52** was converted to Iodo **57** to facilitate the Sn2 reaction with malonate. After malonate was introduced into the molecule, Krapcho decarboxylation removed one methyl ester from the molecule. Then ketal was deprotected under acidic conditions.

Finally, Michael addition closed the ring. Thus, the bicyclic core of collybolide was achieved in **60**.

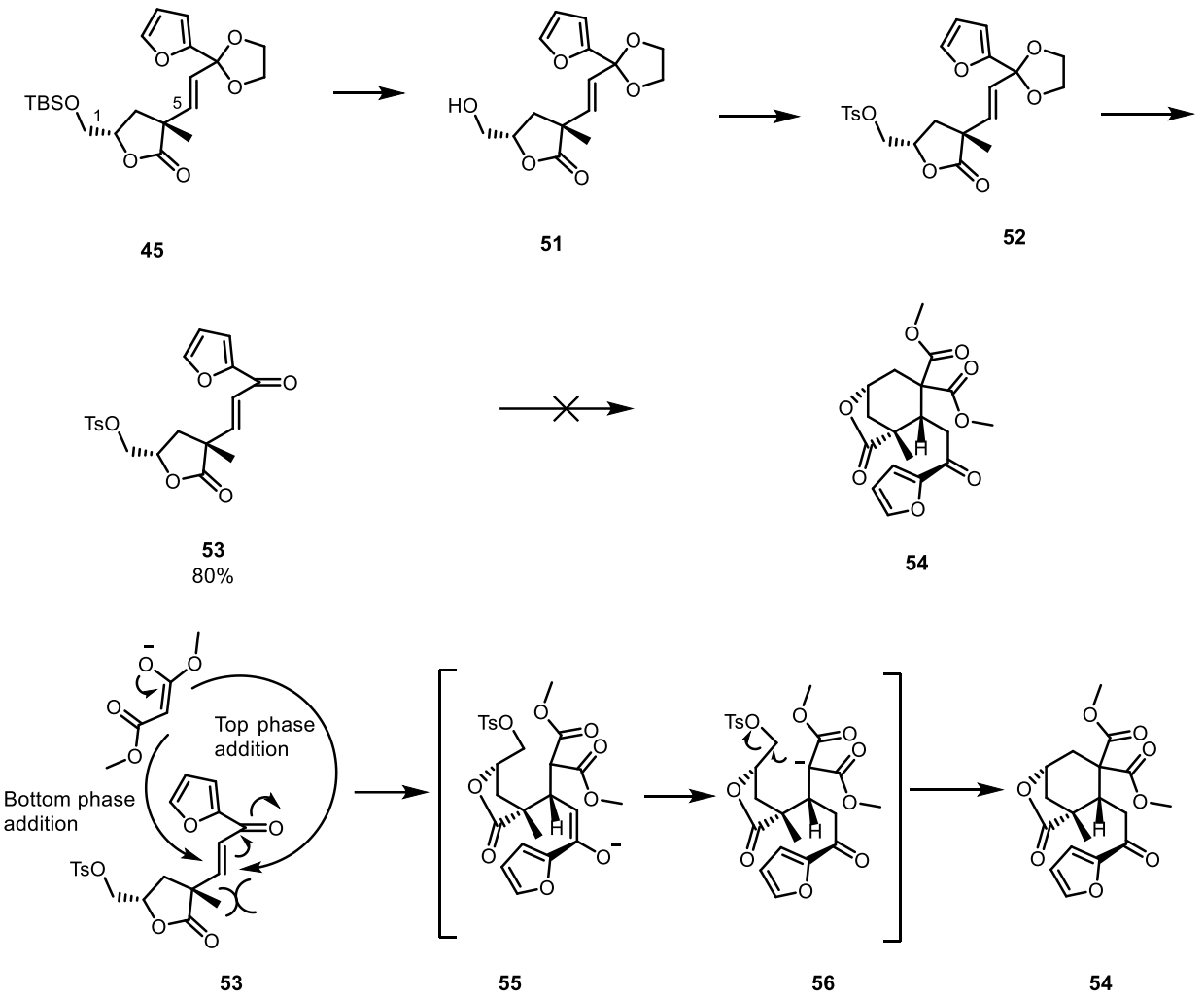

Figure 3.13. Designed one-pot cyclization for synthesis of **54**, which has the bicyclic core in the collybolide molecule

The cyclization from 60 to **61** is an asymmetric Micheal addition. The stereoselectivity originates from the chirality of the molecule rather than utilizing asymmetric catalysts. The lactone ring limits the relative position of the ester and the

conjugate ketene, allowing the attack only from one side. This ring closure generates two additional stereo centers in the molecule without using additional chiral reagents.

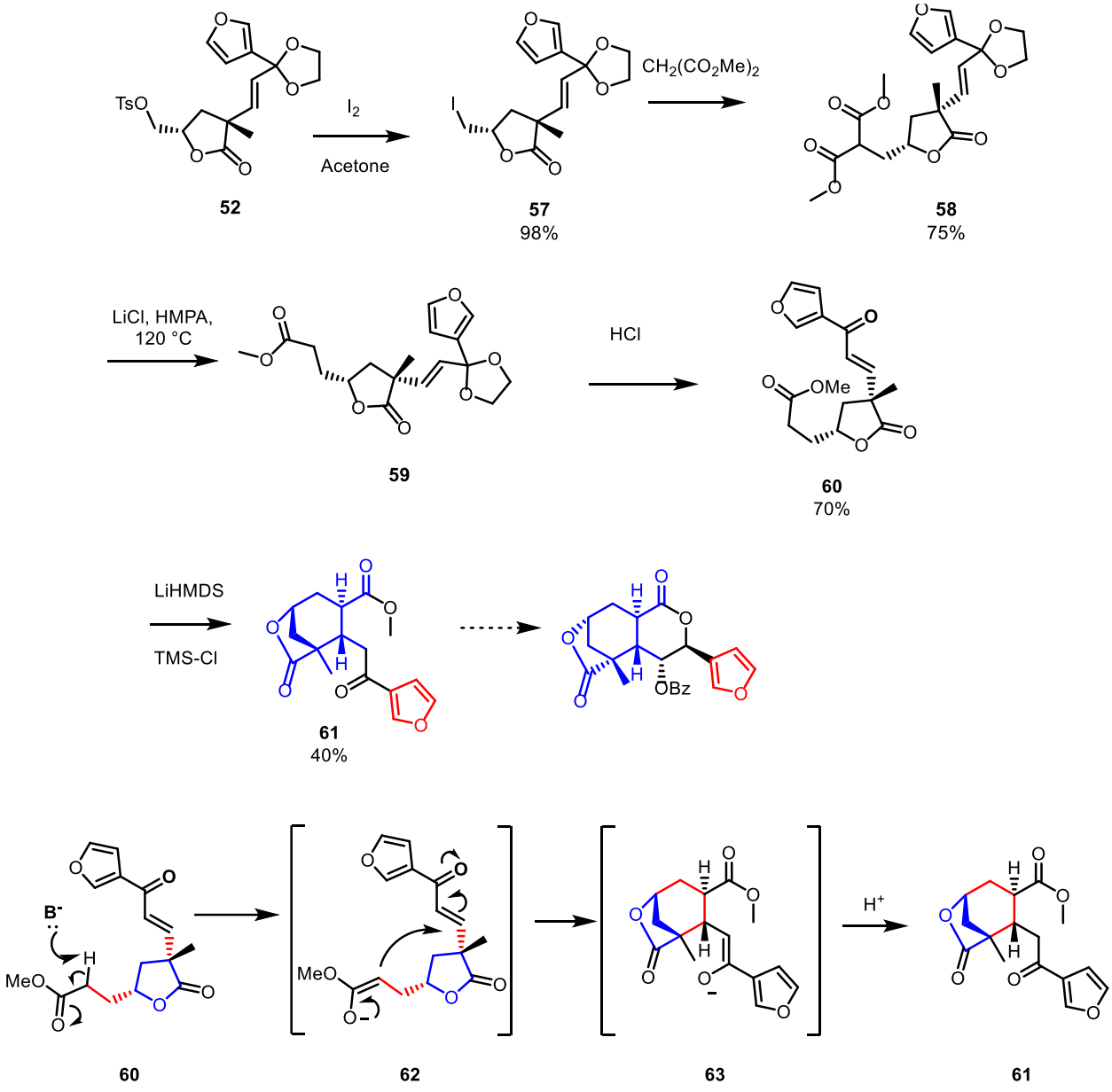

Figure 3.14. Cyclization of the second ring in collybolide leads to intermediate **61**.

3.4. Parallel synthesis of 2-furan isomer of collybolide

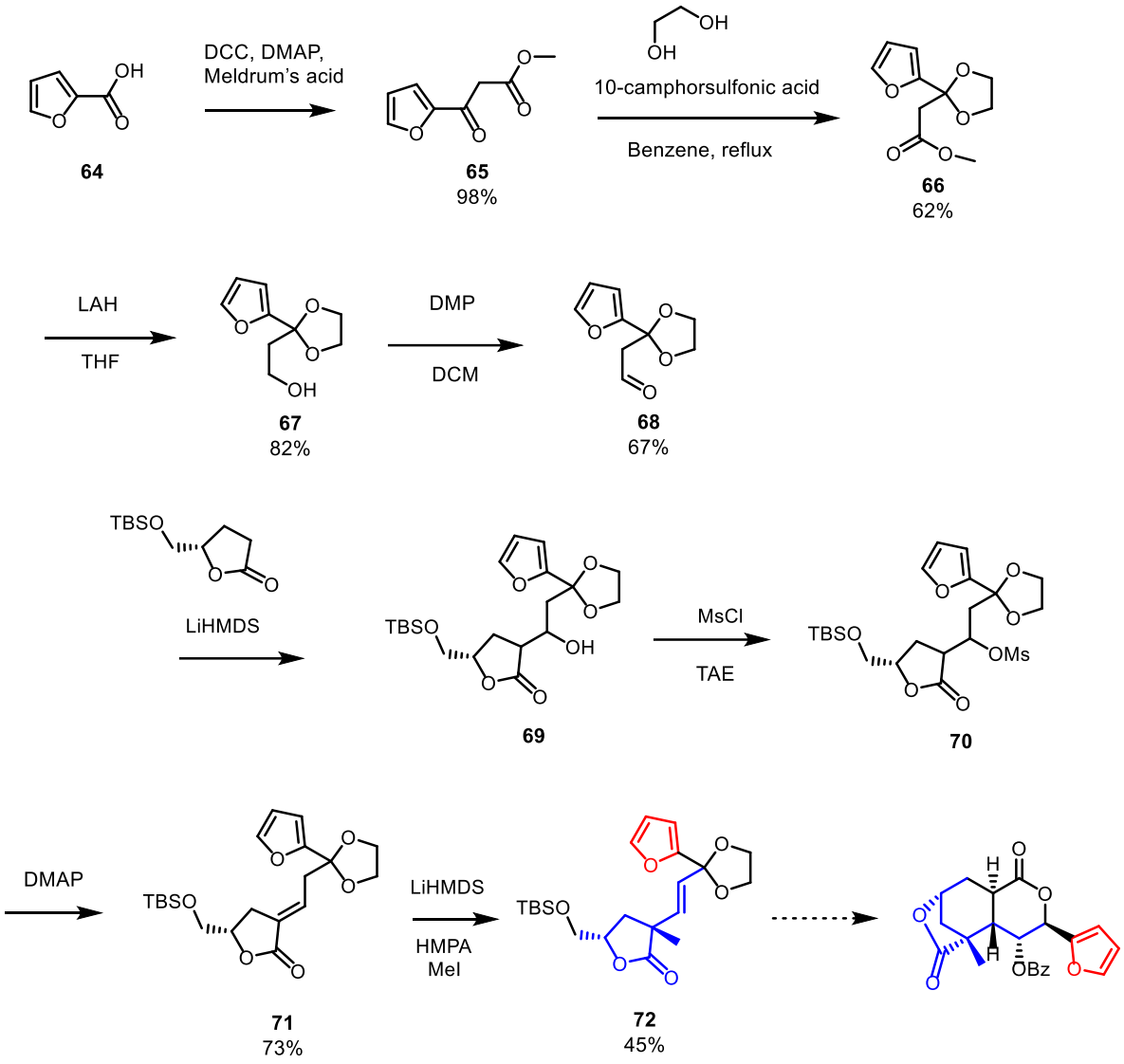

Figure 3.15. Efforts towards synthesis of 2-furan analog of collybolide. Intermediate **72** is achieved after the methylation step with a similar yield as the total synthesis steps.

Based on furan resonance, there is not much reactivity difference between 2-substituted furan and 3-substituted furan. While carrying out Collybolide synthesis, the effort has been put to attempt achieving a 2-furan isomer of collybolide. The synthesis started with 2-furanic acid. All reactions followed the exact same conditions of the

corresponding 3-furan synthesis. The result was achieved with very similar yields as 3-furan synthesis.

3.5. Conclusion and Further Directions

The bicyclic core of collybolide was achieved from a route where furan was installed in an early stage. Until the latest step, the only chiral reagent used was D-glutamic acid as the starting material. So far, the route has exhibited high stereoselectivity. The initial stereo center in lactone contributes to the installation of the methyl group. The chirality of the ring further leads to the asymmetric cyclization of the second ring. Compared with the published route, such an exploit of stereoselectivity showed a huge advantage. In addition, the existence of the furan substructure was proven essential in this route. These two factors demonstrated the significant potential of this synthetic route. After twelve steps, fifteen out of twenty-two carbon atoms, four out of six stereo centers, and two out of three cyclic cores of the collybolide molecule are achieved. The route was very close to the total synthesis of collybolide. There are only two steps away from the final compound, installation of benzo ester, and final cyclization of the third ring. In addition, 2-furan isomer synthesis was attempted. So far, there is no obvious reactivity difference between 2-furan and 3-furan. Thus, once collybolide is synthesized, the 2-furan isomer can be immediately carried out. This isomer is untouchable from semi-synthesis.

3.6. REFERENCES FOR CHAPTER 3

1. McDowell, J.; Kitchen, I., Development of opioid systems: peptides, receptors and pharmacology. *Brain Res. Rev.* **1987,** *12* (4), 397-421.

2. Brownstein, M. J., A brief history of opiates, opioid peptides, and opioid receptors. *Proc. Natl. Acad. Sci.* **1993,** *90* (12), 5391-5393.

3. Duarte, D. F., Opium and opioids: a brief history. *Rev. Bras. Anestesiol.* **2005,** *55*, 135-146.

4. Schiff, P. L., Opium and its alkaloids. *Am. J. Pharm. Educ.* **2002,** *66* (2), 188-196.

5. Kerrigan, S.; Goldberger, B. A., Opioids. *Principles of forensic toxicology* **2020**, 347-369.

6. Volkow, N. D.; Blanco, C., The changing opioid crisis: development, challenges and opportunities. *Mol. Psychiatry* **2021,** *26* (1), 218-233.

7. Martin, W. R.; Jasinski, D. R.; Haertzen, C. A.; Kay, D. C.; Jones, B.; Mansky, P. A.; Carpenter, R. W., Methadone—a reevaluation. *Arch. Gen. Psychiatry* **1973,** *28* (2), 286-295.

8. Campbell, N. D.; Lovell, A. M., The history of the development of buprenorphine as an addiction therapeutic. *Ann. N.Y. Acad. Sci.* **2012,** *1248* (1), 124-139.

9. Joseph, H.; Stancliff, S.; Langrod, J., Methadone maintenance treatment (MMT): a review of historical and clinical issues. *Mt. Sinai J. Med.* **2000,** *67* (5-6), 347-364.

10. Payte, J. T., A brief history of methadone in the treatment of opioid dependence: a personal perspective. *J. Psychoactive Drugs* **1991,** *23* (2), 103-107.

11. Maglione, M. A.; Raaen, L.; Chen, C.; Azhar, G.; Shahidinia, N.; Shen, M.; Maksabedian, E.; Shanman, R. M.; Newberry, S.; Hempel, S., Effects of medication

assisted treatment (MAT) for opioid use disorder on functional outcomes: a systematic review. *J. Subst. Abuse Treat.* **2018,** *89*, 28-51.

12. Lutfy, K.; Cowan, A., Buprenorphine: a unique drug with complex pharmacology. *Curr. Neuropharmacol.* **2004,** *2* (4), 395-402.

13. Pergolizzi, J.; Aloisi, A. M.; Dahan, A.; Filitz, J.; Langford, R.; Likar, R.; Mercadante, S.; Morlion, B.; Raffa, R. B.; Sabatowski, R., Current knowledge of buprenorphine and its unique pharmacological profile. *Pain Practice* **2010,** *10* (5), 428-450.

14. Beckett, A.-H.; Casy, A., Synthetic analgesics: stereochemical considerations. *J. Pharm. Pharmacol.* **1954,** *6* (1), 986-1001.

15. Goldstein, A.; Lowney, L. I.; Pal, B., Stereospecific and nonspecific interactions of the morphine congener levorphanol in subcellular fractions of mouse brain. *Proc. Natl. Acad. Sci.* **1971,** *68* (8), 1742-1747.

16. Ogura, T.; Egan, T. D., Opioid agonists and antagonists. *Physiology and Pharmacology for Anesthesia: Foundations and Clinical Application* **2013**, 253-271.

17. Martin, W. R.; Eades, C.; Thompson, J.; Huppler, R.; Gilbert, P., The effects of morphine-and nalorphine-like drugs in the nondependent and morphine-dependent chronic spinal dog. *J. Pharmacol. Exp. Ther.* **1976,** *197* (3), 517-532.

18. Dhawan, B. N.; Cesselin, F.; Raghubir, R.; Reisine, T.; Bradley, P.; Portoghese, P.; Hamon, M., International Union of Pharmacology. XII. Classification of opioid receptors. *Pharmacol. Rev.* **1996,** *48* (4), 567-592.

19. Ninković, J.; Roy, S., Role of the mu-opioid receptor in opioid modulation of immune function. *Amino Acids* **2013,** *45*, 9-24.

20. Dripps, I. J.; Jutkiewicz, E. M., Delta opioid receptors and modulation of mood and emotion. *Delta Opioid Receptor Pharmacology and Therapeutic Applications* **2018**, 179-197.

21. Cullen, J. M.; Cascella, M., *Physiology, Enkephalin*. StatPearls Publishing, Treasure Island (FL): 2022.

22. Bruchas, M.; Land, B.; Chavkin, C., The dynorphin/kappa opioid system as a modulator of stress-induced and pro-addictive behaviors. *Brain Res.* **2010,** *1314*, 44-55.

23. Mores, K. L.; Cummins, B. R.; Cassell, R. J.; Van Rijn, R. M., A review of the therapeutic potential of recently developed G protein-biased kappa agonists. *Front. Pharmacol.* **2019,** *10*, 407.

24. Stein, C., Opioid receptors. *Annu. Rev. Med.* **2016,** *67*, 433-451.

25. Schmitz, R., Friedrich Wilhelm Sertürner and the discovery of morphine. *Pharm. Hist.* **1985,** *27* (2), 61-74.

26. LASAGNA, L., Nalorphine (N-allylnormorphine): practical and theoretical considerations. *Arch. Intern. Med.* **1954,** *94* (4), 532-558.

27. Andrew Bowdle, T., Adverse effects of opioid agonists and agonist-antagonists in anaesthesia. *Drug Saf.* **1998,** *19*, 173-189.

28. Fürst, S.; Hosztafi, S., The chemical and pharmacological importance of morphine analogues. *Acta Physiol. Hung.* **2008,** *95* (1), 3-44.

29. Kolbe, L.; Fins, J. J., The birth of naloxone: An Intellectual history of an ambivalent opioid. *Camb. Q. Healthc. Ethics* **2021,** *30* (4), 637-650.

30. Strang, J.; Metrebian, N.; Lintzeris, N.; Potts, L.; Carnwath, T.; Mayet, S.; Williams, H.; Zador, D.; Evers, R.; Groshkova, T., Supervised injectable heroin or injectable

methadone versus optimised oral methadone as treatment for chronic heroin addicts in England after persistent failure in orthodox treatment (RIOTT): a randomised trial. *The Lancet* **2010,** *375* (9729), 1885-1895.

31. Vadivelu, N.; Kai, A. M.; Kodumudi, V.; Sramcik, J.; Kaye, A. D., The opioid crisis: a comprehensive overview. *Current pain and headache reports* **2018,** *22*, 1-6.

32. Mital, S.; Wisdom, A. C.; Wolff, J. G., Research Full Report: Improving Partnerships Between Public Health and Public Safety to Reduce Overdose Deaths: An Inventory From the CDC Overdose Data to Action Funding Initiative. *J. Public Health Manag. Pract.* **2022,** *28* (6), S279.

33. Carlezon Jr, W. A.; Béguin, C.; Knoll, A. T.; Cohen, B. M., Kappa-opioid ligands in the study and treatment of mood disorders. *Pharmacol. Ther.* **2009,** *123* (3), 334-343.

34. Pradhan, A. A.; Smith, M. L.; Kieffer, B. L.; Evans, C. J., Ligand-directed signalling within the opioid receptor family. *Br. J. Pharmacol.* **2012,** *167* (5), 960-969.

35. Redila, V. A.; Chavkin, C., Stress-induced reinstatement of cocaine seeking is mediated by the kappa opioid system. *Psychopharmacology* **2008,** *200*, 59-70.

36. Roth, B. L.; Baner, K.; Westkaemper, R.; Siebert, D.; Rice, K. C.; Steinberg, S.; Ernsberger, P.; Rothman, R. B., Salvinorin A: a potent naturally occurring nonnitrogenous κ opioid selective agonist. *Proc. Natl. Acad. Sci.* **2002,** *99* (18), 11934-11939.

37. Prisinzano, T. E., Neoclerodanes as Atypical Opioid Receptor Ligands. *J. Med. Chem.* **2013,** *56* (9), 3435-3443.

38. Bruchas, M. R.; Chavkin, C., Kinase cascades and ligand-directed signaling at the kappa opioid receptor. *Psychopharmacology* **2010,** *210* (2), 137-147.

39. Gupta, A.; Gomes, I.; Bobeck, E. N.; Fakira, A. K.; Massaro, N. P.; Sharma, I.; Cavé, A.; Hamm, H. E.; Parello, J.; Devi, L. A., Collybolide is a novel biased agonist of κ-opioid receptors with potent antipruritic activity. *Proc. Natl. Acad. Sci.* **2016,** *113* (21), 6041-6046.

40. French, A. R.; van Rijn, R. M., An updated assessment of the translational promise of G-protein-biased kappa opioid receptor agonists to treat pain and other indications without debilitating adverse effects. *Pharmacol. Res.* **2022,** *177*, 106091.

41. Nozawa, M.; Suka, Y.; Hoshi, T.; Suzuki, T.; Hagiwara, H., Total Synthesis of the Hallucinogenic Neoclerodane Diterpenoid Salvinorin A. *Org. Lett.* **2008,** *10* (7), 1365-1368.

42. Shevick, S. L.; Freeman, S. M.; Tong, G.; Russo, R. J.; Bohn, L. M.; Shenvi, R. A., Asymmetric Syntheses of (+)-and (−)-Collybolide Enable Reevaluation of kappa-Opioid Receptor Agonism. *ACS Cent. Sci.* **2022,** *8* (7), 948-954.

43. Dake, G. R.; Fenster, E. E.; Patrick, B. O., A Synthetic Approach to the Fusicoccane A−B Ring Fragment Based on a Pauson−Khand Cycloaddition/Norrish Type 1 Fragmentation. *J. Org. Chem.* **2008,** *73* (17), 6711-6715.

44. Monfette, S.; Fogg, D. E., Equilibrium Ring-Closing Metathesis. *Chem. Rev.* **2009,** *109* (8), 3783-3816.

45. Grubbs, R. H., Olefin metathesis. *Tetrahedron* **2004,** *60* (34), 7117-7140.

46. Nguyen, S. T.; Johnson, L. K.; Grubbs, R. H.; Ziller, J. W., Ring-opening metathesis polymerization (ROMP) of norbornene by a Group VIII carbene complex in protic media. *J. Am. Chem. Soc.* **1992,** *114* (10), 3974-3975.

47. Connon, S. J.; Blechert, S., Recent Developments in Olefin Cross-Metathesis. *Angew. Chem. Int. Ed.* **2003,** *42* (17), 1900-1923.

48. Zhang, J.; Yang, W.-L.; Zheng, H.; Wang, Y.; Deng, W.-P., Regio- and Enantioselective γ-Allylic Alkylation of In Situ-Generated Free Dienolates via Scandium/Iridium Dual Catalysis. *Angew. Chem. Int. Ed.* **2022,** *61* (19), e202117079.

49. Kumar, V.; Klimovica, K.; Rasina, D.; Jirgensons, A., 2-Vinyl Threoninol Derivatives via Acid-Catalyzed Allylic Substitution of Bisimidates. *J. Org. Chem.* **2015,** *80* (11), 5934-5943.

50. Wang, L.; Wang, L.; Li, M.; Chong, Q.; Meng, F., Cobalt-Catalyzed Diastereo- and Enantioselective Reductive Allyl Additions to Aldehydes with Allylic Alcohol Derivatives via Allyl Radical Intermediates. *J. Am. Chem. Soc.* **2021,** *143* (32), 12755-12765.

51. Baxter, A. D.; Binns, F.; Javed, T.; Roberts, S. M.; Sadler, P.; Scheinmann, F.; Wakefield, B. J.; Lynch, M.; Newton, R. F., Synthesis and use of 7-substituted norbornadienes for the preparation of prostaglandins and prostanoids. *J. Chem. Soc., Perkin Trans. 1* **1986**, 889-900.

3.7. EXPERIMENTAL SECTION FOR CHAPTER 3

Reagents

Reagents and solvents were obtained from Sigma-Aldrich, Chem-Impex, VWR International, and Acros Organics and used without further purification unless otherwise indicated. Dichloromethane and Acetonitrile were distilled over CaH under N_2 unless stated otherwise. Tetrahydrofuran was distilled over Na under N_2 with benzophenone indicator.

Glassware

All reactions were performed in flame-dried glassware under positive N_2 pressure with magnetic stirring unless otherwise noted.

Chromatography

Thin layer chromatography (TLC) was performed on 0.25 mm E. Merck silica gel 60 F254 plates and visualized under UV light (254 nm) or by staining with potassium permanganate (KMnO4), cerium ammonium molybdate (CAM), phosphomolybdic acid (PMA), and ninhydrin. Silica flash chromatography was performed on Sorbtech 230-400 mesh silica gel 60.

Analytical Instrumentation

NMR spectra were recorded on a Varian VNMRS 300, 400, 500, and 600 MHz NMR spectrometer at 20 ºC in CDCl3 unless otherwise indicated. Chemical shifts are expressed in ppm relative to solvent signals: CDCl3 (1H, 7.26 ppm, 13C, 77.0 ppm); coupling constants are expressed in Hz. IR spectra were recorded on a Cary 760 FTIR

spectrometer with peaks reported in cm-1. Mass spectra were obtained on an Advion Expression CMS TLC Mass Spectrometer.

Nomenclature

Chemical structure named in accordance with IUPAC guidelines, automatically generated using ChemDraw 20.1

PUBLICATION AND CONTRIBUTIONS STATEMENT

The research within this section is unpublished. Only materials synthesized by Chenxin will be reported within.

3.7.1. Efforts towards total synthesis of collybolide.

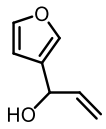

1-(furan-3-yl)prop-2-en-1-ol (32). Synthesized following the reported procedure. Characterization data was in accordance with previous reports. [1]

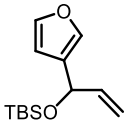

tert-butyl((1-(furan-3-yl)allyl)oxy)dimethylsilane (33). Synthesized following the reported procedure. Characterization data was in accordance with previous reports. [2]

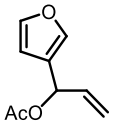

1-(furan-3-yl)allyl acetate (34). Synthesized following the reported procedure. Characterization data was in accordance with previous reports. [3]

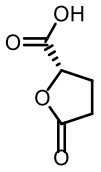

(S)-5-oxotetrahydrofuran-2-carboxylic acid (21). Synthesized following the reported procedure. Characterization data was in accordance with previous reports.[4]

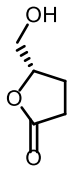

(S)-5-(hydroxymethyl)dihydrofuran-2(3H)-one (22). Synthesized following the reported procedure. Characterization data was in accordance with previous reports.[5]

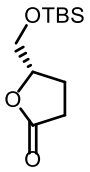

(S)-5-(((tert-butyldimethylsilyl)oxy)methyl)dihydrofuran-2(3H)-one (23). Synthesized following the reported procedure. Characterization data was in accordance with previous reports.[5]

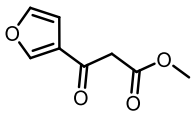

methyl 3-(furan-3-yl)-3-oxopropanoate (38). Synthesized following the reported procedure. Characterization data was in accordance with previous reports. [6]

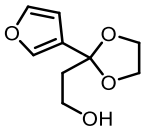

2-(2-(furan-3-yl)-1,3-dioxolan-2-yl)ethan-1-ol (40). Synthesized following the reported procedure. Characterization data was in accordance with previous reports. [6]

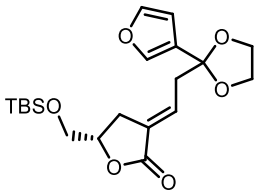

(S,E)-5-(((tert-butyldimethylsilyl)oxy)methyl)-3-(2-(2-(furan-3-yl)-1,3-dioxolan-2-yl)ethy-lidene)-dihydrofuran-2(3H)-one (44). At -40 °C, to **23** in THF solution was added LiHMDS. After 20 min stirring, **41** was added. The reaction was quenched with ammonium chloride after 10 min. The reaction mixture was filtered through silica plug. The solvent was evaporated. The remaining oil was dissolved in DCM and was added with triethylamine and methanesulfonyl chloride at 0 °C. After 2 h stirring, the reaction was quenched with ammonium chloride. The organic layer was collected and filtered through silica plug. After solvent being evaporated, the remining oil was dissolved in DCM again, heated with DBU at 60 °C for 4 h. The reaction was quenched with ammonium chloride. After solvent being evaporated, the remining oil was purified by column chromatography eluting with 1:20 ethyl acetate:hexanes gradient to 1:5 ethyl acetate:hexanes to furnish pure **44**. ^{1}H NMR (400 MHz, Chloroform-*d*) δ 7.41 (d, *J* = 1.2 Hz, 1H), 7.39 – 7.35 (m, 1H), 6.73 (t, *J* = 7.3 Hz, 1H), 6.34 (dt, *J* = 1.9, 1.0 Hz, 1H), 4.67 – 4.39 (m, 1H), 4.01 (d, *J* = 5.0 Hz, 2H), 3.90 (d, *J* = 3.2 Hz, 2H), 3.78 (dd, *J* = 10.8, 3.5 Hz, 1H), 3.71 – 3.55 (m, 1H), 2.77 (d, *J* = 7.7 Hz, 4H), 0.85 (d, *J* = 1.1 Hz, 9H), 0.05 (dd, *J* = 4.7, 1.1 Hz, 6H).

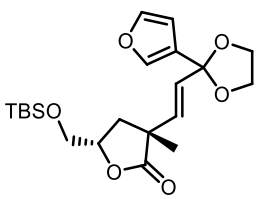

(3R,5S)-5-(((tert-butyldimethylsilyl)oxy)methyl)-3-((E)-2-(2-(furan-3-yl)-1,3-dioxolan-2-yl)vinyl)-3-methyldihydrofuran-2(3H)-one (45). At -40 °C, to **44** in THF solution was added LiHMDS. After 20 min stirring, the reaction mixture was cooled to -78 °C. HMPA and MeI were added sequentially. After 30 min stirring, the reaction was quenched with ammonium chloride. The organic layer was collected, purified by column chromatography eluting with 1:20 ethyl acetate:hexanes gradient to 1:5 ethyl acetate:hexanes to furnish pure **45.** ^{1}H NMR (400 MHz, Chloroform-*d*) δ 7.44 (dd, *J* = 1.7, 0.9 Hz, 1H), 6.37 (dd, *J* = 1.9, 0.9 Hz, 1H), 6.11 (d, *J* = 15.8 Hz, 1H), 5.78 (d, *J* = 15.8 Hz, 1H), 4.03 – 3.97 (m, 2H), 3.81 (dd, *J* = 11.4, 4.0 Hz, 1H), 3.72 (dd, *J* = 11.3, 4.5 Hz, 1H), 2.30 (dd, *J* = 12.8, 9.3 Hz, 1H), 2.07 (dd, *J* = 12.8, 6.5 Hz, 1H), 0.88 (d, *J* = 5.5 Hz, 8H), 0.06 (d, *J* = 5.0 Hz, 5H).

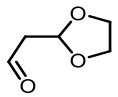

2-(1,3-dioxolan-2-yl)acetaldehyde (49) Synthesized following the reported procedure. Characterization data was in accordance with previous reports.[7]

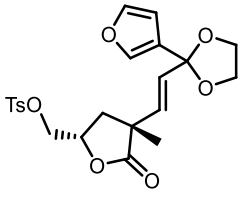

((2S,4R)-4-((E)-2-(2-(furan-3-yl)-1,3-dioxolan-2-yl)vinyl)-4-methyl-5-oxotetrahydrofuran-2-yl)methyl 4-methylbenzenesulfonate (52). At 0 °C, to **44** in THF solution was added TBAF. The mixture was stirred for 4 h. The reaction mixture was washed with water and dried over Na_2SO_4. After solvent being evaporated, the remining

oil was redissolved in DCM. Triethylamine (3 equiv.) and 4-Toluenesulfonyl chloride (1.5 equiv.) was added. The reaction mixture was stirred overnight and quenched with ammonium chloride. The organic layer was collected, purified by column chromatography eluting with 1:20 ethyl acetate:hexanes gradient to 1:5 ethyl acetate:hexanes to furnish pure **52**. ^{1}H NMR (400 MHz, Chloroform-*d*) δ 7.79 (d, *J* = 8.1 Hz, 2H), 7.43 (d, *J* = 2.0 Hz, 1H), 7.40 – 7.35 (m, 3H), 6.35 (dd, *J* = 1.8, 0.9 Hz, 1H), 6.04 (d, *J* = 15.8 Hz, 1H), 5.81 – 5.71 (m, 1H), 4.20 (dd, *J* = 11.0, 4.1 Hz, 1H), 4.14 – 4.08 (m, 1H), 4.04 – 3.97 (m, 4H), 2.46 (s, 3H), 2.17 (dd, *J* = 7.9, 4.1 Hz, 2H), 1.36 (d, *J* = 5.0 Hz, 3H), 1.26 (t, *J* = 7.1 Hz, 1H).

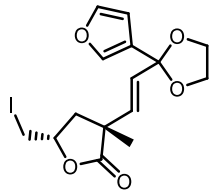

(3R,5S)-3-((E)-2-(2-(furan-3-yl)-1,3-dioxolan-2-yl)vinyl)-5-(iodomethyl)-3-methyldihydrofuran-2(3H)-one (57). 52 in acetone was heat with NaI (5 equiv) under reflux and dark condition overnight. The product was purified by column chromatography eluting with 1:20 ethyl acetate:hexanes gradient to 1:5 ethyl acetate:hexanes to furnish pure **57**. ^{1}H NMR (400 MHz, Chloroform-*d*) δ 7.45 (s, 1H), 7.39 (s, 1H), 6.36 (s, 1H), 6.10 (dd, *J* = 15.6, 2.3 Hz, 1H), 5.81 (d, *J* = 15.8 Hz, 1H), 4.56 (s, 1H), 4.01 (t, *J* = 3.7 Hz, 4H), 3.43 (d, *J* = 10.3 Hz, 1H), 3.22 (t, *J* = 9.2 Hz, 1H), 2.40 (dd, *J* = 13.4, 6.2 Hz, 1H), 2.11 (dd, *J* = 12.8, 9.4 Hz, 1H), 1.44 – 1.34 (m, 3H).

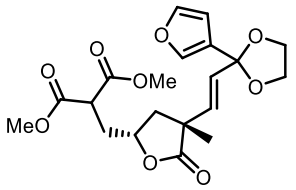

dimethyl 2-(((2R,4R)-4-((E)-2-(2-(furan-3-yl)-1,3-dioxolan-2-yl)vinyl)-4-methyl-5-oxotetrahydro-furan-2-yl)methyl)malonate (58). To **52** in DMF was added Cesium carbonate (2 equiv.) and methyl malonate (1.2 equiv). The mixture was stirred for overnight. and quenched with ammonium chloride. The organic layer was collected, purified by column chromatography eluting with 1:20 ethyl acetate:hexanes gradient to 1:5 ethyl acetate:hexanes to furnish pure **58**. ^{1}H NMR (400 MHz, Chloroform-*d*) δ 7.44 (s, 1H), 7.38 (d, *J* = 1.6 Hz, 1H), 6.36 (d, *J* = 1.7 Hz, 1H), 6.08 (d, *J* = 15.8 Hz, 1H), 5.77 (d, *J* = 15.9 Hz, 1H), 4.52 (d, *J* = 9.2 Hz, 1H), 4.06 – 3.96 (m, 6H), 3.76 (dd, *J* = 9.5, 1.2 Hz, 9H), 3.69 (dd, *J* = 9.9, 4.8 Hz, 1H), 2.39 – 1.96 (m, 6H), 1.36 (s, 3H).

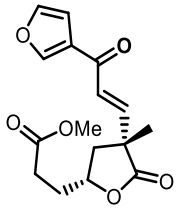

methyl 3-((2R,4R)-4-((E)-3-(furan-3-yl)-3-oxoprop-1-en-1-yl)-4-methyl-5-oxotetrahydrofuran-2-yl)propanoate (60). To **58** (30 mg) in 5 ml HMPA was added with LiCl (4 equiv.). The reaction mixture was heated at 120 °C for 4 h. Then, 1 N HCl was added to quench the reaction and stirred for 4 h. The product was purified by column chromatography eluting with 1:20 ethyl acetate:hexanes gradient to 1:5 ethyl acetate:hexanes to furnish pure **60** (4 mg). ^{1}H NMR (400 MHz, Chloroform-d) δ 8.09 (d, J = 1.1 Hz, 1H), 7.47 (d, J = 1.6 Hz, 1H), 7.05 (d, J = 15.7 Hz, 1H), 6.84 (dd, J = 1.9, 0.9

Hz, 1H), 6.70 (d, J = 15.8 Hz, 1H), 4.67 – 4.48 (m, 2H), 3.70 (s, 4H), 2.68 – 2.50 (m, 3H), 2.37 (dd, J = 12.8, 6.1 Hz, 2H), 2.15 – 2.02 (m, 3H), 2.02 – 1.93 (m, 1H), 1.48 (s, 5H).

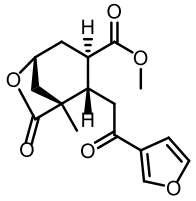

methyl (1R,2S,3R,5R)-2-(2-(furan-3-yl)-2-oxoethyl)-1-methyl-7-oxo-6-oxabicyclo[3.2.1]octane-3-carboxylate (61). To **60** (5 mg) in THF solution was added with LiHMS (2 equiv.) at -78 °C. The reaction mixture was slowly warmed to 0 °C and quenched with ammonium chloride. The organic layer was collected, dried over Na_2SO_4. The product was purified by column chromatography eluting with 1:20 ethyl acetate:hexanes gradient to 1:5 ethyl acetate:hexanes to furnish pure **60**.

^{1}H NMR (400 MHz, Chloroform-*d*) δ 8.08 (d, *J* = 1.3 Hz, 1H), 7.45 (d, *J* = 1.6 Hz, 1H), 6.77 (d, *J* = 1.9 Hz, 1H), 4.81 (dd, *J* = 6.1, 4.7 Hz, 1H), 3.60 (d, *J* = 0.8 Hz, 3H), 3.17 (dd, *J* = 18.0, 6.9 Hz, 1H), 2.95 (ddd, *J* = 11.1, 6.8, 3.5 Hz, 1H), 2.75 – 2.45 (m, 2H), 2.31 (ddd, *J* = 24.8, 13.1, 6.9 Hz, 2H), 2.03 (d, *J* = 11.8 Hz, 1H), 1.87 (dd, *J* = 13.8, 11.7 Hz, 1H), 1.12 (s, 3H).

3.7.2. Synthetic efforts towards 2-furan Analogue of collybolide

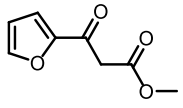

methyl 3-(furan-2-yl)-3-oxopropanoate Synthesized following the reported procedure same as **38**. [6] Characterization data was in accordance with previous reports.[8]

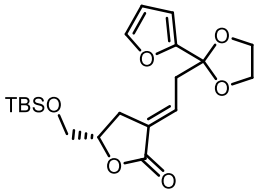

(S,E)-5-(((tert-butyldimethylsilyl)oxy)methyl)-3-(2-(2-(furan-2-yl)-1,3-dioxolan-2-yl)ethy-lidene)-dihydrofuran-2(3H)-one (71) Synthesized following the procedure same as **44** (32 mg 53%). ^{1}H NMR (500 MHz, Chloroform-*d*) δ 7.38 (dd, *J* = 1.8, 0.9 Hz, 1H), 6.72 (ddd, *J* = 7.5, 4.4, 3.0 Hz, 1H), 6.38 – 6.23 (m, 2H), 4.64 – 4.48 (m, 1H), 4.19 – 3.93 (m, 3H), 3.79 (dd, *J* = 11.2, 3.9 Hz, 1H), 3.68 (dd, *J* = 11.1, 3.5 Hz, 1H), 2.91 (dd, *J* = 7.6, 1.7 Hz, 2H), 2.87 – 2.74 (m, 1H), 0.86 (s, 10H), 0.05 (d, *J* = 6.2 Hz, 6H).

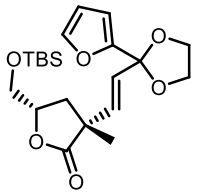

(3R,5S)-5-(((tert-butyldimethylsilyl)oxy)methyl)-3-((E)-2-(2-(furan-2-yl)-1,3-dioxolan-2-yl)vinyl)-3-methyldihydrofuran-2(3H)-one (72). Synthesized following the procedure same as **45.** ^{1}H NMR (400 MHz, Chloroform-*d*) δ 7.40 (d, *J* = 1.7 Hz, 1H), 6.37 (t, *J* = 4.4 Hz, 1H), 6.32 (dd, *J* = 3.3, 1.8 Hz, 1H), 6.17 (d, *J* = 15.8 Hz, 1H), 5.90 (d,

J = 15.9 Hz, 1H), 4.54 (t, *J* = 7.8 Hz, 1H), 4.16 – 3.97 (m, 5H), 3.88 – 3.58 (m, 3H), 2.32 (dd, *J* = 12.8, 9.1 Hz, 1H), 2.20 – 1.98 (m, 2H), 1.41 (s, 4H), 0.87 (d, *J* = 6.4 Hz, 9H), 0.06 (dd, *J* = 6.7, 4.0 Hz, 6H).

3.8. APPENDIX 2

Spectra Relevant to Chapter 3

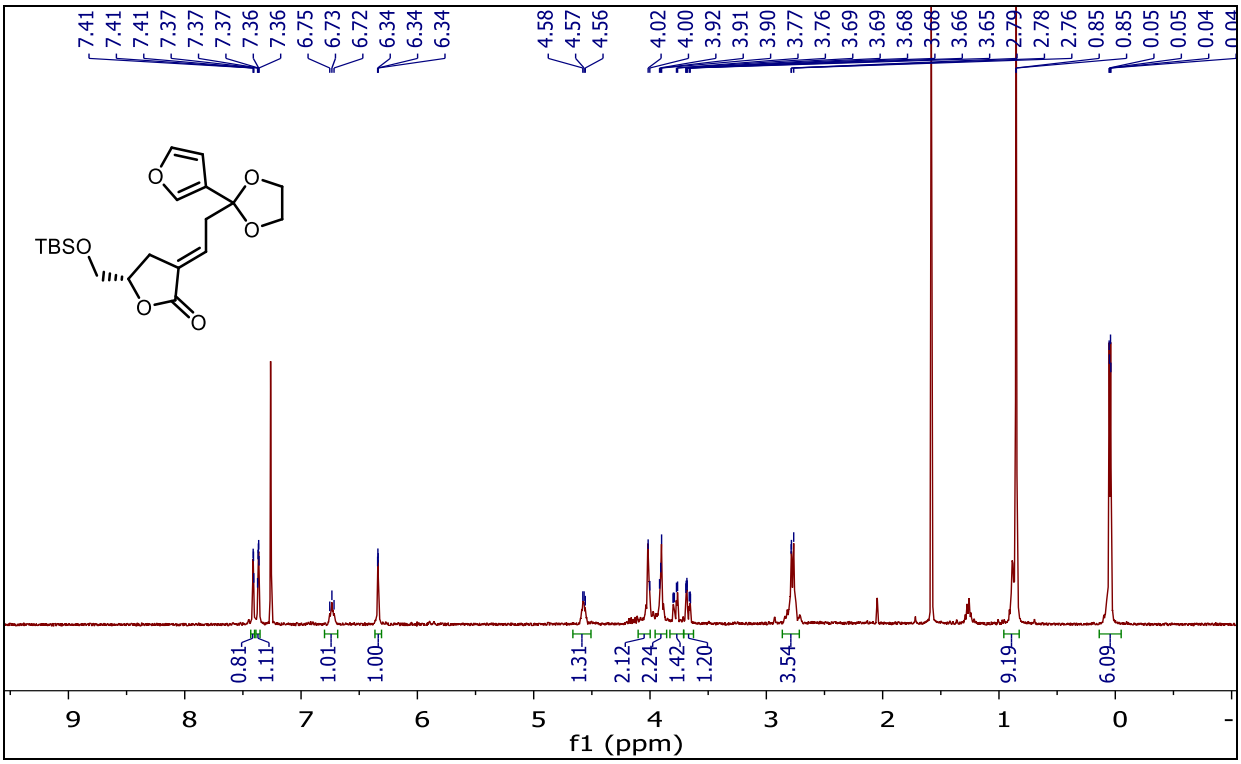
TBSO
f1 (ppm)

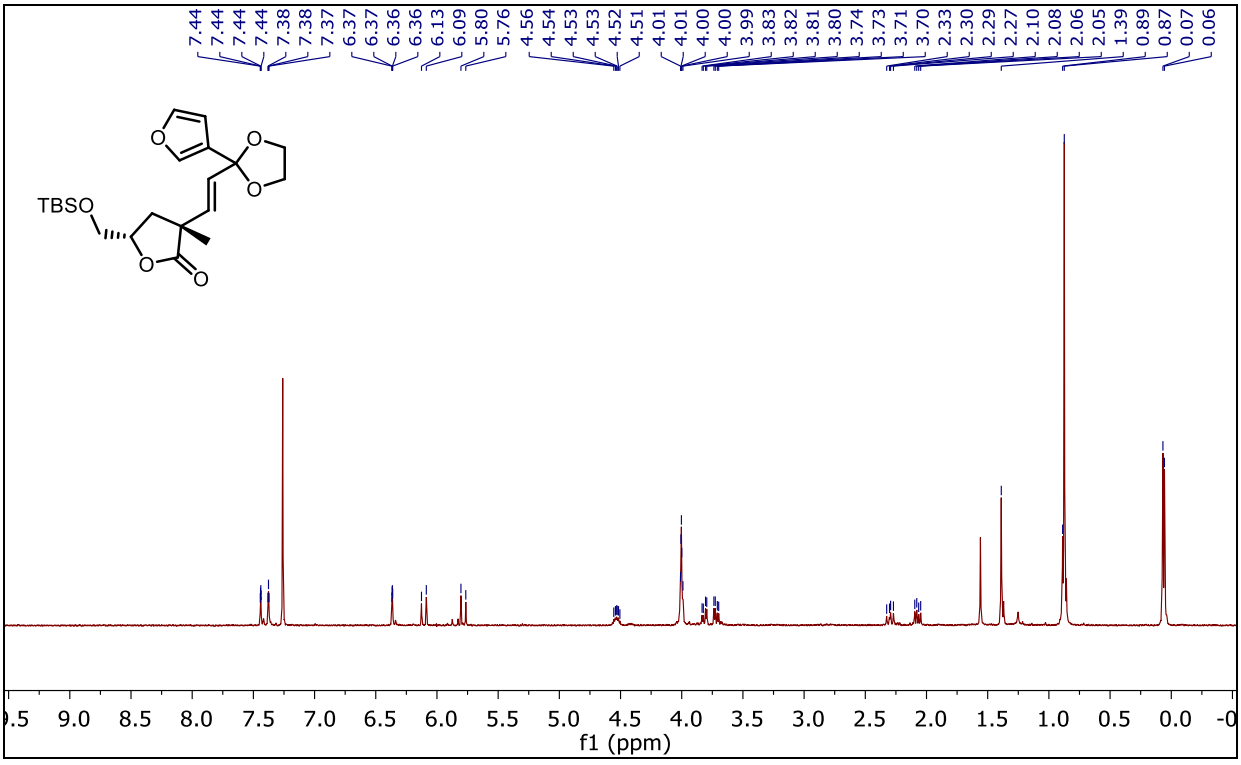
TBSO
f1 (ppm)

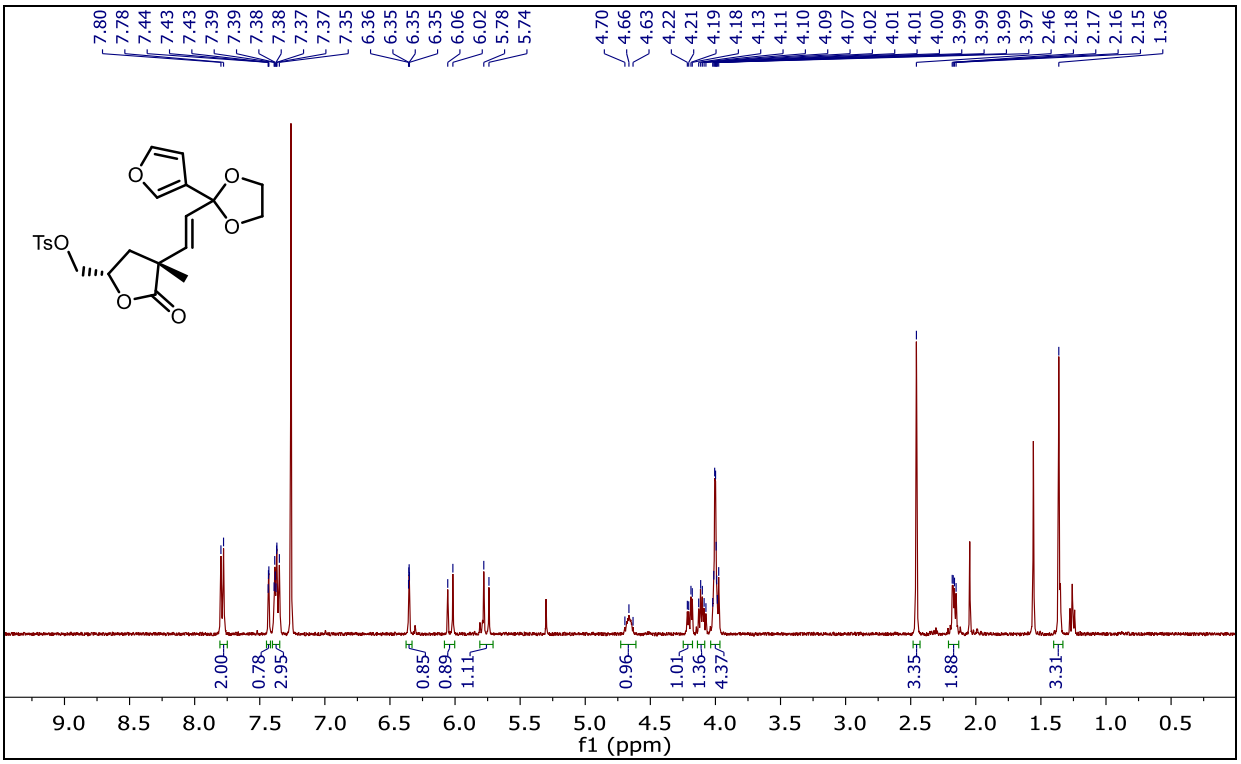
TsO
f1 (ppm)

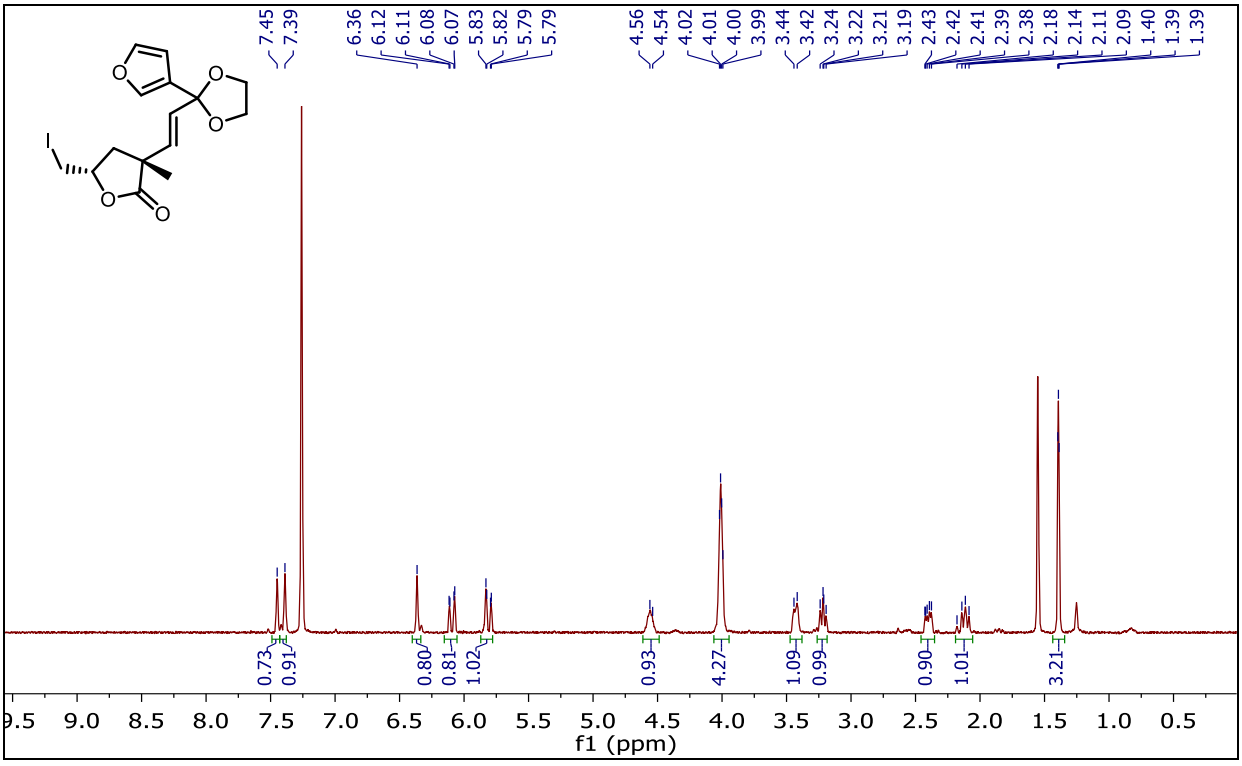
I
f1 (ppm)

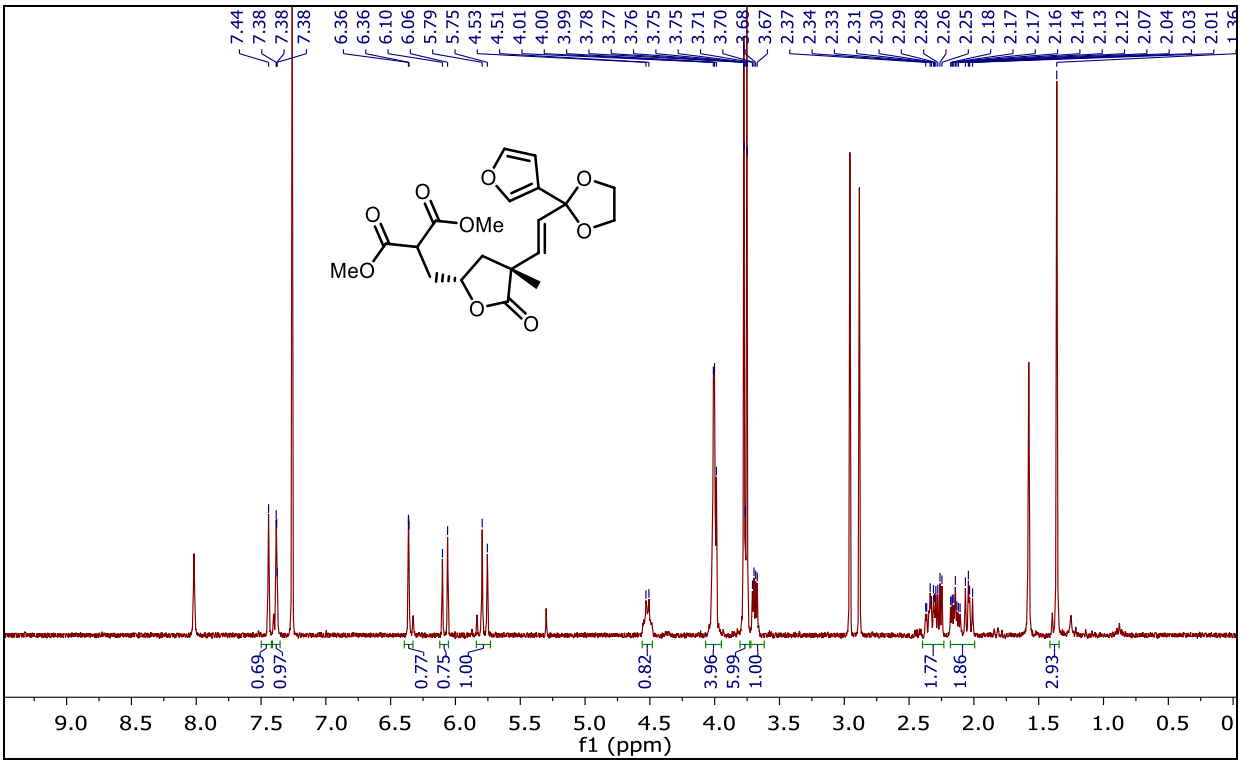
7.44 7.38 7.38 7.38 6.36 6.36 6.10 6.06 5.79 5.75 4.53 4.51 4.01 4.00 3.99 3.78 3.77 3.76 3.75 3.75 3.71 3.70 3.68 3.67 2.37 2.34 2.33 2.31 2.30 2.29 2.28 2.26 2.25 2.18 2.17 2.17 2.16 2.14 2.13 2.12 2.07 2.04 2.03 2.01
O
O
OMe
MeO
O
O
O
O
0.69 0.97 0.77 0.75 1.00 0.82 3.96 5.99 1.00 1.77 1.86 2.93
9.0 8.5 8.0 7.5 7.0 6.5 6.0 5.5 5.0 4.5 4.0 3.5 3.0 2.5 2.0 1.5 1.0 0.5 0
f1 (ppm)

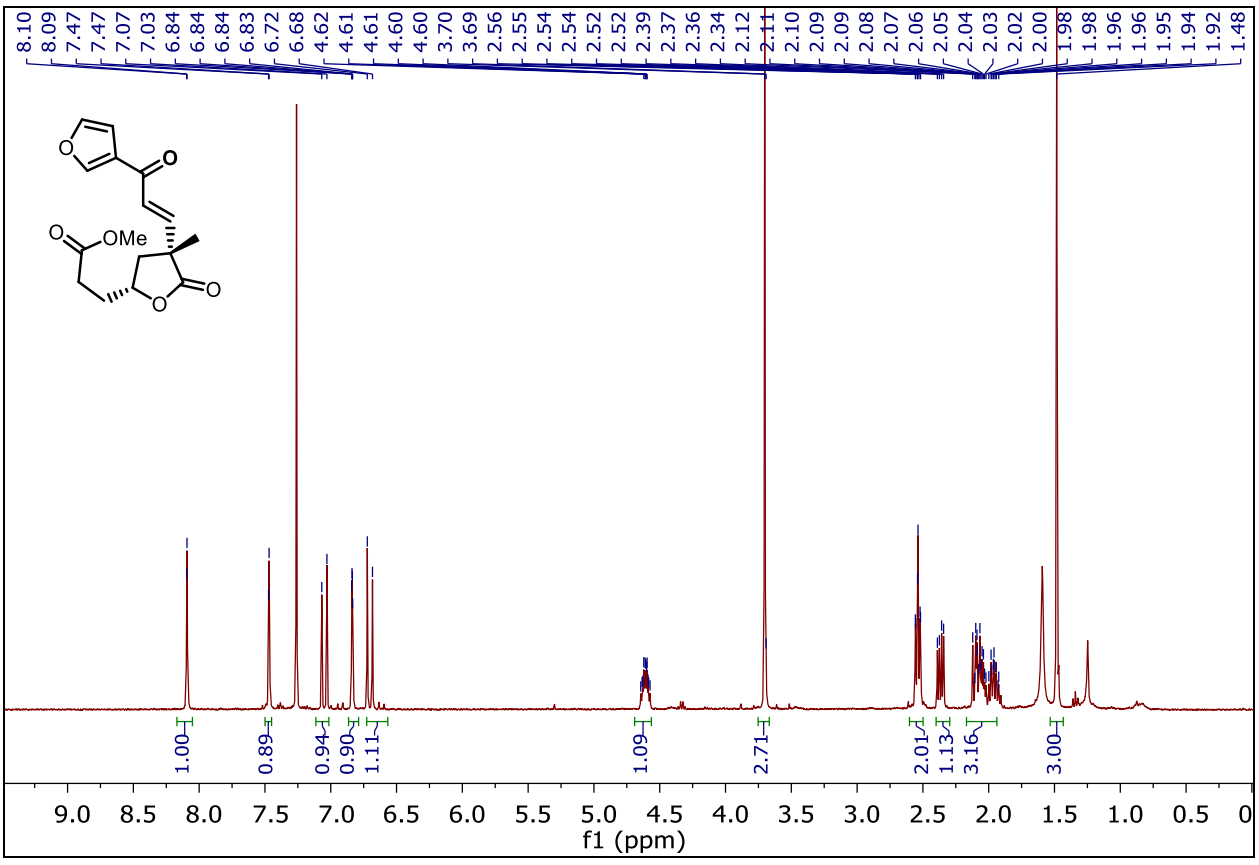
8.10 8.09 7.47 7.47 7.07 7.03 6.84 6.84 6.84 6.83 6.72 6.68 4.62 4.61 4.61 4.60 4.60 3.70 3.69 2.56 2.55 2.54 2.54 2.52 2.52 2.39 2.37 2.36 2.34 2.12 2.11 2.10 2.09 2.09 2.08 2.07 2.06 2.05 2.04 2.03 2.02 2.00 1.98 1.98 1.96 1.96 1.95 1.94 1.92 1.48
O
O
O
OMe
O
O
1.00 0.89 0.94 0.90 1.11 1.09 2.71 2.01 1.13 3.16 3.00
9.0 8.5 8.0 7.5 7.0 6.5 6.0 5.5 5.0 4.5 4.0 3.5 3.0 2.5 2.0 1.5 1.0 0.5 0
f1 (ppm)

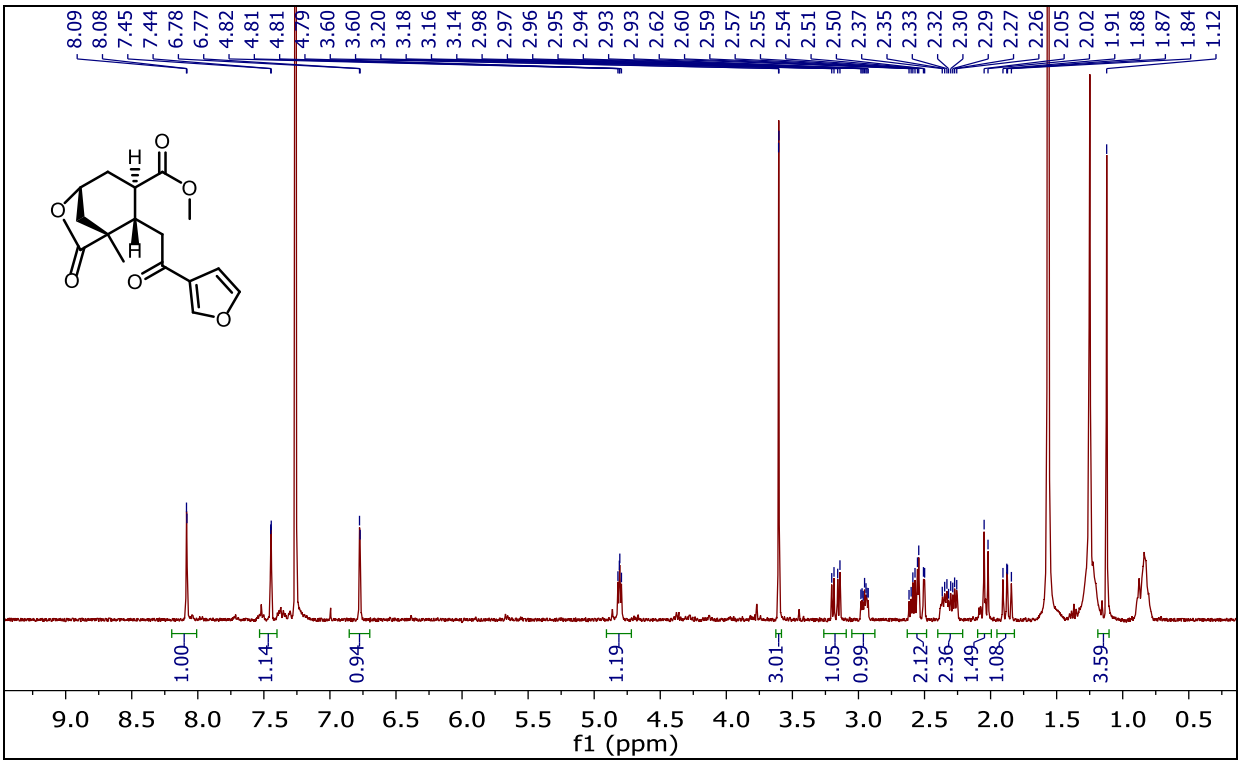
8.09 8.08 7.45 7.44 6.78 6.77 4.82 4.81 4.81 4.79 3.60 3.60 3.20 3.18 3.16 3.14 2.98 2.97 2.96 2.95 2.94 2.93 2.93 2.62 2.60 2.59 2.57 2.55 2.54 2.51 2.50 2.37 2.35 2.33 2.32 2.30 2.29 2.27 2.26 2.05 2.02 1.91 1.88 1.87 1.84 1.12
1.00 1.14 0.94 1.19 3.01 1.05 0.99 2.12 2.36 1.49 1.08 3.59
9.0 8.5 8.0 7.5 7.0 6.5 6.0 5.5 5.0 4.5 4.0 3.5 3.0 2.5 2.0 1.5 1.0 0.5
f1 (ppm)

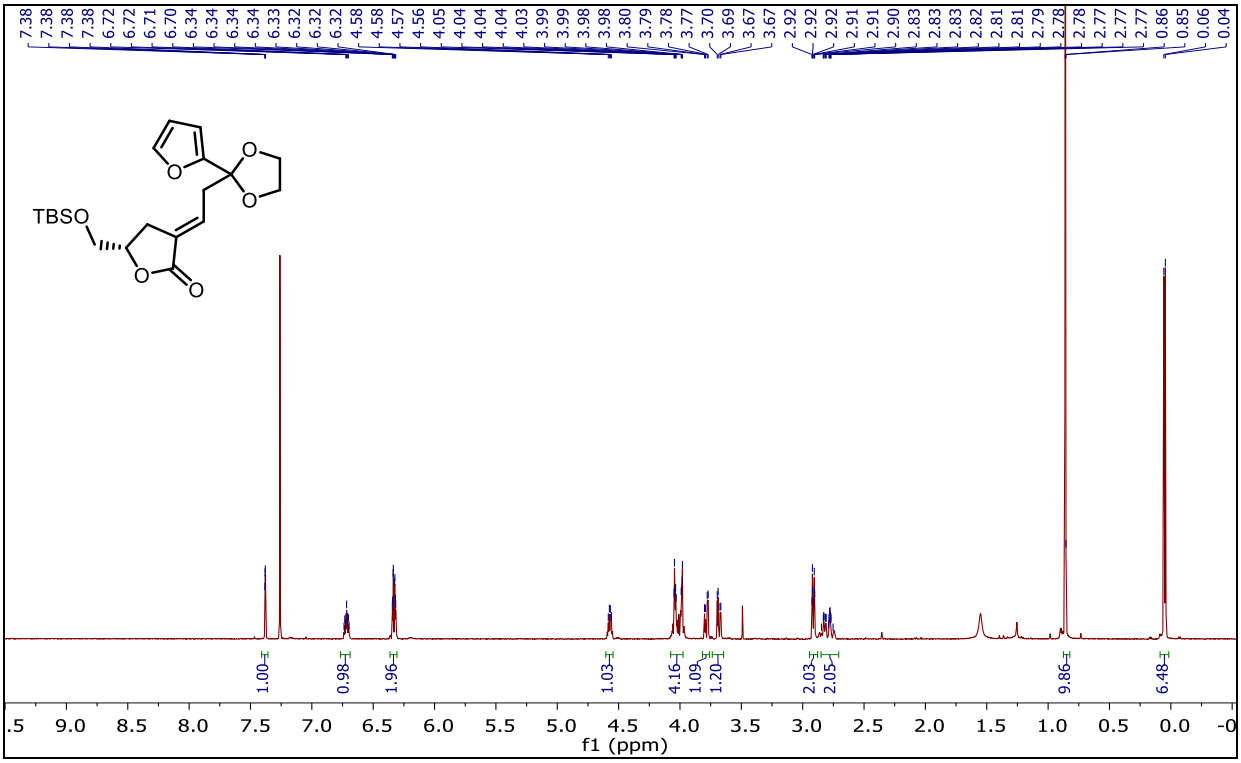
7.38 7.38 7.38 7.38 6.72 6.72 6.71 6.70 6.34 6.34 6.34 6.34 6.33 6.32 6.32 6.32 4.58 4.58 4.57 4.56 4.05 4.04 4.04 4.04 4.03 3.99 3.99 3.98 3.98 3.80 3.79 3.78 3.77 3.70 3.69 3.67 3.67 2.92 2.92 2.92 2.91 2.91 2.90 2.83 2.83 2.83 2.82 2.81 2.81 2.79 2.78 2.78 2.77 2.77 2.77 0.86 0.85 0.06 0.04
TBSO
1.00 0.98 1.96 1.03 4.16 1.09 1.20 2.03 2.05 9.86 6.48
.5 9.0 8.5 8.0 7.5 7.0 6.5 6.0 5.5 5.0 4.5 4.0 3.5 3.0 2.5 2.0 1.5 1.0 0.5 0.0 -0
f1 (ppm)

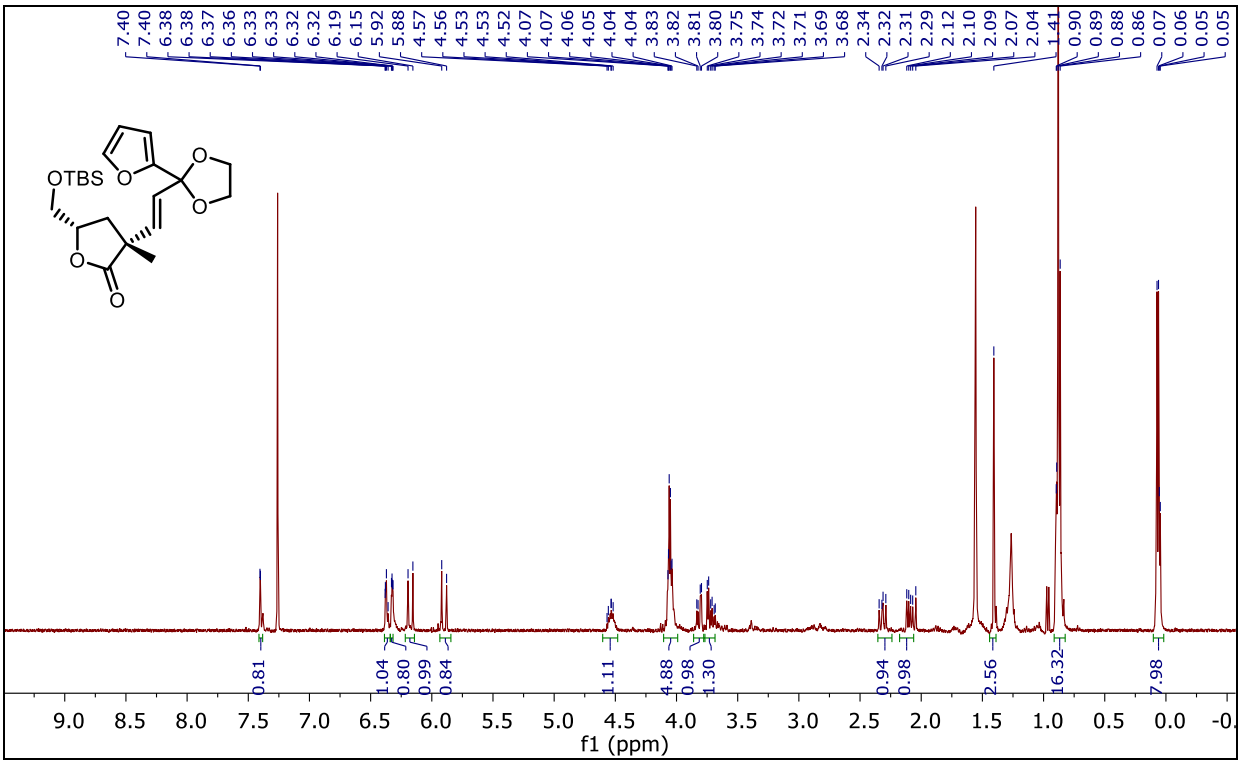
7.40 7.40 6.38 6.38 6.37 6.36 6.33 6.33 6.32 6.32 6.19 6.15 5.92 5.88 4.57 4.56 4.53 4.53 4.52 4.07 4.07 4.06 4.05 4.04 4.04 3.83 3.82 3.81 3.80 3.75 3.74 3.72 3.71 3.69 3.68 2.34 2.32 2.31 2.29 2.12 2.10 2.09 2.07 2.04 1.41 0.90 0.89 0.88 0.86 0.07 0.06 0.05 0.05
OTBS
O
O
O
O
O
0.81 1.04 0.80 0.99 0.84 1.11 4.88 0.98 1.30 0.94 0.98 2.56 16.32 7.98
9.0 8.5 8.0 7.5 7.0 6.5 6.0 5.5 5.0 4.5 4.0 3.5 3.0 2.5 2.0 1.5 1.0 0.5 0.0
f1 (ppm)

3.9. REFERENCES FOR CHAPTER 2 EXPERIMENTAL

1. Zhang, J.; Yang, W.-L.; Zheng, H.; Wang, Y.; Deng, W.-P., Regio- and Enantioselective γ-Allylic Alkylation of In Situ-Generated Free Dienolates via Scandium/Iridium Dual Catalysis. *Angew. Chem. Int. Ed.* **2022,** *61* (19), e202117079.

2. Kumar, V.; Klimovica, K.; Rasina, D.; Jirgensons, A., 2-Vinyl Threoninol Derivatives via Acid-Catalyzed Allylic Substitution of Bisimidates. *J. Org. Chem.* **2015,** *80* (11), 5934-5943.

3. Wang, L.; Wang, L.; Li, M.; Chong, Q.; Meng, F., Cobalt-Catalyzed Diastereo- and Enantioselective Reductive Allyl Additions to Aldehydes with Allylic Alcohol Derivatives via Allyl Radical Intermediates. *J. Am. Chem. Soc.* **2021,** *143* (32), 12755-12765.

4. Kumar, P.; Rahman, M. A.; Haque, A.; Singh Yadav, J., A transition metal-catalyzed enyne metathesis for the preparation of pyrrolizidine alkaloid core: Application towards the total synthesis of stemaphylline. *Tetrahedron Lett.* **2021,** *68*, 152906.

5. Wrona, I. E.; Gozman, A.; Taldone, T.; Chiosis, G.; Panek, J. S., Synthesis of Reblastatin, Autolytimycin, and Non-Benzoquinone Analogues: Potent Inhibitors of Heat Shock Protein 90. *J. Org. Chem.* **2010,** *75* (9), 2820-2835.

6. Li, H.; He, Z.; Guo, X.; Li, W.; Zhao, X.; Li, Z., Iron-catalyzed selective oxidation of N-methyl amines: highly efficient synthesis of methylene-bridged bis-1, 3-dicarbonyl compounds. *Org. Lett.* **2009,** *11* (18), 4176-4179.

7. Ducho, C.; Hamed, R. B.; Batchelar, E. T.; Sorensen, J. L.; Odell, B.; Schofield, C. J., Synthesis of regio-and stereoselectively deuterium-labelled derivatives of L-glutamate semialdehyde for studies on carbapenem biosynthesis. *Org. Biomol. Chem.* **2009,** *7* (13), 2770-2779.

8. Zhang, Y.; Zhang, Y., Trace amount of metallic samarium catalysed aroyl substitution reactions of a β-keto ester in air. *Journal of Chemical Research* **2004,** *2004* (7), 510-512.

CHAPTER 4

Conclusion and Future Directions

Compounds featuring the furan moiety are of significant importance in pharmaceutical chemistry, capturing the attention of synthetic chemists worldwide. This thesis delves into two primary synthetic strategies: the broad-spectrum synthesis and targeted synthesis of furan derivatives. Both approaches have witnessed remarkable successes, underscoring the versatility and potential of furan-containing compounds in the realm of medicinal chemistry.

A groundbreaking approach to constructing furyl-pyrrolidine has been introduced, which leverages enynals as carbene progenitors in the presence of zinc catalysts that are both economical and abundant. Despite the progress, several pivotal inquiries remain unaddressed. Initially, while experimental outcomes lend credence to the anticipated mechanism involving aminoketone coordination to zinc, conclusive evidence remains elusive. Theoretical studies, particularly computational models, could provide crucial insights to substantiate this interaction. Additionally, disparate reactivity profiles have been noted when enynals interact with diazo compounds. Another enigma revolves around the specificity of enynals bearing ester functionalities as the sole successful precursors in generating the desired end product, while their ketone or amide counterparts gave unwanted products. Delving deeper into these phenomena could

greatly enhance our understanding of the underlying principles governing enynal and enynone reactivity, potentially unlocking further synthetic applications.

The synthetic journey toward collybolide's bicyclic structure begins by incorporating a furan moiety early in the sequence. Remarkably, throughout the progression up to the penultimate steps, D-glutamic acid remains the sole chiral source. This route has consistently exhibited exceptional enantioselectivity. The initial chiral center in the lactone framework is pivotal for introducing the methyl group, which subsequently orchestrates the asymmetric formation of the second ring. When contrasted with previously reported methodologies, this strategy's exploitation of stereochemical control is considerably advantageous. Moreover, the incorporation of the furan unit is not just strategic but crucial for the success of this synthetic route. Collectively, these attributes underscore the significant promise of this approach.

After a dozen steps, the synthesis has faithfully constructed fifteen of the twenty-two carbon atoms, four of the six stereocenters, and two of the three core rings inherent to the collybolide structure. The synthesis stands on the brink of completion, with the incorporation of a benzoate ester and the ultimate cyclization to forge the third ring as the final challenge. Furthermore, explorations into synthesizing the 2-furan isomer have been conducted, which thus far indicates no discernible reactivity contrast with its 3-furan counterpart. This opens the possibility that, following the successful synthesis of collybolide, the 2-furan isomer synthesis could proceed forthwith, presenting an opportunity to explore avenues beyond what is achievable through semi-synthesis.